

STUDY OF THE SPATIAL VARIABILITY OF THE SOUTHERN ROOT-KNOT  
NEMATODE (*MELOIDOGYNE INCOGNITA*) AND ITS IMPACT ON COTTON YIELD

by

BRENDA VALESKA ORTIZ URIBE

(Under the Direction of George Vellidis)

ABSTRACT

Site-specific management (SSM) is a promising strategy for reducing yield losses caused by the southern root-knot nematode [*Meloidogyne incognita* (Kofoid & White) Chitwood] (RKN) across the U.S Cotton Belt. To address this opportunity, this dissertation addresses the analysis of the spatial variability of RKN and its spatial relationship to edaphic, terrain, and chemical field properties. Additionally, simulations of RKN damage on different cotton biomass components, through adaptations to the CROPGRO-Cotton growth model, were used to estimate the damage of RKN within zones with a high likelihood for high RKN population.

The work was conducted in the Tifton-Vidalia Upland (TVU) ecoregion of the southeastern Coastal Plain. Data were collected from eleven producers' fields and one university-owned field used for a RKN long-term research project during 2005, 2006, and 2007. The fields were located in Colquitt, Tift, and Worth Counties of Georgia, USA.

Two different approaches were used to identify field features related to the presence or absence of RKN: (i) geostatistical analyses (factorial kriging) to decompose the variability of RKN and soil properties into different spatial components allowing the computation of correlation coefficients for different spatial scales; and (ii) canonical correlation analyses (CCA)

to determine which properties explained the greatest amount of variability in RKN population density. Areas at risk for different levels of RKN population were identified by indicator kriging and fuzzy clustering of canonical predictors derived from the CCA.

The simulation of growth and yield of cotton plants infected with RKN was conducted by modifying the Cropping System Model (CSM)-CROPGRO-Cotton. The model was modified by coupling RKN population for removal of daily assimilate and decreasing root length per unit root weight as strategies to mimic RKN damage.

This study showed that: (1) small patches with high RKN population were associated with the flat areas within a field and large patches were associated with low values of apparent soil electrical conductivity shallow ( $EC_{a-s}$ , 0-30 cm depth) and deep ( $EC_{a-d}$ , 0-90 cm depth); (2) areas at risk for RKN population above a threshold value can be delineated from a reduced number of RKN population samples and a dense data set of  $EC_{a-d}$ ; (3) low values of  $EC_{a-d}$ , slope (SL), and NDVI can be associated with areas having high population of RKN; (4) RKN management zones can be delineated from edaphic terrain properties; (5)  $EC_{a-s}$  and  $EC_{a-d}$  properties offer much more stable information than terrain properties to characterize areas with low and high risk for having presence of RKN population; (6) RKN parasitism reduces cotton growth and development and induces a delay in maturity; (7) the adaptations of the Cropping System Model (CSM)-CROPGRO-Cotton in DSSAT v4.0 by coupling RKN population density and reducing the root length per unit root weight allowed the simulation of growth and yield for the DP 458 BR cotton variety impacted by various levels of RKN population; and (8) the use CSM-CROPGRO-Cotton model to simulate the seed cotton weight for different management zones with various risk levels for RKN allowed the quantification of potential yield losses due to RKN parasitism.

Overall, this research contributes to the knowledge of RKN population variability as a function of edaphic and terrain attributes within fields of south Georgia, and develops techniques for applying site specific management to the pervasive problem of the southern root-knot nematode.

INDEX WORDS: Cotton, crop modeling, geostatistics, growth and yield, *Meloidogyne incognita*, precision agriculture, site-specific management, southern root-knot nematode, spatial variability.

STUDY OF THE SPATIAL VARIABILITY OF THE SOUTHERN ROOT-KNOT  
NEMATODE (MELOIDOGYNE INCOGNITA) AND ITS IMPACT ON COTTON YIELD

by

BRENDA VALESKA ORTIZ URIBE

FORB, Universidad Nacional de Colombia-Universidad del Valle,

Colombia, 1997

A Dissertation Submitted to the Graduate Faculty of The University of Georgia in Partial  
Fulfillment of the Requirements for the Degree

DOCTOR OF PHILOSOPHY

ATHENS, GEORGIA

2008

© 2008

Brenda Valeska Ortiz Uribe

All Rights Reserved

STUDY OF THE SPATIAL VARIABILITY OF THE SOUTHERN ROOT-KNOT  
NEMATODE (MELOIDOGYNE INCOGNITA) AND ITS IMPACT ON COTTON YIELD

by

BRENDA VALESKA ORTIZ URIBE

Major Professor: George Vellidis

Committee: Calvin Perry  
Dana Sullivan  
Gerrit Hoogenboom  
Glen Rains  
John Beasley

Electronic Version Approved:

Maureen Grasso  
Dean of the Graduate School  
The University of Georgia  
December 2008

## ACKNOWLEDGEMENTS

To my major professor, Dr. George Vellidis, for his guidance, encouragement, and time. I thank him very much for giving me the freedom to conduct research in the areas of my interest: geostatistics, GIS, remote sensing, and precision agriculture.

To the members of my advisory committee: Dana Sullivan, Gerrit Hoogenboom, Calvin Perry, Glen Rains, and John Beasley for their guidance, commitment and insightful suggestions. Also, Dr. Richard Davis for his guidance and assistance, providing comments and corrections to early version of some of the manuscripts presented here.

Special recognition to Dr. Kenneth Boote and Dr. James W. Jones from the University of Florida, for their guidance and assistance in many aspects related to crop growth modeling.

To the sponsors of this project especial thanks: Cotton Inc., the Georgia Cotton Commission, the Flint River Water Planning and Policy Center, the Georgia Agricultural Experiment Stations, the USDA-ARS CRIS project.

To the technicians and students for their assistance in the field data collection: Dewayne Dales, Gary Murphy, Rodney Hill, Katia Rizzardi Manuel Renga, Melanie Blomenhoer, Eleni Tzanakouli, Jason Tood. Additional thanks to Andrea Milton and Keith Rucker at the Tifton Campus.

I appreciate the support and guidance of the modeling group at the University of Georgia-Griffin Campus, especially Dr. Cecilia Tojo Soler and Dr. Axel Garcia-Garcia.

My classmates and friends in Athens for their friendship and support: Maria Mosqueda, Kauslendra Singh, Praveen Kolar, Jesus Garcia, Elizabeth and David Conway, Esperanza Mejia, Constanza and Rafael De La Torre, Maria Laura Ramos.

I would like to thank my parents, Carlos Arturo y Martha, and my sister Claudia Gisela, in addition to my extended family, for their guidance, support, encouragement, understanding, love and patience. They were the energy that kept me up every day.

## TABLE OF CONTENTS

	Page
ACKNOWLEDGEMENTS .....	iv
LIST OF TABLES .....	ix
LIST OF FIGURES .....	xiv
CHAPTER	
1 INTRODUCTION AND LITERATURE REVIEW .....	1
References .....	13
2 GEOSTATISTICAL MODELING OF THE SPATIAL VARIABILITY OF SOUTHERN ROOT-KNOT NEMATODES IN RELATION TO SOIL PROPERTIES .....	18
Abstract .....	19
2.1 Introduction .....	20
2.2 Materials and Methods .....	23
2.3 Results and Discussion .....	30
2.4 Summary and Conclusions .....	46
Acknowledgements .....	47
References .....	49

3	DELINEATION OF MANAGEMENT ZONES FOR SOUTHERN ROOT-KNOT NEMATODE USING FUZZY CLUSTERING OF TERRAIN AND EDAPHIC FIELD CHARACTERISTICS .....	70
	Abstract .....	71
	3.1 Introduction .....	72
	3.2 Materials and Methods .....	75
	3.3 Results and Discussion .....	85
	3.4 Summary and Conclusions .....	97
	Acknowledgements .....	99
	References .....	100
4	IMPACT OF SOUTHERN ROOT-KNOT NEMATODE PARASITISM ON COTTON BIOMASS AND YIELD .....	118
	Abstract .....	119
	4.1 Introduction .....	120
	4.2 Materials and Methods .....	123
	4.3 Results .....	128
	4.4 Discussion .....	136
	4.5 Conclusions .....	141
	Acknowledgements .....	141
	References .....	143
5	MODELING THE IMPACT OF SOUTHERN ROOT-KNOT NEMATODE ON COTTON BIOMASS AND YIELD .....	165
	Abstract .....	166

5.1 Introduction .....	167
5.2 Materials and Methods .....	171
5.3 Results and Discussion.....	182
5.4 Summary and Conclusions.....	195
Acknowledgements .....	196
References .....	198
6 SUMMARY AND CONCLUSIONS .....	225
REFERENCES .....	232

## LIST OF TABLES

	Page
Table 2.1: Descriptive statistics of the cotton RKN population density and the soil physical and chemical properties at the CC and PG fields. ....	53
Table 2.2: Parameters of fitted semivariogram models of cotton RKN population density and soil properties for the CC and PG fields. ....	54
Table 2.3: Scale dependent correlation for the nested spatial structures of cotton RKN population density with soil physical and chemical properties at the CC field. ....	55
Table 2.4: Scale dependent correlation for the nested spatial structures of cotton RKN population density with soil physical and chemical properties at the PG field. ....	56
Table 2.5: Indicator semivariogram parameters calculated using hard data and residual semivariogram parameters calculated using hard and soft data for different data sets, CC and PG fields. ....	57
Table 2.6: Number and percentage occurrence of RKN observations above (Risk) or below (No Risk) the threshold value in different levels of estimated probability of risk for RKN above the threshold of 100 RKN second stage juveniles per 100 cm <sup>3</sup> of soil. Jackknife cross-validation results using two data sets, CC field.....	58
Table 2.7: Number and percentage occurrence of RKN observations above (Risk) or below (No Risk) the threshold value in different levels of estimated probability of risk for RKN above the threshold of 100 RKN second stage juveniles per 100 cm <sup>3</sup> of soil. Jackknife cross-validation results using two data sets, PG field.....	59

Table 2.8: Results of the logistic regression between RKN2 and $EC_{a-d}$ using different numbers of RKN observations, CC and PG fields.....	60
Table 3.1: Location, planting and harvesting date, and soil characteristics for the study fields.	105
Table 3.2: Descriptive statistics of RKN, edaphic and terrain data for the CC, PG, and CMP fields.....	106
Table 3.3: Pearson's linear correlation coefficients for RKN population density with edaphic and terrain variables in the CC, PG, and CMP fields. ....	107
Table 3.4: Results from the canonical correlation analysis between the $\text{Log}_{10}$ (RKN Second stage juveniles $100 \text{ cm}^{-3}$ of soil +1) and edaphic and remotely sensed data for each of the studied fields.....	108
Table 3.5: Pooled variances ( $S_p^2$ ) of the data set-zone number combinations for $\text{Log}_{10}$ RKN-S2 and the explanatory variables (EL,SL, $EC_{a-s}$ , $EC_{a-d}$ , and NDVI), CC field. ....	109
Table 3.6: Variability of management zones delineated of fuzzy clustering of canonical predictor variables of RKN calculated from different combination of edaphic and terrain variables, CC field. ....	110
Table 3.7: Pooled variances ( $S_p^2$ ) of the data set-zone number combinations for $\text{Log}_{10}$ RKN-S2 and the explanatory variables (EL,SL, $EC_{a-s}$ , $EC_{a-d}$ , and NDVI), PG field. ....	111
Table 3.8: Variability of management zones delineated of fuzzy clustering of canonical predictor variables of RKN calculated from different combination of edaphic and terrain variables, PG field.....	112
Table 3.9: Pooled variances ( $S_p^2$ ) of the data set-zone number combinations for $\text{Log}_{10}$ RKN-S2 and the explanatory variables (EL,SL, $EC_{a-s}$ , $EC_{a-d}$ , and NDVI), CMP field. ....	113

Table 3.10: Variability of management zones delineated of fuzzy clustering of canonical predictor variables of RKN calculated from different combination of edaphic and terrain variables, CMP field. ....	114
Table 3.11: Validation results of the management zone delineation method tested on six fields located in the Tifton-Vidalia Upland (TVU) ecoregion of the southeastern Coastal Plain. ....	115
Table 4.1: Locations for cotton growth study grouped by root galling rates in the BJ field. ....	146
Table 4.2: Differences in RKN population density by drought stress and fumigation treatments at the Gibbs farm field. Average across four sampling times over six replications. ....	147
Table 4.3: Time series of RKN population density by drought stress and fumigation treatments at the Gibbs farm field. ....	148
Table 4.4: Plant height, LAI, dry matter biomass, and yield as affected by different galling groups, averaged across four harvest dates for the BJ field.....	149
Table 4.5: Plant height differences between galling groups for nine different plating dates in the BJ field. ....	150
Table 4.6: Plant height, LAI, and dry matter biomass as affected by drought and fumigation treatments, averaged across drought-fumigation treatment combinations and four harvest dates for the Gibbs farm field.....	151
Table 4.7: Plant height differences between fumigation treatments for three drought stress treatments, averaged across six replications for the Gibbs farm field. ....	152
Table 4.8: LAI differences between galling groups for nine different plating dates for the BJ field. ....	153

Table 4.9: LAI differences between fumigation treatments for three drought stress treatments, averaged across six replications for the Gibbs farm field.....	154
Table 4.10: Cotton dry matter and yield differences between galling groups measured at four harvest dates, averaged across six replications in the BJ field. ....	155
Table 4.11: Cotton dry matter differences between fumigation treatments for three drought stress treatments measured at four harvest dates, averaged across six replications in the Gibbs farm field. ....	156
Table 4.12: <i>P</i> values for the analysis of variance fixed effects on lint plus seed yield measured at harvest in the Gibbs farm field.....	158
Table 4.13: Cotton dry matter differences between fumigation treatments for three drought stress treatments measured at harvest, averaged across six replications in the Gibbs farm field. ....	159
Table 5.1: Description of the Tifton soil profile for the experiment conducted at the Gibbs farm, GA, USA.....	202
Table 5.2: Cultivar coefficients of cultivar DP 458 B/RR used for model simulations in 2001 and 2007.....	203
Table 5.3: Average RKN population (second stage juveniles-J2 per 150,000 cm <sup>3</sup> soil) measured at different days after planting for the six treatments in the calibration and evaluation experiments.....	204
Table 5.4: Simulated and observed total biomass at harvest for the six treatments in 2007 at the Gibbs farm, GA, USA.....	205
Table 5.5: Simulated and observed bolls weight and seed cotton weight at maturity for the six treatments in 2007 at the Gibbs farm, GA, USA. ....	206

Table 5.6: Prediction accuracy of simulated maximum leaf area index before and after modeling RKN damage. Values correspond to the nonfumigated treatment (-) with low (1), medium (2), and severe (3) drought stress. ....	207
Table 5.7: Simulated and observed maximum leaf area index for the six treatments in 2007 at the Gibbs farm, GA, USA. ....	208
Table 5.8: Prediction accuracy of simulated volumetric soil water content for the six treatment combinations of drought stress and fumigation evaluated at the 15- to 30- cm, 30- to 45- cm, and 45- to 60- cm soil depth. ....	209
Table 5.9: Simulated and observed seed cotton weight at harvest for the six treatments in 2001 at the Gibbs farm, GA, USA. ....	210
Table 5.10: Description of the Albany and Kershaw soil profiles predominant one each of the management zones at the producer field in Norman Park, GA, USA. ....	211
Table 5.11: Simulated and observed average seed cotton weight at harvest for the three management zones in 2006 at the producer field in Norman Park, GA, USA. ....	212

## LIST OF FIGURES

	Page
Figure 2.1: Normalized semivariograms for cotton RKN samples and soil physical and chemical properties at the CC field. Squares indicate the empirical semivariogram and the solid line is the fitted model .....	61
Figure 2.2: Cotton RKN spatio-temporal distribution evaluated RKN1 (a), RKN2 (b), and RKN3 (c) at the CC field in 2006 .....	62
Figure 2.3: Normalized semivariograms for cotton RKN samples and soil physical and chemical properties at the PG field. Squares indicate the empirical semivariogram and the solid line is the fitted model .....	63
Figure 2.4: Cotton RKN spatio-temporal distribution evaluated RKN1 (a), RKN2 (b), and RKN3 (c) at the PG field in 2006 .....	64
Figure 2.5: Indicator semivariograms of the RKN2 population above a threshold of 100 RKN second stage juveniles per 100 cm <sup>3</sup> soil calculated using hard data of 99 (a), 64 (b), and 35 RKN observations (c). Residual semivariograms using hard and soft data of 99 (d), 64 (e), and 35 RKN observations (f), CC field.....	65
Figure 2.6: Maps of predicted RKN risk over the threshold of 100 RKN second stage juveniles per 100 cm <sup>3</sup> soil. Indicator kriging maps of hard data alone based on 99 (a), 64 (b), and 35 (c) RKN observations. Soft indicator kriging maps using EC <sub>a-d</sub> as secondary information based on 99 (d), 64 (e), and 35 (f) RKN observations. Indicator kriging	

with a combination of hard and soft data based on 99 (g), 64 (h), and 35 (i) RKN observations, CC field .....	66
Figure 2.7: Indicator semivariograms of the RKN2 population above a threshold of 100 RKN second stage juveniles per 100 cm <sup>3</sup> soil calculated using hard data of 105 (a) and 70 RKN observations (b). Residual semivariograms using hard and soft data of 105 (d) and 70 RKN observations (e), PG field.....	67
Figure 2.8: Maps of predicted RKN risk over the threshold of 100 RKN second stage juveniles per 100 cm <sup>3</sup> soil. Indicator kriging maps of hard data alone based on 105 (a) and 70 RKN observations (b). Soft indicator kriging maps using EC <sub>a-d</sub> as secondary information based on 105(c) and 70 RKN observations (d). Indicator kriging with a combination of hard and soft data based on 105 (e) and 35 (f) RKN observations, PG field.....	68
Figure 2.9: Ordinary kriging maps of EC <sub>a-d</sub> for the CC field (a) and PG field (b) .....	69
Figure 3.1: Clustering performance based on the fuzziness performance index (FPI), normalized classification entropy (NCE), and pooled variances ( $S_p^2$ ) for the CC field. ....	116
Figure 3.2: Map of the CC field including the management zones (MZ) using (a) strategy one, (b) RKN population density – RKNS2, (c) MZ using strategy two, (d) MZ using strategy three, (e) elevation, (f) EC <sub>a-d</sub> , (g) slope, (h) NDVI.....	117
Figure 4.1: Scheme of the biomass sampling at the BJ field .....	160
Figure 4.2: Monthly total rainfall, and monthly total irrigation applied on the drought stress treatments in 2006 at the BJ field (a) and 2007 at the Gibbs farm field (b), and the climatic average rainfall at each field, Tifton, USA.....	161

- Figure 4.3: Differences in the proportion of roots at different soil depths between fumigation treatments measured between 0-90 cm soil depth for the Gibbs farm field. Root biomass was extracted from soil cores collected next to cotton plants (a) and between plants on a row (b). Error bars represent one standard deviation of measured data..162
- Figure 4.4: Plant height (a) and LAI (b) differences between drought stress treatments [low (1), medium (2), severe (3)] and fumigation treatments [nonfumigated (-), and fumigated (+)]. Average of six replications from the Gibbs farm field .....163
- Figure 4.5: Total biomass (a) and stem plus petiole (b), boll biomass (c), and number of closed bolls  $m^{-2}$  differences between drought stress treatments [low (1), medium (2), severe (3)] and fumigation treatments [nonfumigated (-), and fumigated (+)]. Average of six replications from the Gibbs farm field .....164
- Figure 5.1: RKN management zones for a producer field (Zone 1 = Low risk, Zone 2 = Moderate risk, Zone 3 = High risk for RKN damage).....213
- Figure 5.2: Average monthly solar radiation, average monthly total rainfall, and monthly total irrigation applied on the low drought stress treatment [1] in 2007 (a) and 2001 (b), and the climatic average rainfall (1912-2003) at the Gibbs farm, Tifton, USA.....214
- Figure 5.3: Differences in RKN-J2 population density (dots) and daily assimilate removal (lines) by calculated by the CMS-CROPGRO-Cotton model for the treatment combinations of drought stress [low (1), medium (2), and high (3)] with fumigation levels [ (a) fumigated (+), and (b) nonfumigated (-)].....215
- Figure 5.4: Simulated and observed total biomass for the 2007 experiment corresponding to treatment combinations: low (1), medium (2), and severe (3) drought stress with the

fumigated (+) and nonfumigated (-). Error bars represent one standard deviation, and points represent the mean of measured data.....	216
Figure 5.5: Simulated and observed boll dry weight and seed weight for the 2007 experiment corresponding to treatment combinations: low (1), medium (2), and severe (3) drought stress with the fumigated (+) and nonfumigated (-). Error bars represent one standard deviation, and points represent the mean of measured data .....	217
Figure 5.6: Simulated and observed leaf area index for the 2007 experiment corresponding to treatment combinations: low (1), medium (2), and severe (3) drought stress with the fumigated (+) and nonfumigated (-). Error bars represent one standard deviation, and points represent the mean of measured data.....	218
Figure 5.7: Simulated and observed volumetric soil water content at the 0- to 60- cm soil depth during the 2007 experiment for the treatment combinations: low (1) drought stress with the fumigated (+) and nonfumigated (-) levels.....	219
Figure 5.8: Simulated and observed volumetric soil water content at the 0- to 60- cm soil depth during the 2007 experiment for the treatment combinations: medium (2) drought stress with the fumigated (+) and nonfumigated (-) levels.....	220
Figure 5.9: Simulated and observed volumetric soil water content at the 0- to 60- cm soil depth during the 2007 experiment for the treatment combination severe drought stress (3) with fumigated (+) and nonfumigated (-) levels .....	221
Figure 5.10: Simulated and observed seed weight for the 2001 experiment corresponding to treatment combinations: low (1), medium (2), and severe (3) drought stress with the fumigated (+) and nonfumigated (-). Error bars represent one standard deviation, and points represent the mean of measured data.....	222

Figure 5.11: Differences in RKN-J2 population density (dots) and daily assimilate removal (lines) calculated by the CROPGRO-Cotton model for the three management zones [low risk (Zone 1), moderate risk (Zone 2), and high risk for RKN damage (Zone 3)] at the producer field.....	223
Figure 5.12: Simulated seed plus lint weight in 2006 for the three management zones [low risk (Zone 1), moderate risk (Zone 2), and high risk for RKN damage (Zone 3)] at the producer field .....	224

## CHAPTER 1

### INTRODUCTION AND LITERATURE REVIEW

Cotton (*Gossypium hirsutum L.*), a tropical perennial plant, is grown as an annual crop for fiber and seed production. In the last five years, one quarter of the total world lint has been produced in the United States (U. S.), on approximately five million hectares (Starr et al., 2007). Cotton production in the southern Coastal Plain of Georgia, U. S.A., has grown from 50,000 harvested hectares in 1983 to 580,000 harvested hectares in 2006. Although cotton production area has increased since the late nineteenth century, nematodes have impacted cotton yield. The most important yield losses attributed to nematode pressure across the U. S. cotton belt occurred through the period 1987-2000, increasing from 1.0% to 4.39% (NCC, 2008).

Southern root-knot nematode [*Meloidogyne incognita* (Kofoid & White) Chitwood] (RKN) is considered the most harmful plant-parasitic nematode for cotton production in the U. S. A. In Georgia, the third largest upland cotton producer in the U. S. A. (USDA, 2008), estimated losses attributed to nematodes in 2007 totaled \$50.2 million dollars with RKN contributing to 75% of those losses compared with 19% from reniform (*Rotylenchulus reniformis*) and 6% from Columbia lance (*Hoplolaimus columbus*) nematodes (UGA, 2007a). A survey carried out between 2002 and 2003 showed that major cotton-producing counties in Georgia had RKN population densities above the threshold (100 second juveniles of RKN per 100 cm<sup>3</sup> of soil), indicating that cotton producers lost about 77,000 bales of cotton annually from RKN damage (Blasingame and Patel, 2001; Kemerait et al., 2004).

The management of RKN in the southern U. S. has been characterized mainly by crop rotation in which the host plant, cotton, is replaced by a non-host or poor-host plant. Moderately resistant or tolerant cotton cultivars have been grown to suppress nematode reproduction, resulting in reduced nematode population densities. The use of chemical nematicides, which are usually applied at uniform rates to control population density, has continued to be the primary means of managing nematodes. However, the success of these and other strategies in relation to better management of on-farm resources and optimization of profitability is associated with the identification of areas at risk for RKN damage and forecast of the potential yield losses for a particular production area.

The goal of this study was to analyze the spatial variability of RKN in relation to edaphic and terrain field properties and their impact on cotton yield productivity. If we find that RKN population densities follow an aggregated pattern, is temporarily stable, and can be related with particular field properties, then site specific management (SSM) could be the most promising option. Therefore, the research conducted at experimental plots and production fields was focused on identifying field properties related to the spatial variability of RKN population. This data will then be used as surrogate data for management zone delineation. Additionally, a study of the potential impact of the interaction of RKN population-drought stress on cotton growth and development will be included, as well as the adaptation and evaluation of a cropping system model to simulate the growth of different cotton biomass components and yield under RKN infection. The methods used to accomplish these goals as well as the results are presented in four different chapters.

The different aspects of the RKN-plant-environment system will be addressed for conditions of the Tifton-Vidalia Upland (TVU) ecoregion of the southeastern Coastal Plain.

Southern root-knot nematode population density data and different edaphic and terrain properties collected from 11 cotton fields located in the TVU are the basic information for these studies. Cotton biomass data collected from a producer field in 2006 and an experimental field in 2007 are also part of this study.

The results from this research will contribute to the identification of better management strategies for RKN by proposing a methodology for delineation of management zones which might have different damage threshold levels for RKN population densities. Additionally, the study and simulation of cotton growth and development under different levels of RKN population and drought stress will contribute to an understanding of the effect of these stressor factors when ecological and environmental conditions might change. Also, the identification and evaluation of strategies for modeling RKN damage on cotton plants will bring new options of accounting for RKN damage when running simulations for SSM.

In *chapter two*, the spatial variability of root-knot nematodes in relation to soil properties is studied and areas exceeding a threshold value for RKN population are identified through geostatistical methods. Southern root-knot nematodes usually aggregate in irregular patches with preference for coarse-textured, sandy soils (Noe and Barker, 1985; Starr et al., 1993; Koenning et al., 2004; Monfort et al., 2007). In addition, soil properties such as fertility (Noe and Barker, 1985), pH (Melakeberhan et al., 2004) and moisture (Wheeler et al., 1991) have also been related with RKN presence or absence. The distribution and abundance of nematodes are commonly estimated by collecting soil samples from producer fields; however high sampling cost restricts the number of samples typically collected. Thus, a poor characterization of the within-field spatial distribution of nematodes can result in missed population patches, thus making the implementation of a site-specific management difficult.

Geostatistical analyses have been used in plant pathology to determine the best strategies for sampling and detection of nematode infestations (Webster and Boag, 1992; Avendaño et al., 2003; Wyse-Pester et al. 2002); and to describe the spatial relationships between nematode populations and soil properties (Noe and Barker, 1985). Geostatistics have been defined as a means to describe spatial patterns through the calculation of semivariograms, predict attribute values at unsampled locations by kriging interpolation (Vieira et al., 1983), and also to assess uncertainty and simulate the spatial distribution of attribute values, and the modeling of space–time processes (Goovaerts, 1999). The application of geostatistics requires that observations close to each other tend to be more similar than those further apart (Goovaerts, 1999).

In this chapter, it is hypothesized that by studying the spatial distribution of selected soil properties it is possible to explain the patchy behavior of RKN and delineate areas at risk for high RKN populations. The research questions in this chapter are: (i) is the spatial variability of RKN population aggregated and are the patches of high population density spatially stable throughout time?, (ii) do within-field soil properties follow different spatial scales of variation and are these related with the variability of RKN population density?, (iii) what are the soil properties related to the short and large scale of RKN variation?, (iv) is it possible to use RKN population data to delineate within-field areas above the threshold value used in Georgia to trigger the application of nematicide?, and (v) is it possible to use few RKN samples along with apparent soil electrical conductivity ( $EC_a$ ) data to delineate areas at risk for RKN above the threshold value of 100 second juveniles per 100  $cm^3$  of soil?.

Two geostatistical methods will be evaluated to study the within-field spatial distribution of RKN population densities and soil physico-chemical properties (*method “a”*) as well as to

delineate areas at risk for RKN through a combination of RKN samples and surrogate data for RKN (*method “b”*).

*a. Factorial kriging.*

Factorial kriging (FK) aims to understand the origins of a specific value within a geographic space rather than estimate its value. Through FK it is possible to detect multiple scales of variation and decompose that variation into the corresponding spatial components (Goovaerts, 1997; Goovaerts, 1998). Factorial kriging has been used in soil science to separate sources of variation according to their spatial scales enhancing the relation between variables (Goovaerts, 1994; Castrignanò et al., 2007). In this chapter, factorial kriging is used to establish scale-dependent correlations between the different spatial components of RKN population and soil properties. Therefore, it is possible to identify sources of RKN variation and understand spatial patterns of RKN population densities. Soil properties strongly correlated with RKN spatial variability can be used as surrogate data to indirectly identify areas at risk of encountering RKN population densities above a critical threshold.

*b. Indicator kriging.*

When the main research goal is the identification of areas exceeding a particular value, for example a regulatory threshold, indicator kriging (IK) can be used to estimate the probability that an attribute at a particular location does not exceed a fixed threshold (Goovaerts, 1998). According to Goovaerts (1997), the use of secondary information (surrogate data) can improve prediction of probabilities by indicator kriging.

Previous studies have included IK as a method to estimate and map the risk of exceeding threshold values in watershed management (Lyon et al., 2006), soil pollution (Goovaerts et al., 1997; Lin et al., 2002) groundwater contamination (Goovaerts et al., 2005) as well as studying

the grouping behavior within patches of cereal cyst nematode (*Heterodera avenae*) and potato cyst nematode (*Globodera rostochiensis*) (Webster and Boag, 1992). Indicator kriging will be used in this dissertation for mapping the probability that the RKN population density will exceed an advisory threshold of 100 RKN second stage juveniles per 100 cm<sup>3</sup> of soil (UGA, 2007b). This threshold is typically used by cotton producers in Georgia to trigger nematicide applications.

The results reported in this chapter contribute to the understanding of the within-field spatial variability of RKN and soil properties and to the identification of areas that may be at risk for high RKN population densities. Also, it has a methodological contribution to plant-soil borne pathogen studies by integrating data from physical and chemical soil properties and using tools from geographic information science (GIScience), geostatistics, statistics, and mapping.

In *chapter three*, a framework of procedures for delineating potential RKN management zones based on the fuzzy clustering of surrogate data is presented. For precision agriculture, the delineation of management zones is an effective approach that facilitates crop management and reduces potential harmful environmental impacts (Franzen et al., 2002). A management zone (MZ) is described as a sub-region of a field that expresses a relatively homogenous combination of yield limiting and reducing factors for which a single rate of a specific input is appropriate according to its yield potential (Doerge, 1999). Multiple management zones may indicate different needs within a field resulting in specific management strategies for each zone. Management zones have been used mainly to study variability in crop yield and variable application of inputs (Aaron et al., 2004; Basnet et al., 2003; Boydell and McBratney, 2002; Fridgen et al., 2000). In the case of RKN, management zones may indicate different levels of RKN occurrence and damage which imply a need for variable rate application of inputs,

especially nematicides. The approaches followed for delineation of RKN management zones have focused mainly on the use of soil texture data. Monfort et al. (2007), using initial population of RKN and percent sand fraction, explained 65 - 86% of cotton yield variability measured in plots of similar geographic locations. Overstreet et al. (2007) delineated soil textural zones based on apparent soil electrical conductivity data in six production fields. When applying fumigant through the various zones, they found differences between zones with respect to yield response to the nematicide application.

This chapter evaluates the hypothesis that measurable field features are related with the presence or absence of RKN population density and can serve as surrogate data for RKN; and therefore can be used to develop a preliminary framework of procedures for delineating potential RKN management zones. The data used in this particular manuscript were collected in 2005 and 2006 from 11 cotton fields, exemplifying a series of conditions in the TVCU for reproduction of RKN population density.

The research questions for this chapter are: (i) what are the edaphic and terrain properties associated with the RKN population?, (ii) is it possible to use canonical correlation analyses to calculate single predictor variables for RKN based on the correlation between edaphic-terrain data and RKN population data?, (iii) is it possible to use fuzzy-*c* clustering of RKN predictor variables to identify different clusters or management zones?, (iv) what are the ranges of variation of edaphic and terrain properties characterizing zones with low and high risk for RKN population?, and (v) what is the minimum set of data that can be used to discriminate zones with different risk levels for RKN population?.

When delineating management zones, different statistical approaches have been adopted. Principal component analysis (PCA), partial least square regression (PLS), and canonical

discriminant analysis have been used to screen out variables from a data set and identify association between groups of variables (Noe and Baker, 1985; Fraisse et al., 2001; Aaron et al., 2004; Ping et al., 2005). In this chapter canonical correlation analysis (CCA) will be applied because of the advantage in assessing the correlation between the linear combination of a set of Y variables and a linear combination of a set of X variables (Johnson and Wichern, 2002). Additionally, CCA will allow one to generate canonical predictor variables based on the canonical correlation of the X and Y variables. Canonical correlation analyses have been used to study the relationship between: soil properties and nematode population densities (Noe and Barker, 1985), soil properties and weed populations (Dieleman et al., 2000), field characteristics and soybean plant performance expressed as yield and canopy development (Martin et al., 2005).

In addition to the identification of variables strongly related with the phenomenon under study, it is necessary to select an optimum number of clusters or zones in which the variables should be grouped. Fuzzy *c*-means classification has been used to classify continuous data such as soils (Fridgen et al., 2004; McBratney and DeGrujter, 1992; Tarr et al., 2003), yield (Boydell and McBratney, 2002; Doberman et al., 2003; Fridgen et al., 2000; Jaynes et al., 2003; Li et al., 2007), and remotely sensed images (Boydell and McBratney, 2002; Sullivan et al., 2005). Therefore, fuzzy *c*-means will be used in this study to identify the optimum number of RKN management zones for a particular producer field.

The results reported in this chapter can be used to delineate management zones for site specific application of inputs, especially nematicides, and also for a guided sampling where the highest priority for sampling are the zones with the highest risk for RKN.

*Chapter four*, will include a study of the effects of RKN parasitism on cotton biomass and yield. Studies related with RKN parasitism have had different goals: study the changes in

root morphology of resistant and susceptible cotton cultivars (Shepherd and Huck, 1989), study the differences between susceptible and moderately resistant cotton cultivars in relation to RKN penetration and reproduction (Creech et al., 1995) as well as post penetration and development (Jenkins et al., 1995), study the effects of RKN on plant-water relations of cotton grown in microplots (Kirkpatrick et al., 1991; Kirkpatrick et al., 1995), evaluate cotton breeding lines for resistance and tolerance to RKN based on differences in yield (Davis and May, 2003), evaluate the relationship between root galling and cotton growth characteristics in terms of RKN reproduction and damage (Zhang et al., 2006). However, the changes on different biomass components and yield as a consequence of combined effects of RKN parasitism and drought stress at the level of small plots and producer field have not been previously investigated.

Patches of cotton plants infected by RKN exhibit symptoms that include chlorosis, stunting, and inhibition of leaf expansion (Kirkpatrick et al., 1995), as well as increase of root/shoot ratio (Wilcox-Lee and Loria, 1987). These symptoms could be attributed to the sink of assimilate ( $\text{CH}_2\text{O}$ ) by adult female nematodes feeding on the roots which generates a change in partitioning that impacts the growth of above-ground biomass (McClure, 1977; Williamson and Gleason, 2003). Other causes are related to a reduction in the flow of water and nutrients through intact roots due to the presence of galls (Kirkpatrick et al., 1991), low stomatal conductance and a reduction in the transpiration rate, a reduction in photosynthesis, and an increase in leaf temperature (Kirkpatrick et al., 1995; Wallace, 1987; Wilcox-Lee and Loria, 1987).

This chapter evaluates the hypothesis that RKN infection impacts different components of cotton biomass and also the reduction in biomass and yield increases with elevated levels of drought. The research questions in this chapter are: (i) is cotton biomass reduced under different levels of RKN population densities?, (ii) what are the biomass components highly reduced by

elevated RKN population densities?, (iii) what could be the physiological reasons for the reduced yield?, and (iv) do cotton biomass and yield losses by RKN population increase under severe drought conditions?.

The results from this chapter contribute to understand the effects of RKN population and drought stress on the different components of cotton biomass and yield, and develop better management strategies which might decrease the risk for yield losses. The definition and quantification of the type of RKN damage in cotton plants will be the first step for coupling the effects of RKN to cotton plant growth simulators. The identification in this study of particular biomass components highly susceptible to nematode infection can be also used as a guide during processes of cotton breeding.

*Chapter five*, is focused on simulations of growth and development of cotton plants infected by RKN and under the combined effects of high RKN population and drought stress. In agriculture, the Cropping System Model (CSM) has been used broadly to simulate a crop response to different biotic and abiotic factors (Hoogenboom et al., 2004; Jones et al., 2003). One of the advantages of these type of models is its use to simulate pest damage on a crop. Damage by pests or diseases and their effects can be simulated with crop models by coupling population density or specific damage type, expressed in percentage or rate basis, to state variables (leaf, stem, seed, shell, or root mass), LAI, as well as photosynthetic rate or rate of tissue senescence (Batchelor et al., 1992). Boote et al. (1983) simulated the reduction of water uptake from damaged roots by SCN through an increment of carbon allocation to roots using CROPGRO-Soybean. Batchelor et al. (1992) simulated the effect of soybean defoliation caused by velvet bean caterpillar (*Anticarsia gemmatalis*) using the SOYGRO model. They coupled weekly data of the cumulative defoliation levels to leaf area through the cumulative leaf damage

variable (LAID). Pinnschmidt et al. (1995) coupled the damage effects of defoliators, weed competition, leaf blast, and sheath blight disease to the CERES-Rice model. Simulations using different pest scenarios of onset times and pest intensity indicated nonlinear increases in yield losses when the pest intensities were increased and onset times decreased. The CROPGRO-Soybean model was used to quantify the effects of soybean cyst nematodes (SCN) on soybean yield (Fallick et al., 2002; Irmak et al., 2002; Paz et al., 2001). Fallick et al. (2002) developed and evaluated a monomolecular function for coupling damage of various levels of SCN population to daily photosynthesis and root water uptake of soybean. Nabb et al. (2004) simulated yield losses in peanut caused by leaf defoliation associated with the late leafspot disease (*Cercosporidium personatum*). To simulate the impact of late leafspot on leaf weight, total biomass and pod weight, they provided a scouting report to the CROPGRO-Peanut model, in which the observed leaf damage was presented.

The Cropping System Model (CSM)-CROPGRO-Cotton will offer the opportunity to simulate different scenarios of RKN damage, thus guiding the definition of the most effective RKN management strategies for different production areas.

This chapter evaluates two hypotheses to simulate RKN damage: (i) RKN acting as a sink of soluble assimilate, and (ii) RKN inducing a reduction of root length per root mass and root density. These two hypotheses were tested as part of the steps followed to adapt the Cropping System Model (CSM)-CROPGRO-Cotton to stimulate growth and yield of cotton plants infected with RKN. The research questions in this chapter are: is it possible to use coupling points to reduce the daily assimilate [ $\text{g}(\text{CH}_2\text{O}) \text{m}^{-2}\text{d}^{-1}$ ] available for growth and respiration? Is it possible to reduce the root length per root weight inside the CSM-CROPGRO-Cotton model to simulate leaf area index reductions due to RKN infection? Is it possible to calibrate the CSM-CROPGRO-

Cotton model for simulation of cotton biomass and yield of cotton plants under RKN infection?  
Is it possible to simulate biomass and yield of cotton plants experiencing RKN infection as well as drought stress? and Is it possible to simulate cotton yield for a producer field having three management zones with different levels of RKN population density?. The results reported in this chapter can be used to evaluate the performance of the model for simulating RKN damage on cotton grown under different environmental conditions.

## References

- Aaron, R.S., J.F. Shanahan, M.A. Liebig, J.S. Schepers, S.H. Johnson, and A.J. Luchiari. 2004. Appropriateness of management zones for characterizing spatial variability of soil properties and irrigated corn yields across years. *Agron. J.* 96: 195-203.
- Avendaño, F., O. Schabenberger, F.J. Pierce, and H. Melakeberhan. 2003. Geostatistical analysis of field spatial distribution patterns of soybean cyst nematode. *Agron. J.* 95: 936-948.
- Basnet, B., R. Kelly, T. Jensen, W. Strong, A. Apan, and D. Butler. 2003. Delineation of management zones using multiple crop yield data. In *Proc. International Soil Tillage Research Organization Conference, 16th Triennial Conference*, 69-75. Brisbane, AU.: The University of Queensland.
- Batchelor, W. D., J. W. Jones, and K. J. Boote. 1992. Assessing pest and disease damage with DSSAT. *Agrotech. Trans.* 16: 1-8.
- Blasingame, D. and Patel, and M. V. 2001. Cotton disease loss estimate committee report. In *Proc. 2001 Beltwide Cotton Conference*. Anaheim, CA.: National Cotton Council.
- Boote, K. J., J. W. Jones, J. W. Mishoe, and R. D. Berger. 1983. Coupling pest to growth simulators to predict yield reductions. *Phytopathology* 73: 1581-1587.
- Boydell, B., and B. McBratney. 2002. Identifying potential within-field management zones from cotton-yield estimates. *Prec. Agric.* 3: 9-23.
- Castrignanò, A., G. Buttafuoco, R. Puddu, and C. Fiorentino. 2007. A multivariate geostatistical approach to delineate areas at soil salinization risk. In *Proc. Sixth European Conference of Precision Agriculture (6ECPA)*, 199-205. Stafford, J., and A. Werner, eds. Skiathos. Greece.
- Creech, R.G., J.N. Jenkins, B. Tang, G.W. Lawrance, and J.C. McCarthy. 1995. Cotton Resistance to root-knot nematode: I. Penetration and reproduction. *Crop Sci.* 35: 365-368.
- Davis, R.F., and O.L. May. 2005. Relationship between yield potential and percentage yield suppression caused by the southern root-knot nematode in cotton. *Crop Sci.* 45: 2312-2317.
- Dieleman J. A., D. A. Mortensen, D. D. Buhler, C. A. Cambardella, and T. B. Moorman. 2000. Identifying associations among site properties and weed species abundance: I Multivariate analysis. *Weed Sci.* 48: 567-575.
- Doberman, A., J.L. Ping, V.I. Adamchuk, G.C. Simbahan, and R.B. Ferguson. 2003. Classification of crop yield variability in irrigated production fields. *Agron. J.* 95: 1105-1120.

- Doerge, T.A. 1999. Management zone concepts. In *Site-Specific Management Guidelines*. P. P. Institute. Series Norcross.
- Fallick, J. B., W. D. Batchelor, G. L. Tylka, T. L. Niblack, and J. O. Paz. 2002. Coupling soybean cyst nematode damage to CROPGRO Soybean. *Trans. ASAE* 45: 433-441.
- Fraisse, C. W., K. A. Sudduth, and N. R. Kitchen. 2001. Delineation of site-specific management zones by unsupervised classification of topographic attributes and soil electrical conductivity. *Trans. ASAE* 44(1): 155-166.
- Franzen, D.W., D.H. Hopkins, M.D. Sweeney, M.K. Ulmer, and A.D. Halvorson. 2002. Evaluation of soil survey scale for zone development of site-specific nitrogen management. *Agron. J.* 94: 381-389.
- Fridgen, J.J., C.W. Fraisse, N.R. Kitchen, K.A. Sudduth. 2000. Delineation and analysis of site-specific management zones. In *Proc. 2<sup>nd</sup> International Conference on Geospatial Information in Agriculture and Forestry*, CD-ROM. Lake Buena Vista, FL.
- Fridgen, J.J., N.R. Kitchen, K.A. Sudduth, S.T. Drummond, W.J. Wiebold, and C.W. Fraisse. 2004. Management zone analyst (MZA): software for subfield management zone delineation. *Agron. J.* 96: 100-108.
- Goovaerts, P. 1994. Study of spatial relations between two set of variables using multivariate geostatistics. *Geoderma* 62: 93-107
- Goovaerts, P. 1997. *Geostatistics for Natural Resources*. Oxford University Press, New York.
- Goovaerts, P. 1998. Geostatistical tools for characterizing the spatial variability of microbiological and physico-chemical soil properties. *Biol. Fert. Soils* 27: 315-334.
- Goovaerts, P. 1999. Geostatistics in soil science: state-of-the-art and perspectives. *Geoderma* 89:1-45.
- Goovaerts, P., G. AvRusking, J. Meliker, M. Slotnick, G. Jacquez, J. Nriagu. 2005. Geostatistical modeling of the spatial variability of arsenic in ground water of southeast Michigan. *Water Resour. Res.* 41: 1-19.
- Hoogenboom, G., J. W. Jones, P. W. Wilkens, C. H. Porter, W. D. Batchelor, L. A. Hunt, K. J. Boote, U. Singh, O. Uryasev, W. T. Bowen, A. J. Gijsman, A. S. Du Toit, J. W. White, G. Y. Tsuji. 2004. *Decision Support System for Agrotechnology Transfer*. Ver. 4.0. Honolulu, HI.:University of Hawaii.
- Irmak, A., J. W. Jones, W. D. Batchelor, and J. O. Paz. 2002. Linking multiple layers of information for diagnosing causes of spatial yield variability in soybean. *Trans. ASAE* 45: 839-849.

- Jaynes, D.B., T.C. Kaspar, T.S. Colvin, and D.E. James. 2003. Cluster analysis of spatiotemporal corn yield patterns in an Iowa field. *Agron. J.* 95: 574-586.
- Jenkins, J.N., R.G. Creech, B. Tang, G.W. Lawrance, and J.C. McCarthy. 1995. Cotton resistance to root-knot nematode: II. Post-penetration development. *Crop Sci.* 35: 369-373.
- Johnson, R. A., and D. W. Wichern. 2002. Applied multivariate analysis. 5th ed. Upper Saddle River, NJ.: Prentice Hall.
- Jones, J. W., G. Hoogenboom, C. H. Porter, K. J. Boote, W. D. Batchelor, L. A. Hunt, P. W. Wilkens, U. Singh, A. J. Gijsman, and J. T. Ritchie. 2003. DSSAT cropping system model. *Eur. J. Agron.* 18: 235-265.
- Kemerait, R. C., R. F. Davis, P. H. Jost, C. L. Brewer, S. N. Brown, B. Mitchell, W. E. Harrison, R. Joyce, and E. McGriff. 2004. Assessment of nematicides for management of the southern root-knot nematode, *Meloidogyne incognita*, in Georgia. Tifton, GA. In 2004 Georgia cotton research and extension reports.: The University of Georgia. Available at: <http://commodities.caes.uga.edu/fieldcrops/cotton/rerpubs/2004/p202.pdf>. Accessed 10 October 2008
- Kirkpatrick, T.L., D.M. Oosterhuis, and S.D. Wullschleger. 1991. Interaction of *Meloidogyne incognita* and water stress in two cultivars. *J. Nematol.* 23: 462-467.
- Kirkpatrick, T.L., M.W. van Iersel, and D.M. Oosterhuis. 1995. Influence of *Meloidogyne incognita* on the water relations of cotton growth in microplots. *J. Nematol.* 27: 465-471.
- Koenning, S.R., T.L. Kirkpatrick, J.L. Starr, J.A. Wrather, N.R. Walker, and J.D. Mueller. 2004. Plant-parasitic nematodes attacking cotton in the United States: Old and emerging production challenges. *Plant Dis.* 88: 100-113.
- Li, Y., Z. Shi, F. Li, and H.Y. Li. 2007. Delineation of site-specific management zones using fuzzy clustering analysis in a coastal saline land. *Comput. Electron. Agric.* 56: 174-186.
- Lin, Y., T. Chang, C. Shih, and C. Tseng. 2002. Factorial and indicator kriging methods using a geographic information system to delineate spatial variation and pollution sources of soil heavy metals. *Environ. Geol.* 42: 900-909.
- Lyon, S. W., A. J. Lembo Jr, M. T. Walter, T. S. Steenhuis. 2006. Defining probability of saturation with indicator kriging on hard and soft data. *Adv. Water Resour.* 29: 181-193.
- Martin, N. F., G. Borrero, and D. G. Bullock. 2005. Association between field characteristics and soybean plant performance using canonical correlation analysis. *Plant and Soil* 237: 39-55.
- McBratney, A.B., and J.J. DeGrujter. 1992. A continuum approach to soil classification by modified fuzzy means with extragrades. *J. Soil Sci.* 43: 159-175.

- McClure, M.A. 1977. Meloidogyne incognita: A metabolic sink. *J. Nematol.* 9: 88-90.
- Melakeberhan, H., J. Dey, V.C. Baligar, and T.E. Carter Jr. 2004. Effect of soil pH on the pathogenesis of *Heterodera glycines* and *Meloidogyne incognita* on Glycine max genotypes. *Nematology* 6: 585-592.
- Monfort, W.S., T.L. Kirkpatrick, C.S. Rothrock, and A. Mauromoustakos. 2007. Potential for site-specific management of meloidogyne incognita in cotton using soil textural zones. *J. Nematol.* 39: 1-8.
- Naab, J. B., P. Singh, K. J. Boote, J. W. Jones, and K. O. Marfo. 2004. Using the CROPGRO-peanut model to quantify yield gaps of peanut in the guinean savanna zone of Ghana. *Agron. J.* 96: 1231-1242.
- NCC. 2008. Beltwide yield losses to nematode damage. Cordova, TN.: National Cotton Council of America. Available at: [www.cotton.org/tech/pest/nematode/losses.cfm](http://www.cotton.org/tech/pest/nematode/losses.cfm). Accessed August 17, 2008.
- Noe, J. P., and K. R. Barker. 1985. Relation of within-field spatial variation of plant-parasitic nematode population densities and edaphic factors. *Phytopatology* 75: 247-252.
- Overstreet, C., M. Wolcott, G. B. Padgett, E. Burris. 2007. Defining management zones in cotton. In Proc. 46th Annual meeting Society of nematologists. *J. Nematol.* 39(1): 84-85. San Diego, CA.: Society of nematologists.
- Paz, J. O., W. D. Batchelor, G. L. Tylka, and R. G. Hartzler. 2001. A modeling approach to quantify the effects of spatial soybean yield limiting factors. *Trans. ASAE* 44: 1329-1334.
- Ping, J.L., C.J. Green, K.F. Bronson, R.E. Zartman, and A. Doberman. 2005. Delineating potential management zones for cotton based on yields and soil properties. *Soil Sci.* 170: 371-385.
- Pinnschmidt, H. O., W. D. Batchelor, and P. S. Teng. 1995. Simulation of multiple species pest damage in rice using CERES-Rice. *Agric. Syst.* 48: 193-222.
- Shepherd, R.L., and M.G. Huck. 1989. Progression of root-knot nematode symptoms and infection on resistant and susceptible cotton. *J. Nematol.* 21: 235-241.
- Starr, J.L., C.M. Heald, A.F. Robinson, R.G. Smith, and J.P. Krausz. 1993. *Meloidogyne incognita* and *Rotylenchulus reniformis* and associated soil textures from some cotton production areas of Texas. *J. Nematol.* 25: 895-899. Suppl.
- Starr, J.L., S.R. Koenning, T.L. Kirkpatrick, A.F. Robinson, P.A. Roberts, and R.L. Nichols. 2007. The future of nematode management. *J. Nematol.* 39: 283-294.

- Sullivan, D.G., J.N. Shaw, and D. Rickman. 2005. IKONOS imagery to estimate surface property variability in two Alabama physiographies. *Soil Sci. Soc. Am. J.* 69: 1789-1798.
- Tarr, A.B., K.J. Moore, P.M. Dixon, C.L. Burras, and M.H. Wiedenhoef. 2003. Use of soil electroconductivity in a multistage soil-sampling scheme. *Crop Mgmt.* 10:1094/CM-2003-1029.
- UGA. 2007a. 2007 Georgia plant disease loss estimate. Cooperative Extension Service.: The University of Georgia. Available at : <http://pubs.caes.uga.edu/caespubs/pubcd/SB41-10/SB41-10.htm>. Accessed 02 September 2008.
- UGA. 2007b. 2007 Georgia cotton production guide. Cooperative Extension Service.: The University of Georgia. Available at: <http://commodities.caes.uga.edu/fieldcrops/cotton/2007cottonguide/appendixIII.pdf>. Accessed 06 October 2008.
- USDA. 2008. Crop production. National Agricultural Statistics Service. Washington, D.C.: USDA National Agricultural Statistics Service. Available at: [www.usda.gov/nass/PUBS/TODAYRPT/crop0808.txt](http://www.usda.gov/nass/PUBS/TODAYRPT/crop0808.txt). Accessed 17 August 2008.
- Vieira, G., J.L. Hatfield, D.R. Nielsen, and J.W. Biggar. 1983. Geostatistical theory and application to variability of some agronomical properties. *Hilgardia* 51:1-75.
- Wallace, H.R. 1987. Effects of nematode parasites on photosynthesis. In *Vistas on nematology*, 253-259. Hyattsville, MD. Society of Nematologists.
- Webster, R., and B. Boag. 1992. Geostatistical analysis of cyst nematodes in soil. *J. Soil Sci.* 43: 583-595.
- Wheeler, T.A., K.R. Barker, and S.M. Schneider. 1991. Yield-loss models for tobacco infected with *Meloidogyne incognita* as affected by soil-moisture. *J. Nematol.* 23: 365-371.
- Wilcox-Lee, D.A., and R. Loria. 1987. Effects of nematode parasitism on plant-water relations. In *Vistas on nematology*, 260-266. Hyattsville, MD. Society of Nematologists.
- Williamson, V.M., and C.A. Gleason. 2003. Plant-nematode interactions. *Curr. Opin. Plant Biol.* 6:4: 327-333
- Wyse-Pester, D.Y., L.J. Wiles, and P. Westra. 2002. The potential for mapping nematode distribution for site-specific management. *J. Nematol.* 34: 80-87.
- Zhang, J., C. Waddell, C. Sengupta-Gopalan, C. Potenza, and R.G. Cantrell. 2006. Relationships between root-knot nematode resistance and plant growth in upland cotton: galling index as a criterion. *Crop Sci.* 46: 1581-1586.

CHAPTER 2

GEOSTATISTICAL MODELING OF THE SPATIAL VARIABILITY OF SOUTHERN  
ROOT-KNOT NEMATODES IN RELATION TO SOIL PROPERTIES<sup>1</sup>

---

<sup>1</sup> Ortiz, B.V., C. Perry, G. Vellidis, D. Sullivan, P. Goovaerts. To be submitted to *Agronomy Journal*. October 2008.

## Abstract

Site-specific management (SSM) of cotton (*Gossypium hirsutum* L.) fields at risk for southern root-knot nematode [*Meloidogyne incognita* (Kofoid & White) Chitwood] (RKN) infection may offer producers better management of on-farm resources and optimization of profitability. The objectives of this study were to (i) evaluate the spatial dependency of RKN population density over time; (ii) establish the relationship between RKN occurrence and the spatial variability of soil properties; and (iii) delineate areas at risk for RKN based on indicator kriging (IK) of hard data (i. e., measured RKN population density), soft data (i.e., logistic regression between RKN and soil properties), and the combination of hard and soft data. The spatial relations between soil physico-chemical properties with RKN population density were studied in two cotton fields in southern Georgia, USA, in 2006. Soil samples for assessment of RKN population density were collected at the center of a 50 × 50 m grid three times during the growing season. Nested semivariograms indicated that RKN samples exhibited a local and regional scale of variation which described small and large clusters of RKN. Factorial kriging was used to decompose the variability of RKN and soil properties into different spatial components, allowing the computation of correlation coefficients for different spatial scales. Scale-dependent correlations between RKN data showed that the locations of clusters with high RKN population density remained stable though the growing season. Among soil physical properties, slope (SL) exhibited a strong correlation at local scale and apparent soil electrical conductivity deep ( $EC_{a-d}$ ) at both local and regional scales. The correlation with soil chemical properties was soil texture mediated. Apparent soil electrical conductivity deep ( $EC_{a-d}$ ) showed potential as surrogate data for RKN population density because of its strong and stable correlation at local and regional scales. Indicator kriging (IK) maps depicted the probability for RKN population density to exceed the threshold of 100 second stage juveniles/100 cm<sup>3</sup> of soil. The incorporation of  $EC_{a-d}$  as soft data supplemented the hard data resulting in improved predictions and a reduction of the number of RKN observations required to map areas at risk for high RKN population densities.

Keywords: Cotton, factorial kriging, indicator kriging, logistic regression, nematodes, risk map, semivariogram, soil properties, southern root-knot nematode, spatial variability.

## 2.1 Introduction

Southern root-knot nematode [*Meloidogine incognita* (Kofoid & White) Chitwood] (RKN) is considered the major yield-limiting pest across the United States cotton belt (NCC, 2006). Yield losses attributed to southern root-knot nematode (RKN) account for 72% of the total losses caused by different species of nematodes found in U.S. cotton fields.

The spatial distribution of RKN has been described as aggregated and manifested in irregular patches (Goodell and Ferris, 1980) with high occurrence in coarse-textured sandy soils (Koenning et al., 1996). Because cotton plants do not typically exhibit obvious above-ground symptoms of nematode damage, it is difficult to identify patches infested by RKN before serious damage to the crop has been caused. The patchy behavior of RKN is regulated by biotic and abiotic factors which control their reproduction, movement, and distribution within fields. Therefore, if the relationship between RKN and these controlling factors can be established, they can be used for assessing areas at risk for high RKN populations. Areas identified as high risk can be targeted for site-specific management (SSM).

Geostatistical analyses have been used to determine the best strategies for sampling, detection of nematode infestations, description of the spatial relationships between variables, and estimation of uncertainty in terms of risk among others. Semivariograms have been widely used to describe the spatial variability of nematodes. Through a nested sampling design, Webster and Boag (1992) showed that the spatial dependency of cereal cyst nematode (*Heterodera avenae*) and potato cyst nematode (*Globodera rostochiensis*) in the topsoil ranged from 5 to 50 meter. Indicator and cross- semivariograms showed the population increasing from patch edges towards their centers. Avendaño et al. (2003) found a poorly structured spatial variability of soybean cyst nematodes-SCN (*Heterodera Glycines*) in two Michigan fields (U.S.). From the same fields,

Avendaño et al. (2004) reported a positive correlation between SCN population density and percentage of sand. Wyse-Pester et al. (2002) explained the spatial dependence of three different nematode species within two corn fields through semivariograms. Nematode samples were correlated over distances of 115 to 649 m and varied with direction (anisotropy). When they tried to associate nematode population density with soil texture and organic matter content, correlations were inconsistent. Noe and Barker (1985) evaluated 26 different edaphic properties with respect to the spatial distribution of RKN and found that high levels of clay or organic matter, low copper concentrations, and small changes in percent soil moisture were strongly correlated with RKN spatial distributions. Monfort et al. (2007) explained 65 - 86% of cotton yield variability measured in plots from similar geographic locations using the initial concentrations of RKN and sand content. Other studies have correlated the abundance of RKN with soil pH (Melakeberhan et al., 2004) and soil moisture (Wheeler et al., 1991; Windham and Barker, 1993).

### *Factorial Kriging*

Even though some soil properties have been related to the spatial variability of nematodes, the use of factorial kriging to detect multiple scales of variation and to decompose the variation into the corresponding spatial components, has not been explored with nematode populations. Factorial kriging has been used in soil science to separate sources of variation according to their spatial scales which enhances the relationship between variables. A detailed explanation of factorial kriging is presented in the methods section.

Castrignanò et al. (2007) used factorial kriging to define one regionalized factor that summarized the effect of soil pH, electrical conductivity, exchange sodium percentage, and total clay plus fine silt content on soil salinization. Goovaerts (1994) separated the local and regional

variation of soil and vegetation properties using factorial kriging. He attributed local variation to field-to-field differences and regional variation to the presence of different soil types.

Using factorial kriging to identify sources of variation improves our understanding of the spatial patterns of RKN population densities. It also allows us to use these sources of variation as surrogate data in order to estimate the probability or risk of encountering RKN population densities above a critical threshold. Previous studies have included indicator kriging (IK) as a method to estimate and map the risk of exceeding threshold values in watershed management (Lyon et al., 2006), soil pollution (Goovaerts et al., 1997; Lin et al., 2002) as well as groundwater contamination (Goovaerts et al., 2005). Indicator kriging allows one to estimate the probability that an attribute value does not exceed a target threshold at an unsampled location by using a kriging estimator similar to the one developed for continuous variables (Goovaerts, 1998).

Encouraging results from previous research support the use of a geostatistical approach to verify the hypotheses that the spatial distribution of selected soil properties might be used to explain the patchy behavior of RKN and to delineate areas at risk for high RKN populations. To test these hypotheses, multivariate geostatistical techniques were used to: (i) evaluate the spatial dependency of RKN population density over time; (ii) establish the relationship between RKN occurrence and the spatial variability of soil properties; and (iii) delineate areas at risk for RKN based on indicator kriging (IK) of hard data (i. e., measured RKN population density), soft data (i.e., logistic regression between RKN and soil properties), and the combination of hard and soft data.

## 2.2 Materials and Methods

### 2.2.1 Study fields description and data collection

The study was conducted in two irrigated producer fields located near Tifton, Georgia, USA. The area is within the southeastern coastal plain physiographic region of the USA and is characterized by sandy soils, small differences in topographic relief, and a subtropical climate. In this paper, the two study fields will be identified as the 20 ha CC field and the 25 ha PG field. Both fields were planted to cotton (*Gossypium hirsutum* L.) during May 2006 with the Delta & Pine Land Company DP 555 BG/RR cotton cultivar.

A 50 x 50 m grid (0.25 ha cell size) was superimposed over the fields and sampling nodes were established at the center of each grid. A total of 99 grid cells were established at the CC field and 105 at the PG field. The nodes were georeferenced using an AgGPS 114 DGPS (Trimble<sup>®</sup>, Sunnyvale, CA) receiver. Soil samples for nutrients, RKN, and texture analyses were collected from random locations within a 1.5 m radius of the central node of each grid. The data generated from these samples are termed discrete data. Five 30 cm soil cores were collected and combined into a composite sample for phosphorus (P), potassium (K), calcium (Ca), magnesium (Mg), and soil pH determination. These samples were collected one month after planting. Soil samples for RKN population density determination (second stage juveniles) were collected three times during the growing season – 75, 110, and 167 days after planting (DAP) which coincided with early season (first flower), mid season, and harvest. These sampling events were designated as RKN1, RKN2, and RKN3, respectively. At each sampling event, eight individual subsamples were collected around the center of each grid and composited into a single sample representing RKN population density within each grid cell. The subsamples were collected with a 3 cm

diameter sampler which was inserted 15 - 20 cm deep into the soil adjacent to plant tap roots. Nematodes were extracted from 100 cm<sup>3</sup> of soil by centrifugal flotation (Jenkins, 1964).

Continuous data are defined as data collected at high densities by sensors pulled through the field such as apparent soil electrical conductivity and elevation or information derived from these data (such as slope derived from elevation). Both apparent soil electrical conductivity and elevation data were collected in each field once prior to planting in May 2006. Apparent soil electrical conductivity (EC<sub>a</sub>) has been widely used as an indirect method to identify changes in soil texture (Fridgen et al., 2000; Kitchen et al., 1999; Kitchen et al., 2003; Sudduth et al., 2005). In this study, the VERIS® 3100 implement was used to measure EC<sub>a</sub> between 0 - 30 cm (shallow, EC<sub>a-s</sub>) and 0 - 90 cm (deep, EC<sub>a-d</sub>) in 9 m parallel swaths throughout the fields. Each EC<sub>a-s</sub> and EC<sub>a-d</sub> reading was coupled with its GPS coordinates using a Trimble AgGPS 114. Data points were collected at 2 s intervals which corresponded to about 3 m of linear travel.

Elevation data (EL) were collected at the same time as EC<sub>a</sub> data with a Trimble AgGPS 214 real-time kinematic (RTK) GPS receiver mounted on the tractor pulling the VERIS® 3100 implement. Data were recorded at 4 s intervals which corresponded to about 12 m of linear travel.

### **2.2.2 Data processing**

Although the EL and EC<sub>a</sub> data sets comprised more than 7000 observations spatially distributed through each field, the parallel swaths used to collect the data were not collocated with the sampling nodes (grid cell centers). To overcome this, ordinary punctual kriging was used to estimate the values of EL and EC<sub>a</sub> at the sampling nodes (Kerry and Oliver, 2003) using TerraSeer STIS software (Avruskin et al., 2004).

Raster maps of terrain slope (SL) were derived from EL raster maps using the Spatial Analyst extension of ArcVIEW v. 9.0 (ESRI, 2004a). The slope at the sampling node was estimated by averaging the pixel values of slope contained within the 1.5 m radius sampling area surrounding each sampling node. This average slope was then associated with the corresponding RKN data.

### **2.2.3 Classical statistical analyses**

Descriptive statistics of RKN population density and soil physical and chemical properties at the CC field (n = 99) and the PG field (n = 105) were calculated to ascertain in-field variability as a first step. When RKN population density or the soil properties data exhibited skewness values above + 1 or below -1 failing the assumption of normality, a normal score transformation of the data was performed. The normal score transform replace each observation with the corresponding quantile in the standard normal distribution, allowing the normalization of any distribution regardless of its shape (Goovaerts et al., 2005).

### **2.2.4 Geostatistical analyses**

Experimental semivariograms were used to describe the spatial variability of RKN population density (each sampling event) as well as the measured soil properties. An experimental semivariogram, the core of geostatistics, measures the average dissimilarity between observations separated by a vector  $h$  (Goovaerts, 1997). Therefore, it describes the spatial variation in terms of magnitude, spatial scale and pattern (Rodges and Oliver, 2007). According to Matheron (1963), the semivariance  $[\gamma(h)]$  at a given separation distance (h) is computed as half the average squared difference  $[z(u_\alpha) - z(u_\alpha + h)]^2$  between the data pair of a

variable  $z$ :

$$\gamma(h) = \frac{1}{2N(h)} \sum_{\alpha=1}^{N(h)} [z(u_{\alpha}) - z(u_{\alpha} + h)]^2 \quad (1)$$

where  $N(h)$  denotes the number of data pairs separated by the distance  $h$ .

The experimental semivariogram is usually fitted by a mathematical model or function that best describes the variability of the data. Three important parameters can be determined from each semivariogram model: *range*, *sill* and *nugget*. The *range* of autocorrelation ( $a$ ) corresponds to the distance at which the semivariogram reaches a plateau or *sill* value, then observations separated by distances larger than the range are statistically independent; the *sill* or *total variance* ( $C_0+C$ ) corresponds to the semivariance value at which the semivariogram reaches a plateau. The *nugget* occurs when the fitted model does not pass through the origin of the semivariogram but instead intercepts the y-axis at a positive value of semivariance. The y-intercept ( $C_0$ ) is called the *nugget* which has also been described as a measure of the error and/or sources of variation that were not captured by the shortest sampling distance (Goovaerts, 1997).

The variability of RKN population density and soil properties could be nested as a result of the interaction of several biotic or abiotic processes that may operate at different spatial scales. This translates into an experimental semivariogram that is modeled as a linear combination of different structures  $g_l(h)$  with unique ranges of spatial dependence; semivariogram that is described nested semivariogram:

$$\gamma(h) = \sum_{l=0}^L b_l g_l(h) \quad \text{with } b \geq 0 \quad (2)$$

where  $b_l$  is the variance of the corresponding semivariogram model  $g_l(h)$ . The variance  $b_0$  is called nugget effect and  $g_1(h)$  and  $g_2(h)$  are models with short,  $a_1$ , and long ranges,  $a_2$  (Goovaerts, 1997). In this paper, the models were fitted using least-square regression. The linear

model of regionalization (equation 2) assumes that the random process  $Z(x)$  can be decomposed into orthogonal functions, called spatial components, and a local mean  $m(x)$ :

$$Z(x) = \sum_{l=0}^L Z_l(x) + m(x) \quad (3)$$

where  $Z_0(x)$  is a micro-scale component, and  $Z_1(x)$  and  $Z_2(x)$  are the short-range and long-range spatial components associated with the semivariogram model  $b_1g_1(h)$  and  $b_2g_2(h)$  respectively.

Factorial kriging also allows the estimation and mapping of each spatial component identified in the nested semivariogram by filtering out the  $L$  other components (Matheron, 1982; Goovaerts, 1998). The filtered spatial components can be also grouped into local variability (short range), regional variability (long range plus local mean or trend), and trend component or local mean. Factorial kriging was used here to model nested semivariograms for each variable under study and to estimate the different spatial components of variation. Moreover, each spatial component from the RKN population density and soil property data was used to calculate scale-dependent or structural correlations at different spatial scales.

Statistical and geostatistical analyses were performed using SAS (SAS Institute, 2007), TerraSeer STIS (Avruskin et al. 2004), ISATIS (Geovariances, 2007), and the Geostatistical Analyst extension of ArcVIEW v. 9.0 (ESRI, 2004b)

### **2.2.5 Delineating areas at risk for RKN population over threshold values using indicator kriging**

The identification of areas at risk for high populations of RKN is an important step in the establishment of SSM. Most useful to the producer is a map of the probability that the RKN population density will exceed an advisory threshold. With that information, resources to further

quantify and address the risk can be allocated to areas with high probability levels. Such probability mapping can be accomplished using indicator kriging (IK) that requires a prior transform of the data (i.e. RKN population density) into a new binary or indicator variable which represents observations above and below a threshold value. In this study, RKN samples exceeding a threshold of 100 RKN second stage juveniles / 100 cm<sup>3</sup> of soil were assigned a value of 1. RKN samples were assigned a value of 0 if they did not exceed the threshold. This threshold is typically used by cotton producers in Georgia to trigger nematicide applications.

The indicator semivariogram was computed by applying the traditional semivariogram formula to the indicator data. Indicator semivariograms were modeled with ISATIS (Geovariances, 2007) and the probability that the RKN population density exceeds 100 was created using TerraSeer STIS (Avruskin et al. 2004) and the Geostatistical Analyst extension of ArcVIEW v. 9.0.

Direct measurements of the indicator variable, in our case RKN second stage juveniles / 100 cm<sup>3</sup> of soil exceeding the threshold population density, are also referred to as “hard data”. In our case, collecting “hard data” is expensive and labor intensive. The IK map based on density data (hard data) may be improved with the integration of “soft data” or secondary data which are ubiquitous and more easily and cheaply collected and which may serve as surrogate data for the indicator variable.

In this study, we hypothesized that soil properties may serve as “soft” or surrogate data. We estimated the probability that RKN at a sampling location  $i$  exceeds a threshold value based

on one or multiple soil properties ( $X_1, X_2, \dots, X_i$ ) through the following binary logistic regression (Kleinschmidt et al., 2000; Lyon et al., 2006):

$$\text{RKN}_i = \log(1 / 1 - p_i) = c + \beta_1 X_1 + \beta_2 X_2 + \dots + \beta_i X_i \quad (4)$$

where  $p_i$  is the probability of having a RKN population density above the threshold;  $\beta_i$  corresponds to the parameter estimates; and  $X_i$  represents the soil properties or explanatory variables. Therefore, the calculation of the probability of a population of RKN above the threshold ( $p$ ) based on RKN surrogate data becomes:

$$p = e^{(\alpha + \beta * X)} / (1 + e^{(\alpha + \beta * X)}) \quad (5)$$

Logistic regression is a technique that has been used successfully as an intermediate step in the delineation of probability maps (Grunwald et al., 2006; Lyon et al., 2006; Kleinschmidt et al., 2000). In this study the explanatory variable(s) in equation 4 was the local mean of the soil property with the highest and most stable spatial correlation with RKN as determined from the structural correlation analysis. These local means were estimated at the RKN sampling locations by factorial kriging. The significance of the logistic regression model was evaluated using a likelihood ratio (-2LogL) with an approximated chi-square distribution. The prediction formula (equation 5) was applied to the ordinary kriging map of secondary data using the TerraSeer STIS software to produce a probabilistic or prior probability map based on soft data.

The hard data and soft data were combined following the method suggested by Goovaerts et al. (1997): 1) indicator residuals are computed by subtracting, at each RKN sampling location, prior probabilities (i.e. soft data) from the indicator variable, 2) the residual semivariogram was

calculated and the model was used to interpolate residuals through simple kriging, and 3) the final probability map was obtained by adding the soft data to the kriged residuals.

To simulate the impact of a smaller number of RKN data on the accuracy of indicator maps and to assess the benefit of using soft data, the procedure described above was repeated using a training data set composed of 65% and 37% of the initial RKN sampling observations which were selected at random. The remaining observations were used to validate the accuracy of the IK maps.

## **2.3 Results and Discussion**

### **2.3.1 Classical statistical analyses**

The RKN population data exhibited both spatial and temporal variability. The soil chemical properties of both fields exhibited less variation, expressed as coefficient of variation (CV), than the RKN population density and the soil physical properties (Table 2.1).

#### CC field

At the CC field, the high standard deviation (SD), coefficient of variation (CV), and broad range of RKN values are evidence of within field variability. The highest mean RKN population density was observed during RKN2 which contradicts the generally accepted rule that the highest population density occurs near harvest (Table 2.1). Even though the cotton was irrigated, this finding may be related to drought conditions experienced towards the end of the growing season (September and October of the 2006) and with limited availability of infection sites as a result of root decay (Stanton, 1986).

The CC field exhibited small changes in EL as indicated by the low SD and CV (Table 2.1). The CV of slope and  $EC_{a-d}$  were fairly high compared to soil chemical properties which

indicates that the RKN population density and soil physical properties were not evenly distributed across the field. The  $EC_{a-d}$  readings seemed to be sensitive to changes in soil particle size. A correlation analysis between sand fraction, measured at this field and four other nearby fields showed a strong negative correlation between  $EC_{a-d}$  and soil particle size. Therefore, low values of  $EC_{a-d}$  imply the presence of coarse textured soil particles – i.e. coarse sand.

### PG field

At the PG field, even though the CV of RKN population density was fairly high, the mean population densities at the three sampling events (RKN1, RKN2, RKN3) was low compared to the CC field because high RKN population density was measured at only a few sampling nodes. However, EL, SL, and  $EC_{a-d}$  were more variable compared to the CC field.

### **2.3.2 Geostatistical analyses**

The existence of several sources of variation operating at different scales yielded nested semivariograms with particular spatial structures in most of the cases (Table 2.2). Because the range of the semivariograms summarizes the extent of the spatial structures present, the analysis of the results for this section will be focused on the variability described by the range of spatial correlation.

### CC field

Visual inspection of the experimental semivariograms (square symbol) and the parameters of fitted models (solid line) for the RKN data in most cases suggested the presence of three spatial structures (Figure 2.1a-2.1c). The first structure was a nugget effect (y-intercept other than 0) which may be associated with measurement errors due to the sampling procedure itself or to micro-variation not captured by the 50 m sampling interval. The second structure,

indicated by  $a_1$  in Table 2.2, characterizes the variability of RKN population density at short distances which is represented by cluster with high populations located at the north-west part of the field in Figure 2.1a-2.1c. The third structure, indicated by  $a_2$  in Table 2.2, corresponds to large clusters with long ranges.

The large value of  $a_1$  (277 m – Table 2.2) for RKN1 explains the low spatial variability of RKN population density in the field at first flower. The range of 277 m represents the distance up to which RKN samples are spatially correlated with their neighbors. The low mean of RKN1 suggests low spatial variability which was also explained by a longer range of 422 m ( $a_2$ ) at the regional scale.

The nested semivariogram of RKN2 (Figure 2.1b) shows that RKN2 population density also varied at two different scales: (i) short with a range of 71.3 m between RKN observations delineating small clusters of high population density (> 500 second stage juveniles) located in the central and north-eastern parts of the field, and (ii) large with a range of 216 m indicating large clusters with moderate population density (100-300 second stage juveniles) (Figure 2.2b).

The RKN3 semivariogram (Figure 2.1c) describes small RKN clusters at a shorter scale than RKN2 (range of 65 m versus 71.3 m). However the range of the large clusters at RKN3 is much greater than that of RKN2 (481 m versus 216 m). This may be the result of a decrease in the high population of RKN at shorter scales (Figure 2.2c). Although the size and shape of the RKN clusters changed between RKN1, RKN2 and RKN3, short scale correlations of 0.20 and 0.18, and long scale correlations of 0.46 and 0.51 between RKN1-RKN2 and RKN2-RKN3, respectively, indicated that the locations of high RKN population density, especially the large clusters, remained stable until the end of the growing season (Figure 2.2).

Among the soil properties evaluated, the semivariograms of  $EC_{a-d}$ , soil pH, K and Ca had ranges with similar orders of magnitude. The short scale ranges were between 102-125 m and the long scale ranges between 595-1299 m (Table 2.2). The correlation at short scale of  $EC_{a-d}$  with soil pH, K, Ca, and Mg produced correlation coefficients of 0.37, 0.21, 0.60, and 0.48, respectively. This positive correlation indicates that low values of these soil chemical properties were found in areas with low values of  $EC_{a-d}$ , which are associated with sandy areas. From this we conclude that areas with low  $EC_{a-d}$  values are prone to leaching of soil minerals.

The semivariograms of, RKN2, RKN3, and SL were also similar, especially for the short range (Figure 2.1b, 2.1c, 2.1f), which reflects the similarity of their distributions at a short scale.

### PG field

As for the CC field, the shape of the semivariograms suggested the existence of more than one scale of variation. The RKN population density measured through the growing season showed similar ranges at short and large spatial scales (Figure 2.3a-2.3c). Although the ordinary kriging map of the RKN1 showed population density as low and uniformly distributed throughout the field (Figure 2.4a), factorial kriging analysis separated the total variability into short and long spatial scales. The short scale of variation (range = 91 m) describes the size of small clusters of RKN population density three standard deviations above the mean (Table 2.2).

The nested semivariograms of RKN2 and RKN3 had ranges with similar orders of magnitude. In this case, the short range of variation corresponded to the size of the small clusters with high population density (> 500 second stage juveniles) mainly located in the central part of the field (dark colors in Figure 2.4b-2.4c). The long range was greater than 200 m and described clusters of large size having moderate population density (100-300 second stage juveniles) (Table 2.2). As with the CC field, the locations with high RKN population density

remained stable until the end of the growing season which was explained by the correlation between the short range (0.42) and long range (0.53) for RKN2 and RKN3.

For the soil physical properties evaluated, the semivariograms of  $EC_{a-d}$ , and soil pH, had ranges with similar orders of magnitude to the RKN population density. Two main spatial scales, short with ranges of about 63-96 m and large with ranges of about 215-242 m, were common to these variables. This may suggest a good correlation between RKN population density and these soil properties at short and large scales (Table 2.2). The soil chemical properties, except for soil pH, had ranges with similar orders of magnitude. Therefore, these variables may vary in a similar fashion throughout the field as well.

### **2.3.3 Scale-dependent correlation between RKN population density and soil properties**

Tables 2.3 and 2.4 report the linear correlation coefficient as well as the structural correlation coefficients between RKN population densities measured at three different times during the growing season, and soil physical and chemical properties for the CC and PG fields.

Structural correlations were calculated between the nugget, local (short range), and regional (long range plus local mean or trend) components of each group of variables. Unlike the linear correlation coefficient that ignores the spatial coordinates of the data, filtering the noise by factorial kriging improved the accuracy of the estimations of spatial correlations and helped the identification of the potential sources of variation. For example, the linear correlation coefficient between RKN2 and  $EC_{a-d}$  at CC field was only -0.50. However, the coefficient grew to -0.77 when the noise and local components were filtered out. The discussion of the results presented in tables 2.3 and 2.4 will focus on the local (short range) and regional (trend or local mean plus long range) components of variation.

### CC field

The correlation between RKN population density and soil physical properties changed as a function of spatial scale. At short-range scale, SL exhibited a most consistent correlation with RKN throughout the growing season and it was negative. This can be explained by the correspondence between the models at short scale of both nested semivariograms which had similar ranges of spatial correlation (Table 2.2, Figure 2.1a-2.1c, Figure 2.1f). The negative spatial correlation between RKN population density and SL suggested that high population density of RKN could be found in areas of a field with little or no slope. At regional scale, a strong and negative correlation between RKN1, RKN2, and RKN3 and  $EC_{a-d}$  was observed. The strongly negative correlation between the trend components of RKN and  $EC_{a-d}$  also reflected a regional correlation among these variables, indicating that they shared similar distributions at large scales. This negative spatial correlation suggests that high RKN population density were likely to be found in large areas with low values of  $EC_{a-d}$ .

Sandy or coarse-textured soil has been related to low  $EC_{a-d}$  values (Khalilian et al., 2001; Perry et al., 2006). Therefore, the data here agree with the findings by Monfort et al. (2007) showing higher RKN population density in sandy areas. Although the correlation between RKN population density and EL (which was positive) was the highest at regional scale, it can be considered as erratic due to the low variation which EL exhibited in this field ( $CV = 2.1\%$ ). However, the negative correlation between RKN3 and the trend component of EL (- 0.63) agrees with the findings by Ortiz et al. (2006) showing an inverse relationship between EL and RKN ( $r = - 0.36$ ) when data from six cotton fields harvested in 2005 were pooled. They attributed these findings to the erosional deposition of coarse sand particles in low lying areas where nematodes

are mainly found, suggesting that a high population densities of RKN3 were more likely in low lying areas.

Soil chemical properties were more strongly correlated with RKN population density at the long-range scale than the short-range scale. However, for some properties, the correlations changed as function of the spatial scale. Even though soil pH was the only variable that correlated with RKN population density at short scale throughout the growing season, this correlation was very poor (-0.14) (Table 2.3). At a regional scale, RKN population density was strongly negatively correlated with soil pH. Therefore, high population density of RKN were present in more acidic soils (low soil pH). This could be considered an indirect relationship and related to the loss of nematicide activity by ammonia-releasing organic and inorganic fertilizers due to low levels of soil pH (Oka et al., 2006). According to Oka et al. (2007), an increase in soil pH can increase the nematicidal activities of ammonia-releasing amendments.

Along with soil pH, the negative correlation of Ca and Mg with RKN population density at regional scale was also very strong indicating that RKN clusters of large size and high populations were spatially correlated with large areas where the levels of Ca and Mg were low in relation to the average of the field. Even though the levels of Ca (mean of 897 kg ha<sup>-1</sup>) measured one month after planting did not indicate a nutritional deficiency of this element in the soil (> 247 kg ha<sup>-1</sup> of Ca is adequate for coastal plain soils), the spatial correlation of Ca and Mg with EC<sub>a-d</sub> indicated a strong positive correlation at the local scale (0.42 in average) and at regional scale (0.86 in average). Therefore, low levels of Ca and Mg corresponded with areas of low EC<sub>a-d</sub> which again indicates leaching of Ca and Mg in coarse textured areas where low values of EC<sub>a-d</sub> tend to occur.

The relationship between soil chemical properties and RKN population density presented above can be considered direct and/or indirect (plant mediated). Studies have shown that mineral salts such as NaCl, NaNO<sub>3</sub>, KCl, KNO<sub>3</sub>, CaCl<sub>2</sub>, Ca(NO<sub>3</sub>)<sub>2</sub>, MgCl<sub>2</sub>, MgSO<sub>4</sub>, FeCl<sub>2</sub>, and FeSO<sub>4</sub> exhibit a degree of repellency toward *M. javanica* and *M. incognita* (Cadet et al., 2004; Castro et al., 1990). Again, this indicates that special attention must be paid to sandy areas where salts may leach preferentially.

### PG field

A negative correlation was found between RKN population density and soil physical properties at the PG field. Even though the strength of the correlation of some properties changed as a function of the spatial scale, the strongest negative correlation with RKN population density at short and regional scale was exhibited by EC<sub>a-d</sub> (Table 2.4) suggesting its use as potential surrogate data for RKN. The high negative spatial correlation at short-range and trend components of variation suggest that small clusters with high RKN population density were likely in small patches with low values of EC<sub>a-d</sub>. The negative spatial correlation between these two variables validates the hypothesis that it is possible to identify areas at risk for high population of RKN based on surrogate data. At short-range scale, the correlation between SL and RKN1 (-0.17) and RKN2 (-0.27) was negative. The negative spatial correlation between these two variables indicates that RKN aggregates in the flattest areas of a field.

As in the CC field, soil chemical properties at the PG field had a negative spatial correlation with RKN population density at short and long scale. K and Mg exhibited the strongest negative correlation with RKN2 and RKN3.

### *Potential surrogate data*

The spatial correlation results from the two fields discussed above show that the relationship between RKN population density and soil chemical properties is at best weak but it does point out that site specific management of soil nutrients may reduce the risk for having high population density of RKN. The relationship with soil physical properties is stronger and in particular, the results point to EC<sub>a-d</sub> as potential surrogate data for RKN population density because of its correlation at short and long scale but also because of the stability of the correlation with respect to space, time and location.

### **2.3.4 Delineating areas at risk for RKN population over threshold values using indicator kriging**

Indicator kriging was used to predict the areas in CC and PG fields where the RKN2 population density likely exceeds the threshold of 100 second stage juveniles / 100 cm<sup>3</sup> of soil. The indicator variable required for the IK analysis was generated from the RKN2 data because of their strong spatial correlation with the soil physical and chemical properties. As described earlier, IK maps were created with three strategies: “hard” data, “soft” data, and a combination of “hard” and “soft” data. Because measured RKN2 population density best correlated with EC<sub>a-d</sub> at both the short and long scales, EC<sub>a-d</sub> data were used as the “soft” data for these analyses.

#### CC field – “hard” data

Figures 2.5a-2.5c present the indicator semivariograms used to predict the areas at risk of having RKN2 population density above the threshold of 100 second stage juveniles / 100 cm<sup>3</sup> of soil using only “hard” data. The data used were measured RKN population density from 99

(Figure 2.5a), 64 (Figure 2.5b), and 35 (Figure 2.5c) randomly selected sampling nodes from the RKN2 sampling event. The corresponding IK maps are presented in Figures 2.6a-2.6c.

Each semivariogram was calculated using 6 lags of 50 meters, and the corresponding model parameters are listed in table 2.5. The indicator semivariogram calculated from 99 RKN observations (Figure 2.5a) suggests two scales of variation. The short scale (range of 180 m) described the clusters located in the center of the field (Figure 2.6a). These clusters have a high risk (probability > 75%) for RKN population density to exceed the threshold. The long scale (range of 400 m) described the large high-risk clusters located in the northwest part of the field (Table 2.5, Figure 2.6a). The white square symbols on the maps represent RKN2 sampling nodes where RKN population density exceeded the threshold. Thirty-four or 87% of these observations coincided with areas in the field identified as high-risk. An additional 13% of the RKN observations exceeding the threshold were located in moderately high risk areas (50 - 75% probability range of risk) (Figure 2.6a). These results are summarized in Table 2.6.

The delineation accuracy of high-risk areas (probability > 75%) decreased 13% when 64 RKN observations were used to create the IK map (Figure 2.6b). Now, 76% of the observations above the threshold were found to be in the predicted high-risk area and 21% were predicted to be in the moderately high risk areas (Figure 2.6b). This decrease in accuracy may be associated with a reduction in the short range of spatial correlation (from 180 to 130 m) of the indicator semivariogram.

The IK map calculated from a smaller data set (35 RKN observations) showed a few scattered spots of predicted high risk (Figure 2.6c). Out of the RKN observations above the threshold, only 15% were found to be in the predicted high-risk area, while the remaining fall in the moderately high risk areas (Table 2.6). The lower accuracy of this IK map could be

associated with the weak spatial structure (nugget:sill ratio of 0.80) caused by sparse RKN observations above the threshold throughout the field (Table 2.5, Figure 2.5c). Because the observations were randomly selected, even fewer observations exceeded the threshold. The low accuracy of this IK map illustrates what could happen if producers use only a relatively small and randomly selected sampling points to quantify nematode infestations in their fields.

#### PG field – “hard” data

The indicator semivariograms for the PG field calculated using data sets of 105 and 70 RKN observations are shown on the figures 2.7a, and 2.7b, respectively. The model parameters calculated from each indicator semivariogram are summarized in Table 2.5. The short scale has a range of 103 m and a high nugget value ( $C_0$ ) with respect to the sill ( $C_1$  and  $C_2$ ). This describes small areas with RKN values above the threshold. It also infers that these areas are not spatially well connected. Although there were several RKN observations above the threshold, the IK map did not show any high risk zones (Figure 2.8a).

As with the CC field, the exercise was repeated for a smaller data set. But in this field, we had some surprising results. The data set was reduced to 70 RKN observations –considerably smaller than the original. Nevertheless, the nugget effect was reduced indicating a better spatial relationship between samples. This appeared to improve the delineation of clusters with high risk (Figure 2.8b). Even more surprising was that all of the observations above the threshold, coincided with areas in the field identified as high-risk (white square symbols of Figure 2.8b, Table 2.7). In this case, the random selection of a smaller sample set resulted in better spatial relationship between the samples.

Based on field histories, we expected RKN population density to be similar in both fields. But, the RKN population density in the PG field was lower and less variable than the CC field.

Furthermore, only 18 of the 105 observations were above the threshold. Low RKN population density in this field could be associated with past management practices as well as specific soil properties. The CC field has a Kershaw sandy soil characterized by having 91% sand, 6% silt, 3% clay in the first 85- cm soil depth. In contrast, the PG field has a Tifton loamy sand soil with 85% sand, 11% silt, 4% clay in the first 30- cm soil depth. These differences were observed on the soil  $EC_{a-d}$  maps of these two fields (Figure 2.9). Apparent soil electrical conductivity ( $EC_a$ ) measurements in these fields were taken within a few days of each other with similar soil moisture conditions. At the PG field, 73% of the total area had an average soil  $EC_{a-d}$  above 2.7 mS/m contrasting with only 7.2% at the CC field. Conversely, at the CC field 56% of the total area had average soil  $EC_{a-d}$  below 0.9 mS/m. These differences corroborate that the CC field had relatively deep coarse sandy soils compared to the PG and could help explain why lower RKN population densities were observed in the PG field throughout the 2006 growing season.

#### CC field – “soft” data

A logistic regression between the indicator variable and  $EC_{a-d}$  (trend component or local mean) was used to model the probability of risk of RKN2 population density above the threshold. The results from the logistic regression using data sets of 99, 64 and 35 RKN observations are presented in Table 2.8. Although the overall significance of the logistic models was not very high, the contribution of  $EC_{a-d}$  is significant ( $\alpha=0.05$ ). Using only soft data decreases the accuracy of the delineation of areas with high risk (probability > 75%) relative to using “hard” data alone. The resulting IK maps are presented in Figures 2.6d, 2.6e, and 2.6f.

On the map created using logistic regression with the set of 99 observations (Figure 2.6d), only 18% of the RKN2 observations above the threshold coincided with predicted high risk areas (Table 2.6). When the number of RKN observations used in the logistic regression was reduced

from 99 to 64 (Figure 2.6e), 31% of the RKN observations above the threshold were classified as being in areas with high risk. In contrast, when the data set was reduced from 99 to 35 observations, no areas of high risk were delineated and consequently, none of the RKN observations above the threshold were classified as being in areas with high risk (Figure 2.6f, Table 2.6). In all three maps, however, the area delineated as having moderately high risk (50 – 75%) remained relatively stable and contained between 31% and 43% of the observations exceeding the threshold.

The IK maps generated from soft data were not as accurate as the IK maps created from the hard data in terms of delineating the areas with the highest level of risk. However, a cotton producer may be able to use maps created this way to target the areas with more than 50% probability of having RKN population density above the threshold.

#### *PG field – “soft” data*

The results from the logistic regression between the indicator variable and  $EC_{a-d}$  using a data set of 105 and 70 RKN observations at the PG field are presented in Table 2.8. Although the overall significance of the logistic models was very poor,  $EC_{a-d}$  showed a significantly negative correlation with respect to the variability of the indicator variable which indicates that areas with low  $EC_{a-d}$  were associated with clusters of RKN observations above the threshold.

The small power of  $EC_{a-d}$  to explain the variability of the indicator variable is due to the presence of few RKN S2 observations (18) above the threshold. As a result, the accuracy on the delineation of areas with high risk (probability > 75%) decreased with respect to the IK hard data maps (Figures 2.8c and 2.8d). The RKN2 observations (105 and 70 data) above the threshold were classified as having between 0-25% and 25-50% probability of risk (Table 2.7).

### CC field – “hard” and “soft” data

The IK maps for the CC field combining hard and soft data generated from 99, 64 and 35 observations are presented in figures 2.6g, 2.6h, and 2.6i respectively. The accuracy of these maps improved with respect to the IK maps created from soft data, especially for the areas with high risk due to the addition of the kriging residuals calculated from the hard and soft data. Figures 2.5d-2.5f show the semivariograms of the residuals calculated for data sets of 99, 64, and 35 RKN observations, respectively. All three semivariograms showed that the residuals are spatially related at a short scale with a range of spatial dependence of around 120 m. The fact that residuals were correlated at the short scale may suggest an increase in accuracy using this method.

The advantage of combining hard and soft data was truly tested by reducing the initial number of RKN observations (99) used to delineate the IK maps. When 64 RKN observations were used to calculate the IK map, all the RKN observations above the threshold coincided with the areas predicted to have a high risk of exceeding the threshold. In contrast, only 76% and 31% of these observations were classified within that range in the maps created with the hard data alone and soft data alone, respectively (Table 2.6). A jackknife validation using a data set of 35 RKN observations also showed an increased accuracy of 60% and 160% in predicting high risk areas when compared to the IK maps created with the hard data alone and soft data alone, respectively.

When a reduced data set of 35 observations was used to delineate the IK maps, the combination of hard and soft data showed the best results for delineating zones at risk for RKN population density above the threshold value. The IK map created from the hard data alone using 35 observations (Figure 2.6c) greatly under predicted the extent of the high risk area

compared to the map from the combined data set (Figure 2.6i). All the RKN observations in the reduced data set which were above the threshold coincided with the predicted high risk zone while only 15% of the observations coincided in the hard data map and none coincided in the soft data map (Figures 2.6c, 2.6f, and 2.6i, Table 2.6). A jackknife validation using a data set of 64 RKN observations showed that the accuracy of the combined data map increased from 4% to 38% in the high risk area over the hard data map. Accuracy was also improved for the lower risk areas.

The purpose of this exercise is to create a technique for predicting areas at high risk of RKN populations exceeding the established threshold from the smallest number of RKN observations. It is most valuable, therefore, to compare the hard data map created from the 99 RKN concentration observations (Figure 2.6a) to the combined hard and soft data map created from the 35 RKN observations (Figure 2.6i). There are both visual and quantitative similarities and differences between these two maps.

If we assume that the distribution of RKN in this field is best represented by the dense data set used to create the hard data map in Figure 2.6a, then the most striking difference is that the combined map (Figure 2.6i) under estimates by about 40% the area identified as being at high risk by the hard data map (Figure 2.6a). Nevertheless, the combined data map does well in predicting areas with at least a moderately high (probability > 50%) risk of RKN population density exceeding the established threshold. In light of the earlier discussion on the cost and difficulty of collecting samples for RKN analyses, the slight loss in accuracy is justified by the reduced cost of creating a combined hard and soft data map with fewer observations. This type of map may be used to delineate RKN management zones.

In addition, the IK maps using soft data and the combination of soft and hard data showed that the zone with the highest probability of having RKN population density exceeding the threshold corresponded to the zone of  $EC_{a-d} < 0.9$  mS/m in the field (Figure 2.9a). This indicates the ability of  $EC_{a-d}$  to predict RKN risk zones in this field. The zones which together exceeded the 50% probability level on the IK maps were characterized by having the lowest values of  $EC_{a-d}$  ( $< 0.9$  mS/m). In contrast, the zone with less than 25% probability level had the highest values of  $EC_{a-d}$  ( $> 1.8$  mS/m). Therefore, these  $EC_{a-d}$  values can be used as guidelines for SSM in this field.

#### PG field – “hard” and “soft” data

The IK maps generated from hard and soft data using 105 and 70 observations are presented in figures 2.8e and 2.8f, respectively. The accuracy of the IK maps improved compared to the maps created from soft data alone and especially in the areas with high risk (probability  $> 75\%$ ). The semivariogram of the residuals calculated from the 105 data set suggested the presence of two scales of variation: short with a range of 81 m and long with a range of 209 m (Table 2.5, Figure 2.7d). The fact that residuals were correlated within the short and long scale explains the improved accuracy of the combined IK map especially at the short scale (Figure 2.8c). The low significance of the logistic models between the indicator variable with only 15 RKN observations above the threshold and  $EC_{a-d}$  may explain the poor improvement in the delineation of high risk areas in the combined map when compared to the map created from hard data.

The low number of RKN2 observations above the threshold in the data set used for jackknife validation of the combined IK map made it difficult to derive conclusions about the reliability of this map especially in the areas with high risk.

## 2.4 Summary and Conclusions

The aggregation pattern, spatial variability, and stability of RKN population density throughout the 2006 growing season observed in the two fields meet some of the requirements for site specific management (SSM). The short range of spatial dependence can be used as a guideline for sampling RKN population density in fields with low topographic relief. Structural spatial correlations, derived from the spatial components of each variable calculated with factorial kriging, allowed the identification of the most appropriate variables to use as surrogate data for delineating RKN risk areas or management zones for SSM. The moderate to strong spatial dependence of RKN population density observed at mid season (RKN2) and the spatial stability of areas with high populations throughout the growing season favored their high correlation with the soil properties. The aggregated pattern of RKN distribution facilitated the segregation of RKN risk areas based on low values of  $EC_{a-d}$  through the development of indicator kriging maps combining RKN observations (hard data) and  $EC_{a-d}$  data (soft data).

The results from the CC and PG fields showed that the incorporation of  $EC_{a-d}$  as soft data supplementing the hard data resulted in improved predictions. The combination of hard and soft data takes advantage of the dense set of  $EC_{a-d}$  data which is less expensive and easier for a producer to collect than the RKN samples. In the absence of soil movement or the addition of large volumes of soil amendments,  $EC_a$  data need only be collected once.

The advantage of combining hard and soft data was shown when 35 RKN observations were combined with  $EC_{a-d}$  data to map the areas at risk with a result similar to the map delineated using a much large data set of RKN observations. However, the logistic regression analysis demonstrated that  $EC_{a-d}$  alone may not capture the total spatial distribution of RKN population density and predict the areas at risk for high populations. The integration of other surrogate data

for soil texture, such as slope and elevation along with  $EC_{a-d}$ , may improve the accuracy of combined hard and soft data maps as well as soft data maps.

The biggest advantage of combining soft data with hard data to develop probabilistic maps is the reduced number of RKN observations required to assess the areas at risk for high population of RKN. Additionally, these maps may be used to target zones for additional sampling and/or application of nematicides. However, it should be noted that the identification of surrogate data and estimation of areas at risk may be difficult if the RKN population density follows a random pattern of spatial variation or if RKN are not present.

The fact that RKN population density increase in areas of coarse textured soils where leaching of nematicides is most likely to occur indicates the importance of having a probability map of RKN risk which can be used not only for RKN population management but also for soil fertility management. The strong spatial correlation between the RKN and  $EC_{a-d}$ , a relatively stable variable, indicates that  $EC_{a-d}$  can be used to delineate management zones for RKN which will capture most of the variation of RKN. Future research must be focused on the effect that soil chemical properties have on the reproduction and survival of nematodes.

### **Acknowledgements**

This work was supported by grant funds from Cotton Inc., the Georgia Cotton Commission, the Flint River Water Planning and Policy Center, Hatch and State funds allocated to the Georgia Agricultural Experiment Stations and by USDA-ARS CRIS project funds. Many thanks to the cotton producers who participated in this study and shared their time and records with us. Many thanks also to Dr. Robert Nichols who supported this project. Finally, special thanks to Dewayne Dales, Rodney Hill, Gary Murphy, Andrea Milton, and Katia Rizzarda who assisted with the extensive field work required to complete this project.

Mention of commercially available products is for information only and does not imply endorsement.

## References

- Avendaño, F., O. Schabenberger, F. J. Pierce, and H. Melakeberhan. 2003. Geostatistical analysis of field spatial distribution patterns of soybean cyst nematode. *Agron. J.* 95: 936-948.
- Avendaño, F., F. J. Pierce, O. Schabenberger, and H. Melakeberhan. 2004. The spatial distribution of soybean cyst nematode in relation to soil texture and soil map unit. *Agron. J.* 96: 181-194.
- Avruskin G., G. Jacquez, J. Meliker, M. Slotnick, A. Kaufmann, and J. Nriagu. 2004. Visualization and exploratory analysis of epidemiologic data using a novel space time information system. *Intl. J. Health Geogr.* 3: 26.
- Cadet, P., S. Berry, and V. Spaul. 2004. Mapping of interactions between soil factors and nematodes. *Eur. J. Soil Biol.* 40(2): 77-86.
- Castro, C. E., N. O. Belser, H. E. McKinney, and I. J. Thomasson. 1990. Strong repellency of the root knot nematode, *Meloidogine incognita* by specific inorganic ions. *J. Chem. Ecol.* 16(4): 1199-1205.
- Castrignanò, A., G. Buttafuoco, R. Puddu, and C. Fiorentino. 2007. A multivariate geostatistical approach to delineate areas at soil salinization risk. In Proc. *Sixth European Conference of Precision Agriculture (6ECPA)*, 199-205. Stafford, J., and A. Werner, eds. Skiathos. Greece.
- ESRI. 2004a. ArcGIS Spatial Analyst 9.0. ESRI, Redlands, CA.
- ESRI. 2004b. ArcGIS Geostatistical Analyst. ESRI, Redlands, CA.
- Fridgen, J.J., C.W. Fraisse, N.R. Kitchen, and K.A. Sudduth. 2000. Delineation and analysis of site-specific management zones. In Proc. *2<sup>nd</sup> International Conference on Geospatial Information in Agriculture and Forestry*, CD-ROM. Lake Buena Vista, FL.
- Geovariances, 2007. ISATIS technical references, version 7.0.6.
- Goodell, P. B., and H. Ferris. 1980. Plant-parasitic nematode distributions in an alfalfa field. *J. Nematol.* 12: 136-141.
- Goovaerts, P. 1994. Study of spatial relations between two set of variables using multivariate geostatistics. *Geoderma* 62: 93-107
- Goovaerts, P. 1997. *Geostatistics for Natural Resources*. Oxford University Press, New York, USA.

- Goovaerts, P., R. Webster, and J. P. Dubois. 1997. Assessing the risk of soil contamination in the Swiss Jura using indicator geostatistics. *Environ. Ecol. Stat.* 4: 31-48.
- Goovaerts, P. 1998. Geostatistical tools for characterizing the spatial variability of microbiological and physico-chemical soil properties. *Biol. Fert. Soils* 27: 315-334.
- Goovaerts, P., G. AvRusking, J. Meliker, M. Slotnick, G. Jacquez, and J. Nriagu. 2005. Geostatistical modeling of the spatial variability of arsenic in ground water of southeast Michigan. *Water Resour. Res.* 41: 1-19.
- Grunwald, S., P. Goovaerts, C. M. Bliss, N. B. Comerford, and S. Lamsal. 2006. Incorporation of auxiliary information in the geostatistical simulation of soil nitrate nitrogen. *Vadose Zone J.* 5: 391-404
- Jenkins, W.R. 1964. A rapid centrifugal flotation technique for separating nematodes from soil. *Plant Dis.* 48: 692.
- Khalilian A., J. D. Mueller, S. C. Blackville, Y. J. Han, and F. J. Wolak. 2001. Predicting cotton nematodes distribution utilizing soil electrical conductivity. In *Proc. 2001 Beltwide Cotton Conference*, 146-149. Memphis, TN.:National Cotton Council.
- Kerry, R., M. A. Oliver. 2003. Co-kriging when soil and ancillary data are not co-located. In *Proc. 4<sup>th</sup> European Confence of Precision Agriculture*. 303-308. Wageningen Academic Publishers.
- Kitchen, N. R., K.A. Sudduth, and S. T. Drummond. 1999. Soil electrical conductivity as a crop productivity measure for claypan soils. *J. Prod. Agric.* 12: 607-617.
- Kitchen, N. R., S. T. Drummond, E. D. Lund, K.A. Sudduth, and G. W. Buchleiter. 2003. Soil electrical conductivity and topography related to yield for three contrasting soil-crop systems. *Agron. J.* 95: 483-495.
- Kleinschmidt, I., M. Bagayoko, GPY. Clarke, M. Craig, and D. Le Sueur. 2000. A spatial statistical approach to malaria mapping. *Intl. J. Epidemiol.* 29: 355-361.
- Koenning, S. R., S. A. Walters, and K. R. Barker. 1996. Impact of soil texture on the reproductive and damage potential of *Rotylenchulus reniformis* and *Meloidogyne incognita* on Cotton. *J. Nematol.* 28: 527-536.
- Lin, Y., T. Chang, C. Shih, and C. Tseng. 2002. Factorial and indicator kriging methods using a geographic information system to delineate spatial variation and pollution sources of soil heavy metals. *Environ. Geol.* 42: 900-909.
- Lyon, S. W., A. J. Lembo Jr, M. T. Walter, and T. S. Steenhuis. 2006. Defining probability of saturation with indicator kriging on hard and soft data. *Adv. Water Resour.* 29: 181-193.

- Matheron, G. 1963. Principles of geostatistics. *Econ. Geol.* 58: 1246-1266.
- Matheron, G. 1982. Pour une analyse krigéante de données régionalices. Centre de Géostatistique, Report N-732, Fontainebleau.
- Melakeberhan, H., J. Dey, V. C. Baligar, and T. E. Carter Jr. 2004. Effect of soil pH on the pathogenesis of *Heterodera glycines* and *Meloidogyne incognita* on *Glycine max* genotypes. *Nematology* 6: 585-592.
- Monfort, W. S., T. L. Kirkpatrick, C. S. Rothrock, and A. Mauromoustakos. 2007. Potential for site-specific management of *Meloidogyne incognita* in cotton using soil textural zones. *J. Nematol.* 39 (1): 1-8.
- NCC. 2006. Beltwide yield losses to nematode damage. Cordova, TN.: National Cotton Council of America. Available at: [www.cotton.org/tech/pest/nematode/losses.cfm](http://www.cotton.org/tech/pest/nematode/losses.cfm). Accessed August 17, 2008.
- Noe, J. P., and K. R. Barker. 1985. Relation of within-field spatial variation of plant-parasitic nematode population densities and edaphic factors. *Phytopatology* 75: 247-252.
- Oka, Y., N. Tkachi, S. Shuker, R. Rosenberg, S. Suriano, L. Roded, and P. Fine. 2006. Field studies on the enhancement of nematicidal activity of ammonia-releasing fertilizers by alkaline amendments. *Nematology* 8(6): 881-893.
- Oka, Y., N. Shapira, and P. Fine. 2007. Control of root-knot nematodes in organic farming systems by organic amendments and soil solarization. *Crop Prot.* 26(10): 1556-1565.
- Ortiz, B. V., D. G. Sullivan, C. Perry, and G. Vellidis. 2006. Geospatial solutions for precision management of cotton root knot nematodes. ASAE paper No. 061147. Portland, OR.: ASAE.
- Perry, C., G. Vellidis, D. G. Sullivan, K. Rucker, and R. Kemerait. 2006. Predicting nematode hotspots using soil EC<sub>a</sub> data. In *Proc. 2006 Beltwide Cotton Conference*. San Antonio, TX.: National Cotton Council.
- Rodgers, S. E., and M. A. Oliver. 2007. A geostatistical analysis of soil, vegetation, and image data characterizing land surface variation. *Geogra. Anal.* 39: 195-216.
- SAS Institute Inc. 2007. SAS OnlineDoc (R) 9. 1. 3. Cary, NC: SAS Institute Inc.
- Stanton, M. A. 1986. Effects of root-knot nematode (*Meloidogyne* spp.) on growth and yield of 'Cobb' soybean (*Glycine max* (L.) merrill). MS thesis. Gainesville, Fl.: University of Florida, Agronomy Department.

- Sudduth, K. A., N. R. Kitchen, W.J. Wiebold, W. D. Batchelor, G. A. Bollero, D. G. Bullock, D. E. Clay, H. L. Palm, F. J. Pierce, R. T. Schuler, and K. D. Thelen. 2005. Relating apparent electrical conductivity to soil properties across the north-central USA. *Comp. Electron. Agric.* 46: 263-283.
- Webster, R., and B. Boag. 1992. Geostatistical analysis of cyst nematodes in soil. *J. Soil Sci.* 43: 583-595.
- Wheeler, T. A., K.R. Barker, and S. M. Schneider. 1991. Yield-loss models for tobacco infected with *Meloidogyne incognita* as affected by soil-moisture. *J. Nematol.* 23: 365-371.
- Windham, G. L. and K. R. Barker. 1993. Spatial and temporal interactions of *Meloidogyne incognita* and soybean. *J. Nematol.* 25: 738-745 Suppl. S.
- Wyse-Pester, D. Y., L.J. Wiles, and P. Westra,. 2002. The potential for mapping nematode distribution for site-specific management. *J. Nematol.* 34: 80-87.

Table 2.1. Descriptive statistics of the cotton RKN population density and the soil physical and chemical properties for the CC and PG fields.

Field	Variable	Descriptive statistics				
		Mean	Min.-Max.	SD†	CV (%)‡	Skewness
CC (99) <sup>§</sup>						
	RKN1††	43.9	1-1281	139.4	319.7	7.5
	RKN2††	132.1	1-1629	226.4	171.4	4.3
	RKN3††	116.2	1-729	145.8	125.5	2.0
	EL (m)	78.2	74-81	1.7	2.1	-0.5
	SL (%)	1.2	0.13-3.54	0.6	50.4	0.6
	EC <sub>a-d</sub> (mS/m)	1.2	0.45-7.95	1.1	89.5	4.0
	soil pH	6.4	5.34-7.49	0.4	6.5	0.1
	P (kg/ha)	83.9	45-141	20.1	24	0.7
	K (kg/ha)	80.2	41-163	22.5	28	1.2
	Ca (kg/ha)	897.0	276-1924	324.9	36.2	0.6
	Mg (kg/ha)	122.1	30-345	55.0	45	1.3
PG (105) <sup>§</sup>						
	RKN1††	1.6	0-52	6.4	395.7	5.7
	RKN2††	64.6	0-876	158.5	245.3	3.7
	RKN3††	97.3	0-2006	242.5	249.4	5.5
	EL (m)	107.7	103-112	2.3	2.1	-0.1
	SL (%)	2.8	0.43-14.65	1.7	62.9	2.6
	EC <sub>a-d</sub> (mS/m)	3.9	0.66-10.39	2.1	52.7	1.1
	soil pH	6.1	5.37-7.29	0.3	5.5	1.1
	P (kg/ha)	100.2	43.1-193.2	29.8	29.7	0.8
	K (kg/ha)	118.1	65.1-201.3	34.1	28.9	0.6
	Ca (kg/ha)	736.8	366.2-1599	197.7	26.8	1.0
	Mg (kg/ha)	105.9	43.3-313.1	36.8	34.7	1.9

† Standard deviation.

‡ Coefficient of variation, percentage.

§ Sample size.

†† Counts from 100 cm<sup>3</sup> soil.

Table 2.2. Parameters of fitted semivariogram models of cotton RKN population density and soil properties for the CC and PG fields.

Variable	Semivariogram model parameters						Model 1	Model 2
	C <sub>0</sub>	C <sub>1</sub>	C <sub>2</sub>	a <sub>1</sub> (m)	a <sub>2</sub> (m)			
<i>CC field</i>								
RKN1†	0.375	0.119	0.701	277.0	422.7	Cubic	Cubic	
RKN2†	6.40E-09	0.480	0.309	71.3	216.5	Cubic	Cubic	
RKN3†	0.310	0.486	0.213	65.2	481.2	Spherical	Cubic	
EL (m)	1.98E-08	2.072		1001.6		Cubic		
SL (%)	0.216	0.405	0.331	51.4	241.6	Spherical	Cubic	
EC <sub>a-d</sub> (mS/m) †	0.047	0.463	3.004	125.6	972.3	Spherical	Gaussian	
soil pH	0.352	0.539	0.579	132.5	1299.0	Spherical	Spherical	
P (kg/ha)	0.019	0.747	0.440	48.1	476.3	Spherical	Cubic	
K (kg/ha)†	0.391	0.199	2.212	102.6	1288.6	Exponential	Cubic	
Ca (kg/ha)	1.38E-08	0.510	0.678	117.9	595.6	Exponential	Cubic	
Mg (kg/ha)†	2.15E-07	0.380	0.747	63.9	318.8	Cubic	Spherical	
<i>PG field</i>								
RKN1†	4.75E-08	0.181	0.816	90.8	215.5	Cubic	Spherical	
RKN2†	8.37E-09	0.436	0.582	96.8	242.0	Cubic	Cubic	
RKN3†	0.175	0.471	0.361	70.4	224.8	Spherical	Spherical	
EL (m)	4.64E-07	1.185		438.5		Cubic		
SL (%)†	0.511	0.292	0.131	92.4	233.4	Cubic	Exponential	
EC <sub>a-d</sub> (mS/m)†	0.091	0.292	0.704	63.3	216.4	Spherical	Spherical	
soil pH†	1.68E-09	0.769	0.341	84.5	231.4	Cubic	Cubic	
P (kg/ha)	0.416	0.252	0.937	151.5	1275.4	Spherical	Spherical	
K (kg/ha)	7.15E-02	0.421	0.503	132.1	281.6	Cubic	Spherical	
Ca (kg/ha)	2.11E-07	0.575	0.523	103.0	255.4	Cubic	Cubic	
Mg (kg/ha)†	3.80E-06	0.471	0.653	105.8	236.8	Cubic	Cubic	

† Semivariogram was performed on normal score transformed data.

The model parameters are: C<sub>0</sub> - nugget variance, C<sub>1</sub> – sill variance of the first structure, C<sub>2</sub> - sill variance of the second structure, a<sub>1</sub> – range of spatial dependence for the first structure, a<sub>2</sub> – range of the second structure, model 1 – model fitted to the first structure of the semivariogram, model 2 – model fitted to the second structure of the semivariogram.

Table 2.3. Scale dependent correlation for the nested spatial structures of cotton RKN population density with soil physical and chemical properties at the CC field.

Variables	Linear correlation coefficient	Structural correlation coefficients				
		Spatial components				
		Nugget	Short-range	Long-range	Trend‡	Regional‡‡
<i>RKN1† with</i>						
EC <sub>a-d</sub> †	-0.39	0.00	0.06	0.01	-0.63	-0.54
EL	0.46	0.00	0.00	-0.02	0.48	0.64
SL	-0.35	0.00	-0.19	-0.18	-0.59	-0.61
soil pH	-0.19	-0.11	-0.14	0.03	-0.80	-0.49
P	-0.09	-0.16	-0.04	0.08	-0.24	-0.07
K†	-0.07	-0.01	-0.23	-0.28	0.35	0.00
Ca	-0.30	-0.23	-0.08	-0.06	-0.88	-0.46
Mg†	-0.21	-0.17	-0.06	0.00	-0.85	-0.31
<i>RKN2† with</i>						
EC <sub>a-d</sub> †	-0.50	0.00	0.17	0.01	-0.69	-0.77
EL	0.63	0.00	0.00	0.07	0.96	0.90
SL	-0.37	0.00	0.05	-0.16	-0.51	-0.59
soil pH	-0.26	-0.14	-0.07	-0.35	-0.89	-0.76
P	-0.09	-0.06	-0.03	0.05	-0.14	-0.18
K†	-0.28	-0.04	-0.05	-0.20	0.36	-0.46
Ca	-0.45	-0.09	-0.08	-0.42	-0.88	-0.80
Mg†	-0.35	-0.18	-0.06	-0.36	-0.88	-0.63
<i>RKN3† with</i>						
EC <sub>a-d</sub> †	-0.26	0.00	0.01	0.19	-0.65	-0.61
EL	0.41	0.00	0.00	-0.11	-0.63	0.88
SL	-0.19	0.00	-0.14	-0.08	-0.53	-0.42
soil pH	-0.23	-0.06	-0.14	-0.32	-0.88	-0.70
P	0.04	0.04	0.00	-0.01	0.04	0.19
K†	-0.15	0.06	0.04	0.09	0.49	-0.55
Ca	-0.22	0.06	-0.04	-0.09	-0.77	-0.69
Mg†	-0.20	0.02	-0.05	-0.20	-0.82	-0.53

‡ Trend component corresponds to local mean

‡‡ Regional component corresponds to the long-range component plus local mean or trend component

† Spatial correlation was performed on normal score transformed data.

Table 2.4. Scale dependent correlation for the nested spatial structures of cotton RKN population density with soil physical and chemical properties at the PG field.

Variables	Linear correlation coefficient	Structural correlation coefficients				
		Spatial components				
		Nugget	Short-range	Long-range	Trend‡	Regional‡‡
<i>RKNI † with</i>						
EC <sub>a-d</sub> †	-0.09	0.00	-0.13	-0.06	-0.35	-0.10
EL	-0.67	0.00	0.00	-0.28	-0.43	-0.76
SL †	-0.08	0.00	-0.17	-0.14	0.17	0.05
soil pH †	0.33	0.11	0.21	0.62	-0.33	0.37
P	0.49	0.24	0.20	0.42	0.90	0.74
K	-0.25	-0.03	-0.01	0.09	-0.75	-0.43
Ca	0.18	0.09	0.18	0.38	-0.28	-0.19
Mg†	0.25	0.26	0.17	0.49	-0.36	0.25
<i>RKN2 † with</i>						
EC <sub>a-d</sub> †	-0.40	0.00	-0.24	-0.17	-0.39	-0.47
EL	-0.15	0.00	0.00	0.03	-0.36	-0.21
SL †	-0.05	0.00	-0.27	0.00	0.24	0.14
soil pH †	-0.14	0.09	-0.02	-0.40	-0.38	-0.36
P	0.22	0.18	0.03	-0.05	0.83	0.49
K	-0.51	-0.36	-0.21	-0.57	-0.76	-0.67
Ca	-0.38	-0.25	-0.08	-0.61	-0.61	-0.39
Mg†	-0.41	-0.15	-0.22	-0.64	-0.62	-0.58
<i>RKN3 † with</i>						
EC <sub>a-d</sub> †	-0.37	0.00	-0.19	-0.16	-0.30	-0.49
EL	-0.13	0.00	0.00	0.26	-0.34	-0.32
SL †	0.14	0.00	0.16	0.20	0.16	0.06
soil pH †	-0.29	-0.01	-0.14	-0.67	-0.50	-0.59
P	0.11	0.14	-0.03	-0.21	0.77	0.37
K	-0.35	-0.23	-0.11	-0.45	-0.81	-0.71
Ca	-0.39	-0.21	-0.18	-0.74	-0.29	-0.10
Mg†	-0.37	-0.06	-0.18	-0.69	-0.51	-0.58

‡ Trend component corresponds to local mean

‡‡ Regional component corresponds to the long-range component plus local mean or trend component

† Spatial correlation was performed on normal score transformed data.

Table 2.5. Indicator semivariogram parameters calculated using hard data and residual semivariogram parameters calculated using hard and soft data for different data sets, CC and PG fields.

Field	Number of data	Semivariogram model parameters						
		$C_0$	$C_1$	$C_2$	$a_1$ (m)	$a_2$ (m)	Model 1	Model 2
CC		<u>Indicator semivariogram</u>						
	99	0.12	0.07	0.03	180	400	Spherical	Cubic
	64	0.13	0.02	0.09	130	400	Spherical	Cubic
	35	0.19	0.02	0.03	112	277	Cubic	Spherical
		<u>Residuals semivariogram</u>						
	99	0.10	0.08		140		Spherical	
PG		<u>Indicator semivariogram</u>						
	105	0.12	0.00	0.04	103	224	Spherical	Spherical
	70	0.08	0.05	0.05	94	213	Cubic	Cubic
		<u>Residuals semivariogram</u>						
	105	0.03	0.11	0.01	81	209	Spherical	Spherical
	70	0.01	0.17		118		Cubic	

The model parameters are:  $C_0$  - nugget variance,  $C_1$  – sill variance of the first structure,  $C_2$  - sill variance of the second structure,  $a_1$  – range of spatial dependence for the first structure,  $a_2$  – range of the second structure, model 1 – model fitted to the first structure of the semivariogram, model 2 – model fitted to the second structure of the semivariogram.

Table 2.6. Number and percentage occurrence of RKN observations above (Risk) or below (No Risk) the threshold value in different levels of estimated probability of risk for RKN above the threshold of 100 RKN second stage juveniles per 100 cm<sup>3</sup> of soil. Jackknife cross-validation results using two data sets, CC field.

Estimated probability of RKN above threshold (%)	Hard Data		Soft Data		Hard and Soft Data	
	Risk	No Risk	Risk	No Risk	Risk	No Risk
	No.	No.	No.	No.	No.	No.
	(%)	(%)	(%)	(%)	(%)	(%)
<u>99 Observations</u>						
0 – 25	0 (0)	58 (97)	3 (8)	35 (58)	0 (0)	52 (86)
25 – 50	0 (0)	2 (3)	12 (31)	14 (23)	0 (0)	7 (12)
50 – 75	5 (13)	0 (0)	17 (43)	10 (16)	9 (33)	1 (2)
75 – 100	34 (87)	0 (0)	7 (18)	3 (5)	30 (59)	0 (0)
<u>64 Observations</u>						
0 – 25	0 (0)	30 (86)	3 (10)	18 (52)	0 (0)	35 (100)
25 – 50	0 (0)	5 (14)	6 (21)	11 (31)	0 (0)	0 (0)
50 – 75	6 (21)	1 (3)	11 (38)	4 (11)	0 (0)	0 (0)
75 – 100	22 (76)	0 (0)	9 (31)	2 (6)	29 (100)	0 (0)
<u>35 Observations</u>						
0 – 25	0 (0)	15 (68)	0 (0)	9 (41)	0 (0)	22 (100)
25 – 50	0 (0)	7 (32)	9 (69)	9 (41)	0 (0)	0 (0)
50 – 75	11 (85)	0 (0)	4 (31)	4 (18)	0 (0)	0 (0)
75 – 100	2 (15)	0 (0)	0 (0)	0 (0)	13 (100)	0 (0)
<u>Jackknife Validation – 64 observations (35 observations - Testing)</u>						
0 – 25	0 (0)	12 (48)	0 (0)	14 (56)	0 (0)	15 (60)
25 – 50	0 (20)	5 (20)	2 (20)	5 (20)	1 (10)	2 (8)
50 – 75	5 (50)	5 (20)	5 (50)	4 (16)	1 (10)	4 (16)
75 – 100	5 (50)	3 (12)	3 (30)	2 (8)	8 (80)	4 (16)
<u>Jackknife Validation – 35 observations (64 observations - Testing)</u>						
0 – 25	1 (4)	11 (29)	1 (4)	20 (52)	1 (4)	20 (52)
25 – 50	11 (42)	25 (66)	13 (50)	17 (45)	6 (23)	14 (37)
50 – 75	13 (50)	2 (5)	10 (38)	1 (3)	9 (35)	4 (11)
75 – 100	1 (4)	0 (0)	2 (8)	0 (0)	10 (38)	0 (6)

Table 2.7. Number and percentage occurrence of RKN observations above (Risk) or below (No Risk) the threshold value in different levels of estimated probability of risk for RKN above the threshold of 100 RKN second stage juveniles per 100 cm<sup>3</sup> of soil. Jackknife cross-validation results using two data sets, PG field.

Estimated probability of RKN above threshold (%)	Hard data		Soft data		Hard and soft data	
	Risk (%)	No risk (%)	Risk (%)	No risk (%)	Risk (%)	No risk (%)
<u>105 observations</u>						
0-25	0 (0)	78 (90)	13 (72)	76 (87)	0 (0)	85 (98)
25-50	14 (78)	9 (10)	5 (28)	11 (13)	1 (5)	2 (2)
50-75	4 (22)	0(0)	0 (0)	0 (0)	17 (95)	0 (0)
75-100	0 (0)	0 (0)	0 (0)	0 (0)	0 (0)	0 (0)
<u>70 observations</u>						
0-25	0 (0)	55 (100)	8 (53)	39 (70)	0 (0)	55 (100)
25-50	0 (0)	0 (0)	7 (46)	16 (29)	0 (0)	0 (0)
50-75	0 (0)	0 (0)	0 (0)	0 (0)	0 (0)	0 (0)
75-100	15 (100)	0 (0)	0 (0)	0 (0)	15 (100)	0 (0)
<u>Jackknife validation</u>						
<u>70 observations (35 observations - Testing)</u>						
0-25	2 (66)	16 (50)	2 (66)	22 (69)	2 (66)	17 (53)
25-50	1 (24)	11 (35)	0 (0)	10 (31)	1 (34)	11 (34)
50-75	0 (0)	3 (9)	1 (34)	0 (0)	0 (0)	3 (9)
75-100	0 (0)	2 (6)	0 (0)	0 (0)	0 (0)	1 (4)

Table 2.8. Results of the logistic regression between RKN2 and  $EC_{a-d}$  using different numbers of RKN observations, CC and PG fields.

Number of observations	Indicator variable (RKN2 $\geq$ Threshold $\dagger$ )					
	-2LogL	Pr>F <sup>a</sup>	$\beta^b$	$c$	$R$	$R^2$
<i>CC field</i>						
99	101.50	< 0.0001	-1.584	-0.547	-0.529	0.27
64	64.42	< 0.0001	-1.747	-0.296	-0.572	0.31
35	41.89	0.052	-0.869	-0.583	-0.340	0.11
<i>PG field</i>						
105	91.97	0.045	-0.646	-1.636	-0.200	0.04
70	68.99	0.060	-0.702	-1.367	-0.228	0.05

$\dagger$  Threshold value equal to 100 second stage juveniles per 100 cm<sup>3</sup> of soil

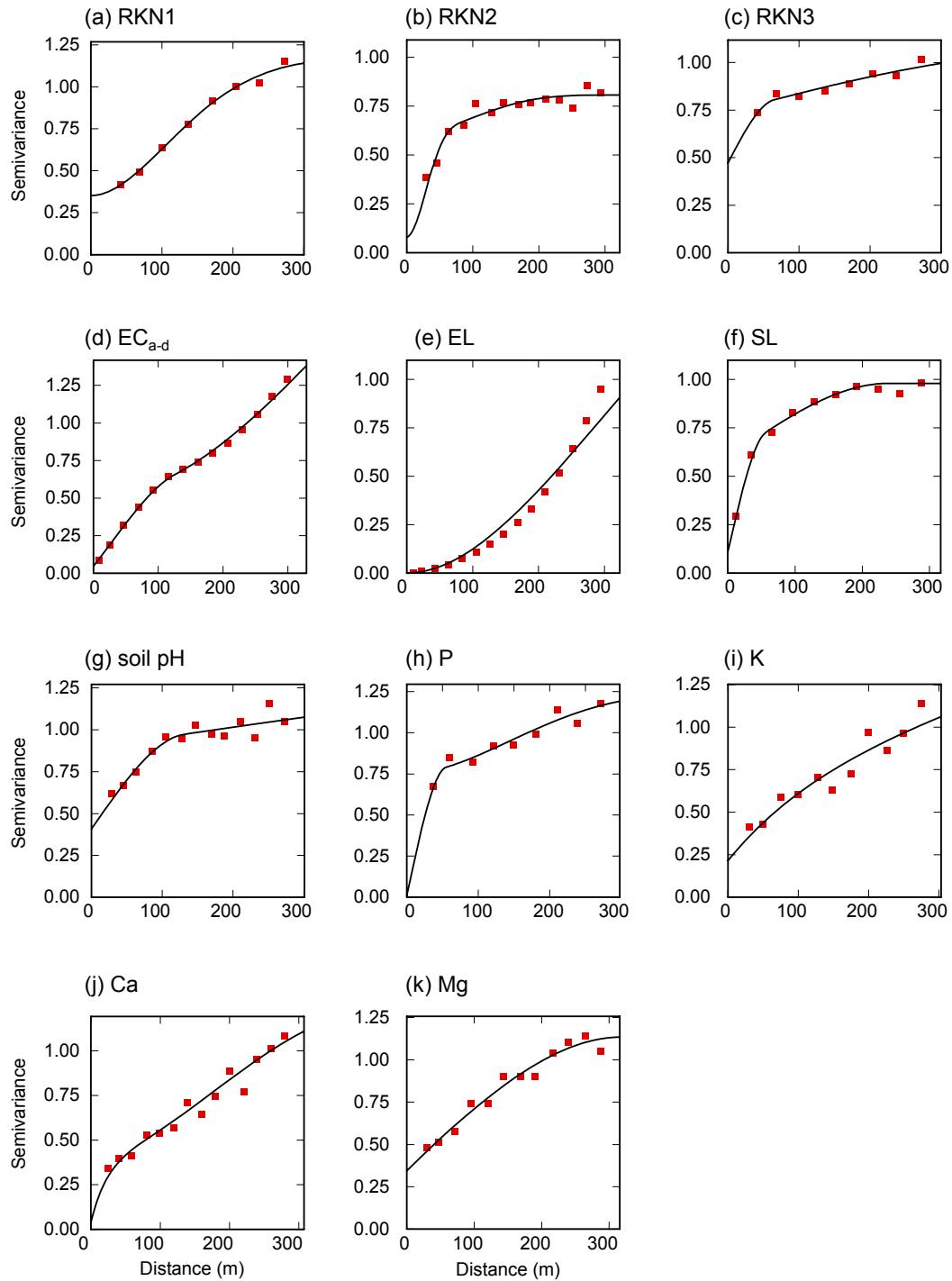


Figure 2.1. Normalized semivariograms for cotton RKN samples and soil physical and chemical properties at the CC field. Squares indicate the empirical semivariogram and the solid line is the fitted model.

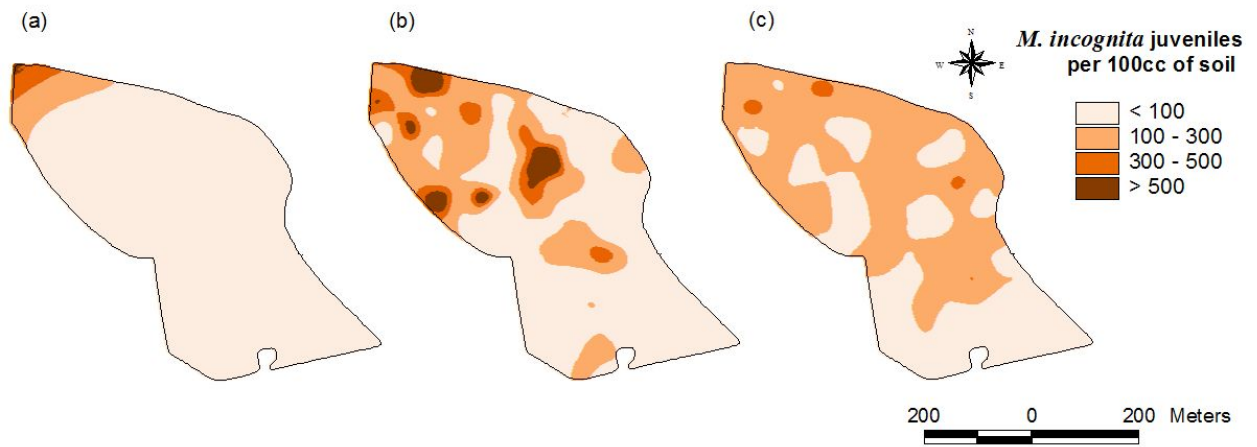


Figure 2.2. Cotton RKN spatio-temporal distribution evaluated RKN1 (a), RKN2 (b), and RKN3 (c) at the CC field in 2006.

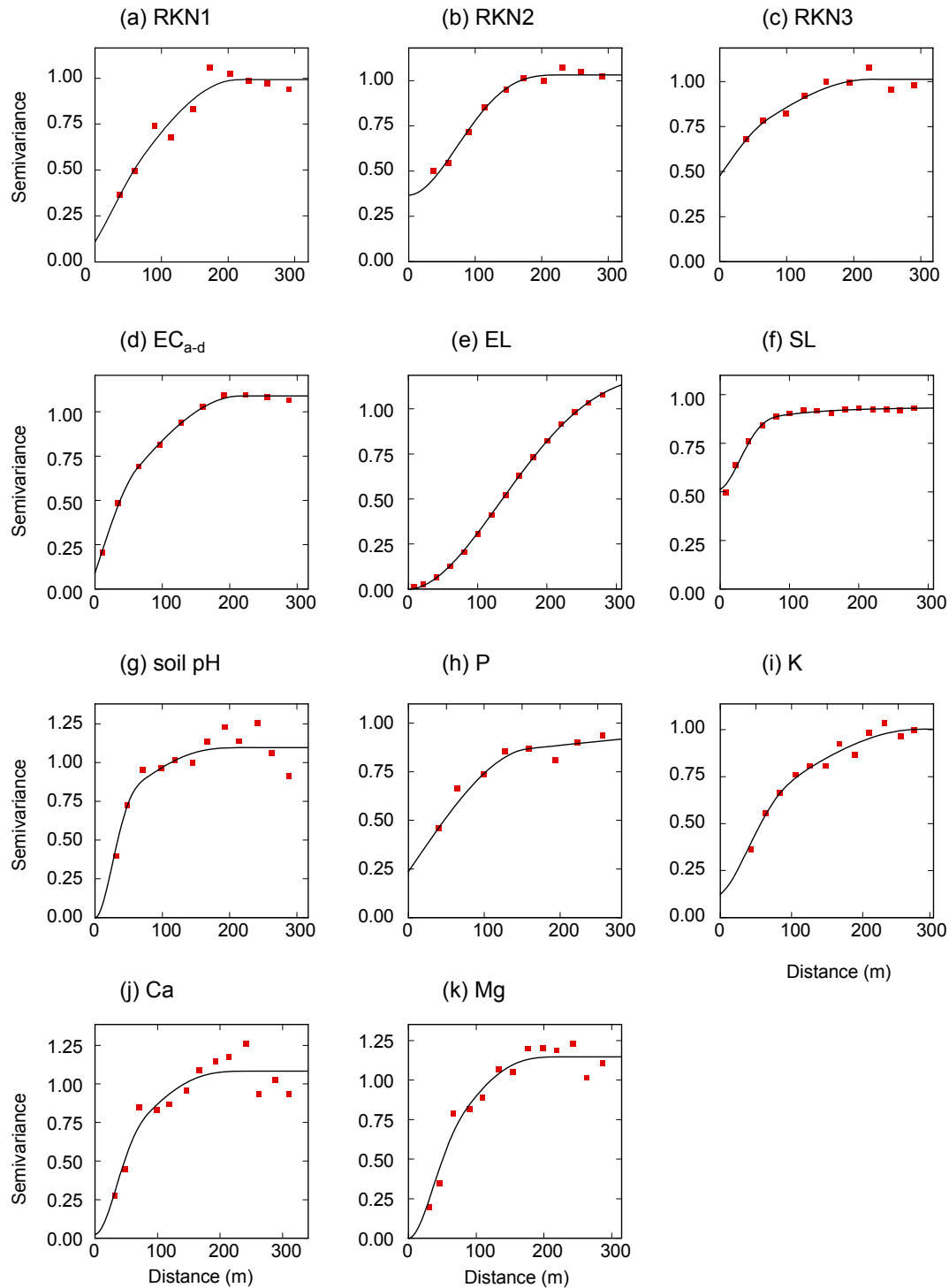


Figure 2.3. Normalized semivariograms for cotton RKN samples and soil physical and chemical properties at the PG field. Squares indicate the empirical semivariogram and the solid line is the fitted model.

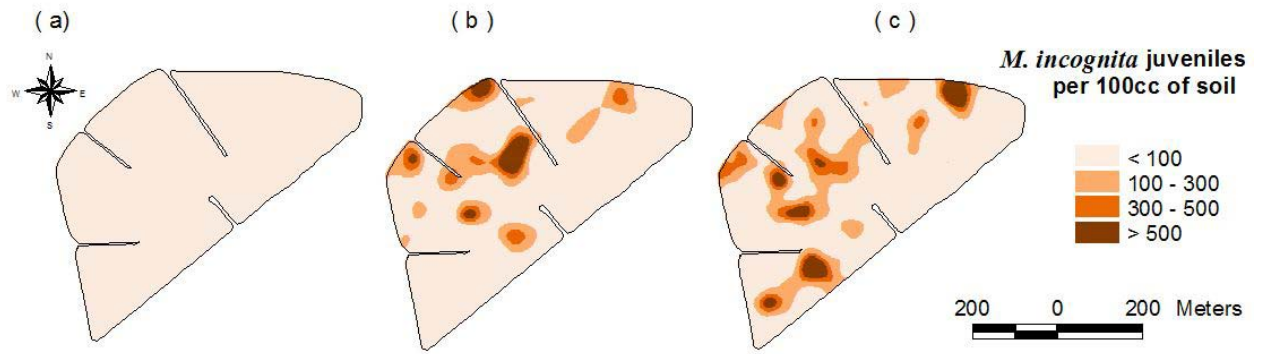


Figure 2.4. Cotton RKN spatio-temporal distribution evaluated RKN1 (a), RKN2 (b), and RKN3 (c) at the PG field in 2006.

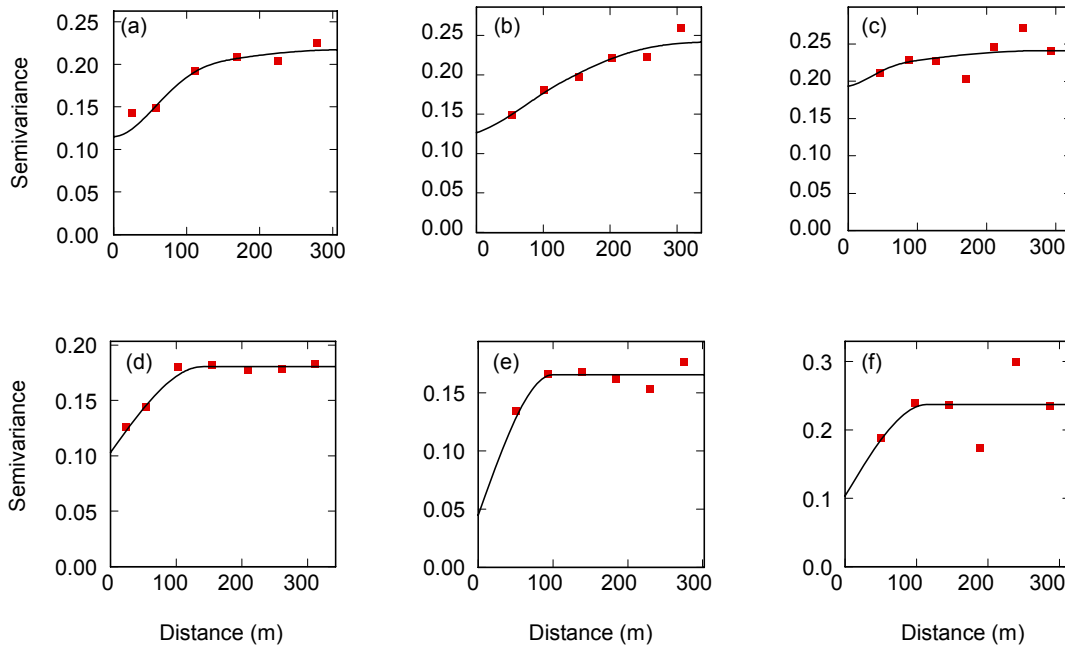


Figure 2.5. Indicator semivariograms of the RKN2 population above a threshold of 100 RKN second stage juveniles per 100 cm<sup>3</sup> soil calculated using hard data of 99 (a), 64 (b), and 35 RKN observations (c). Residual semivariograms using hard and soft data of 99 (d), 64 (e), and 35 RKN observations (f), CC field.

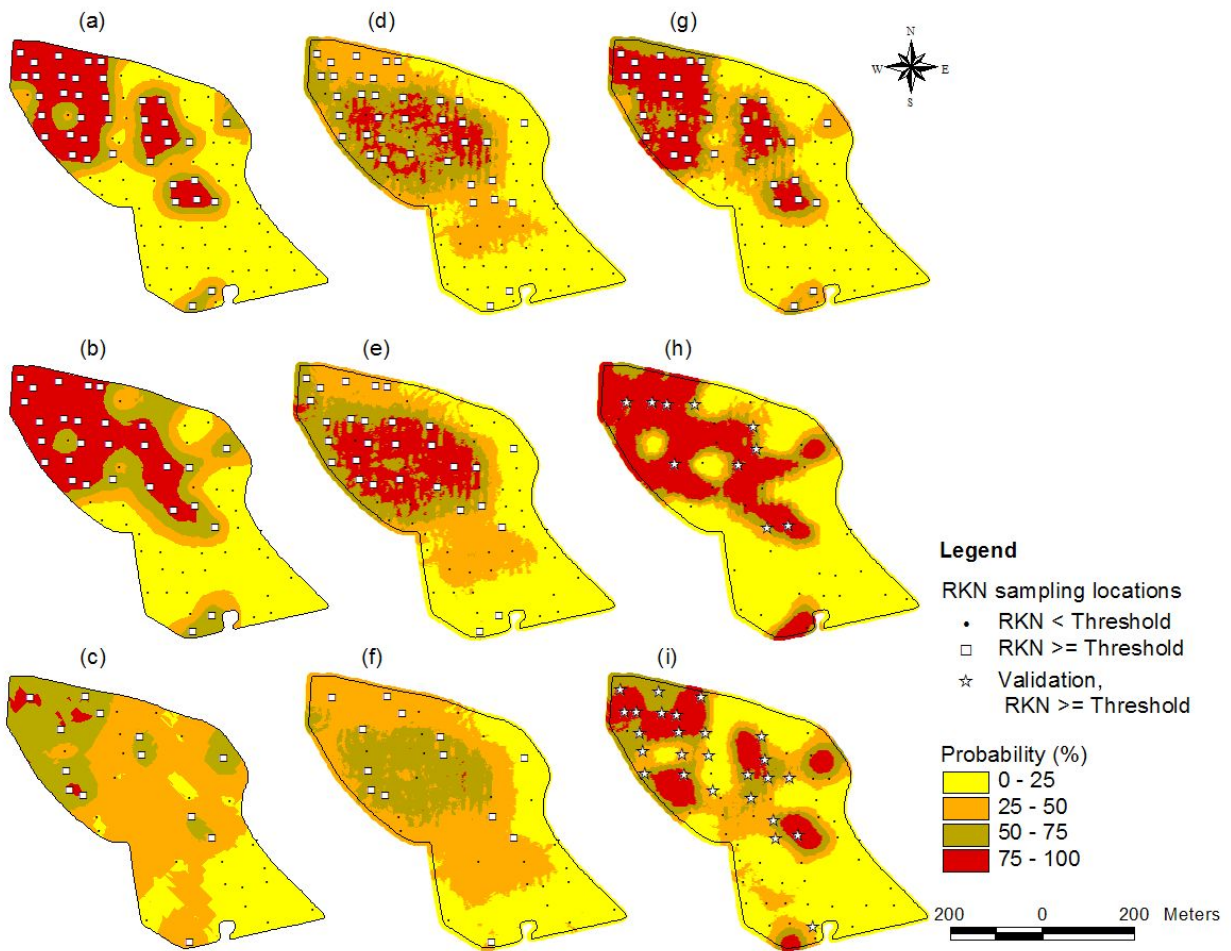


Figure 2.6. Maps of predicted RKN2 risk over the threshold of 100 RKN second stage juveniles per 100 cm<sup>3</sup> soil. Indicator kriging maps of hard data alone based on 99 (a), 64 (b), and 35 (c) RKN2 observations. Soft indicator kriging maps using EC<sub>a-d</sub> as secondary information based on 99 (d), 64 (e), and 35 (f) RKN2 observations. Indicator kriging with a combination of hard and soft data based on 99 (g), 64 (h), and 35 (i) RKN2 observations, CC field.

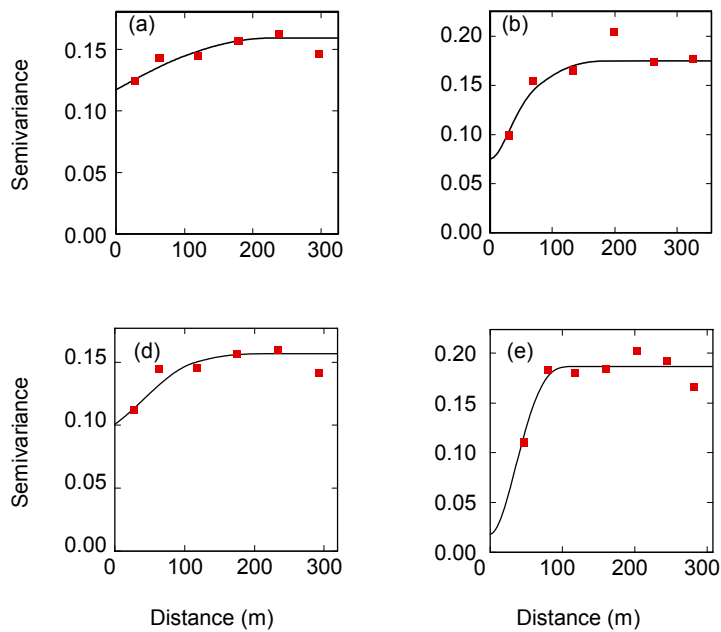


Figure 2.7. Indicator semivariograms of the RKN2 population above a threshold of 100 RKN second stage juveniles per 100 cm<sup>3</sup> soil calculated using hard data of 105 (a) and 70 RKN observations (b). Residual semivariograms using hard and soft data of 105 (d) and 70 RKN observations (e), PG field.

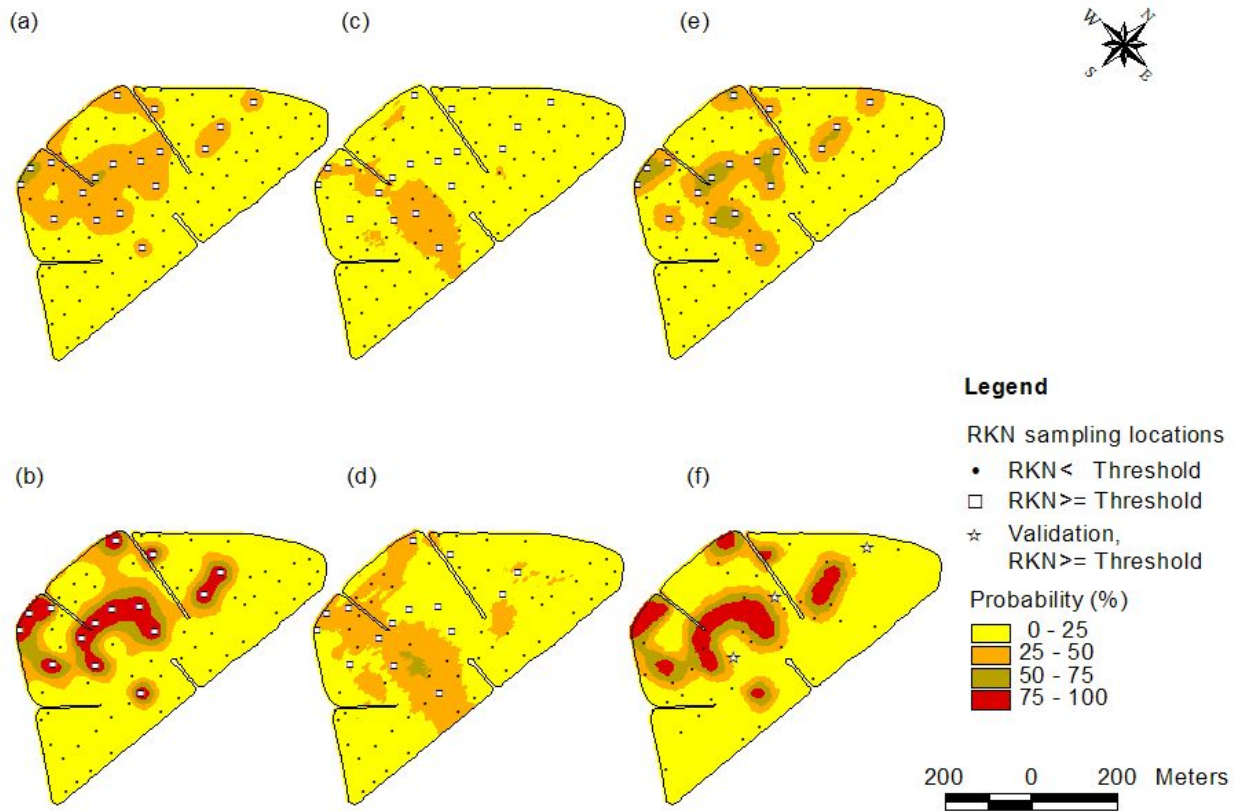


Figure 2.8. Maps of predicted RKN2 risk over the threshold of 100 RKN second stage juveniles per 100 cm<sup>3</sup>soil. Indicator kriging maps of hard data alone based on 105 (a) and 70 RKN2 observations (b). Soft indicator kriging maps using EC<sub>a-d</sub> as secondary information based on 105(c) and 70 RKN2 observations (d). Indicator kriging with a combination of hard and soft data based on 105 (e) and 35 (f) RKN2 observations, PG field.

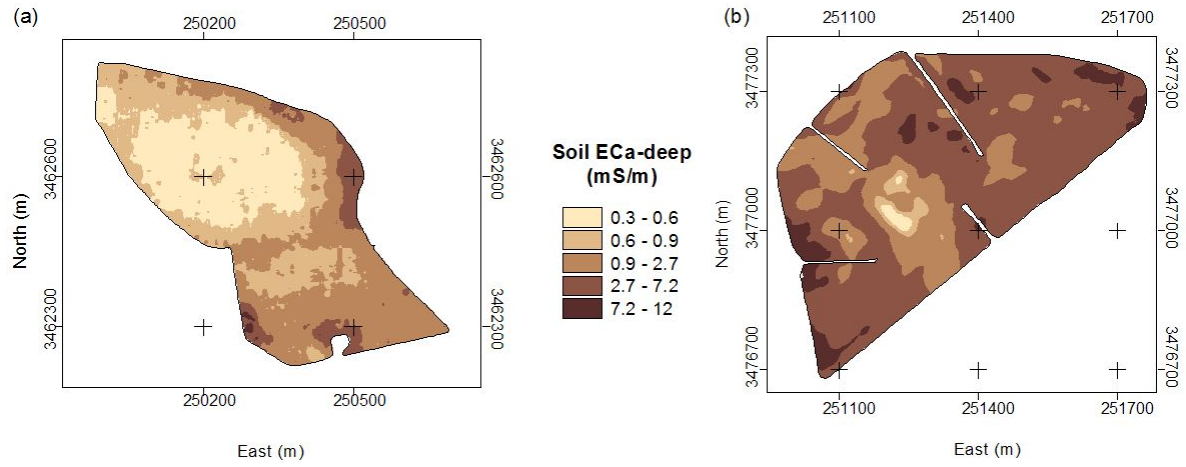


Figure 2.9. Ordinary kriging maps of EC<sub>a-d</sub> for the CC field (a) and PG field (b).

## CHAPTER 3

### DELINEATION OF MANAGEMENT ZONES FOR SOUTHERN ROOT-KNOT NEMATODE USING FUZZY CLUSTERING OF TERRAIN AND EDAPHIC FIELD CHARACTERISTICS<sup>1</sup>

---

<sup>1</sup> Ortiz, B.V., D. Sullivan, C. Perry, G. Vellidis. To be submitted to *Transactions of ASABE*. October 2008.

## Abstract

Delineation of management zones (MZ) for site-specific management of southern root-knot nematode [*Meloidogine incognita* (Kofoid & White) Chitwood] may be used to improve nematode sampling strategies and site-specific application of inputs, in order to reduce yield losses and maximize profitability. Southern root-knot nematode (RKN) occurs in irregular patches and prefers coarse sandy soils. We hypothesized that the integration of terrain (TR) and edaphic (ED) data may be used to identify field features that favor nematode abundance and delineate MZ. The MZ approach suggested here was tested in 11 cotton fields in southern Georgia, USA, during 2005 and 2006. RKN population density within each field was measured four times during each growing season. Apparent soil electrical conductivity [shallow ( $EC_{a-s}$ ) and deep ( $EC_{a-d}$ )], elevation (EL), slope (SL), and changes in bare soil spectral reflectance (Red and NIR reflectance) analyzed through the use of the normalized difference vegetation index (NDVI) were used in a canonical correlation analysis to determine which properties explained the greatest amount of variability in RKN population density. This paper presents a summary of the canonical correlation analysis between RKN and ED/TR variables for the 11 cotton fields, detailed results of the MZ delineation procedure for three fields are presented. The MZ delineation procedure was validated on six of the eleven fields and results are presented. Different combinations of significant ED and TR properties were used to calculate canonical predictors that were entered into a fuzzy clustering algorithm and used to determine the best MZ delineation strategy. The results showed that the combination of all five variables can be used to separate MZ having low and high risk for high nematode population levels. However,  $EC_{a-d}$  alone can also be used for MZ delineation. The zones with elevated risk for high RKN population density were associated with the lowest values of  $EC_{a-s}$ ,  $EC_{a-d}$ , NDVI and SL with respect to the mean values of the variables in each field. The delineation of MZ for RKN using the method presented here can be used for guided sampling and also site specific application of inputs, especially nematicides.

Keywords: Apparent soil electrical conductivity ( $EC_a$ ), Cotton, Fuzzy clustering, Management zones, *Meloidogine incognita*, Spatial variability, Southern root-knot nematodes, Precision Agriculture.

### 3.1. Introduction

Site specific management has emerged as a promising strategy for better management of on-farm resources and optimization of profitability through variable rate application of inputs such as fertilizers, pesticides, nematicides, seeds, and water. This approach could reduce cotton (*Gossypium hirsutum L.*) yield losses up to 10<sup>8</sup> kg caused by the southern root-knot nematode [*Meloidogyne incognita* (Kofoid & White) Chitwood] (RKN) across the U.S. cotton belt, (Blasingame and Patel, 2001). In Georgia, the third largest cotton producer in the U.S. (USDA, 2008), a survey conducted between 2002 and 2003 showed that 69% of fields evaluated were infected with nematodes and high populations of RKN above economic threshold values (100 stage juveniles per 100 cm<sup>3</sup> of soil) were found in 23 of the states' 78 cotton producing counties (Kemerait et al., 2004; Shurley et al., 2004; UGA, 2005).

Although nematodes are found in a variety of soils, RKN prefers coarse-textured, sandy soils and aggregates in irregularly distributed patches (Koenning et al., 2004; Starr et al., 1993). Soil samples are commonly collected to evaluate levels of population densities and decide the need for nematicide application; however high sampling cost restricts the number of samples typically collected. Thus, a poor characterization of the within field spatial distribution of nematodes can result in missed population patches and make the implementation of site-specific management difficult.

The identification of management zones (MZ) with different risk levels for RKN population would be possible if specific biotic or abiotic factors are used as indirect indicators of the presence or absence of this pathogen. Various studies have found nematodes related with soil texture, terrain, soil fertility and soil moisture. Monfort et al. (2007), using initial population of RKN and percent sand fraction, explained 65 - 86% of cotton yield variability measured in

plots of similar geographic locations. Avendaño et al. (2003) found, for example, that patches of soybean cyst nematode (*Heterodera glycines*) not detected by a geostatistical sampling were detected by remotely-sensed images and yield maps. Khalilian et al. (2001) found a strong correlation between the spatial variability of the Columbia lance (*Hoplolaimus Columbus*) nematode and sandy areas identified by measuring apparent soil electrical conductivity (EC<sub>a</sub>). Other research has related abundance of RKN to changes in soil pH (Melakeberhan et al., 2004) and soil moisture (Wheeler et al., 1991). Noe and Barker (1985) evaluated 26 soil physical and chemical properties (soil texture, acidity, base saturation, cation-exchange capacity, percent organic matter, and others) with respect to the spatial distribution of RKN population density. Canonical analyses of the data showed that 50% of the variability in nematode population density was related to high levels of clay, organic matter, low copper concentration, and small changes in percent soil moisture.

A management zone (MZ) is a sub-region of a field that expresses a relatively homogenous combination of yield limiting and reducing factors for which a single rate of a specific input is appropriate according to its yield potential (Doerge, 1999). Multiple management zones may indicate different needs within a field which result in specific management strategies for each zone. Management zones have been used mainly to study variability in crop yield and variable application of inputs (Aaron et al., 2004; Basnet et al., 2003; Fridgen et al., 2000).

The spatial data used to delineate MZ very often exhibit multicollinearity, which makes it necessary to screen out variables or to create a new set of uncorrelated variables based on the original ones. Fraisse et al. (2001a) used principal component analysis (PCA) to screen out covariables used to define clay soil management zones. Partial least squares regression was

employed by Bronson et al. (2005) to create new variables or factors extracted from a relationship between soil  $EC_a$  and seven soil properties.

Canonical correlation analysis (CCA) has been used as another method to determine the relationship between groups of variables because of its potential to account for multicollinearity (Jaynes et al., 2005). It assesses the correlation between the linear combination of a set of Y variables and a linear combination of a set of X variables (Johnson and Wichern, 2002). In this study, CCA was used to study the correlation between RKN population density (Y variable) and edaphic and terrain properties measured from cotton fields (X variables). Canonical correlation analyses have been used to study the relationship between: soil properties and nematode population densities (Noe and Barker, 1985), soil properties and weed populations (Dieleman et al., 2000), field characteristics and soybean plant performance expressed as yield and canopy development (Martin et al., 2005).

In addition to the identification and clustering of different variables strongly related with the phenomenon under study, it is necessary to select the optimum number of clusters or zones in which the variables should be grouped. According to Fraisse et al. (2001b), a cluster analysis allows the identification of areas with similar edaphic, terrain, and plant growth characteristics and the quantification of variability in patterns. Different from a typical cluster analysis, fuzzy *c*-means, a clustering algorithm for continuous classification, allows individual pixels of a data set to have partial class membership in multiple groups which improves the representation of continuous variability found in nature (Fridgen et al., 2000). Fuzzy *c*-means classification has been used to classify continuous data such as soils (Fridgen et al., 2004; McBratney and DeGrujter, 1992; Tarr et al., 2003), yield (Doberman et al., 2003; Fridgen et al., 2000; Jaynes et al., 2003; Li et al., 2007), and remotely sensed images (Boydell and McBratney, 2002; Sullivan

et al., 2005). Therefore, it will be used in this study to identify the optimum number of RKN management zones for a particular producer's field.

Research has shown the need for the identification of areas that are likely to have different levels of RKN, which will allow cotton producers to target the application of nematicides in contrast to the more common approach of a uniform rate (Evans et al., 2002; Wyse-Pester et al., 2002). Therefore, the overall goal of our research was to develop a methodology for creating RKN MZs in cotton fields. The objectives of this study were: (i) to measure the strength of association between edaphic-terrain properties and RKN population through a CCA. If correlation is found, then the hypothesis that measurable field features can serve as surrogate data for RKN will be tested, and (ii) to develop a preliminary framework of procedures for delineating potential RKN MZs based on the fuzzy clustering of surrogate data. The purpose of the MZs is to identify areas with an increased risk of having high RKN population levels, facilitate the definition of nematode sampling strategies, and promote site-specific nematicide control.

## **3.2 Material and Methods**

### **3.2.1 Study fields description and data collection**

Eleven fields from 8 to 25 ha in size located in Colquitt, Tift, and Worth Counties of Georgia, USA, were selected for this study in 2005 (6 fields) and 2006 (5 fields). Because of the large number of fields and large volumes of data collected during the study, three fields having different edaphic and terrain properties were selected for detailed discussion (Table 3.1). All fields were planted with the Delta & Pine Land Company DP 555 BG/RR cotton cultivar. These fields were located in the Tifton-Vidalia Upland (TVU) ecoregion of the southeastern Coastal Plain. The TVU is characterized by relatively homogeneous geology, soils, parent materials,

land use, agricultural management, and economic and social patterns and has become the most intensely row-cropped region of Georgia. Topographically, this is an area of floodplains, river terraces, and gently sloping uplands. Bottom lands are nearly level and most valley flanks are less than 5 percent slope although some slopes of 5 to 15 percent exist. The soils are generally considered sandy to loamy within the first 30 cm of the soil profile (USDA, 2002).

A 50 x 50 m grid (0.25 ha cell size) was superimposed over each study field and sampling locations for RKN population density determination were established at the center of each grid. Soil samples were collected four times during the growing season: June (planting, RKN0), July (first square, RKN1), late August (flowering, RKN2), and October-November (harvest, RKN3). This sampling strategy was adopted because the nematode population density is usually low in spring, but increases through the growing season and reaches peak densities near harvest. At each grid sampling location, eight individual subsamples were collected within a 1.5 m radius and then composited into a single sample representing average RKN per grid cell. Soil probes with a 3 cm diameter opening and approximately 20 cm long were used to extract the soil samples for nematode density analysis. Probes were inserted 15 - 30 cm deep into the soil adjacent to the plant tap root. Nematodes were extracted from 100 cm<sup>3</sup> of soil by centrifugal flotation (Jenkins, 1964).

A Trimble AgGPS 114 Global Position System (GPS) differentially corrected with the Wide Area Augmentation System (WAAS) was used to georeference the location of the RKN samples. This GPS system will be subsequently referred to as DGPS.

### **3.2.2 Apparent soil Electrical conductivity and topography**

Because the spatial variability of RKN has been associated with variability in soil texture and terrain, continuous apparent soil electrical conductivity (EC<sub>a</sub>) and elevation data were

collected for every field one time prior to planting. Apparent soil electrical conductivity has been broadly used as an indirect method to identify changes in soil texture as well as other soil properties (Fridgen et al., 2000; Kitchen et al., 1999; Kitchen et al., 2003; Sudduth et al., 2005). In this study, the VERIS<sup>®</sup> 3100 implement was used to measure  $EC_a$  at two depths into the soil. The implement uses the Wenner or contact method of measuring soil  $EC_a$  with six coulter-electrodes (disks) mounted on a toolbar (Corwin and Lesch, 2005). As the instrument is pulled through the field, one pair of coulter electrodes transmits an electrical current through the soil while another pair of electrodes measures the voltage created by the current (Kitchen et al., 2003). The voltage is then associated with apparent soil electrical conductivity which changes with texture, moisture, pH and other soil properties. The 6-coulter configuration allows the implement to alternatively use two different pairs of electrodes to measure  $EC_a$  at two depths. In our configuration,  $EC_a$  was measured between 0 - 30 cm (shallow,  $EC_{a-s}$ ) and 0 -90 cm (deep,  $EC_{a-d}$ ). An average of 5000  $EC_a$  data points were collected per field. Every  $EC_a$  data point was associated with its corresponding coordinates as recorded using DGPS. Apparent soil electrical conductivity data were collected in 9 m parallel swaths.

Soil cores of 1 m depth and 25 mm diameter were collected at different locations within each field for soil texture determination. The locations were identified based on a proportional stratified random sampling design where the strata were areas of different  $EC_a$  values. Each core was divided into 0-30 and 30-90 cm depth increments and analyzed for soil texture (% sand, silt, clay) determined by the Bouyoucos hydrometer method (Bouyoucos, 1936) and sand particle size (0.044 mm to 2 mm) of each soil sample determined by the pipette method (Day, 1965). The depth increments were selected to coincide with soil electrical conductivity measurements

described above. These data were collected to correlate or relate the differences in  $EC_a$  with respect to within-field variability of soil texture.

Terrain properties such as elevation (EL) and slope (SL) have been considered limiting factors in crop development because of their relation with microclimate, soil particle deposition, and water availability (Fraisie et al., 2001a). Elevation data were collected at the same time as  $EC_a$  data using a Trimble AgGPS 214 real-time kinematic (RTK) GPS mounted on the tractor pulling the  $EC_a$  implement. The system's base-station was located at the edge of the field. Data were recorded at 4 s intervals which corresponded to about 12 m of linear travel

### **3.2.3 Remotely sensed data**

Multispectral airborne and satellite images are recognized to be very useful for describing changes in soil texture and elevation (Barnes and Baker, 2000; Li et al., 2001), iron content variability (Sullivan et al., 2005), and spatial variation of organic C from bare soil images (Chen et al., 2000) among others. Spectral reflectance data of bare soil from QuickBird satellite images were acquired for all fields as an alternative means to evaluate soil texture measured differences. The QuickBird satellite captures reflectance in four spectral bands: blue (450 to 520 nm), green (520 to 600 nm), red (630 to 690 nm) and near infrared- NIR (760 to 900 nm). The images were georeferenced and rectified to the Universal Transverse Mercator projection (UTM), World Geodetic Survey 1984 datum (WGS-84), Zone 17 north. The pixel size of these images is 2.4 meters.

Li et al. (2001) reported high near infrared (NIR) reflectance and low red reflectance on low lying- sandy areas of cotton fields. Based on this, the Normalized Difference Vegetation Index (NDVI) was applied to the multispectral bare soil images to enhance soil texture differences, reduce atmospheric effects and changes in illumination, while reducing the

dimensionality of the data. Normalized Difference Vegetation Index maps showing differences in soil texture were calculated from the red and NIR bands for all fields using equation 1.

$$\text{NDVI} = (\text{NIR} - \text{Red}) / (\text{NIR} + \text{Red}) \quad (1)$$

### **3.2.4 Data processing**

Although the EL and EC<sub>a</sub> data sets comprised more than 7000 observations spatially distributed through each field, the parallel swaths used to collect the data were not always collocated with sampling nodes (grid cell centers). To overcome this, ordinary punctual kriging was used to estimate values of EL and EC<sub>a</sub> at RKN sampling locations (Kerry and Oliver, 2003) using TerraSeer STIS software (Avruskin et al. 2004). Because interpolation by kriging bases the estimations at unsampled locations on their distances to observed data that in this case are spatially dense, the interpolation error will be small.

Raster maps of terrain slope (SL) were derived from EL raster maps using the Spatial Analyst extension of ArcVIEW v. 9.0 (ESRI, 2004). Using ArcVIEW v. 9.0, polygons or buffer areas of 1.5-m radius were created around each RKN sampling location and pixel values from SL as well as NDVI maps within the buffer were extracted, averaged and integrated with the RKN data for further analyses.

### **3.2.5 Data analysis**

#### *Classical statistical analyses*

The departure of RKN data from normality was tested by assessing skewness and by the Shapiro-Wilk and Kolmogorov-Smirnov statistic. Root-knot nematode data with skewness values above + 1 or below -1, data were log-transformed. Descriptive statistics comprised of

mean, minimum (Min), maximum (Max), standard deviation (SD), coefficient of variation (CV), and skewness were calculated for all variables.

The relationship between each of the RKN sampling events (RKN-S0, RKN1, RKN3, RKN-S4) edaphic ( $EC_{a-s}$ ,  $EC_{a-d}$ , NDVI), and terrain (EL, SL) variables was evaluated through Pearson correlation analyses. These analyses were done to identify which RKN sampling event best correlated with edaphic (ED) and terrain (TR) properties and evaluate these relationships through time. Data from the RKN sampling event which best correlated with ED and TR properties were used in the canonical correlation (CCA) and fuzzy clustering analyses.

#### Canonical correlation analysis

Canonical correlation analysis (CCA) assesses the relationship between a linear combination of a set of Y variables (RKN data) and a linear combination of a set of X variables (ED and TR properties). This procedure reduces the dimensionality of the data set and maximizes the separability of different clusters while minimizing the variance within each cluster (Johnson and Wichern, 2002). In this study, CCA was used to measure the strength of association between ED and TR properties and RKN population density, identify ED and TR properties that best explained the largest portion of spatial variability in RKN, and generate a single canonical predictor variable based on different linear combinations of the original variables. The level of significance of the canonical correlation was assessed through the Wilkes-Lambda statistic. If  $P < 0.05$ , the pair of canonical variables was significantly associated by canonical correlation. The eigenvalue is the squared canonical correlation and corresponds to the proportion of variance in the canonical predictor variable explained by the canonical correlation relating a pair of canonical variables. The canonical correlation value in this study corresponded to a bivariate correlation between an edaphic-terrain canonical variable (linear

combination of ED and TR properties) and a RKN canonical variable (RKN data) (Garson, 2007).

The loadings, or canonical structure correlation in the CCA, indicate the simple linear relation between the original variables and the canonical predictor. Variables having a high contribution to the predictor are those that exhibit large loadings. In this case, based on the loadings of the ED and TR properties to the edaphic-terrain canonical variable, different combinations of ED and TR properties were used to calculate canonical composites or canonical predictor variables for RKN which latter should be used in the clustering analysis (Jaynes et al., 2005). New canonical predictor variables were calculated using the following three strategies:

1. all the ED and TR properties,
2. three of the properties having the highest loadings in the edaphic-terrain canonical variable, and
3. two of the properties having the highest loadings in the edaphic-terrain canonical variable.

Every new canonical predictor variable based on strategies one to three was entered into a fuzzy *c*-means algorithm to identify the optimum number of MZs derived from it.

#### *Cluster analysis and optimum number of zones*

Cluster analysis of predictor variables was chosen to identify areas that are comprised of ED and TR features with a high likelihood of having RKN. By delineating “at risk zones”, targeted sampling and variable rate application strategies can be more effectively used.

Scores of the three different canonical predictor variables (strategies) at each sampling location for each field were separately entered into the Management Zone Analyst v1.0.1 (MZA) software (Fridgen et al., 2004) for the fuzzy clustering analysis. The MZA utilizes a fuzzy *c*-

means algorithm and the Euclidean or Mahalanobis distances to separate the data into clusters or zones. The maximum number of permissible zones was set at six. Consequently, the software generated five different MZ scenarios for each strategy – two, three, four, five and six clusters or zones. Thus, a total of 15 possible MZ options (up to five type of zones by three predictor scenarios) were available for evaluation per field. Each one of these MZ options was separately evaluated to determine the optimal number of MZs in each field.

MZA generates two different performance indices – normalized classification entropy (NCE) and the fuzziness performance index (FPI) – which were used as a first step towards identifying the optimum number of MZs. In general, the optimum classification is the one having the lowest values of FPI and NCE with the least number of clusters used (Fridgen et al., 2004).

In addition to the FPI and NCE indices, pooled variances ( $S_p^2$ ) of RKN population density and the ED-TR properties were calculated for each predictor variable and zones scenarios. The pooled variance ( $S_p^2$ ) was calculated based on the mean and variance ( $S_i^2$ ) for each zone and the number of zones. Pooled variances ( $S_p^2$ ) were calculated based on the  $S_i^2$  within each zone using the equation:

$$S_p^2 = \frac{\sum_{i=1}^z (n_i - 1)s_i^2}{\left[ \sum_{i=1}^z (n_i) - z \right]} \quad (2)$$

where  $z$  represents the number of sampling zones previously defined by the fuzzy clustering analysis,  $n_i$  corresponds to number of observation or sampling locations within the zone  $i$ , and the  $s_i^2$  was the within-zone variance calculated for zone  $i$  (Steel and Torrie, 1980).

The field variance was calculated for each data set using the equation:

$$S^2_{field} = \sum_{i=1}^n (x_i - \bar{x})^2 / (n - 1) \quad (3)$$

where  $x_i$  was the RKN or ED-TR value at each sampling location  $i$  and  $\bar{x}$  was the whole field mean. Significant reductions in pooled variances for a specific number of zones-predictor variable and the whole field variance were determined by an  $F$  value ( $S^2_{field} / S^2_p$ ) at  $P \leq 0.1$  as indicated by Chang et al. (2003). The best number of zones explaining the variability of RKN was selected according with the results of performance indices and pooled variance. These analyses were performed to determine: how much was gained in terms of nematode population homogeneity within a zone by dividing the field in additional zones (Fraisie et al., 2001a) and the impact of a specific number of zones on explaining within-zone RKN population density (Chang et al., 2003).

Figure 3.1 shows an example of the change in FPI and NCE values as the number of MZs increase in the CC field. Figure 3.1 also shows the pooled variances calculated for a specific canonical predictor and number of zones. Fuzziness performance index-FPI decreases as the number of zones increase, reaching a minimum value when the zones are four (0.26) or six (0.36). However, the NCE values indicated that the best delineation (lowest values) could be one with three or six zones. Because of the disagreement between the FPI and NCE indices with respect to the best number of zones, the pooled variances ( $S^2_p$ ) for each zone number were calculated and compared to the whole field variance. When the number of zones or clusters increases, some of them tend to have few observations which sometimes are scattered through the field making the process of interpretation and association with field features more difficult. The results from fuzzy clustering and pooled variance showed that the best management zone

delineation corresponded with three zones. For every field, the same procedure was implemented to establish the optimum number of MZs for each of the three strategies.

#### Assessing management zone delineation

Ideally the management zone delineation will result in homogenous zones, each of which has a much lower variability in RKN population as well as ED and TR features compared to the entire field. For each field and management zone delineation strategy, the mean and coefficient of variation (CV) of each zone with respect to RKN population density and the ED and TR properties was compared to the means and CVs of the whole field. This procedure allowed one to identify the differences in each zone with respect to RKN population density and also the ED and TR features associated with a low or high likelihood of having RKN. Pooled variances were also used to determine differences between whole field variance and variance accounted for each predictor-number of zones combination.

### **3.2.6 Validation of the management zone delineation procedure**

The RKN management zones' procedure was validated on six producer's fields using data collected from 5 fields during the 2005 growing season and 1 field during the 2006 growing season. For each field, management zones were delineated from fuzzy clustering of ED and TR properties. The best number of clusters or zones in which the data set should be divided was based on the values of the FPI and NCE indices reported from the MZA software.

Subsequently, the mean and coefficient of variation (CV) of RKN population density and the ED and TR properties within zone were calculated for zones comparison.

### 3.3 Results and Discussion

#### 3.3.1 Classical statistical analyses

Descriptive statistics of RKN assay results and ED and TR properties are presented in Table 3.2. Data sets with skewness values above + 1 or below -1 were log-transformed for calculation of Pearson's correlation coefficients and canonical correlation analyses.

Root-knot population density varied significantly within and between fields across sampling dates. The mean RKN population density showed an increase from RKN1 to RKN2 (approximate mid season) (Table 3.2). The high mean RKN population density observed in late August (RKN2) contradicts the generally accepted premise that the highest population density is found at harvest. This finding may be related to drought conditions during September and October of the 2006 growing season and with the observed decay of root biomass towards the end of the growing season. Root-knot population density measured in the three fields was highly skewed and not normally distributed (Table 3.2).

There were both similarities and differences between the ED and TR properties of the three fields. The fields exhibited small changes in EL as indicated by the low standard deviation (SD) and coefficient of variation (CV) (Table 3.2). In contrast, SL exhibited more variability, especially at the CC and CMP fields. The SL at PG field exhibited a broader range of variation and a high CV even though most of the field exhibited a slope range of 2% to 6%. Low values of  $EC_a$  (shallow and deep) and low variability were common for all the fields and indicated sandy soils.

Although RKN population densities changed through time, significant correlations between RKN1 and RKN2 and between RKN2 and RKN3 suggest that the spatial distribution of

RKN was consistent over time (Table 3.3). In the CC and PG fields, there were significant negative correlation between  $EC_a$  (shallow and deep) and RKN population.

### **3.3.2 Canonical correlation**

Because RKN population density sampled in late August (RKN2, flowering) best correlated with ED and TR properties in more than 50% of the 11 fields included in this research, these data were used for the CCA (Tables 3.3-3.4).

Canonical correlation analyses (CCA) between the edaphic-terrain canonical variable and the RKN canonical variable were performed individually for the 11 fields (Table 3.4). Significant canonical correlations ( $P < 0.05$ , Wilk's Lambda) were observed in four of the six fields studied in 2005 and four of the five studied fields in 2006. The eigenvalues indicated that more than 50% of the variability of the canonical predictor variable was explained by the canonical correlation between the edaphic-terrain canonical variable (strategy one) and RKN canonical variable in six of the eleven fields. The properties with high influence on the single canonical predictor variable were those that exhibited large loadings (Table 3.4). For the edaphic-terrain canonical variable, the properties with the highest loadings between all the fields were  $EC_a$  (shallow or deep), EL, and SL, respectively.

Overall, higher loadings were observed for the edaphic properties than the terrain properties. Both  $EC_{a-s}$  and  $EC_{a-d}$  had similar contributions in explaining the variability of RKN between fields and their relation was inverse in 60% of the fields (Table 3.4). Low  $EC_a$  values have been related to sandy or coarse-textured soils by other researchers (Khalilian et al., 2001). Therefore, our data reaffirmed that nematodes prefer sandy areas. Perry et al. (2006) reported an inverse relationship between  $EC_a$  and sand content for the 2005 fields included in this study.

Data from the 2006 fields showed a negative correlation between  $EC_a$  and increasing soil particle size [from medium (0.25 mm) to coarse (2 mm)] and a positive correlation with decreasing particle size (medium to fine). This evidenced the sensitivity of  $EC_a$  for segregating areas of different particle size.

A positive correlation between EL and RKN population was observed on eight of the eleven fields in this study (Table 3.4), however this relationship was not very strong because most fields exhibited small changes in elevation which is typical for the southern Coastal Plain (Table 3.3). In contrast, Ortiz et al. (2006) found an inverse relationship between elevation and nematodes ( $r = - 0.36$ ) using data pooled from all the 2005 fields. This relation could be explained through the positive correlation between elevation and  $EC_a$  found when 2005 and 2006 data were pooled. Therefore, this data reaffirmed that low-lying areas in our landscape typically exhibit coarser textured soils as a result of erosional deposition where nematodes are prone.

Although the relationship between bare soil NDVI and RKN was not consistent between fields, a strong negative correlation was observed at the RB and CC fields indicating that areas with low values of bare soil NDVI were associated with areas of high RKN population density (Table 3.4). A similar relationship was observed by Ortiz et al. (2006) using data only from the 2005 fields. The coarser sandy areas with low values of  $EC_a$  in the studied fields exhibited lower NDVI values than the finer sandy soils or soils with increased clay content (Table 3.3). Because the soils in the southern Coastal Plain are mainly sandy, soil spectral reflectance in the NIR band is higher than the red band. However, smaller differences in soil spectral reflectance between these two bands were found in the coarser sandy areas than in the finer sandy areas. Similarly, Li et al. (2001) found that low lying areas with sand content higher than 740-828  $g\ kg^{-1}$  in the first 30 cm depth had high reflectance in the NIR and low reflectance in the red and middle infrared

(MIR). Sullivan et al. (2005) found a negative correlation between clay content and Red (630 to 690 nm) and NIR (760 to 900 nm) reflectance on soils from the Tennessee Valley and Coastal Plain of Alabama. They also found that visible and NIR reflectance increase as the clay content in the soil decreased.

### 3.3.3 Fuzzy clustering and optimum number of zones

The loadings or canonical structure correlations between the edaphic-terrain canonical variable and the ED and TR properties for the CC, PG, and CMP fields are presented in table 3.4. At the CC field, the edaphic-terrain canonical variable and EL were strongly correlated (0.96), however it was not included into the strategies two and three for MZ delineation because of the small changes in terrain observed throughout this field. Therefore, the second strategy included the variables of SL,  $EC_{a-d}$ , and NDVI while the third strategy included the  $EC_{a-d}$  and SL variables. At the PG field, the variables of  $EC_{a-s}$ ,  $EC_{a-d}$ , and NDVI with the three highest loadings were used for MZ delineation-strategy 2 while the third strategy only included the  $EC_{a-s}$ ,  $EC_{a-d}$  variables. Finally, at the CMP field the three highest correlations were observed for EL,  $EC_{a-s}$ , and NDVI in that order while the two most contributing variables were  $EC_{a-s}$  and NDVI. Therefore, these variables were used to calculate canonical predictors that were later used for MZ delineation.

The results and evaluation of the different MZ delineation strategies for the CC, PG and CMP fields are presented in tables 3.5 to 3.10. Overall, there were significant reductions of RKN pooled variance ( $S^2_p$ ) with respect to the RKN field variability ( $S^2_{field}$ ) for each of the MZ delineation strategies evaluated on the three fields. However, the percentage of reduction in

RKN variability depended on the type and number of variables used to estimate the canonical predictor variable.

The evaluation of each MZ delineation strategy was also based on the comparison of between-zones mean  $\text{Log}_{10}$  RKN and CV respect to the whole field. Overall, the zone having the highest mean  $\text{Log}_{10}$  RKN2 had the lowest CV with respect to the CV of the whole field and was significantly different from the zone having the lowest RKN population density. This indicates that the ED and TR variables evaluated in this study can be used to segregate areas having high and low risk for high RKN population density.

#### CC field

At the CC field, the  $S_p^2$  of RKN was reduced 51% using strategy one and three MZs (Table 3.5). Strategy two with four zones reduced  $S_p^2$  of RKN by 24% while strategy three with three zones reduced  $S_p^2$  of RKN by 28% (Table 3.5). For the strategies one and two, the EL, SL,  $\text{EC}_{a-d}$  variables exhibited significant reductions in  $S_p^2$  with respect to the whole field. However, no significant reductions in  $S_p^2$  were observed for NDVI which may be explained by its low within-field variability (CV = 35%).

In general, for each MZ delineation strategy the most homogeneous zone was the one having the highest RKN population density with the lowest CV compared to the whole field (Table 3.6). The variability of  $\text{Log}_{10}(\text{RKN2})$  within this zone compared to the whole field was reduced by 59%, 57%, and 60% for the strategies one, two and three, respectively. The zone with the highest RKN occurrence was associated with the lowest values of  $\text{EC}_{a-d}$  ( $\leq 0.67 \text{ mS m}^{-1}$ ), SL ( $\leq 0.7\%$ ) and NDVI ( $\leq 0.06$ ) which mainly characterized sandy areas (Table 3.6).

### *Strategy one*

Zone three, having the highest RKN population density was the most homogeneous, with a within zone RKN variation reduction of 59% respect to the whole field. The ED and TR properties with the highest CV reduction were EL and  $EC_{a-d}$ , 77 % and 71.6%, respectively. This indicates that these two variables were the primary contributing variables differentiating this zone. Zone three was mainly characterized by having the lower  $EC_{a-d}$  ( $\leq 0.60 \text{ mS m}^{-1}$ ), SL ( $\leq 0.7\%$ ), and NDVI ( $\leq 0.06$ ) mean values compared to zones one and two. Soil samples randomly collected at a depth of 0-90 cm within this zone showed that soil was composed of more than 93% sand, 3% clay, and 4% silt. A sand fraction analysis showed that 55% of the sand in this area had particle size in a range of 0.25mm to 2 mm. Therefore, the low values of  $EC_a$  can be related with an increase in coarse sand in the  $\geq 0.25 \text{ mm}$  range. Data are consistent with previous findings, which have shown that RKN tend to occur at higher densities in sandier soils, which in turn are associated with low  $EC_a$  readings (Khalilian et al., 2001; Monfort et al., 2007). Although zone three had the highest EL, the effective range in elevation throughout the field was very low (76.0 to 79.8 m) with a CV of 2.1%. This indicates that no meaningful relationship existed between elevation and RKN distributions.

A map depicting the three MZs delineated using strategy one is shown in figure 3.2a. This map illustrates good spatial distinction of zones having different levels of RKN population density. The MZ map also has similarities with spatial patterns in the  $EC_{a-d}$  map (Figure 3.2f) which reaffirm the impact of this variable on the segregation of zones having high and low risk for RKN occurrence.

The lowest RKN population density was found in zone one (Figure 3.2a) in which the RKN variability was not reduced with respect to the whole field. However, the variability of SL

and NDVI was reduced 54 % and 46 %, respectively. This zone was mainly characterized by having higher  $EC_{a-d}$ , SL, and NDVI mean values than zones two and three. The mean  $EC_{a-d}$  values within this zone ( $2.0 \text{ mS m}^{-1}$ ) increased 70% with respect to the mean  $EC_{a-d}$  of the field ( $1.17 \text{ mS m}^{-1}$ ). Compared to zone three, this zone was composed of 89% sand, 2% clay, and 9% silt with 49 % of the sand particles having a sand size fraction between 0.106 and 0.044 mm. The increase in silt percent and decrease in sand particle size as well as the increase in slope may be related with the decrease in RKN population density and an increase in soil moisture. Increases in soil water matric pressure and soil moisture associated with increases in fine soil particle size classes have been reported as detrimental for nematode reproduction, hatching and movement (Koenning and Barker, 1995).

The mean NDVI values within zone one (0.10) increased 66% with respect to the mean NDVI of zone three (0.06) and 25% with respect to the mean NDVI of the whole field. The high values of NDVI in zone one may indicate a darker soil with an increase in soil moisture which might be related with the increase in fine particles where nematodes seem to be less prone.

#### *Strategy two*

Although the pooled variance analysis indicated that RKN variability was only reduced by 24% using strategy two compared to 51% of strategy one, the  $S_p^2$  of the ED and TR properties used in strategy two were reduced (Table 3.5). Zones three and four reduced the within zone RKN variability by 35 and 57 %, respectively (Table 3.6). The highest RKN population densities were observed in zones three and four (Table 3.6, Figure 3.2c). In zone four, the variables with the highest CV reduction were  $EC_{a-d}$  and NDVI, 76 % and 20.6%, respectively. Therefore, this zone is homogeneous with respect to  $EC_{a-d}$  and NDVI which indicates homogeneity of soil textural conditions. The low values of NDVI in this zone agree with the low values of  $EC_{a-d}$ .

There was a large positive correlation between NDVI with  $EC_{a-s}$  (0.76) and  $EC_{a-d}$  (0.47) demonstrating the strong relationship of high NIR reflectance and coarser sandy textures. These findings support the idea of using bare soil NDVI as a surrogate data of soil texture and indirect factor for assessing areas at risk for high RKN population levels. The low values of  $EC_{a-d}$  ( $\leq 0.60$   $mS\ m^{-1}$ ), SL ( $\leq 0.56$ ), and NDVI ( $\leq 0.06$ ) in zone four mainly characterized areas of coarse texture in which there is high occurrence of high RKN population density (Figure 3.2c).

When comparing the zones, similarities with respect to the mean values of  $\text{Log}_{10}(\text{RKN2})$ , EL,  $EC_{a-d}$ , SL, and NDVI were found (Table 3.6). Root-knot nematode population levels [ranging from 1.11 to 1.27  $\text{Log}_{10}(\text{RKN2})$  population] in zones one and two were similar but the CVs did not decrease with respect to the whole field. In contrast, zones three and four were similar, homogeneous, and had higher RKN population than zones one and two. Similarities between zones three and four were also related with the  $EC_{a-d}$ , and NDVI average values. Hence, data suggest that the overall number of zones for the strategy two could be reduced. The similar CVs for RKN, EL, and NDVI for zones one and two suggested that these two zones could be grouped in one zone. These zones were mainly characterized by high values of  $EC_{a-d}$ , SL and NDVI and low RKN population density, and then a low risk for RKN occurrence could be established. Similarly, the zones three and four with close CV values can be grouped in a zone with the highest risk for RKN occurrence. These results show that strategy two is useful for segregating two distinctive areas having low and high risk for RKN occurrence.

### *Strategy three*

When the zones were delineated using the strategy three, only 45% of the  $EC_{a-d}$  and SL variability was linearly associated with the RKN variability. The within zone RKN variability was reduced by 60% in zone three, with 2.12  $\text{Log}_{10}(\text{RKN2})$  population. Also in this zone, the

variability in  $EC_{a-d}$  and SL was reduced 61% and 13%, respectively, with respect to the whole field. Therefore,  $EC_{a-d}$  seemed to be the primary factor for MZ delineation using this strategy. The map depicting the three MZs delineated using strategy three is shown in figure 3.2d. This map shows that zone three, highest risk for RKN occurrence, resembles the area with the highest RKN population density in figure 3.2b. The random pattern followed by the few locations assigned to zone one explains the high variability in RKN population and  $EC_{a-d}$ .

### PG field

At the PG field, the  $S^2_p$  of RKN was reduced 30%, 42%, and 26 % for strategies one, two and three, respectively (Table 3.7). The  $S^2_p$  of  $EC_{a-s}$  and  $EC_{a-d}$  was also significantly reduced with respect to the whole field for each one of the strategies. However, no significant reductions in the  $S^2_p$  were observed for SL and NDVI on any of the evaluated strategies (Table 3.7).

In the PG field as well as the CC field, each MZ delineation strategy identified a zone, zone three, with the highest RKN population density, which was the most homogeneous and had the lowest CV compared to the whole field (Table 3.8). The variability (CV) of  $\text{Log}_{10}(\text{RKN}2)$  within this zone compared to the whole field was reduced by 38%, 44%, and 36% for the strategies one, two and three, respectively. The zone with the highest RKN population density was mainly characterized by having the lowest  $EC_{a-s}$  ( $\leq 1.15 \text{ mS m}^{-1}$ ) and  $EC_{a-d}$  ( $\leq 2.5 \text{ mS m}^{-1}$ ). Soil samples randomly collected at a depth of 0-30 cm within zone three-strategy one showed that soil was composed of 92% sand, 2% clay, and 5% silt. Data emphasized the preference of RKN for sandy areas characterized by having low values of  $EC_{a-s}$  and  $EC_{a-d}$ . In contrast to the CC field, this zone had the highest mean values of SL. This disparity could be associated with a poor differentiation of areas with abrupt changes in slope. Contrasting with zone three, zones one and two with the lowest RKN population density represented the low risk areas for high RKN

population levels. These zones had the highest  $EC_{a-s}$ ,  $EC_{a-d}$  and NDVI mean values compared to mean values for the field. The high mean values of  $EC_{a-s}$ ,  $EC_{a-d}$  and NDVI in zone two – strategy one can be related with the increase in clay (12%) and silt (11%), and a decrease in sand content (67%) compared with zone three.

The homogeneity in EL and bare soil NDVI expressed by the low CV values indicated the low contribution of these variables to MZ delineation (Table 3.4). This low contribution could be expected considering low canonical correlations with values of 0.48, 0.43, 0.41 for strategies one to three, respectively. Data suggest that in each of the three strategies evaluated the zones can be combined and the overall number of zones discriminating between low and high risk for high RKN population levels could be reduced from three to two. For most of the strategies, the variability in RKN population, EL, SL and NDVI with respect to the whole field was not reduced in zones one and two which justify the combination of them into a single zone with low risk for RKN occurrence

The high contribution of soil texture, expressed by changes in  $EC_{a-s}$  and  $EC_{a-d}$  to the discrimination of areas at risk for RKN population occurrence was evidenced by small differences between strategy one (all the ED and TR properties), strategy two (properties related to soil texture differentiation) and strategy three ( $EC_a$  which is related to soil texture differentiation). It shows the potential of  $EC_a$  (shallow and deep) as surrogate data for RKN MZ delineation in this field.

### CMP field

At the CMP field, the RKN population density evaluated at mid season and harvest exhibited low variability throughout the field compared with the CC and PG fields. The CV values for RKN2 and RKN3 were 79 and 75.2 respectively (Table 3.2). Because of RKN3

exhibited a significant correlation with  $EC_{a-s}$  and NDVI, these data were used to evaluate their potential for MZ delineation (Table 3.3).

At the CMP field, the  $S_p^2$  of RKN was reduced 60 % when using strategies 2 and 3 . Contrasting with the other two fields, none of the  $S_p^2$  for the ED and TR properties tested as surrogate data for RKN was reduced with respect to the  $S_p^2$  for whole field (Table 3.9).

Different from the CC and PG fields, there were no distinct field features strongly related with the zone of the highest RKN population density which might suggested a poor level of aggregation followed by RKN3 (Table 3.10). When a semivariogram of RKN3 was calculated, a pure nugget effect (0.16) was found. Therefore, the poor distinction of areas with low and high RKN population density made the process of identification of surrogate data for RKN management zone delineation very difficult.

For all the strategies, because two locations having very low RKN population were only included in zone one, the discussion will be focused on the results from the other zones. In general, for each MZ delineation strategy the most homogeneous zone was the one having the highest RKN population density and lowest CV compared to the whole field (Table 3.10). Zone three, for strategies two and three was significantly different from the other two zones with respect to RKN population and within-zone bare soil NDVI. Positive correlations between bare soil NDVI and  $EC_{a-s}$  for zone three derived from strategies two (0.32) and three ( 0.71) reemphasized previous findings relating low NDVI values with coarser sandy areas where RKN population is prone.

Although fuzzy clustering analysis divided the canonical predictor calculated from strategy one into four zones, there were zones having similar RKN population density as well as ED and TR features. For example, zones three and four were similar with respect to RKN

population, EL and  $EC_{a-s}$ , but different with respect to  $EC_{a-d}$ , SL, and NDVI. The canonical correlation indicated that  $EC_{a-s}$  was the variable most highly correlated with RKN population density. However, zones two, three, and four had similar average  $EC_{a-s}$  which may be associated with the low within-field variability with respect to RKN population as well  $EC_{a-s}$  (Table 3.4, 3.10). The variability in zone four, the zone with the highest RKN population density, was only reduced 7% with respect to the field average of RKN population (Table 3.10).

Even though there were significant differences in RKN population density between zone two and three when strategies two and three were evaluated, there was not much difference between ED and TR features. The low variability of the RKN population density and the random pattern of the sampling locations with high RKN population made the identification of ED and TR features associated with RKN occurrence very complex. The conditions observed in this field illustrate the difficulties of delineating MZ for site-specific RKN management when the RKN population density is not highly structured and there is not enough within-field variability of field features.

### **3.3.4 Validation of the management zone delineation procedure**

For each one of the six fields where the MZ procedure was validated, the results from fuzzy clustering of ED and TR properties showed that it was possible to segregate a zone having the highest RKN population and the lowest CV with respect to the mean and CV for the whole field (Table 3.11). Zone 3 for the fields 1, 2, and 6 as well as zone 4 for the fields 3, 5 and 8 had the highest RKN population with respect to the whole field mean. These zones consistently had low  $EC_{a-s}$  and  $EC_{a-d}$  values compared to the whole field mean. In contrast, the characteristics of these zones with respect to EL, SL, and NDVI change from field to field. In most of the fields,

zone 1, with the lowest RKN population, exhibited higher  $EC_{a-s}$  and/or  $EC_{a-d}$  values compared to the  $EC_{a-s}$  and/or  $EC_{a-d}$  values of the zones having the highest RKN population density.

The percentage increase in RKN population for the zone with the highest RKN population with respect to the whole field RKN mean was 33%, 7%, 360%, 78%, 58%, and 18% for the fields 1, 2,3,5,6, and 8 respectively. For the same fields, the reduction in  $EC_{a-d}$  values within that zone with respect to the whole field  $EC_{a-d}$  mean was 14%, 25%, 69%, 74%, 22%, and 34%, respectively (Table 3.11).

These results show that the ED and TR properties can be used to segregate areas having high and low risk for high RKN population density. However, the  $EC_{a-s}$  and  $EC_{a-d}$  properties offer much more stable information to characterize areas with low and high risk for having presence of RKN population.

### **3.4 Summary and Conclusions**

The results from this research showed that zones with high and low risk for RKN population occurrence can be delineated using edaphic (ED) and terrain (TR) properties. The three fields presented in detail this study had both similarities and differences with respect to the variability in RKN population density as well as the ED and TR properties which can be viewed as three different scenarios faced by the cotton producers. The analysis of the results from the MZ delineation for these fields as well as the fields used for the validation indicated that areas likely to have high levels of RKN population might be mainly identified through the within field changes in apparent soil electrical conductivity (shallow-  $EC_{a-s}$  or deep- $EC_{a-d}$ ). However, if the field exhibits significant variability in terrain properties, flat areas will be more likely to have high RKN levels.

At the CC and PG fields, the zone with the highest RKN population (high risk zone) was the most homogeneous (the lowest CV with respect to the whole field) and was characterized by having the lowest mean values of  $EC_{a-s}$ ,  $EC_{a-d}$ , NDVI and SL. In contrast, the zone with the lowest RKN population density (low risk zone) exhibited the highest values of  $EC_{a-s}$ ,  $EC_{a-d}$ , NDVI and SL with respect to the average values of the field. This zone also did not have a significant reduction in RKN variability compared to the whole field. This phenomenon was likely due to the random pattern that nematodes exhibit in nature, particularly under conditions in southern Georgia, USA.

Although the discrimination of zones with different levels of risk for RKN occurrence have been viewed as the differentiation between sand, clay and silt areas within a field with sandy areas being the ones with high risk; this type of strategy does not directly apply to south Georgia. In south Georgia there is not high variability in soil textural classes within the fields. In contrast, there is a high predominance for coarse sandy textures. Therefore the differentiation of the zones at risk for nematode occurrence must be based on the segregation of sandy areas with different particle size. Similar conclusions were reached by Monfort et al. (2007). The on-the-go sensing of changes in apparent soil electrical conductivity ( $EC_a$ ) through a field brings an alternative for the discrimination of areas with differences in soil texture and particle size. A correlation analysis between sand fraction data and  $EC_a$  supported the hypothesis that  $EC_a$  (shallow or deep) is sensitive to changes in particle size with  $EC_{a-d}$  being more sensitive. When  $EC_a$  (shallow or deep) was evaluated for MZ delineation, significant differences between zones with high and low RKN population density were observed. This shows the potential for  $EC_a$  to serve as surrogate data for RKN MZ delineation. The positive correlation between  $EC_a$  and NDVI calculated at bare soil conditions and the significant differentiation of RKN risk areas

suggested that NDVI also can be used as surrogate data for RKN. Although this type of data did not provide strong discrimination of the areas with a high likelihood for having high RKN population as the EC<sub>a-s</sub> or deep-EC<sub>a-d</sub> data did. The differentiation of MZ improved when NDVI and EC<sub>a-s</sub> or deep-EC<sub>a-d</sub> were combined. The validation results of the RKN MZ delineation from six fields reaffirmed that the EC<sub>a-s</sub> and EC<sub>a-d</sub> properties offer much more stable information to characterize areas with low and high risk for having presence of RKN population

Results from this study indicate that RKN management zones delineated from surrogate edaphic data could facilitate the SSM of RKN, especially the site specific application of nematicides. The results also showed that if there is neither structured within-field spatial variability for RKN population nor edaphic or terrain properties; no discrimination by management zones is recommended.

In addition to the results presented here, the MZ approach might bring the opportunity to decide various threshold values for nematicide application within a single field.

### **Acknowledgments**

This work was supported by funds from Cotton Inc., the Georgia Cotton Commission, the Flint River Water Planning and Policy Center, Hatch and State funds allocated to the Georgia Agricultural Experiment Stations and by USDA-ARS CRIS project funds. Many thanks also to Dr. Robert Nichols from Cotton Inc. whom supported this project. Finally, special thanks to Dewayne Dales, Gary Murphy, Rodney Hill, Andrea Milton, Keith Rucker, Katia Rizzardi, Manuel Renga, Melanie Blomenhoer, Eleni Tzanakouli, Jason Tood, who assisted with the extensive field work required to complete this study.

Mention of commercially available products is for information only and does not imply endorsement

## References

- Aaron, R.S., J.F. Shanahan, M.A. Liebig, J.S. Schepers, S.H. Johnson, and A.J. Luchiari. 2004. Appropriateness of management zones for characterizing spatial variability of soil properties and irrigated corn yields across years. *Agron. J.* 96: 195-203.
- Avendaño, F., O. Schabenberger, F.J. Pierce, and H. Melakeberhan. 2003. Geostatistical analysis of field spatial distribution patterns of soybean cyst nematode. *Agron. J.* 95: 936-948.
- Avruskin G., G. Jacquez, J. Meliker, M. Slotnick, A. Kaufmann, and J. Nriagu. 2004. Visualization and exploratory analysis of epidemiologic data using a novel space time information system. *Intl. J. Health Geogr.* 3: 26
- Barnes, E.M., and M.G. Baker. 2000. Multispectral data for mapping soil texture: possibilities and limitations. *Trans. ASAE* 16(6): 731-741.
- Basnet, B., R. Kelly, T. Jensen, W. Strong, A. Apan, and D. Butler. 2003. Delineation of management zones using multiple crop yield data. In *Proc. International Soil Tillage Research Organization Conference, 16th Triennial Conference*. Brisbane, AU.: The University of Queensland.
- Blasingame, D., and M. V. Patel. 2001. Cotton disease loss data base . In *Proc. 2002 Beltwide Cotton Conference*. Anaheim, CA.: National Cotton Council.
- Bouyoucos, G.J. 1936. Directions for making mechanical analysis of soils by the hydrometer method. *Soil Sci.* 42: 3.
- Boydell, B., and B. McBratney. 2002. Identifying potential within-field management zones from cotton-yield estimates. *Prec. Agric.* 3:9-23.
- Bronson, K.F., J.D. Booker, S.J. Officer, R.J. Lascano, S.J. Maas, S.W. Searcy, and J. Booker. 2005. Apparent electrical conductivity, soil properties and spatial covariance in the U.S. Southern High Plains. *Prec. Agric.* 6: 297-311.
- Chang, J., D.E. Clay, C.G. Carlson, S.A. Clay, D.D. Malo, R. Berg, J. Kleinjan, and W.J. Wiebold. 2003. Different techniques to identify management zones impact nitrogen and phosphorus sampling variability. *Agron. J.* 95: 1550-1559.
- Chen, F., D.E. Kissel, L.T. West, and W. Adkins. 2000. Field-scale mapping of surface soil organic carbon using remotely sensed imagery. *Soil Sci. Soc. Am. J.* 64: 746-753.
- Corwin, D.L., and S.M. Lesch. 2005. Apparent soil electrical conductivity measurements in agriculture. *Comput. Electron. Agric.* 46: 11-43.
- Day, P.R. 1965. Particle fractionation and particle-size analysis. Black, C. A., Madison, Wisconsin.

- Dieleman J. A., D. A. Mortensen, D. D. Buhler, C. A. Cambardella, and T. B. Moorman. 2000. Identifying associations among site properties and weed species abundance: I Multivariate analysis. *Weed Sci.* 48: 567–575.
- Doberman, A., J.L. Ping, V.I. Adamchuk, G.C. Simbahan, and R.B. Ferguson. 2003. Classification of crop yield variability in irrigated production fields. *Agron. J.* 95: 1105-1120.
- Doerge, T.A. 1999. Management zone concepts. In *Site-Specific Management Guidelines*. P. P. Institute. Series Norcross.
- ESRI. 2004. ArcGIS Spatial Analyst. Ver. 9.0. Redlands, CA.: ESRI.
- Evans, K., R.M. Webster, P.D. Halford, A.D. Barker, and M.D. Russell. 2002. Site-specific management of nematode - Pitfalls and practicalities. *J. Nematol.* 34: 194-199.
- Fraisse, C.W., K.A. Sudduth, and N.R. Kitchen. 2001a. Delineation of site-specific management zones by unsupervised classification of topographic attributes and soil electrical conductivity. *Trans. ASAE* 44(1): 155-166.
- Fraisse, C.W., K.A. Sudduth, and N.R. Kitchen. 2001b. Calibration of the ceres-maize model for simulating site-specific crop development and yield on claypan soils. *Appl. Eng. Agric.* 17: 547-556.
- Fridgen, J.J., C.W. Fraisse, N.R. Kitchen, and K.A. Sudduth. 2000. Delineation and analysis of site-specific management zones. In Proc. 2<sup>nd</sup> *International Conference on Geospatial Information in Agriculture and Forestry*, CD-ROM. Lake Buena Vista, FL.
- Fridgen, J.J., N.R. Kitchen, K.A. Sudduth, S.T. Drummond, W.J. Wiebold, and C.W. Fraisse. 2004. Management zone analyst (MZA): software for subfield management zone delineation. *Agron. J.* 96: 100-108.
- Garson, D.G. 2007. Canonical Correlation. North Carolina State University. Available at: <http://www2.chass.ncsu.edu/garson/pa765/canonic.htm>. Accessed 24 August 2008.
- Jaynes, D.B., T.S. Colvin, and T.C. Kaspar. 2005. Identifying potential soybean management zones from multi-year yield data. *Comput. Electron. Agric.* 46: 309-327.
- Jaynes, D.B., T.C. Kaspar, T.S. Colvin, and D.E. James. 2003. Cluster analysis of spatiotemporal corn yield patterns in an Iowa field. *Agron. J.* 95: 574-586.
- Jenkins, W.R. 1964. A rapid centrifugal flotation technique for separating nematodes from soil. *Plant Dis.* 48: 692.
- Johnson, R. A., and D. W. Wichern. 2002. Applied multivariate analysis. 5th ed. Upper Saddle River, NJ.: Prentice Hall.

- Kemerait, R.C., R.F. Davis, P.H. Jost, C.L. Brewer, S.N. Brown, B. Mitchell, W.E. Harrsion, R. Joyce, and E. McGriff. 2004. Assessment of nematicides for management of the southern root-knot nematode, *Meloidogyne incognita*, in Georgia 2004. Georgia Cotton Research and Extension Reports. Tifton, GA.: The University of Georgia.
- Khalilian, A., J. D. Mueller, S. C. Blackville, Y. J. Han, and F. J. Wolak. 2001. Predicting cotton nematodes distribution utilizing soil electrical conductivity. In *Proc. 2001 Beltwide Cotton Conference*. Memphis, TN.: National Cotton Council.
- Kerry, R., M. A. Oliver. 2003. Co-kriging when soil and ancillary data are not co-located. In *Proc. 4<sup>th</sup> European Confence of Precision Agriculture*. 303-308. Wageningen Academic Publishers.
- Kitchen, N.R., K.A. Sudduth, and S.T. Drummond. 1999. Soil electrical conductivity as a crop productivity measure for claypan soils. *J. Prod. Agric.* 12: 607-617.
- Kitchen, N.R., S.T. Drummond, E.D. Lund, K.A. Sudduth, and G.W. Buchleiter. 2003. Soil electrical conductivity and topography related to yield for three contrasting soil-crop systems. *Agron. J.* 95: 483-495.
- Koenning, S.R., and K.R. Barker. 1995. Soybean photosynthesis and yield as influenced by *Heterodera glycines*, soil type and irrigation. *J. Nematol.* 27: 51-62.
- Koenning, S.R., T.L. Kirkpatrick, J.L. Starr, J.A. Wrather, N.R. Walker, and J.D. Mueller. 2004. Plant-parasitic nematodes attacking cotton in the United States: old and emerging production challenges. *Plant Dis.* 88: 100-113.
- Li, H., R.J. Lascano, E.M. Barnes, J. Booker, L.T. Wilson, K.F. Bronson, and E. Segarra. 2001. Multispectral reflectance of cotton related to plant growth, soil water and texture, and site elevation. *Agron. J.* 93: 1327-1337.
- Li, Y., Z. Shi, F. Li, and H.Y. Li. 2007. Delineation of site-specific management zones using fuzzy clustering analysis in a coastal saline land. *Comput. Electron. Agric.* 56: 174-186.
- Martin, N. F., G. Borrero, and D. G. Bullock. 2005. Association between field characteristics and soybean plant performance using canonical correlation analysis. *Plant and Soil* 237: 39-55.
- McBratney, A.B., and J.J. DeGrujter. 1992. A continuum approach to soil classification by modified fuzzy means with extragrades. *J. Soil Sci.* 43: 159-175.
- Melakeberhan, H., J. Dey, V.C. Baligar, and T.E. Carter Jr. 2004. Effect of soil pH on the pathogenesis of *Heterodera glycines* and *Meloidogyne incognita* on Glycine max genotypes. *Nematology* 6: 585-592.

- Monfort, W.S., T.L. Kirkpatrick, C.S. Rothrock, and A. Mauromoustakos. 2007. Potential for site-specific management of *Meloidogyne incognita* in cotton using soil textural zones. *J. Nematol.* 39: 1-8.
- Noe, J.P., and K.R. Barker. 1985. Relation of within-field spatial variation of plant-parasitic nematode population densities and edaphic factors. *Phytopatology* 75: 247-252.
- Ortiz, B. V., D. G. Sullivan, C. Perry, and G. Vellidis. 2006. Geospatial solutions for precision management of cotton root knot nematodes. ASAE paper No. 061147. Portland, OR.: ASAE.
- Perry, C., G. Vellidis, D. G. Sullivan, K. Rucker, and R. Kemerait. 2006. Predicting nematode hotspots using soil EC<sub>a</sub> data. In *Proc. 2006 Beltwide Cotton Conference*. San Antonio, TX.: National Cotton Council.
- Shurley, W.D., R.C. Kemerait, S. Brown, E. McGriff, B. Mitchell, and R. Reed. 2004. Economic analysis of southern root knot nematode controls. University of Georgia.
- Starr, J.L., C.M. Heald, A.F. Robinson, R.G. Smith, and J.P. Krausz. 1993. *Meloidogyne incognita* and *Rotylenchulus reniformis* and associated soil textures from some cotton production areas of Texas. *J. Nematol.* 25: S895-899.
- Steel, R.G.D., and J.H. Torrie. 1980. Principles and procedures of statistics. 2<sup>nd</sup> ed. New York, N.Y.: McGraw-Hill.
- Sudduth, K.A., N.R. Kitchen, W.J. Wiebold, W.D. Batchelor, G.A. Bollero, D.G. Bullock, D.E. Clay, H.L. Palm, F.J. Pierce, R.T. Schuler, and K.D. Thelen. 2005. Relating apparent electrical conductivity to soil properties across the north-central USA. *Comput. Electron. Agric.* 46: 263-283.
- Sullivan, D.G., J.N. Shaw, and D. Rickman. 2005. IKONOS imagery to estimate surface property variability in two Alabama physiographies. *Soil Sci. Soc. Am. J.* 69: 1789-1798.
- Tarr, A.B., K.J. Moore, P.M. Dixon, C.L. Burras, and M.H. Wiedenhoef. 2003. Use of soil electroconductivity in a multistage soil-sampling scheme. *Crop Mgmt.* 10:1094/CM-2003-1029.
- UGA. 2005. 2005 Georgia cotton research and extension reports. Cooperative Extension Service.: The University of Georgia. Available at : <http://commodities.caes.uga.edu/fieldcrops/cotton/rerpubs/2005/p242.pdf>. Accessed 25 August 2008.
- USDA. 2002. Soil survey geographic (SSURGO) database. U.S. Department of Agriculture, Natural Resources Conservation Service.

- USDA. 2008. Crop production. National Agricultural Statistics Service. Washington, D.C.: USDA National Agricultural Statistics Service. Available at: [www.usda.gov/nass/PUBS/TODAYRPT/crop0808.txt](http://www.usda.gov/nass/PUBS/TODAYRPT/crop0808.txt). Accessed 17 August 2008.
- Wheeler, T.A., K.R. Barker, and S.M. Schneider. 1991. Yield-loss models for tobacco infected with *Meloidogyne incognita* as affected by soil-moisture. *J. Nematol.* 23: 365-371.
- Wyse-Pester, D.Y., L.J. Wiles, and P. Westra. 2002. The potential for mapping nematode distribution for site-specific management. *J. Nematol.* 34: 80-87.

Table 3.1. Location, planting and harvesting date, and soil characteristics for the study fields.

Field characteristics	Field ID		
	CC	CMP	PG
County	Colquitt	Colquitt	Tift
Field size (ha)	20	25	25
Soils	Albany sand 0-2% slope (Loamy, siliceous, subactive, thermic Grossarenic Paleudults ).	Fuquay loamy sand, 0-5% slope (Loamy, kaolinitic, thermic Arenic Plinthic Kandiudults).	Tifton loamy sand, 2-5% slope (Fine-loamy, kaolinitic, thermic Plinthic Kandiudults)
	Kershaw sand, 0-5% slope (Thermic, uncoated Typic Quartzipsamments)	Tifton loamy sand, 2-5% slope (Fine-loamy, kaolinitic, thermic Plinthic Kandiudults)	
Planting date	15 May 2006	15 May 2006	4 May 2006
Harvest date	30 October	02 November 2006	26 September 2006
RKN samples	99	98	105

Table 3.2. Descriptive statistics of RKN, edaphic and terrain data for the CC, PG, and CMP fields.

Field	Factor	Descriptive Statistics				
		Mean	Min.-Max.	SD <sup>[b]</sup>	CV (%) <sup>[c]</sup>	Skewness
CC (99) <sup>[a]</sup>	RKN - S1	43.9	1-1281	139.4	319.7	7.5
	RKN - S2	132.1	1-1629	226.4	171.4	4.3
	RKN - S3	116.2	1-729	145.8	125.5	2.0
	EL (m)	78.2	74-81	1.7	2.1	-0.5
	SL (%)	1.2	0.13-3.54	0.6	50.4	0.6
	EC <sub>a-s</sub> (mS m <sup>-1</sup> )	0.9	0.40-9.71	1.1	117.7	6.6
	EC <sub>a-d</sub> (mS m <sup>-1</sup> )	1.2	0.45-7.95	1.1	89.5	4.0
	NDVI	0.1	0.02-0.16	0.0	34.8	0.4
PG (105) <sup>[a]</sup>	RKN - S1	1.6	0-52	6.4	395.7	5.7
	RKN - S2	64.6	0-876	158.5	245.3	3.7
	RKN - S3	97.3	0-2006	242.5	249.4	5.5
	EL (m)	107.7	103-112	2.3	2.1	-0.1
	SL (%)	2.8	0.43-14.65	1.7	62.9	2.6
	EC <sub>a-s</sub> (mS m <sup>-1</sup> )	2.1	0.46-9.10	1.5	69.9	2.3
	EC <sub>a-d</sub> (mS m <sup>-1</sup> )	3.9	0.66-10.39	2.1	52.7	1.1
	NDVI	0.1	0.02-0.14	0.0	29.9	2.2
CMP (98) <sup>[a]</sup>	RKN - S1	5.1	0-60	10.3	203.2	3.0
	RKN - S2	328.3	0-1270	259.4	79	1.1
	RKN - S3	225.3	2-1140	169.5	75.2	1.7
	EL (m)	91.9	88-96	1.8	2	0.5
	SL (%)	1.7	0.57-5.54	1.0	59	1.7
	EC <sub>a-s</sub> (mS m <sup>-1</sup> )	0.9	0.34-5.58	0.9	63.1	5.5
	EC <sub>a-d</sub> (mS m <sup>-1</sup> )	1.7	0.49-4.87	0.8	45.7	1.6
	NDVI	0.1	0.01-0.16	0.0	46.2	0.3

<sup>[a]</sup> Data in parenthesis shows the number of RKN samples collected from each field.

<sup>[b]</sup> Standard Deviation.

<sup>[c]</sup> Coefficient of variation, percentage.

Table 3.3. Pearson's linear correlation coefficients for RKN population density with edaphic and terrain variables in the CC, PG, and CMP fields.

Variable	RKN1 <sup>[a]</sup>	RKN2 <sup>[a]</sup>	RKN3 <sup>[a]</sup>	EL (m)	SL (%)	EC <sub>a-s</sub> (mS m <sup>-1</sup> )	EC <sub>a-d</sub> (mS m <sup>-1</sup> )	NDVI
CC field								
RKN1 <sup>[a]</sup>	1							
RKN2 <sup>[a]</sup>	0.48*	1						
RKN3 <sup>[b]</sup>	0.33**	0.39*	1					
EL	0.48*	0.61*	0.34**	1				
SL	-0.30**	-0.39*	-0.16	-0.42*	1			
EC <sub>a-s</sub>	-0.22***	-0.19	-0.19	-0.33**	0.19	1		
EC <sub>a-d</sub>	-0.32***	-0.34**	-0.24***	-0.52*	0.30**	0.94*	1	
NDVI	-0.11	-0.29***	-0.08	-0.56	0.20***	0.39*	0.53*	1
PG field								
RKN1 <sup>[a]</sup>	1							
RKN2 <sup>[a]</sup>	0.21***	1						
RKN3 <sup>[a]</sup>	0.17	0.56*	1					
EL	-0.41*	-0.1	-0.16	1				
SL	-0.02	0.08	0.09	-0.05	1			
EC <sub>a-s</sub>	-0.15	-0.39*	-0.34**	-0.17	-0.15	1		
EC <sub>a-d</sub>	-0.23	-0.40*	-0.36**	-0.06	-0.23	0.88*	1	
NDVI	0.11	-0.27	-0.15	-0.39*	-0.17	0.40*	0.31**	1
CMP field								
RKN1 <sup>[a]</sup>	1							
RKN2 <sup>[a]</sup>	-0.003	1						
RKN3 <sup>[a]</sup>	0.25**	0.22	1					
EL	0.01	0.04	0.23	1				
SL	0.96*	0.02	0.06	-0.16	1			
EC <sub>a-s</sub>	-0.07	0.03	-0.33**	-0.2	0.28	1		
EC <sub>a-d</sub>	-0.01	0.12	-0.08	-0.04	0.37**	0.74*	1	
NDVI	0.24	0.25	0.37**	0.28	0.22	0.22	0.33**	1

<sup>[a]</sup> Log<sub>10</sub> (RKN - Second stage juveniles 100 cm<sup>-3</sup> of soil +1)

<sup>[b]</sup> Square root (RKN - Second stage juveniles 100 cm<sup>-3</sup> of soil)

<sup>[c]</sup> Bare soil NDVI

\* Significance based on  $P < 0.0001$

\*\* Significance based on  $P = 0.01$

\*\*\* Significance based on  $P = 0.05$

Table 3.4. Results from the canonical correlation analysis between the  $\text{Log}_{10}$  (RKN Second stage juveniles  $100 \text{ cm}^{-3}$  of soil +1) and edaphic and remotely sensed data for each of the studied fields.

Parameter	Field ID number										
	2005						2006				
	1 <sup>[a]</sup>	2 <sup>[b]</sup>	3 <sup>[b]</sup>	4 <sup>[a]</sup>	5 <sup>[b]</sup>	6 <sup>[a]</sup>	7 <sup>[b]</sup>	8 <sup>[a][c]</sup>	9 <sup>[a][d]</sup>	10 <sup>[b][e]</sup>	11 <sup>[a][f]</sup>
Eigenvalue	0.70	0.32	0.49	0.52	0.78	0.66	0.17	0.24	0.68	0.50	0.31
Canonical correlation	0.64	0.49	0.58	0.58	0.66	0.63	0.03	0.44	0.64	0.58	0.49
Wilk's Lambda	0.000	0.162	0.014	0.288	0.000	0.000	0.749	0.050	<.0001	<.0001	<.0001
	Loadings or canonical structure correlations <sup>[g]</sup>										
EL	0.30	-0.13	-0.05	<b>-0.64</b>	<b>0.63</b>	<b>-0.76</b>	<b>0.67</b>	<b>0.76</b>	<b>0.96</b>	<b>0.40</b>	0.21
SL	<b>-0.63</b>	<b>0.38</b>	<b>0.75</b>	<b>-0.50</b>	<b>-0.38</b>	<b>0.73</b>	<b>-0.35</b>	<b>-0.38</b>	<b>-0.63</b>	0.11	-0.18
EC <sub>a-s</sub>	<b>-0.55</b>	<b>-0.43</b>	0.26	<b>0.60</b>	<b>0.92</b>		-0.14			<b>-0.57</b>	<b>0.81</b>
EC <sub>a-d</sub>	-0.34	<b>-0.74</b>	-0.02		<b>0.96</b>	<b>-0.77</b>	<b>-0.50</b>	0.16	<b>-0.53</b>	-0.14	<b>0.83</b>
NDVI <sup>[h]</sup>	0.09	0.16		<b>0.46</b>	0.23	-0.15		<b>0.57</b>	<b>-0.46</b>	<b>0.64</b>	<b>0.56</b>

<sup>[a]</sup>  $\text{Log}_{10}$  RKN2 sampled at flowering stage of cotton.

<sup>[b]</sup>  $\text{Log}_{10}$  RKN3 sampled at harvest.

<sup>[c]</sup> Normally distributed data

<sup>[d]</sup> CC field for subsequent references

<sup>[e]</sup> CMP field for subsequent references

<sup>[f]</sup> PF field for subsequent references

<sup>[g]</sup> Correlations greater than 0.35 are shown in bold font

<sup>[h]</sup> Bare soil NDVI

Table 3.5. Pooled variances ( $S_p^2$ ) of the data set-zone number combinations for  $\text{Log}_{10}$  RKN2 and the explanatory variables (EL,SL,  $\text{EC}_{a-s}$ ,  $\text{EC}_{a-d}$ , and NDVI), CC field.

Data Set <sup>[a]</sup>	No. zones (n)	Strategy number <sup>[b]</sup>	$\text{Log}_{10}$ RKN2		EL (m)		SL (%)		$\text{EC}_{a-s}$ ( $\text{mS m}^{-1}$ )		$\text{EC}_{a-d}$ ( $\text{mS m}^{-1}$ )		NDVI	
			$S_p^2$	F <sub>value</sub>	$S_p^2$	F <sub>value</sub>	$S_p^2$	F <sub>value</sub>	$S_p^2$	F <sub>value</sub>	$S_p^2$	F <sub>value</sub>	$S_p^2$	F <sub>value</sub>
EL-SL- $\text{EC}_{a-d}$ -NDVI	3	1	0.22	2.0*	0.19	42*	0.05	2.7*	0.02	1.0	1.66	0.7	$2.5 \times 10^{-7}$	$1.8 \times 10^{-14}$
SL- $\text{EC}_{a-d}$ -NDVI	4	2	0.34	1.3*	3.72	2.1*	0.03	5.2*	0.03	5.0*	0.13	1.2*	$3.1 \times 10^{-7}$	$1.5 \times 10^{-14}$
$\text{EC}_{a-d}$ -SL	3	3	0.32	0.8	4.02	2.0*	0.02	7.5*	8.50	$2.3 \times 10^{-3}$	3.90	0.04	$4.0 \times 10^{-7}$	$1.1 \times 10^{-14}$
$S_{\text{field}}^2$	1		0.45		8.05		0.15		0.02		0.16		$4.6 \times 10^{-7}$	

<sup>[a]</sup> Data set used to calculate an edaphic-terrain canonical variable.

<sup>[b]</sup> Strategies for delineating management zones based on canonical predictors calculated from the canonical correlation between an edaphic-terrain canonical variable and a RKN canonical variable.

\*If a classification method is significantly different from the whole field variance at  $P=0.1$  then  $S_p^{2*}$ . df numerator=99, df denominator=99-n.

Table 3.6. Variability of management zones delineated by fuzzy clustering of canonical predictor variables of RKN calculated from different combination of edaphic and terrain variables, CC field.

Strategy <sup>[a]</sup>	No. zones (n) <sup>[b]</sup>	Log <sub>10</sub> (RKN2/100 cm <sup>3</sup> +1)		EL (m)		EC <sub>a-d</sub> (mS m <sup>-1</sup> )		SL (%)		NDVI	
		Mean	CV	Mean	CV	Mean	CV	Mean	CV	Mean	CV
1 EL-SL- EC <sub>a-d</sub> - NDVI (0.63) <sup>[c]</sup>	1 (32)	0.97	79.9	76.0	1.0	2.0	74.3	1.5	22.9	0.10	18.9
	2 (31)	1.51	46.6	78.5	0.9	1.0	48.7	1.6	37.0	0.07	32.1
	3 (36)	2.19	20.8	79.8	0.5	0.6	25.4	0.7	54.8	0.06	38.3
2 SL-EC <sub>a-d</sub> - NDVI (0.47) <sup>[c]</sup>	1 (31)	1.11	72.7	77.11	1.8	1.25	36.1	1.50	14.8	0.08	20.7
	2 (16)	1.27	76.3	76.91	2.3	2.56	75.6	2.04	28.1	0.10	23.9
	3 (24)	1.76	33.3	78.93	1.5	0.81	34.1	1.12	36.0	0.07	42.7
	4 (28)	2.16	21.8	79.61	0.7	0.60	20.9	0.56	44.5	0.06	27.9
3 EC <sub>a-d</sub> -SL (0.45) <sup>[c]</sup>	1 (6)	1.32	70.8	77.80	2.2	3.59	80.3	2.38	30.7	0.09	32.0
	2 (54)	1.23	66.5	77.30	2.0	1.26	47.6	1.53	18.4	0.08	30.6
	3 (39)	2.12	20.7	79.50	1.0	0.67	35.0	0.62	43.7	0.06	37.7
Whole field	1	1.58	51.6	78.22	2.2	1.17	89.5	1.22	50.3	0.08	34.8

<sup>[a]</sup> Data set used to calculate an edaphic-terrain canonical variable.

<sup>[b]</sup> Data in parenthesis shows the number of observations per zone.

<sup>[c]</sup> Canonical correlation between the edaphic-terrain canonical variable and the RKN canonical variable.

Table 3.7. Pooled variances ( $S_p^2$ ) of the data set-zone number combinations for  $\text{Log}_{10}$  RKN2 and the explanatory variables (EL,SL,  $EC_{a-s}$ ,  $EC_{a-d}$ , and NDVI), PG field.

Data Set	No. zones (n)	Strategy number	$\text{Log}_{10}$ RKN2		EL (m)		SL (%)		$EC_{a-s}$ ( $\text{mS m}^{-1}$ )		$EC_{a-d}$ ( $\text{mS m}^{-1}$ )		NDVI	
			$S_p^2$	$F_{\text{value}}$	$S_p^2$	$F_{\text{value}}$	$S_p^2$	$F_{\text{value}}$	$S_p^2$	$F_{\text{value}}$	$S_p^2$	$F_{\text{value}}$	$S_p^2$	$F_{\text{value}}$
$EL-SL-EC_{a-s}-EC_{a-d}-NDVI$	3	1	0.59	1.4*	26.3	1.00	5.38	0.9	3.30	1.5*	4.99	3.4*	$11 \times 10^{-7}$	0.50
$EC_{a-s}-EC_{a-d}-NDVI$	3	2	0.49	1.7*	28.7	1.0	4.80	1.0	0.7	7.5*	1.7	10.5*	$1.16 \times 10^{-7}$	0.50
$EC_{a-s}-EC_{a-d}$	3	3	0.63	1.3*	29.0	0.9	12.9	0.4	0.95	5.3*	0.8	22.2*	$1.57 \times 10^{-7}$	0.30
$S_{\text{field}}^2$	1		0.85		27.53		5.01		5.01		17.89		$5.6 \times 10^{-8}$	

<sup>[a]</sup> Data set used to calculate an edaphic-terrain canonical variable.

<sup>[b]</sup> Strategies for delineating management zones based on canonical predictors calculated from the canonical correlation between and edaphic-terrain canonical variable and a RKN canonical variable.

\* If a classification method is significantly different from the whole field variance at  $P=0.1$  then  $S_p^{2*}$ . df numerator=105, df denominator=105-n

Table 3.8. Variability of management zones delineated of fuzzy clustering of canonical predictor variables by RKN calculated from different combination of edaphic and terrain variables, PG field.

Strategy <sup>[a]</sup>	No. zones (n) <sup>[b]</sup>	Log <sub>10</sub> (RKN2/100 cm <sup>3</sup> +1)		EL (m)		EC <sub>a-s</sub> (mS m <sup>-1</sup> )		EC <sub>a-d</sub> (mS m <sup>-1</sup> )		SL (%)		NDVI	
		Mean	CV	Mean	CV	Mean	CV	Mean	CV	Mean	CV	Mean	CV
1	1 (9)	0.16	300.1	107.8	2.6	5.28	46.0	7.66	30.8	2.79	59.6	0.07	46.9
EL-SL- EC <sub>a-s</sub> -EC <sub>a-d</sub> - NDVI (0.48) <sup>[c]</sup>	2 (48)	0.45	176.9	108.5	1.7	2.42	37.1	4.62	27.8	2.87	53.1	0.05	17.8
	3 (48)	1.32	71.9	107.0	2.2	1.27	49.8	2.49	49.4	3.48	62.5	0.05	25.3
2	1 (6)	0.00	-	106.1	2.0	6.74	25.9	8.91	18.6	1.98	62.4	0.07	50.6
EC <sub>a-s</sub> -EC <sub>a-d</sub> - NDVI (0.43) <sup>[c]</sup>	2 (52)	0.39	191.5	107.9	2.0	2.51	30.5	4.83	25.0	2.81	54.6	0.06	22.8
	3 (47)	1.40	64.9	107.7	2.2	1.15	35.8	2.25	35.3	3.43	40.2	0.04	20.5
3	1 (8)	0.24	282.8	106.4	2.3	6.13	30.2	8.68	17.0	2.4	77.6	0.06	59.0
EC <sub>a-s</sub> -EC <sub>a-d</sub> (0.41) <sup>[c]</sup>	2 (49)	0.47	171.7	108.1	1.9	2.48	25.9	4.80	18.9	2.7	54.2	0.05	21.9
	3 (48)	1.27	74.87	107.6	2.3	1.12	31.4	2.20	32.1	3.4	40.2	0.05	23.8
Whole field	1	0.82	117	107.7	2.1	2.13	70.0	3.90	52.6	3.14	59.5	0.05	29.8

<sup>[a]</sup> Data set used to calculate an edaphic-terrain canonical variable.

<sup>[b]</sup> Data in parenthesis shows the number of observations per zone.

<sup>[c]</sup> Canonical correlation between the edaphic-terrain canonical variable and the RKN canonical variable.

Table 3.9. Pooled variances ( $S_p^2$ ) of the data set-zone number combinations for  $\text{Log}_{10}$  RKN2 and the explanatory variables (EL,SL,  $\text{EC}_{a-s}$ ,  $\text{EC}_{a-d}$ , and NDVI), CMP field.

Data Set	No. zones (n)	Strategy number	$\text{Log}_{10}$ RKN3		EL (m)		SL (%)		$\text{EC}_{a-s}$ ( $\text{mS m}^{-1}$ )		$\text{EC}_{a-d}$ ( $\text{mS m}^{-1}$ )		NDVI	
			$S_p^2$	F <sub>value</sub>	$S_p^2$	F <sub>value</sub>	$S_p^2$	F <sub>value</sub>	$S_p^2$	F <sub>value</sub>	$S_p^2$	F <sub>value</sub>	$S_p^2$	F <sub>value</sub>
EL-SL- $\text{EC}_{a-s}$ - $\text{EC}_{a-d}$ - NDVI	4	1	0.10	0.2	12.4	0.9	1.0	1.0	0.3	0.4	0.5	0.7	$1.31 \times 10^{-4}$	$7.7 \times 10^{-11}$
EL- $\text{EC}_{a-s}$ - NDVI	3	2	0.01	1.2*	10.1	1.1	1.0	1.0	0.3	0.4	0.5	0.7	$1.02 \times 10^{-7}$	$9.9 \times 10^{-14}$
$\text{EC}_{a-s}$ -NDVI	3	3	0.01	1.9*	11.0	1.0	4.3	0.2	0.3	0.5	0.5	0.7	$1.15 \times 10^{-7}$	$8.8 \times 10^{-14}$
$S_{\text{field}}^2$	1		0.025		10.88		1.01		0.12		0.33		$1.01 \times 10^{-6}$	

<sup>[a]</sup> Data set used to calculate an edaphic-terrain canonical variable.

<sup>[b]</sup> Strategies for delineating management zones based on canonical predictors calculated from the canonical correlation between and edaphic-terrain canonical variable and a RKN canonical variable.

\* If a classification method is significantly different from the whole field variance at  $P=0.1$  then  $S_p^{2*}$ . df numerator=98, df denominator=98-n

Table 3.10. Variability of management zones delineated by fuzzy clustering of canonical predictor variables of RKN calculated from different combination of edaphic and terrain variables, CMP field.

Strategy <sup>[a]</sup>	No. zones (n) <sup>[b]</sup>	Log <sub>10</sub> (RKN3/100 cm <sup>3</sup> +1)		EL (m)		EC <sub>a-s</sub> (mS m <sup>-1</sup> )		EC <sub>a-d</sub> (mS m <sup>-1</sup> )		SL (%)		NDVI	
		Mean	CV	Mean	CV	Mean	CV	Mean	CV	Mean	CV	Mean	CV
1	1 (2)	0.94	69.5	89.1	0.4	4.04	54.0	3.41	60.8	3.18	10.7	0.05	29.7
EL-SL- EC <sub>a-s</sub> -	2 (42)	2.09	14.7	91.1	0.9	0.79	43.4	1.50	47.2	1.31	50.0	0.04	32.5
EC <sub>a-d</sub> - NDVI	3 (14)	2.37	13.5	92.7	2.0	0.93	30.8	1.60	37.3	1.78	64.4	0.09	19.7
(0.58) <sup>[c]</sup>	4 (40)	2.35	16.6	92.5	2.7	0.94	25.5	2.08	36.2	2.47	35.1	0.11	17.3
2	1 (2)	0.94	69.5	89.1	0.4	4.04	54.0	3.41	60.8	3.18	10.7	0.05	29.7
EL- EC <sub>a-s</sub> -	2 (48)	2.10	14.8	91.2	1.1	0.82	44.7	1.58	49.2	1.58	65.7	0.04	40.0
NDVI	3 (48)	2.38	14.0	92.7	2.2	0.92	26.0	1.67	35.8	1.77	53.5	0.10	19.2
(0.56) <sup>[c]</sup>													
3	1 (2)	0.94	69.5	89.1	0.4	4.04	54.0	3.41	60.8	3.18	10.7	0.05	29.7
EC <sub>a-s</sub> - NDVI	2 (46)	2.11	14.9	91.2	1.1	0.82	45.2	1.60	49.0	1.61	65.1	0.04	40.5
(0.56) <sup>[c]</sup>	3 (50)	2.37	14.3	92.6	2.3	0.91	26.3	1.65	36.4	1.73	54.5	0.09	20.5
Whole field	1	2.21	17.9	91.9	2.0	0.93	63.1	1.66	45.6	1.70	58.9	0.07	46.3

<sup>[a]</sup> Data set used to calculate an edaphic-terrain canonical variable.

<sup>[b]</sup> Data in parenthesis shows the number of observations per zone.

<sup>[c]</sup> Canonical correlation between the edaphic-terrain canonical variable and the RKN canonical variable.

Table 3.11. Validation results of the management zone delineation method tested on six fields located in the Tifton-Vidalia Upland (TVU) ecoregion of the Southeastern Coastal Plain. †

Field ID <sup>[a]</sup>	Zone number <sup>[b]</sup>	RKN <sup>[c]</sup>		Variables <sup>[d]</sup>									
				EL		SL		EC <sub>a-s</sub>		EC <sub>a-d</sub>		NDVI	
		Mean	CV	Mean	CV	Mean	CV	Mean	CV	Mean	CV	Mean	CV
1	1 (13)	62	108	109	1.47	3.0	48.3	0.7	162.3	1.3	128.5	0.10	12.8
	2 (19)	158	100	108	0.97	2.3	46.0	1.5	34.7	2.8	21.2	0.15	17.1
	3 (23)	211	69	110	0.90	1.3	58.3	1.0	48.9	1.8	38.8	0.14	20.1
	F <sup>[e]</sup>	<b>158</b>	<b>92</b>	<b>109</b>	<b>1.94</b>	<b>2.2</b>	<b>61.0</b>	<b>1.1</b>	<b>69.7</b>	<b>2.1</b>	<b>56.0</b>	<b>0.13</b>	<b>0.2</b>
2	1 (13)	161	71.5	80.6	0.01	0.8	29.3	0.6	54.7	0.9	61.9	0.31	9.6
	2 (17)	171	66.3	81.2	0.00	0.5	32.3	0.5	49.5	0.9	45.5	0.33	12.2
	3 (14)	185	76.3	80.8	0.00	0.6	32.2	0.0	186.6	0.6	28.8	0.30	23.2
	F <sup>[e]</sup>	<b>173</b>	<b>70</b>	<b>80.8</b>	<b>0.51</b>	<b>0.6</b>	<b>38.0</b>	<b>0.4</b>	<b>87.0</b>	<b>0.8</b>	<b>52.0</b>	<b>0.31</b>	<b>16.0</b>
3	1 (21)	5	165	105	0.41	1.4	50.7	0.5	78.2	1.5	75.0		
	2 (4)	16	105	104	0.54	3.7	22.9	3.5	34.0	7.1	11.0		
	3 (10)	23	220	103	0.97	2.7	23.3	1.1	135.0	2.8	46.0		
	4 (5)	106	60	106	0.53	3.6	56.0	0.3	29.0	0.7	85.0		
	F <sup>[e]</sup>	<b>23</b>	<b>200</b>	<b>105</b>	<b>1.32</b>	<b>2.2</b>	<b>58.0</b>	<b>1.0</b>	<b>129.0</b>	<b>2.3</b>	<b>91.0</b>		
5	1 (12)	61	206	111	0.78	3.5	11.1	4.5	32.0	7.7	23.0	0.17	5.7
	2 (12)	212	100	106	2.46	4.8	12.0	2.7	53.0	6.4	41.0	0.17	11.0
	3 (6)	253	92.4	102	0.6	4.4	16.7	1.8	40.0	2.9	59.0	0.20	7.7
	4 (14)	509	42	105	1.78	4.0	18.0	0.5	40.0	1.2	60.0	0.14	9.1
	F <sup>[e]</sup>	<b>286</b>	<b>103</b>	<b>106</b>	<b>3.28</b>	<b>4.1</b>	<b>18.4</b>	<b>2.4</b>	<b>79.3</b>	<b>4.7</b>	<b>68.0</b>	<b>0.17</b>	<b>14.2</b>
6	1 (14)	253	116	115	0.63	1.9	41.4			6.4	50.5	0.18	7.2
	2 (13)	584	93.8	115	0.55	3.5	18.6			4.8	25.1	0.19	3.5
	3 (19)	1062	77.3	112	0.97	3.0	11.4			3.8	36.1	0.20	17.4
	F <sup>[e]</sup>	<b>673</b>	<b>104</b>	<b>114</b>	<b>1.38</b>	<b>2.9</b>	<b>29.0</b>			<b>4.9</b>	<b>47.4</b>	<b>0.19</b>	<b>12.4</b>
8	1 (6)	98	68.7	93.4	1.01	3.5	45.1			2.0	82.3	0.03	39.1
	2 (5)	162	71.8	93.7	0.48	3.4	19.6			7.7	30.1	0.12	33.2
	3 (11)	217	70.9	93.6	0.8	3.7	14.3			1.6	60.7	0.09	23.2
	4 (26)	293	66.5	95.7	1.06	2.4	24.5			1.5	63.0	0.08	21.1
	F <sup>[e]</sup>	<b>248</b>	<b>77.4</b>	<b>94.7</b>	<b>1.48</b>	<b>2.9</b>	<b>31.4</b>			<b>2.3</b>	<b>97.8</b>	<b>0.08</b>	<b>37.5</b>

† Management zones delineated from fuzzy clustering of edaphic and terrain variables.

<sup>[a]</sup> Field identification number

<sup>[b]</sup> Data in parenthesis shows the number of observations per zone.

<sup>[c]</sup> RKN population density per zones (second stage juveniles per 100 cm<sup>3</sup> soil).

<sup>[d]</sup> Set of edaphic and terrain variables used for the management zones delineation.

<sup>[e]</sup> Field average and coefficient of variation are in bold font.

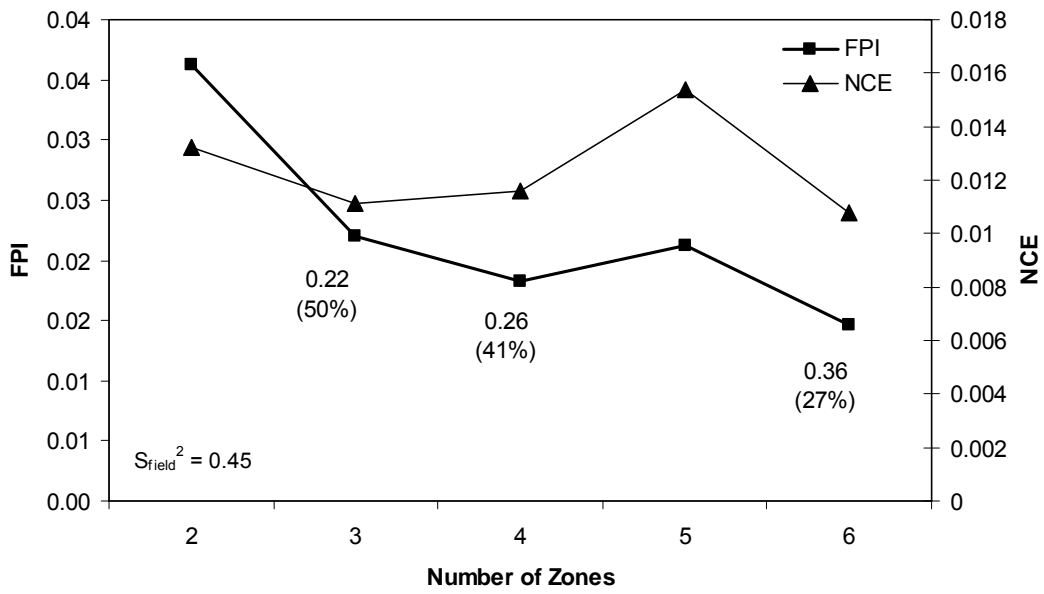


Figure 3.1. Clustering performance based on the fuzziness performance index (FPI), normalized classification entropy (NCE), and pooled variances ( $S_p^2$ ) for the CC field.

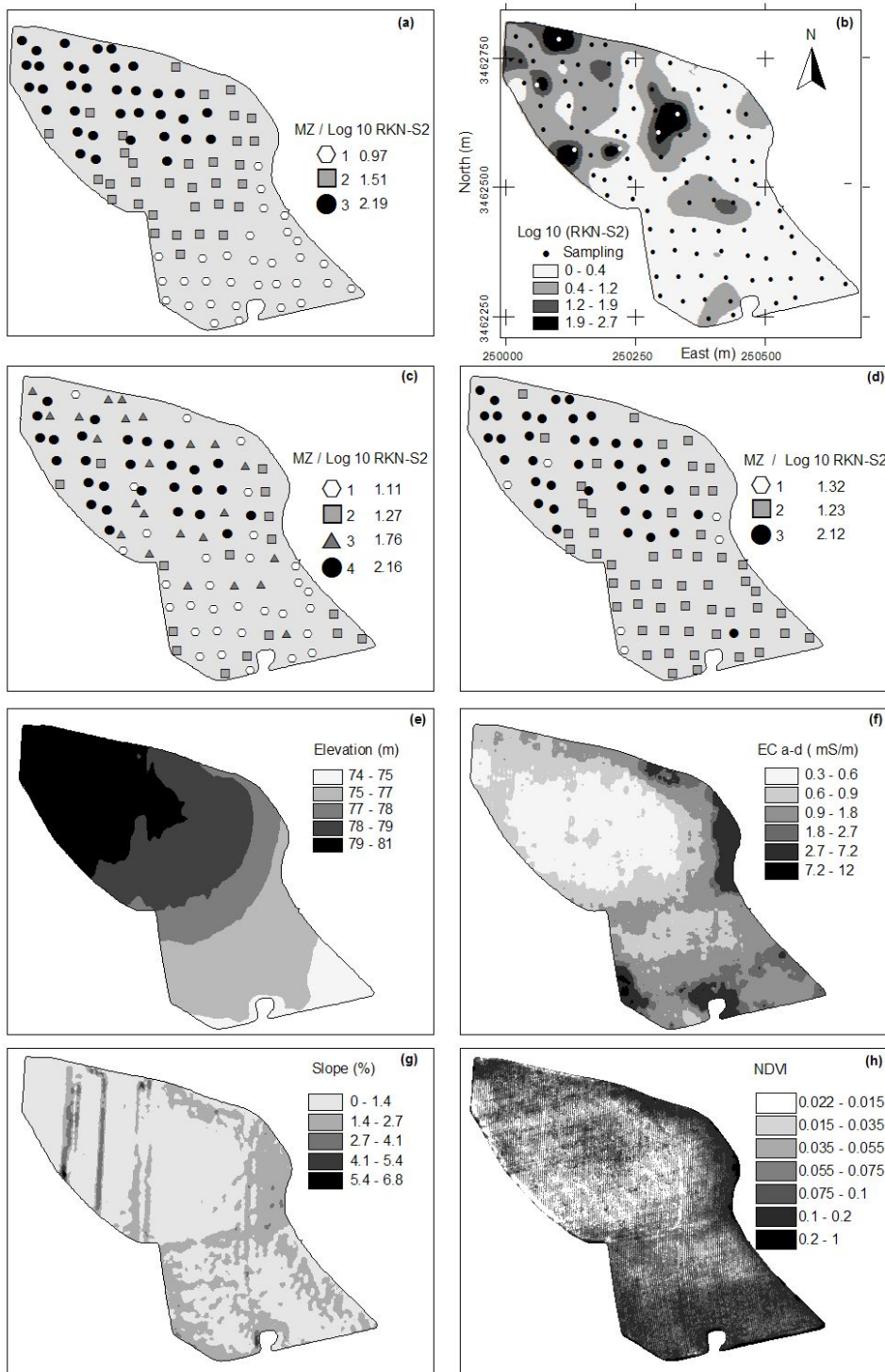


Figure 3.2. Map of the CC field including the management zones (MZ) using (a) strategy one, (b) RKN population density – RKNS2, (c) MZ using strategy two, (d) MZ using strategy three, (e) elevation, (f)  $EC_{a-d}$ , (g) slope, (h) NDVI.

## CHAPTER 4

### IMPACT OF SOUTHERN ROOT-KNOT NEMATODE PARASITISM ON COTTON BIOMASS AND YIELD<sup>1</sup>

---

<sup>1</sup> Ortiz, B. V. R. F. Davis, G. Vellidis, C. Perry, G. Hoogenboom, D. Sullivan. To be submitted to *Nematology*. October 2008.

## Abstract

Southern Root-Knot Nematode [*Meloidogyne incognita* (Kofoid & White) Chitwood] (RKN) is responsible for considerable cotton (*Gossypium hirsutum* L.) yield losses across the U.S. cotton belt. However, the degree of damage varies according to the interaction of RKN population-plant-environment. Our objectives were to study changes in cotton growth, development, and yield production induced by: (i) RKN parasitism and (ii) the interaction RKN population-drought stress. Cotton was grown in a producer's field and in small plots of a controlled experiment. Fourteen sites differing in soil texture within the producer's field were chosen to study the degree of damage by the RKN population on cotton plants. The controlled experiment consisted of six treatments arranged in a split-plot design with three drought stress levels and two fumigation levels [fumigated (65 L of 1,3-dichloropropene ha<sup>-1</sup>) and nonfumigated (0 L ha<sup>-1</sup>)]. RKN population density and above-ground dry matter partitioning were evaluated at four times during the growing season. Gallings severity over locations with the lowest soil EC<sub>a</sub> (shallow and deep) values in a producer's field indicated the increased risk for yield losses on sandy areas. On average, RKN population density on fumigated plots was reduced 52%, 67%, and 47% for the low, medium and severe drought stress treatments compared to nonfumigated plots. The growth and development of the evaluated cotton biomass components (plant height, LAI, stem-petiole, bolls, number of closed bolls, lint plus seed yield) were reduced by RKN parasitism and exacerbated by drought stress. Cotton plants with severe root galling exhibited 11% to 14% lower height than plants with low or no infection. Increase in low plant height and boll dry weight on nonfumigated plots under severe drought stress indicated that high RKN population densities and drought limit vegetative and reproductive growth. Within the nonfumigated treatment in the controlled experiment, the elevated number of closed bolls indicated a delay to maturity occurred as a consequence of RKN parasitism. Lint plus seed yield was suppressed by RKN population from 12% to 14% on nonfumigated plots compared to fumigated plots and these differences increased with increments on the level of drought stress. Damage of RKN population mainly prone on coarse sand area could be reduced if a site specific management is implemented not only to suppress nematodes throughout fumigation but also supply water and nutrients to the areas with elevated risk for parasitism.

Keywords: Cotton, drought, leaf area index, galling, growth, *Meloidogyne incognita*, soil electrical conductivity, southern root-knot nematode, yield.

## 4.1 Introduction

In the last two decades, cotton (*Gossypium hirsutum L.*) production in the U.S. cotton belt has been greatly reduced by plant parasitic nematodes feeding on the plant roots. Yield losses, expressed in cotton lint, caused by these pathogens have increased from 1% to 2% in the 1950s to 4.39% in 2000 (Koenning et al., 2004; NCC, 2008). Southern root-knot nematode [*Meloidogyne incognita* (Kofoid & White) Chitwood] (RKN) is responsible for twice as much yield loss as the other nematodes found across the U.S. cotton belt and its spatial distribution still keeps increasing (Koenning et al., 2004). However, losses are not usually detected until significant damage has been caused.

Southern root-knot nematode has a life cycle that includes several generations in one crop (Ehwaeti et al., 2000). The second stage juveniles of RKN (RKN-J2) emerge into the soil following the first molt, which occurs inside the egg. After penetrating the root near the root tip, RKN-J2 move intercellularly, migrating to the differentiation zone where a permanent feeding site is established and nuclear division is induced causing the formation of galls or root-knots (Williamson and Gleason, 2003; Wyss et al., 1992). After three more molts, egg lying females generate an egg mass which is expelled out of the roots. This cycle repeats several times during the growing season. Although the juveniles and eggs may survive in the soil for multiple months after cotton has been harvested, the decay of root biomass, which serves as a food source for those obligate parasites, causes a significant reduction in reproduction and degree of infection following harvest.

Studies concerning RKN damage have shown a complex variety of effects on cotton growth and yield. The nematodes damage plants through several mechanisms including a change in plant physiology, removal of host carbon compounds, reduction of water and nutrient flow

through intact roots, and suppression of growth, all of which may contribute to diminished cotton yield. Physiological changes have been considered as one of the major causes of growth reduction. The reduction in the photosynthetic rate by RKN can occur in two ways: (i) reduction in the rate of CO<sub>2</sub> fixation due to stomatal closure as a result of water stress caused by the root damage (Bird, 1974), and (ii) decreased production and translocation of photosynthesis regulating factors (cytokinins and gibberellins) in root tissues (Loveys and Bird, 1973). In microplots used to study the effects of RKN on cotton growth and water relations, low stomatal conductance and leaf transpiration rate as well as increases in leaf temperature were observed (Kirkpatrick et al., 1995).

The damage caused by RKN parasitism has also been attributed to delayed maturity (Walker et al., 1998). Nematodes affect carbon allocation and partitioning because of the competition with the host for nutrients in the roots. Research involving tomato plants showed that giant cells, developed at the RKN feeding site, stimulate the allocation of photosynthate to roots instead of shoot (Bird and Loveys, 1975; McClure, 1977). The most common above-ground signs of parasitism are stunting and inhibition of leaf expansion (Kirkpatrick et al., 1995), root/shoot ratio increase (Wilcox-Lee and Loria, 1987), reduction in the number and size of bolls and plant dry weight (Walker et al., 1998), and yield suppression expressed in fewer bolls per plant and reduced cotton seed (Walker et al., 1999) and lint (Davis and May, 2005). Below-ground symptoms are mainly characterized by suppression of root branching, root length and mass, and rate of root growth, which reduces the capacity of the root system to explore the soil (Khoshkhoo et al., 1994; Zhang et al., 2006). The suppression of root biomass causes a reduction in water and nutrient flow. Additionally, the presence of galls or knots in the roots have been shown to decrease water flow to uninfected roots (Kirkpatrick et al., 1991). Even though all of

the processes cited above might impact soil-water-plant relations as well as reduce growth and development of biomass, the degree of damage varies according to the interaction of RKN population, the plant, and the environment.

Most of the research reporting RKN parasitism has been focused on the study of single or multiple cotton physiology and growth processes, the interaction of RKN population with soilborne diseases, and their impact on yield. However, few studies developed under field conditions have quantified how cotton growth and development along with the different components of biomass are affected by RKN parasitism. Additionally, the effects of interactions between RKN population density and abiotic factors on cotton biomass have not been broadly studied. The identification and quantification of which aspects of cotton growth and development are affected most by RKN damage, as well as the interactions with the environment, offers an opportunity to identify new strategies for plant breeding, implement site specific management, and understand the physiological mechanisms of RKN damage for coupling its effects to cotton growth simulations.

Because the level of RKN damage may increase with water stress, comparison of changes in growth and biomass accumulation under different levels of RKN population and soil water content should help to understand the causes of yield losses. The objectives of this study were (1) to study the changes in cotton growth, development, and yield production induced by RKN parasitism, and (2) to study the interaction of RKN populations and drought stress in cotton growth and development and yield production.

## 4.2 Materials and Methods

### 4.2.1 Field experiments

The impact of RKN parasitism and the interaction between RKN population density and drought stress on cotton (*Gossypium hirsutum* L.) growth, biomass and yield were studied in 2006 and 2007 under two different conditions: a producer's cotton field and a controlled experiment conducted at Gibbs Farm of the University of Georgia. Both experiments were located in Tifton, GA (-83° 34' 47.9" N, 31° 26' 24", 90 m elevation above mean sea level) and the soil was a Tifton loamy sand (fine, loamy, siliceous, thermic Plinthic Paleudults; 85% sand, 11% silt, 4% clay at the bottom layer) about 2.0 m deep (Perkins et al., 1986).

The producer field, identified as BJ field in this paper, was planted on 17 May 2006 with the Delta & Pine Land Company DP 555 BG/RR cotton cultivar. Plant density was approximately 36 plants m<sup>-2</sup> with a row spacing of 91 cm. The field was not irrigated. This nonirrigated field was divided into three management zones delineated prior to this study using apparent soil electrical conductivity (EC<sub>a</sub>) measured between 0 - 30 cm (shallow, EC<sub>a-s</sub>) and 0 - 90 cm (deep, EC<sub>a-d</sub>). Because EC<sub>a</sub> has been broadly used as an indirect method to identify changes in soil texture (Fridgen et al., 2000; Kitchen et al., 2003; Sudduth et al., 2005) and has been used to identify areas prone to have greater RKN population densities (Ortiz et al., 2007), the EC<sub>a</sub>-zones represented different levels of water stress and risk for high RKN populations. Therefore, fourteen locations for biomass sampling and growth analysis were identified based on a proportional stratified random sampling design where the strata were the EC<sub>a</sub>-zones. At each of the 14 locations, four cotton plants were selected at random within a 3 m radius of each location and several biomass measurements were collected throughout the growing season (Figure 4.1).

The controlled experiment was located at a field on the Gibbs Farm from the University of Georgia. The experimental design consisted of six treatments in factorial combination of three drought stress levels: low (1), medium (2), and high drought stress (3), and two fumigation levels: nonfumigated (-), and fumigated (+) with 1,3-dichloropropene at 65 L ha<sup>-1</sup> [Telone II, Dow AgroSciences, Indianapolis, Indiana] to create different levels of RKN population densities. The drought stress treatments differed with respect to the frequency and amount of the irrigation water applied (Figure 4.2).

A split-plot design with six replications was used. The three drought stress treatments were assigned to the main plots and the two fumigation levels were assigned to the sub plots. Each plot or experimental unit consisted of four 15.2 m long rows spaced 91 cm. This experiment was planted on May 11, 2007 with the Delta & Pine Land Company DP 458 BG/RR cotton cultivar with seeds sown at 1.2 cm; the same cultivar has been planted in this field for the last five years. Before planting, the field was disc-plowed, harrowed and the winter cover crop, hairy vetch (*Vicia villosa* Roth), incorporated into the soil. The experiment was fertilized two days before sowing with NPK (0-20-20, 392 Kg ha<sup>-1</sup>) and with liquid nitrogen (114 Kg ha<sup>-1</sup>) one month after planting.

#### **4.2.2 Plant measurements**

Biomass samples at the BJ field were collected four times during the growing season including harvest [62, 91, 126, and 161 days after planting ( DAP)]. At 62, 91, and 126 DAP plants covering an area of 0.914 m<sup>2</sup> (1 m of row) were harvested from a place within the area of influence (3 m radius) at each one of the 14 locations. At 161 DAP the field was harvested with a 9965 four-row John Deere picker which had an Ag Leader<sup>®</sup> cotton yield monitor system installed

(Ag Leader Technology, Ames, IA) to record the yield data (cotton seed plus lint), and an AgGPS 132 DGPS receiver with differential correction to calculate the position of the harvester at any time in the field. Ordinary punctual kriging was used to estimate the values of yield at each of the 14 locations.

Biomass samples at the controlled experiment, Gibbs Farm field for future references, were collected four times during the growing season, including harvest (74, 108, 132, and 160 days after planting – DAP). At 74, 108, and 132 DAP, plants covering an area of 0.914 m<sup>2</sup> (1 m of row) were harvested from the central rows of each plot. At 160 DAP, plants covering 1 m of two rows, 1.828 m<sup>2</sup> area were harvested. The lint plus seed from the final harvest (171 DAP) was obtained by mechanical harvest of the remaining plants on the two central rows of each plot. The weight of the lint and seed was separately obtained through several steps: removing a subsample of 22% of the total weight of lint plus seed on each harvested plot, separating the lint from the seed by ginning the bolls in the subsample, calculating the percentage of lint and seed in the subsample, and applying the corresponding percentage values of lint and seed to the total weight of the harvested cotton.

From each biomass sample collected at the two fields, a three-plant subsample was removed and separated into leaves, stem plus petioles, closed and open bolls, lint plus seed, and shell. The number of closed and open bolls from each sample was recorded. All plant material, including the subsample, was oven dried at 70 °C to constant weight and total biomass dry weight was determined. The dry weight per area of each plant component (leaves, stem-petiole, bolls, lint, seed) was calculated as the product of the total biomass dry weight and the fraction of each plant component in the subsample (Fallick et al., 2002).

Leaf area index (LAI) was measured with a LAI-2000 Plant Canopy Analyzer (LI-COR, Lincoln, NE) every two weeks from four plants nearby each one of the 14 locations at the BJ field and at four different locations within each plot of the Gibbs Farm field.

Plant height measured from the soil line to the apex of the terminal bud was recorded weekly. For the BJ field, plant height was measured from the four plants representing the average growth conditions from each location; and at the Gibbs Farm field plants within one meter row of each plot were measured with the average value assigned to each plot.

The proportion of roots on a weight basis was determined from 90 cm long soil cores extracted from the experimental plots at the Gibbs Farm field. Soil cores were extracted next to a cotton plant and between two plants in a row within each plot and they were divided into four sections: 0-15, 15-30, 30-60, and 60-90 cm. The roots in each section of the core were hand picked, washed and dried at 40 °C until constant weight. The proportion of roots was calculated as the weight of root mass in each section of the soil core divided by the total weight of roots in the core.

#### **4.2.3 Nematode population and root galling measurements**

For the BJ field, a 50 x 50 m grid (0.25 ha cell size) was established and soil samples for RKN population density determination [second stage juveniles (RKN-J2)] were collected around the center of each grid cell three times during the growing season: 75, 110, and 167 DAP. The fourteen locations selected for cotton growth analysis were included as part of the sampling grid. For each grid sampling location, eight individual subsamples were collected within a 1.5 m radius and then composited into a single sample representing an average of RKN within each grid cell. Soil probes with a 3 cm diameter opening and approximately 20 cm deep were used to

extract the soil samples for nematode density analysis. The probes were inserted 15 - 30 cm deep into the soil adjacent to the plant tap root. Nematodes were extracted from 100 cm<sup>3</sup> of soil by centrifugal flotation (Jenkins, 1964).

For the Gibbs Farm field, soil samples were collected from each experimental plot four times during the growing season: 18, 65, 127, and 172 DAP. Soil samples consisted of a composite sample of 8 to 10 cores per plot and RKN-J2 were extracted from 150 cm<sup>3</sup> soil by centrifugal flotation (Jenkins, 1964).

Root galls are one of the main cotton expressions of RKN damage. A measure of this root damage, root galling, uses a rating scale where 0 corresponds to scarce or no galls or damage and 10 indicates 100% of the root system galled (Davis and May, 2005). For the BJ field, root galling was evaluated by rating the roots of plants from each biomass sample and at harvest by sampling five plants selected from the area of influence of each one of the 14 locations, four of them corresponding with the plants selected for plant height and LAI data collection throughout the growing season.

#### **4.2.4 Statistical analyses**

For the BJ field, the fourteen sampling locations were combined in three groups to study the effect of RKN infection on biomass. The three groups (low, medium, severe) represented different levels of RKN damage expressed as root galling. The criteria for assigning one location to a group was based not only on the average root galling through the growing season but also the level of galling at each one of the sampling dates.

Biomass data (plant height, LAI, stem-petiole biomass, total biomass, bolls weight, closed bolls number) and yield (lint plus seed) were analyzed by mixed models analysis (Littel et al., 1996)

using PROC MIXED with repeated measures within SAS (SAS Institute, 2007). Statistical differences among galling groups (subjects in the BJ field) and fumigation-drought treatments (subjects in the Gibbs Farm field) were tested with harvest dates or DAP as the repeated factor. In the case of the Gibbs Farm experiment, the autoregressive (AR=1) covariance structure was used to fit the repeated measures and evaluate the effect of the variables fumigation, drought stress, DAP, and the respective interactions. Fumigation treatment and harvest dates were assumed to be fixed because they were not randomly selected from a target population, while drought stress treatments, repetition (replication) and all repetition interactions were considered random. Mean differences between galling groups at each harvest time were compared using least significant ratio (LSD) at  $P \leq 0.1$ . In contrast, means of the Gibbs Farm experiment were obtained and compared with the LSMEANS in SAS at  $P \leq 0.05$ .

## **4.3 Results**

### **4.3.1 Weather**

For the BJ field, rainfall during the period from planting to harvest was lower than the climatic average rainfall. In July, when the squaring and first white flower stages occurred, rainfall was 50% lower (69.2 mm) than the climatic average (139.2 mm) (Figure 4.2a). During the months of July, August, and September the number of days with rainfall were 10, 11, and 9 respectively. Because this field was not irrigated, low rainfall in amount and frequency could impact boll biomass accumulation.

For the Gibbs Farm field, the month of May, which corresponded with the germination and seedling period, had less rainfall than the climatic average (6.5 mm vs. 85.5 mm for the climatic average, Figure 4.2b). However, the deficit of water in the soil profile was mitigated

with irrigation (88.8 mm) reducing the risks of poor germination, root growth and development. Low rainfall during the squaring and flowering stages (79 mm vs. 139 mm of the climatic average for the month of July) was also mitigated with irrigation for the plots that had the low and medium drought stress treatments. The month of August received more rainfall than the climatic average (182 mm compared to the climatic average of 120 mm), resulting in a regrowth of the cotton plants and mitigation of the water stress imposed to the plots receiving the severe drought stress treatment.

#### **4.3.2 Nematode population density, root galling and root biomass**

Data from root galling collected at the fourteen locations within the BJ field were used to group locations into three groups with different levels of RKN damage. Root galling, which has been found to be negatively correlated with plant growth and positively correlated with eggs reproduction, is a reliable method for screening resistant and susceptible cotton cultivars for RKN infection (Davis and May, 2005; Zhang et al., 2006). Therefore, each one of the fourteen locations selected for plant growth analyses were assigned to a group based on the occurrence of high or low root gall ratings throughout the season as well as high, medium, and low root galling season average (Table 4.1). Once the groups were created, differences between the groups with respect to soil  $EC_a$  were observed. Locations within the severe damage group had the lowest soil  $EC_a$  values which confirmed that damage by high RKN population is likely to happen in areas with coarse sand characterized by low shallow  $EC_a$  and low deep  $EC_a$  (Ortiz et al., 2007). Because there was a high variability in RKN population and root galling between the locations, comparisons of plant growth by galling groups facilitated the understanding of the effects of RKN parasitism. The severe galling group included the locations with cotton plants having the

highest root galling across the season and the highest root galling average. In contrast, the low galling group consisted of locations with plants without symptoms of damage.

Root gall ratings were not always consistent with the soil RKN population density. Some locations assigned to the low damage group exhibited a high mid season RKN population density (83 DAP). However, the root gall ratings from plants in close proximity to each location did not indicate severe damage. RKN population density significantly varied among the locations assigned to the galling groups. The low, medium and severe galling groups had an average population of RKN-J2 and coefficient of variation of 166 (95%CV), 329 (106% CV), and 299 (73% CV), respectively.

For the Gibbs Farm field, on average a 56% greater RKN population density was found in nonfumigated plots compared to fumigated plots ( $P = 0.004$ ) (Table 4.2). In contrast, there were no significant differences in population density between the drought stress treatments ( $P = 0.71$ ). A high population density of RKN in nonfumigated plots was observed at 49, 67 and 129 DAP relative to the fumigated plots. The highest population density for the nonfumigated plots was observed after the bolls started cracking (129 DAP) with values increasing from low to severe drought (Table 4.3). By post-harvest (184 DAP), the nematode population was similar for most of the plots. On average, RKN population density on fumigated plots was reduced 52%, 67%, and 47% for the low, medium and severe drought stress treatments compared to nonfumigated plots.

Differences in root biomass expressed as the proportion of roots on a weight basis at different soil layers were found between fumigation treatments (Figure 4.3). The proportion of roots extracted from samples collected next to a cotton plant and between plants was higher for

nonfumigated treatments than fumigated being more evident in the shallow layers (0- to 15- cm and 15- to 30-cm depth).

### **4.3.3 Plant height**

The damage by RKN was shown by a reduction in plant height from cotton plants growing on coarse sandy areas of the BJ field and nonfumigated plots of the Gibbs Farm field. Cotton plants with symptoms of RKN infection exhibited a 11% to 14% reduction in height compared to the plants with low or zero infection. For the BJ field, there were significant differences in plant height throughout the growing season ( $P < .0001$ ) with the lowest mean values observed for the severe galling group (Table 4.4). The highest differences in plant height between the severe and low galling groups occurred early in the season with significant differences at 38, 51, and 60 DAP; and the highest reduction (12.7%) observed at 60 DAP (Table 4.5). Fumigation on plots of the Gibbs Farm field had a significant impact ( $P < .0001$ ), not only on plant height but also other cotton biomass components (Table 4.6). Drought also significantly impacted plant height ( $P = 0.036$ ), especially the severe drought (1.53 cm less in average with respect to low drought). The differences in plant height between fumigated and nonfumigated plots increased with the level of drought which evidenced an interaction drought  $\times$  fumigation ( $P = 0.031$ ) (Table 4.6). On average, plant height for the nonfumigated plots was reduced 11%, 10.7% and 14% for low, medium, and severe drought stress with respect to the fumigated plots (Figure 4.4a). Even though reductions in plant height for the nonfumigated plots were evidenced at 49 DAP, the greatest difference between fumigation treatments was observed just before the early bloom stage (64 DAP) with 11.4 cm lower plant height (18% reduction) occurring for the nonfumigated plots (Table 4.7).

#### **4.3.4 Leaf area index**

For both fields, increasing densities of RKN had a strong negative effect on LAI, which increased with drought stress (Table 4.4 and 4.8). At the BJ field, LAI was significantly different ( $P < .0001$ ) between the galling groups and the lowest LAI was found in locations with severe galling (Table 4.4). Low LAI values for the severe galling group relative to the medium and low galling groups were observed either early in the growing season (42 and 61 DAP) or late in the season (113 and 132 DAP) (Table 4.8). For the Gibbs Farm field, the average reduction in LAI for the nonfumigated plots ( $2.48 \text{ cm}^2 \text{ cm}^{-2}$ ) with respect to the fumigated plots ( $3.03 \text{ cm}^2 \text{ cm}^{-2}$ ) was mainly attributed to the 36% greater RKN population density found in those plots. These significant differences increased in average from 15.6% to 20% with low to severe drought stress levels, respectively (Table 4.5, Figure 4.4b). The maximum LAI occurred at bloom (88 DAP) when the highest difference (23% reduction) in LAI between fumigation treatments was observed (Table 4.9). These differences, expressed as percentage reduction in LAI from nonfumigated plots relative to the fumigated plots, increased from planting to flowering and then declined until physiological maturity.

#### **4.3.5 Total biomass**

On average, above ground biomass decreases were caused by RKN damage and drought stress, especially under conditions of high population of RKN and severe drought. For the BJ field, the cotton plants from the severe galling group had an average total biomass 9% lower than the low and medium galling groups (Table 4.4). More marked differences in total biomass between the severe and the other two galling groups occurred early in the season. During the squaring (62 DAP) and flowering (91 DAP) stages, the reduction in total biomass from plants in

the severe group compared to the low galling group were 31% and 21%, respectively (Table 4.10). For the Gibbs Farm field, total biomass was not only reduced due to RKN damage on nonfumigated plots with respect to the fumigated ( $P = 0.001$ ), but also these differences increased as a consequence of increments in drought (Figure 4.5a). The percent reduction in the average total biomass in nonfumigated plots versus the fumigated plots was 14.4%, 10.6% and 22.5% for the low, medium, and severe drought stress levels, respectively. Similar to the BJ field, significant differences between fumigation treatments were observed at early flowering (74 DAP). However, these differences did not change with the level of drought stress. Once the cotton bolls started cracking (132 DAP) and at harvest, the differences between the fumigation treatments increased as the level of drought increased from low to severe. The impact of drought was more severe at the fruiting stage because that is when the highest demand for water occurs. At 132 DAP and 160 DAP, the percentage reduction in total biomass in nonfumigated compared to fumigated plots was around 14% and 23% for the low and severe drought stress levels, respectively. At this time of the growing season, these differences resulted in more bolls in the plants of the fumigated treatment.

#### **4.3.6 Stem and petiole biomass**

One of the biomass components highly impacted by the fumigation and drought stress treatments was stem and petiole biomass. For the BJ field, even though there were no differences in the average season stem and petiole biomass between the galling groups; the greatest difference between the severe and low galling groups occurred during squaring and cutout (18.2% and 16.4% respectively) (Tables 4.4 and 4.10).

At the Gibbs Farm field, the significant effect of fumigation ( $P = 0.001$ ) and drought ( $P = 0.088$ ) on stem and petiole biomass was shown by an average reduction of 11%, 16.9% and 29.8% for the nonfumigated plots relative to the fumigated plots under low, medium, and severe drought stress, respectively (Table 4.6, Figure 4.5b). Differences between fumigation treatment with respect to the level of drought stress were more evident at the peak of bloom (108 DAP) and when the cotton bolls started cracking (132 DAP) (Table 4.11).

#### **4.3.7 Yield components**

##### *Boll biomass*

Along with stem and petiole biomass, bolls were the biomass component most highly and negatively impacted by nematode population. For the BJ field, boll biomass was 8% lower in the severe galling group than the low galling group (Table 4.4). After cutout (91 DAP), the cotton plants from the severe galling group had 31% less boll dry biomass than the low galling group. These differences were less when the cotton bolls started cracking, but the 15% reduction under the severe galling group suggested a delay in the accumulation of boll biomass and/or a reduction in the number or size of the bolls. At the Gibbs Farm field, the differences between fumigation treatments for the low and severe drought levels were 1170 kg ha<sup>-1</sup> (31% reduction) and 734 kg ha<sup>-1</sup> (25% reduction), respectively (Table 4.6). The significant impact of fumigation ( $P < .0001$ ) in boll biomass was highly evident in plots of low drought compared with severe drought (Figure 4.5c). For the plots that were fully irrigated (low drought stress), the nonfumigated treatment decreased boll biomass 37% at 108 DAP and 42% at 132 DAP relative to fumigated treatment. Although numerically lower, in the plots under severe drought, the nonfumigated treatment reduced bolls biomass 30% at 108 DAP and 26% at 132 DAP respect to

the fumigated treatment (Table 4.11). These results not only indicated an impact of RKN population density on bolls biomass, but also a significant response of the cotton plants to the fumigation where a high boll biomass (number and size of bolls) were produced per unit ground area.

#### Closed boll number

Although there was not much similarity in the results from the BJ field and the Gibbs Farm field with respect to the number of closed bolls per area, the elevated number of closed bolls for the nonfumigated treatment from the Gibbs Farm experiment evidenced a delay in maturity (Figure 4.5d). At the BJ field, the cotton plants in the severe galling group had, on average, about 10% fewer closed bolls relative to the low galling group (Table 4.4). By the end of cutout (91 DAP) and during the boll cracking stage (126 DAP), the number of closed bolls in the severe galling group were 37% and 33% lower than the low galling groups, respectively (Table 4.10). At the Gibbs Farm field, even though there were no significant differences in the number of closed bolls between fumigation or drought treatments ( $P = 0.128$ ), the nonfumigated treatment had, on average, 13% more close bolls than the fumigated treatment (Figure 4.5d). The percentage increase in the average season closed boll number occurring on nonfumigated plots compared to the fumigated plots was 23%, 7% and 8% for the low, medium, and severe drought stress levels, respectively (Table 4.6). The differences between fumigation treatments were more evident at the peak of closed bolls production (108 DAP) where nonfumigated plots under low drought stress had 36% more closed bolls than the fumigated and 13% more under severe drought (Table 4.11).

### Lint plus seed yield

The high number of closed bolls and also the reduction of boll biomass in the nonfumigated plots resulted in the decline of lint plus seed yield. In contrast, the response of cotton plants to the fumigation with 1,3-dichloropropene along with full irrigation resulted in an increase of boll biomass without delay in maturity, which resulted in a higher lint plus seed yield than nonfumigated plants. For the BJ field, there were no differences in average yield between galling groups, however at 91 DAP the low galling group had higher yield than the severe galling group (Table 4.4 and 4.10). In contrast, at the Gibbs Farm field, drought decreased yield ( $P = 0.001$  at 160 DAP,  $P = 0.025$  at 171 DAP) and fumigation increased lint plus seed yield ( $P = 0.028$  at 160 DAP,  $P = 0.055$  at 171 DAP) (Table 4.12). The lint plus seed was reduced 12% to 14% in nonfumigated plots compared to fumigated plots, and these differences increased with increasing level of drought stress (Table 4.13).

### **4.4 Discussion**

The average population densities of RKN exhibited large within-season variation as well as within-field variability with a preference for coarse, sandy areas. In areas without nematicide treatment, the RKN population increased until the bolls started cracking and then declined due to leaf senescence and decline of root biomass. Population densities below the threshold for Georgia, 100 second stage juveniles  $100\text{ cm}^{-3}$  soil, were found in most of the cases in plots fumigated with 1,3-dichloropropene at  $65\text{ L ha}^{-1}$ . However, the increase of population density in the fumigated plots at the end of the growing season indicated a lack of season-long control (Davis and May, 2003; Pettigrew et al., 2005).

Galling severity in locations with the lowest soil  $EC_a$  (shallow and deep) values in a producer's field showed a good response to nematicide applications thereby indicating risk for yield losses on sandy areas. Ortiz et al. (2008) evaluated the response to two nematicides across different management zones and found that 1,3-dichloropropene at  $56 \text{ L ha}^{-1}$  provided the best nematode control and profits for the highest risk zone (lowest  $EC_a$ ). In contrast, the lowest risk areas in this field showed no benefits from fumigation. Increased RKN damage on coarse, sandy areas of cotton fields show the importance of site specific management which can be facilitated by the use of management zones based on soil  $EC_a$  along with other edaphic properties (Ortiz et al., 2007).

Cotton growth and development were impacted by elevated RKN population densities and drought stress. The fumigation treatment used to reduce RKN population density increased growth and development of vegetative and reproductive biomass components (Figure 4.4 - 4.5). The efficacy in the control of RKN population density through fumigation early in the season was shown by the significant differences in plant height and LAI between fumigated and nonfumigated plots. These differences are related to early season root galling (Creech et al., 1995), which occurred in the absence of fumigation. In this study, the increment of root weight in the shallow layers with respect to the total root weight for nonfumigated plots was associated with the presence of root galls in the shallow roots as a result of the RKN infection. Although the proportion of the roots through the soil profile was different for each one of the sampling locations (next to a plant and between plants), the increment in root proportion at the depth 30-cm to 60-cm on nonfumigated plots may be due to root growth compensation for drought caused by the RKN damage. Therefore, early protection against RKN damage causing root malfunctioning and changes in rooting depth and distribution (Shepherd and Huck, 1989) will

prevent reductions in water and nutrient uptake which later may impact biomass accumulation (Kirkpatrick et al., 1991).

Plant height reduction (11%-14%) resulted as a consequence of RKN infection and increased as the RKN population and drought increased (Figure 4.4a). The negative correlation between plant height and root galling for coarse areas, as well as high population density of RKN in nonfumigated plots, showed that plant growth was suppressed as a consequence of RKN infection, which severely increased with the extension of drought periods. These effects can be explained by the decreased water uptake of infected cotton plants experiencing periodic water stress (Kirkpatrick et al., 1995; O'Bannon and Reynolds, 1965). Plant height, along with root galling and fresh plant weight, have been considered important criteria for measuring RKN resistance in cotton (Zhang et al., 2006). Therefore, early season differences in plant height may be used as a surrogate for identifying potential areas of RKN damage. Presumably, the decline in LAI on the severe galling group and on nonfumigated plots was due to a reduction of leaf expansion caused by decreases in stomatal conductance, leaf transpiration rate and increasing leaf temperature (Kirkpatrick et al., 1995).

The greatest reductions in plant height, LAI and stem-petiole biomass were observed at the cutout period. During cutout the rate of vegetative growth and flowering is reduced due to the production of bolls which demand elevated amount of assimilates (Pettigrew et al., 2005). The high demand for assimilates by root galls also contributes to the reductions in vegetative growth at cutout and during boll growth.

The reduction in above ground biomass in nonfumigated plots and the increased losses as drought increased may also be explained by the root damage which significantly impacts water and nutrient absorption (Kirkpatrick et al., 1991). Previous research has shown reduction of

water flow through infected roots as a consequence of nematode parasitism in other plant species. Smit and Vamerali (1998) found that the main effect of potato cyst nematode was a retarded growth length and early root decay which impacted water uptake. Similarly, Dorhout et al. (1991) reported a reduction of total water flow in tomato roots as a consequence of reduced total root length.

Another explanation for the suppressed shoot growth is a change in partitioning due to the diversion or sink of assimilate ( $\text{CH}_2\text{O}$ ) to roots as a result of root parasitism (Williamson and Gleason, 2003). In the controlled experiment of this study, the highest root galling was observed close to the peak of bloom (95 DAP), which may indicate that high amounts of carbon were already used in the production of galls at the cost of reduction in above ground biomass.

Khoshkhoo et al. (1994) associated high levels of glucose in leaves of susceptible cotton genotypes and sucrose in roots with a reduction of root mass and sink of assimilates due to RKN feeding. Research involving tomato plants showed that giant cells, developed around the RKN feeding site, stimulated the allocation of photosynthate to roots instead of shoot where they are used by the nematodes (Bird and Loveys, 1975; McClure, 1977; Williamson and Gleason, 2003). Nematode- infected cotton plants consume slightly more water than noninfected plants if water is supplied continuously (O'Bannon and Reynolds, 1965). Therefore, good practices of irrigation and fertilization could mitigate the impacts of nematodes on plant growth and development.

The yield response to fumigation was observed in the production of 30% more boll biomass per area, which may results in 13% to 16% improvement of lint plus seed yield relative to the nonfumigation. Previous research has shown the benefits on the production of more bolls per unit area when using aldicarb to control reniform nematodes (*Rotylenchulus reniformis*) (Pettigrew et al., 2005) and improvements in lint yield when using 1,3-dichloropropene to

control RKN (Davis and May, 2003; Zimet et al., 2002). The reduction in boll biomass may be associated with a decrease in leaf area, particularly subtending leaves. Ashley (1972) and Brown (1968) found that subtending leaves are coupled to the translocation of assimilate to cotton bolls and considered these leaves as the primary source of photosynthate for the developing cotton bolls. Therefore, the whole-plant LAI decrease in nonfumigated plots could contribute to the losses in boll biomass.

In addition to the overall reduction of boll biomass, a 10% average increase in closed bolls (which can not be harvested) in nonfumigated plots can be considered as one of the main sources for yield losses. The high number of closed bolls found in cotton grown without nematicide treatment is a clear indication of delay in maturity which has been discussed in previous research as one of the results of nematode parasitism in cotton. Then, a delay in maturity, caused mainly by a delay of cotton plants setting bolls as a consequence of RKN damage, could explain the differences in total biomass. Robinson (2007) reported that flowering and fruit set are delayed one or two fruiting branches up the main stem as a consequence of reniform parasitism in cotton. Cotton damage by Columbia lance (*H. Columbus*) nematode has been also associated with delayed onset of fruiting and delay in harvest maturity (Bond and Mueller, 2007). Drought could be another cause of boll biomass reduction which was evident by a low number of close bolls observed under severe drought conditions (McWilliams, 2003).

All the effects of RKN parasitism discussed above indicated that areas at risk for high populations of RKN should receive a different agronomic management which may include a delay of harvest time to allow the cotton plants in those areas to reach full maturity.

## **4.5 Conclusions**

High populations of RKN were found on coarse, sandy areas and plots without fumigation. In contrast, fumigation with 1,3-dichloropropene provided suppression of RKN during most of growing season with less effectiveness towards the harvest time. Root-knot nematode parasitism resulted in a reduction of the growth and development of evaluated cotton biomass components (plant height, LAI, stem-petiole biomass, number of bolls, number of closed bolls, lint plus seed yield). However, the effects of high RKN population density were exacerbated by drought stress. A significant interaction between fumigation and drought stress was highly evidenced by a reduction in plant height and boll dry weight, which showed that a high RKN population density and drought limit vegetative and reproductive growth. Another effect of RKN parasitism was the high number of closed bolls observed on nonfumigated plots, caused by a delay in the onset of fruiting, resulting in a delay in harvest maturity. This delay in maturity and the reduction of boll biomass are directly related with the decline of lint plus seed yield.

Therefore, damage from RKN, which is most likely to occur in coarse sand areas, could be reduced if a site specific management is implemented to suppress nematodes and also to supply water and nutrients to areas with elevated risk for parasitism.

## **Acknowledgments**

This work was supported by funds from Cotton Inc., the Georgia Cotton Commission, the Flint River Water Planning and Policy Center, Hatch and State funds allocated to the Georgia Agricultural Experiment Stations and by USDA-ARS CRIS project funds. Mention of commercially available products is for information only and does not imply endorsement. We

also thank Mr. Jerry Davis Statistician from UGA –Griffin campus for his assistance with different statistical analyses included in this paper.

Finally, special thanks to Dewayne Dales, Gary Murphy, Rodney Hill, Katia Rizzardi, Manuel Renga, Melanie Blomenhoer, Eleni Tzanakouli, Jason Tood, who assisted with the extensive field work required to complete this project.

## References

- Ashley, D.A. 1972.  $^{14}\text{C}$ -Labeled photosynthate translocation and utilization in cotton plants. *Crop Sci.* 12: 69-74.
- Bird, A.F. 1974. Plant response to root- knot nematode. *Ann. Rev. Phytophat.* 12: 69-85.
- Bird, A.F., and R.R. Loveys. 1975. The incorporation of photosynthates by *Meloidogyne javanica*. *J. Nematol.* 7:111-113.
- Bond, C.R., and J. D. Mueller. 2007. Delayed maturity and associated yield loss in cotton infected by the Columbia Lance (*Hoplolaimus Columbus* Sher) nematode. *J. Cotton Sci.* 11: 275-287.
- Brown, K.L. 1968. Translocation of carbohydrate in cotton: Movement to fruting bodies. *Ann. Bot.* 32: 703-713.
- Creech, R.G., J.N. Jenkins, B. Tang, G.W. Lawrance, and J.C. McCarthy. 1995. Cotton Resistance to Root-Knot Nematode: I. Penetration and Reproduction. *Crop Sci.* 35: 365-368.
- Davis, R.F., and O.L. May. 2003. Relationships between tolerance and resistance to *Meloidogyne incognita* in Cotton. *J. Nematol.* 35: 411-416.
- Davis, R.F., and O.L. May. 2005. Relationship between yield potential and percentage yield suppression caused by the southern root-knot nematode in cotton. *Crop Sci.* 45: 2312-2317.
- Dorhout, R., F.J. Gommers, and C. Kollöffel. 1991. Water transport through tomato roots infected with *Meloidogyne incognita*. *Phytopathology* 81: 379-385.
- Ehwaeti, M.E., M.J. Elliott, J.M. McNicol, M.S. Phillips, and D.L. Trudgill. 2000. Modelling nematode population growth and damage. *Crop Prot.* 19: 739-745.
- Fallick, J.B., W.D. Batchelor, G.L. Tylka, T.L. Niblack, and J.O. Paz. 2002. Coupling soybean cyst nematode damage to CROPGRO Soybean. *Trans. ASAE* 45: 433-441.
- Fridgen, J. J., C. W. Fraisse, N. R. Kitchen, and K. A. Sudduth. 2000. Delineation and analysis of site-specific management zones. In *In Proc. 2<sup>nd</sup> International Conference on Geospatial Information in Agriculture and Forestry*, CD-ROM. Lake Buena Vista, FL.
- Jenkins, W.R. 1964. A rapid centrifugal flotation technique for separating nematodes from soil. *Plant Dis.* 48: 692.
- Khoshkhoo, N., P.A. Hedin, and J.C.J. McCarthy. 1994. Free sugars in root-knot nematode susceptible and resistant cotton plant roots and leaves. *J. Agric. Food Chem.* 42: 366-368.

- Kirkpatrick, T.L., D.M. Oosterhuis, and S.D. Wullschleger. 1991. Interaction of *Meloidogyne incognita* and water stress in two cultivars. *J. Nematol.* 23: 462-467.
- Kirkpatrick, T.L., M.W. van Iersel, and D.M. Oosterhuis. 1995. Influence of *Meloidogyne incognita* on the water relations of Cotton growth in microplots. *J. Nematol.* 27: 465-471.
- Kitchen, N.R., S.T. Drummond, E.D. Lund, K.A. Sudduth, and G.W. Buchleiter. 2003. Soil electrical conductivity and topography related to yield for three contrasting soil-crop systems. *Agron. J.* 95: 483-495.
- Koenning, S.R., T.L. Kirkpatrick, J.L. Starr, J.A. Wrather, N.R. Walker, and J.D. Mueller. 2004. Plant-Parasitic Nematodes Attacking Cotton in the United States: Old and Emerging Production Challenges. *Plant Dis.* 88: 100-113.
- Littel, R.C., G.A. Milliken, W.W. Stroup, and R.D. Wolfinger. 1996. *SAS Systems for Mixed Models*, Cary, NC.
- Loveys, R.R., and A.F. Bird. 1973. The influence of nematodes on photosynthesis in tomato plants. *Physiol. Plant Pathol.* 3: 525-529.
- McClure, M.A. 1977. *Meloidogyne incognita*: A metabolic sink. *J. Nematol.* 9: 88-90.
- McWilliams, D. 2003. Drought strategies for cotton. New Mexico State University, Las Cruces. 6 p.
- NCC. 2008. Beltwide yield losses to nematode damage. Cordova, TN.: National Cotton Council of America. Available at: [www.cotton.org/tech/pest/nematode/losses.cfm](http://www.cotton.org/tech/pest/nematode/losses.cfm). Accessed August 17, 2008.
- O'Bannon, J.H., and H.W. Reynolds. 1965. Water consumption and growth of root-knot nematode-infected and uninfected cotton plants. *Soil Sci.* 99: 251-255.
- Ortiz, B. V., D. G. Sullivan, C. Perry, G. Vellidis, L. Seymour, and K. Rucker. 2007. Delineation of management zones for site specific management of parasitic nematodes using geostatistical analysis of measured field characteristics. In *Proc. Sixth European Conference of Precision Agriculture (6ECPA)*., CD-ROM. Stafford, J., and A. Werner, eds. Skiathos. Greece.
- Ortiz, B. V., C. Perry, D. G. Sullivan, R. C. Kemerait, A. Ziehl, R. Davis, G. Vellidis, and K. Rucker. 2008. Evaluation of Variable Rate of Nematicides on Cotton According to Nematode Risk Zones. In *Proc. 2008 Beltwide Cotton Conference*. Nashville, TN.: National Cotton Council.
- Perkins, H.F., J.E. Hook, and N.W. Barbour. 1986. Soil characteristics of selected areas of the coastal plain experiment station and ABAC research farms. The University of Georgia.

- Pettigrew, W.T., W.R. Meredith, Jr., and L.D. Young. 2005. Potassium fertilization effects on cotton lint yield, yield components, and reniform nematode populations. *Agron. J.* 97: 1245-1251.
- Robinson, A.F. 2007. Reniform in U. S Cotton: When, where, why, and some remedies. *Ann. Rev. Phytopathol.* 45: 263-288.
- SAS Institute Inc. 2007. SAS OnlineDoc (R) 9. 1. 3. Cary, NC: SAS Institute Inc.
- Shepherd, R.L., and M.G. Huck. 1989. Progression of root-knot nematode symptoms and infection on resistant and susceptible cotton. *J. Nematol.* 21: 235-241.
- Smit, A.L., and T. Vamerali. 1998. The influence of potato cyst nematodes (*Globodera pallida*) and drought on rooting dynamics of potato (*Solanum tuberosum* L.). *Eur. J. Agron.* 9: 137-146.
- Sudduth, K.A., N.R. Kitchen, W.J. Wiebold, W.D. Batchelor, G.A. Bollero, D.G. Bullock, D.E. Clay, H.L. Palm, F.J. Pierce, R.T. Schuler, and K.D. Thelen. 2005. Relating apparent electrical conductivity to soil properties across the north-central USA. *Comp. Electron. Agric.* 46: 263-283.
- Walker, N.R., T.L. Kirkpatrick, and C.S. Rothrock. 1998. Interaction between *Meloidogyne incognita* and *Thielaviopsis basicola* on cotton (*Gossypium hirsutum*). *J. Nematol.* 30: 415-422.
- Walker, N.R., T.L. Kirkpatrick, and C.S. Rothrock. 1999. The interaction between the root-knot nematode (*Meloidogyne incognita*) and black root rot (*Thielaviopsis basicola*) on cotton (*Gossypium hirsutum*). *J. Nematol.* 30: 415-422.
- Wilcox-Lee, D.A., and R. Loria. 1987. Effects of nematode parasitism on plant-water relations. In *Vistas on nematology*, 260-266. Hyattsville, MD. Society of Nematologists.
- Williamson, V.M., and C.A. Gleason. 2003. Plant-nematode interactions. *Curr. Opin. Plant Biol.* 6:4: 327-333
- Wyss, U., F.M.W. Grundler, and A. Munch. 1992. The parasitic behaviour of second stage juveniles of *Meloidogyne incognita* in root of *Arabidopsis thaliana*. *Nematologica* 38: 98-111.
- Zhang, J., C. Waddell, C. Sengupta-Gopalan, C. Potenza, and R.G. Cantrell. 2006. Relationships between root-knot nematode resistance and plant growth in upland cotton: galling index as a criterion. *Crop Sci.* 46: 1581-1586.
- Zimet, D.J., J.L. Smith, R.A. Kinloch, and J.R. Rich. 2002. Improving cotton returns using nematicides in Northwestern Florida infested with Root-Knot Nematode. *J. Cotton Sci.* 6: 28-33.

Table 4.1. Locations for cotton growth study grouped by root galling rates in the BJ field.

Galling group†	Location	Root galling‡					RKN-J2 per 100 cm <sup>3</sup> soil (83 DAP)	EC <sub>a</sub> Class§
		Days after planting - DAP				Average		
		30	60	95	140			
3 - Severe	3	4	0	8	2.4	3.6	304	1
	10	0	0	7	1.0	2.0	52	1
	11	5	1	6	6.6	4.7	6	2
	9	0	6	3	4.2	3.3	302	2
2 - Moderate	7	0	1	6	2.0	2.3	76	3
	12	0	0	4	2.2	1.6	124	2
	13	1	1	2	2.8	1.7	744	2
	6	2	0	0	2.2	1.1	672	2
	8	1	0	0	1.6	0.7	28	2
1 - Low	14	0	0	0	0.8	0.2	602	2
	5	1	0	0	0.6	0.4	88	2
	2	0	0	0	0.4	0.1	232	2
	4	0	0	0	0.2	0.1	132	3
	1	0	0	0	0.0	0.0	444	2

† The galling group is relative to the RKN damage observed in the root system and evaluated through root galling.

‡ Gall ratings correspond to: 0 = no galling, 1 = 10% of roots are galled, 2 = 11-20% galled, etc., 10 = 91-100% galled.

§ EC<sub>a</sub> Class: (1) EC<sub>a-shallow</sub> = 0.61 mS/m and EC<sub>a-deep</sub> = 1.46 mS/m, (2) EC<sub>a-shallow</sub> = 0.76 mS/m and EC<sub>a-deep</sub> = 1.83 mS/m, (3) EC<sub>a-shallow</sub> = 1.02 mS/m and EC<sub>a-deep</sub> = 2.42 mS/m

Table 4.2. Differences in RKN population density by drought stress and fumigation treatments at the Gibbs Farm field. Average across four sampling times over six replications.

Treatment		Second stage juveniles per 150 cm <sup>3</sup> of soil†
Drought stress	Fumigation	
Low		108
Medium		131
Severe		126
	$P > F‡$	0.710
	0 L ha <sup>-1</sup>	148
	65 L ha <sup>-1</sup>	95
	$P > F§$	0.004

†LSMEAN was utilized as means separation. Means were

‡ Drought stress treatments were significant at  $P \leq 0.05$  calculated from data collected four times during the growing season.

§ Fumigation treatments were significant at  $P \leq 0.05$

Table 4.3. Time series of RKN population density by drought stress and fumigation treatments at the Gibbs Farm field.

DAP	Statistics†	RKN population density (second stage juveniles per 150 cm <sup>3</sup> of soil)					
		Drought stress level					
		Low		Medium		Severe	
		Fumigation levels					
		0 L ha <sup>-1</sup>	65 L ha <sup>-1</sup>	0 L ha <sup>-1</sup>	65 L ha <sup>-1</sup>	0 L ha <sup>-1</sup>	65 L ha <sup>-1</sup>
18	mean (CV)	23 (75)	5 (167)	28 (103)	0 (-)	28 (143)	5 (167)
	LSMEANS <sub>1</sub>	-18		-28*		-23.3	
	LSMEANS <sub>2</sub>	-23*					
66	mean (CV)	37 (131)	10 (167)	38 (58)	17 (73)	7 (-)	0 (181)
	LSMEANS <sub>1</sub>	-27		-22		-6	
	LSMEANS <sub>2</sub>	-8					
118	mean (CV)	210 (47)	100 (47)	345 (61)	111 (129)	361 (68)	191 (70)
	LSMEANS <sub>1</sub>	-110		-233		-170	
	LSMEANS <sub>2</sub>	-171					
175	mean (CV)	212 (70)	265 (71)	288 (48)	212 (93)	205 (78)	213 (41)
	LSMEANS <sub>1</sub>	53		-77		8	
	LSMEANS <sub>2</sub>	-2					

† Mean of RKN population density for each treatment combination over six replications. Coefficient of variation (CV).

LSMEANS<sub>1</sub> corresponds to the difference of least square means between fumigation treatments within one specific level of drought stress. LSMEANS<sub>2</sub> corresponds to the difference of least square means between fumigation treatments over all the drought stress treatments.

\* Significant  $P \leq 0.05$

Table 4.4. Plant height, LAI, dry matter biomass, and yield as affected by different galling groups, averaged across four harvest dates for the BJ field.

Galling group†	Plant Height	LAI	Total biomass dry wt.	Stem and Petiole dry wt.	Bolls dry wt.	Lint plus Seed	Closed boll no.
	cm	m <sup>2</sup> m <sup>-2</sup>	----- kg ha <sup>-1</sup> -----				bolts m <sup>-2</sup>
Low	22.8	1.56	3944.0	936.3	2500.0	2032.0	23.1
Medium	22.7	1.71	3932.0	1042.4	2511.0	1846.0	20.0
Severe	21.1	1.41	3583.0	872.3	2296.0	1948.0	20.8
Galling group $P > F$ ‡	<.0001	<.0000	0.601	0.590	0.900	0.770	0.870

† The galling group is relative to the RKN damage observed in the root system and evaluated through root galling.

‡ Mean differences between galling groups significant at  $P \leq 0.05$

Table 4.5. Plant height differences between galling groups for nine different plating dates in the BJ field.

DAP	Statistics†	Plant Height (cm)		
		Galling group‡		
		Low	Medium	Severe
38	mean	27.1a	28.9a	24.2b
	% reduction		10.7	
44	mean	36.3a	37.8a	31.7a
	% reduction		12.7	
51	mean	47.7a	48.0a	41.91b
	% reduction		12.1	
60	mean	57.9a	56.1a	50.54b
	% reduction		12.7	
71	mean	63.0a	61.0a	57.98a
	% reduction		8.1	
80	mean	63.7a	62.2a	60.4a
	% reduction		5.1	
87	mean	64.5a	62.2a	61.2a
	% reduction		4.1	
98	mean	68.8a	68.8a	67.0a
	% reduction		2.62	
105	mean	75.7a	78.0a	70.1b
	% reduction		7.4	

† Mean of plant height for each galling group at a specific day after planting. Percentage reduction in plant height for severe galling group relative to the low galling group is reported.

‡ Means followed by the same letter within rows and the same DAP are not significantly different at  $P = 0.1$ . Least significant difference (LSD) was utilized as mean separation.

Table 4.6. Plant height, LAI, and dry matter biomass as affected by drought and fumigation treatments, averaged across drought-fumigation treatment combinations and four harvest dates for the Gibbs Farm field.

Drought stress level	Fumigation level	Plant Height	LAI	Total biomass dry wt.	Stem and Petiole dry wt.	Bolls dry wt.	Closed boll no.
		cm	m <sup>2</sup> m <sup>-2</sup>	-----	kg ha <sup>-1</sup> -----		bolles m <sup>-2</sup>
Low	0 L ha <sup>-1</sup>	27.7	2.7	6972.6	2381.4	2586.9	33.2
	65 L ha <sup>-1</sup>	31.1	3.2	8149.6	2674.5	3756.8	27.0
Medium	0 L ha <sup>-1</sup>	26.4	2.4	6222.5	1880.0	2645.8	29.1
	65 L ha <sup>-1</sup>	29.5	2.9	6959.4	2262.5	3084.3	27.1
Severe	0 L ha <sup>-1</sup>	25.8	2.4	5198.8	1506.8	2240.1	27.7
	65 L ha <sup>-1</sup>	30.0	3.0	6707.8	2147.6	2974.2	25.6
<i>Between subjects</i>							
Drought stress	<i>P</i> > <i>F</i>	0.036	0.069	0.063	0.088	0.037	0.583
Fumigation	<i>P</i> > <i>F</i>	<.0001	<.0001	0.001	0.001	<.0001	0.128
Fumigation × Drought stress	<i>P</i> > <i>F</i>	0.031	0.354	0.638	0.531	0.244	0.688
<i>Within subjects</i>							
DAP	<i>P</i> > <i>F</i>	<.0001	<.0001	<.0001	<.0000	<.0001	<.0002
Drought stress × DAP	<i>P</i> > <i>F</i>	0.000	0.099	0.086	0.002	0.232	0.604
Fumigation × DAP	<i>P</i> > <i>F</i>	0.003	0.007	0.927	0.915	0.060	0.073

Table 4.7. Plant height differences between fumigation treatments for three drought stress treatments, averaged across six replications for the Gibbs Farm field.

DAP	Statistics†	Plant Height (cm)					
		Drought stress					
		Low		Medium		Severe	
		Fumigation					
		0 L ha <sup>-1</sup>	65 L ha <sup>-1</sup>	0 L ha <sup>-1</sup>	65 L ha <sup>-1</sup>	0 L ha <sup>-1</sup>	65 L ha <sup>-1</sup>
	mean	20.8	24.7	22.2	25.6	21.0	25.1
49	LSMEANS <sub>1</sub>	3.91*		3.42*		4.15*	
	LSMEANS <sub>2</sub>	3.83*					
	mean	34.4	45.3	36.1	44.7	34.8	45.3
57	LSMEANS <sub>1</sub>	10.93*		8.60*		10.44*	
	LSMEANS <sub>2</sub>	9.99*					
	mean	52.0	63.8	52.6	62.6	49.9	62.3
64	LSMEANS <sub>1</sub>	11.81*		9.95*		12.38*	
	LSMEANS <sub>2</sub>	11.38*					
	mean	70.8	83.1	74.1	79.0	66.0	79.5
70	LSMEANS <sub>1</sub>	12.27*		4.87*		13.44*	
	LSMEANS <sub>2</sub>	10.19*					
	mean	81.0	91.4	77.0	86.7	75.3	87.9
78	LSMEANS <sub>1</sub>	10.33*		9.63*		12.69*	
	LSMEANS <sub>2</sub>	10.88*					
	mean	84.6	94.2	81.4	89.0	81.2	90.0
87	LSMEANS <sub>1</sub>	9.66*		7.57*		8.81*	
	LSMEANS <sub>2</sub>	8.68*					
	mean	84.6	94.0	77.3	88.0	76.1	90.1
94	LSMEANS <sub>1</sub>	9.40*		10.71*		14.06*	
	LSMEANS <sub>2</sub>	11.39*					
	mean	90.3	98.9	83.7	91.2	83.7	93.5
99	LSMEANS <sub>1</sub>	8.56*		7.51*		9.79*	
	LSMEANS <sub>2</sub>	8.62*					
	mean	93.1	97.0	82.2	90.8	83.4	92.7
109	LSMEANS <sub>1</sub>	3.85*		8.58*		9.31*	
	LSMEANS <sub>2</sub>	7.24*					
	mean	92.3	98.4	83.3	93.0	83.6	95.5
116	LSMEANS <sub>1</sub>	6.05*		9.65*		11.96*	
	LSMEANS <sub>2</sub>	9.22*					

† Mean of plant height for each treatment combination over six replications. LSMEANS<sub>1</sub> is the difference of least square means between fumigation treatments within one specific level of drought stress and LSMEANS<sub>2</sub> is difference between fumigation treatments over all the drought stress treatments.

\* Significant  $P \leq 0.05$

Table 4.8. LAI differences between galling groups for nine different plating dates for the BJ field.

DAP	Statistics†	LAI (m <sup>2</sup> m <sup>-2</sup> )		
		Galling group†		
		Low	Medium	Severe
42	mean	0.8a	0.9a	0.5b
	% reduction		32.8%	
61	mean	1.2b	1.5a	1.1b
	% reduction		10.62%	
70	mean	1.4a	1.5a	1.4a
	% reduction		0%	
84	mean	1.6a	1.7a	1.8a
	% reduction		0%	
103	mean	1.6b	1.9a	1.6b
	% reduction		0%	
113	mean	1.9ab	2.1a	1.7b
	% reduction		12.3%	
132	mean	2.2a	2.1a	1.5b
	% reduction		31.5%	

† Mean of LAI for each galling group at a specific day after planting. Percentage reduction in LAI for severe galling group relative to the low galling group is reported.

‡ Means followed by the same letter within rows and the same DAP are not significantly different at  $P = 0.1$ . Least significant difference (LSD) was utilized as mean separation.

Table 4.9. LAI differences between fumigation treatments for three drought stress treatments, averaged across six replications for the Gibbs Farm field.

DAP	Statistics†	Leaf Area Index-LAI (m <sup>2</sup> m <sup>-2</sup> )					
		Drought stress					
		Low		Medium		Severe	
		Fumigation					
		0 L ha <sup>-1</sup>	65 L ha <sup>-1</sup>	0 L ha <sup>-1</sup>	65 L ha <sup>-1</sup>	0 L ha <sup>-1</sup>	65 L ha <sup>-1</sup>
46	mean	0.89	1.03	0.89	1.10	0.75	1.07
	LSMEAN <sub>1</sub>	0.14		0.21*		0.31*	
	LSMEAN <sub>2</sub>	0.22*					
61	mean	1.65	2.06	1.79	1.96	1.60	2.06
	LSMEAN <sub>1</sub>	0.41*		0.17		0.46*	
	LSMEAN <sub>2</sub>	0.35*					
75	mean	3.20	3.84	2.94	3.71	2.92	3.98
	LSMEAN <sub>1</sub>	0.63*		0.78*		1.06*	
	LSMEAN <sub>2</sub>	0.82**					
88	mean	4.27	5.08	3.67	4.61	3.37	4.97
	LSMEAN <sub>1</sub>	0.81*		0.94*		1.59*	
	LSMEAN <sub>2</sub>	1.11*					
101	mean	4.22	4.67	3.17	3.69	3.63	4.35
	LSMEAN <sub>1</sub>	0.45		0.52		0.72	
	LSMEAN <sub>2</sub>	0.56*					
117	mean	2.91	2.90	2.99	2.27	2.38	2.80
	LSMEAN <sub>1</sub>	0.08		0.52		0.09	
	LSMEAN <sub>2</sub>	0.23					
131	mean	1.77	2.54	2.12	2.18	1.78	2.39
	LSMEAN <sub>1</sub>	0.78*		0.05		0.60*	
	LSMEAN <sub>2</sub>	0.48*					

† Mean of LAI for each treatment combination over six replications. LSMEANS<sub>1</sub> corresponds to the difference of least square means between fumigation treatments within one specific level of drought stress. LSMEANS<sub>2</sub> corresponds to the difference of least square means between fumigation treatments over all the drought stress treatments.

\* Significant  $P \leq 0.05$

Table 4.10. Cotton dry matter and yield differences between galling groups measured at four harvest dates, averaged across six replications in the BJ field.

Galling class†	Total biomass dry wt.	Stem and Petiole dry wt.	Bolls dry wt.	Lint plus Seed	Closed boll no.
	----- kg ha <sup>-1</sup> -----				bolts m <sup>-2</sup>
<u>62 DAP</u>					
Low	1400.4	676.1	-	-	-
Medium	1181.6	642.9	-	-	-
Severe	971.0	552.9	-	-	-
D1 (%)‡	30.6	18.0	-	-	-
<u>91 DAP</u>					
Low	3895.0	928.8	2389.0	1144.7	32.0
Medium	3566.7	879.1	1955.0	1132.2	21.0
Severe	3077.1	776.4	1637.0	737.8	20.0
D1 (%)‡	20.9	16.4	31.5	35.5	37.5
<u>126 DAP</u>					
Low	5919.0	1243.2	3068.0	2921.0	20.5
Medium	6539.0	1400.4	2956.0	2560.0	19.0
Severe	5840.0	1120.6	2611.0	3159.2	13.7
D1 (%)‡	1.3	9.8	14.8	8.1§	33.2
<u>161 DAP</u>					
Low	4562.4	897.2	-	-	-
Medium	4442.0	1247.3	-	-	-
Severe	4444.7	1039.4	-	-	-
D1 (%)‡	2.6	15.8§	-	-	-

† The galling group is relative to the RKN damage observed in the root system and evaluated through root galling.

‡ Percentage reduction of weight for severe galling group relative to the low galling group.

Table 4.11. Cotton dry matter differences between fumigation treatments for three drought stress treatments measured at four harvest dates, averaged across six replications in the Gibbs Farm field.<sup>†</sup>

Drought stress	Nematicide level	Total biomass dry wt.	Stem and Petiole dry wt.	Bolls dry wt.	Closed boll no.
		----- Kg ha <sup>-1</sup> -----			bolls m <sup>-2</sup>
<u>74 DAP</u>					
Low	0 L ha <sup>-1</sup>	2769.7	1483.9	53.4	6.3
	65 L ha <sup>-1</sup>	3573.0	1983.1	81.3	8.3
Medium	0 L ha <sup>-1</sup>	2785.3	1506.7	37.1	5.0
	65 L ha <sup>-1</sup>	3611.5	1974.7	90.9	11.8
Severe	0 L ha <sup>-1</sup>	2546.2	1343.5	46.2	4.2
	65 L ha <sup>-1</sup>	3301.6	1806.0	46.0	5.3
LSD (0.05) within low drought stress		803.3	499.2	27.9	2.0
LSD (0.05) within medium drought stress		826.2	468.0	53.8	6.8
LSD (0.05) within severe drought stress		755.4	462.6	-0.2	1.2
LSD (0.05) between nematicide treatments		794.9 *	476.6*	27.8	3.3*
<u>108 DAP</u>					
Low	0 L ha <sup>-1</sup>	10496.7	3287.7	3518.6	61.0
	65 L ha <sup>-1</sup>	12151.2	3661.9	5663.7	44.8
Medium	0 L ha <sup>-1</sup>	8341.3	2126.8	3886.2	56.0
	65 L ha <sup>-1</sup>	9257.9	2390.9	4369.8	50.5
Severe	0 L ha <sup>-1</sup>	7021.8	1685.0	3283.8	57.0
	65 L ha <sup>-1</sup>	8648.0	2129.7	4735.0	50.3
LSD (0.05) within low drought stress		1654.5	374	2145*	-16.2*
LSD (0.05) within medium drought stress		916.6	264.1	483.7	-5.5
LSD (0.05) within severe drought stress		1626.2	44.6	1451.14	-6.6
LSD (0.05) between nematicide treatments		1399.1	360.9	1359.9*	-9.4*

... Continue in the next page

<sup>†</sup>LSMEANS<sub>1</sub> corresponds to the difference of least square means between fumigation treatments within the low drought stress treatment. LSMEANS<sub>2</sub> corresponds to the difference of least square means between fumigation treatments within the medium drought stress treatment. LSMEANS<sub>3</sub> corresponds to the difference of least square means between fumigation treatments within the severe drought stress treatment. LSMEANS<sub>4</sub> corresponds to the difference of least square means between fumigation treatments averaged across drought stress treatments.

\* Significant  $P \leq 0.05$

Table 4.11. Cotton dry matter differences between fumigation treatments for three drought stress treatments measured at four harvest dates, averaged across six replications in the Gibbs Farm field.† (continuation)

Drought stress	Nematicide level	Total biomass dry wt.	Stem and Petiole dry wt.	Bolls dry wt.	Closed boll no.
		----- Kg ha <sup>-1</sup> -----			bolls m <sup>-2</sup>
<u>132 DAP</u>					
Low	0 L ha <sup>-1</sup>	7637.1	2372.6	2246.0	32.3
	65 L ha <sup>-1</sup>	8860.3	2378.6	3894.2	27.8
Medium	0 L ha <sup>-1</sup>	8270.1	2000.6	3072.0	26.5
	65 L ha <sup>-1</sup>	8489.5	2421.8	3657.3	19.2
Severe	0 L ha <sup>-1</sup>	6301.6	1491.9	2407.3	22.2
	65 L ha <sup>-1</sup>	8170.8	2507.2	3265.3	21.2
LSD (0.05) within low drought stress		1223.2	6.02	1648.2*	-4.5
LSD (0.05) within medium drought stress		219.4	415.1	585.40	-7.3
LSD (0.05) within severe drought stress		1869.2	1015.3*	858.10	-1.0
LSD (0.05) between nematicide treatments		1103.9	478.8*	1030*	-4.3
<u>160 DAP</u>					
Low	0 L ha <sup>-1</sup>	6986.9	1987.0	4541.2	-
	65 L ha <sup>-1</sup>	8013.7	2171.7	5346.7	-
Medium	0 L ha <sup>-1</sup>	5493.5	1503.6	3507.5	-
	65 L ha <sup>-1</sup>	6478.8	1750.0	4170.2	-
Severe	0 L ha <sup>-1</sup>	4926.0	1404.7	3222.5	-
	65 L ha <sup>-1</sup>	6709.2	1642.8	3855.8	-
LSD (0.05) within low drought stress		1026.8	184.7	805.5	-
LSD (0.05) within medium drought stress		985.4	247.0	662.7	-
LSD (0.05) within severe drought stress		1783.2*	238.1	633.3	-
LSD (0.05) between nematicide treatments		1265 *	223.3	700.5*	-

†LSMEANS<sub>1</sub> corresponds to the difference of least square means between fumigation treatments within the low drought stress treatment. LSMEANS<sub>2</sub> corresponds to the difference of least square means between fumigation treatments within the medium drought stress treatment. LSMEANS<sub>3</sub> corresponds to the difference of least square means between fumigation treatments within the severe drought stress treatment. LSMEANS<sub>4</sub> corresponds to the difference of least square means between fumigation treatments averaged across drought stress treatments.

\* Significant  $P \leq 0.05$

Table 4.12. *P* values for the analysis of variance fixed effects on lint plus seed yield measured at harvest in the Gibbs Farm field.

DAP	Source	<i>P</i> > <i>F</i>
	Drought stress	0.001
160†	Fumigation treatment	0.028
	Drought stress × Fumigation	0.980
	Drought stress	0.025
171‡	Fumigation treatment	0.055
	Drought stress × Fumigation	0.821

† Cotton plants harvested from an area of 1m × 2 rows (hand picked)

‡ Cotton plants harvested with a cotton picker

Table 4.13. Cotton dry matter differences between fumigation treatments for three drought stress treatments measured at harvest, averaged across six replications in the Gibbs Farm field.<sup>†</sup>

		Lint plus Seed (Kg ha <sup>-1</sup> )					
DAP	Statistics <sup>†</sup>	Drought stress					
		Low		Medium		Severe	
		Fumigation					
		0 L ha <sup>-1</sup>	65 L ha <sup>-1</sup>	0 L ha <sup>-1</sup>	65 L ha <sup>-1</sup>	0 L ha <sup>-1</sup>	65 L ha <sup>-1</sup>
	mean	3536.3	3971.6	2738.5	3181.4	2439.7	2964.2
160‡	LSMEAN <sub>1</sub>	435.4		442.9		524.6	
	LSMEAN <sub>2</sub>	467.6					
	mean	2892.9	3086.6	2374.3	2820.5	2197.1	2582.7
171§	LSMEAN <sub>1</sub>	193.7		446.2		385.6	
	LSMEAN <sub>2</sub>	342.05*					

<sup>†</sup> Mean of lint plus seed for each treatment combination over six replications. LSMEANS<sub>1</sub> corresponds to the difference of least square means between fumigation treatments within one specific level of drought stress. LSMEANS<sub>2</sub> corresponds to the difference of least square means between fumigation treatments over all the drought stress treatments.

<sup>‡</sup> Cotton plants harvested from an area of 1m × 2 rows (hand picked)

<sup>§</sup> Cotton plants harvested with a cotton picker

\* Significant  $P \leq 0.05$

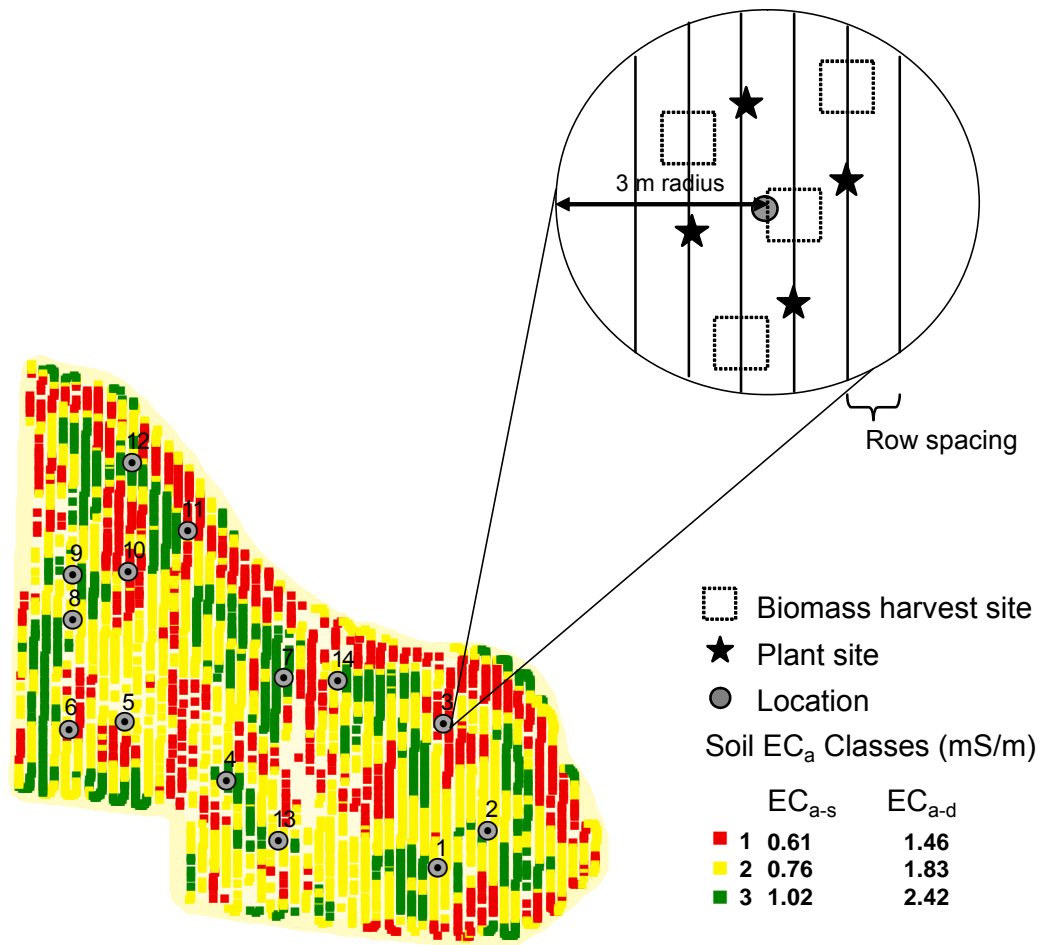


Figure 4.1. Scheme of the biomass sampling at the BJ field.

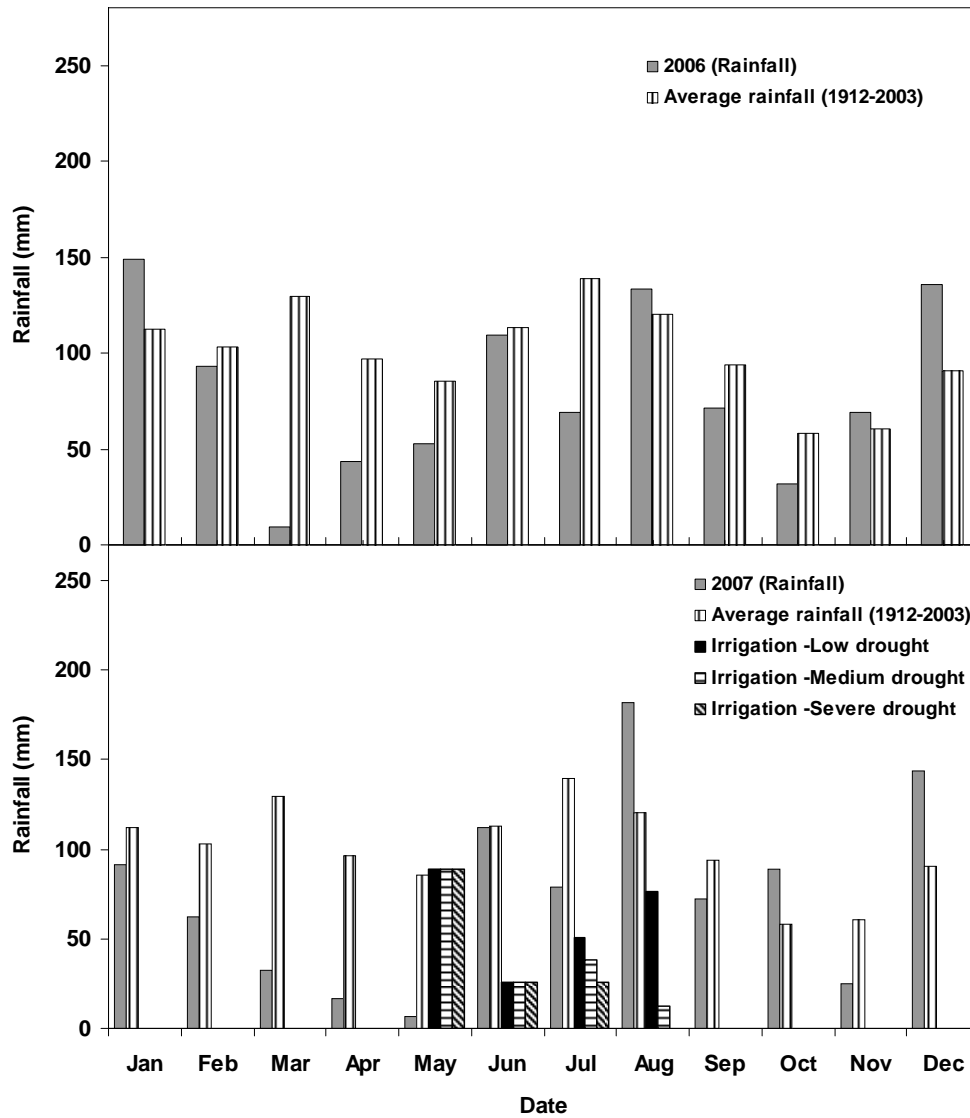


Figure 4.2. Monthly total rainfall, and monthly total irrigation applied on the drought stress treatments in 2006 at the BJ field (a) and 2007 at the Gibbs Farm field (b), and the climatic average rainfall at each field (1912-2003), Tifton, USA.

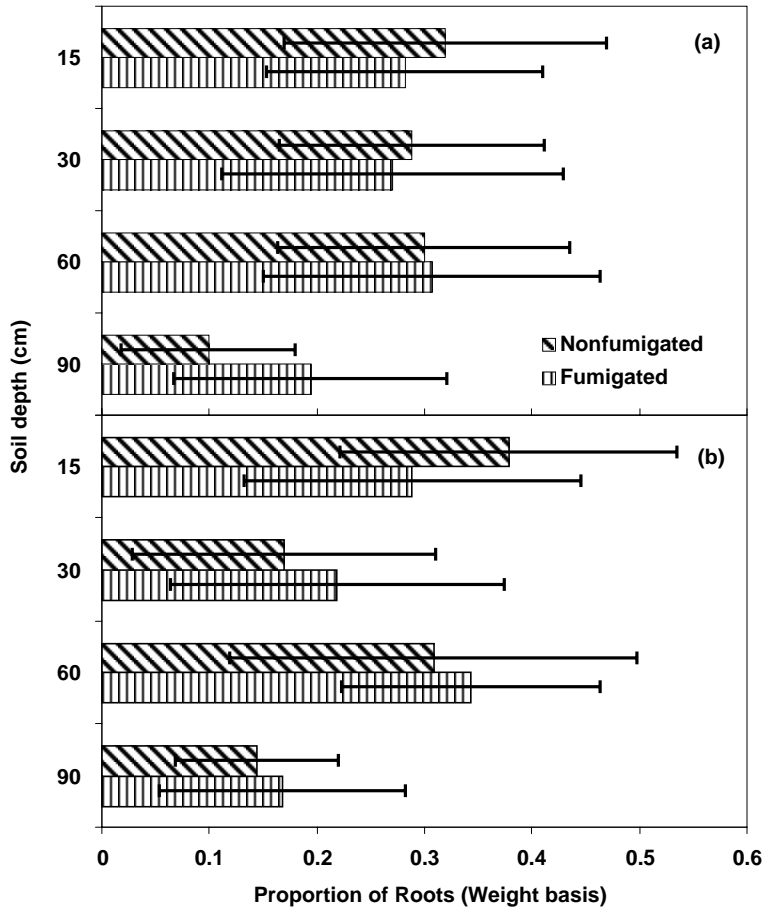


Figure 4.3. Differences in the proportion of roots at different soil depths between fumigation treatments measured between 0-90 cm soil depth for the Gibbs Farm field. Root biomass was extracted from soil cores collected next to cotton plants (a) and between plants on a row (b). Error bars represent one standard deviation of measured data.

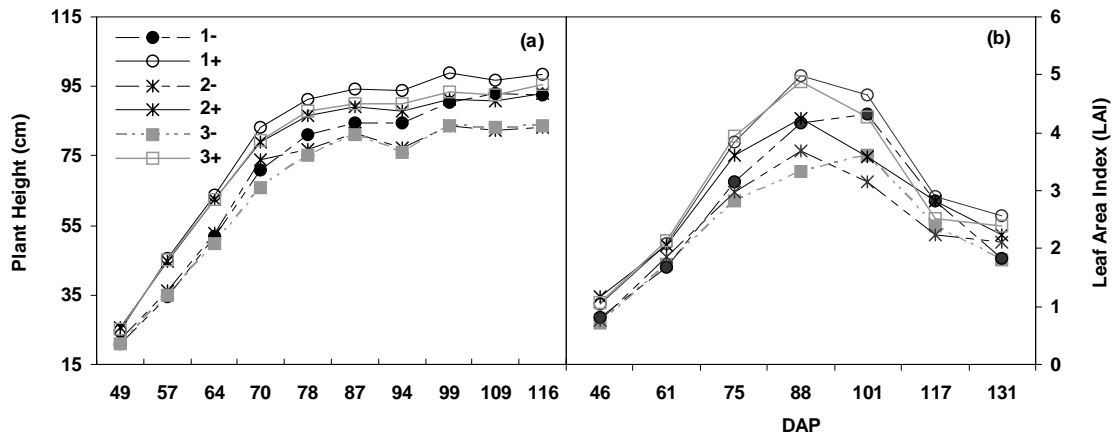


Figure 4.4. Plant height (a) and LAI (b) differences between drought stress treatments [low (1), medium (2), severe (3)] and fumigation treatments [nonfumigated (-), and fumigated (+)]. Average of six replications from the Gibbs Farm field.

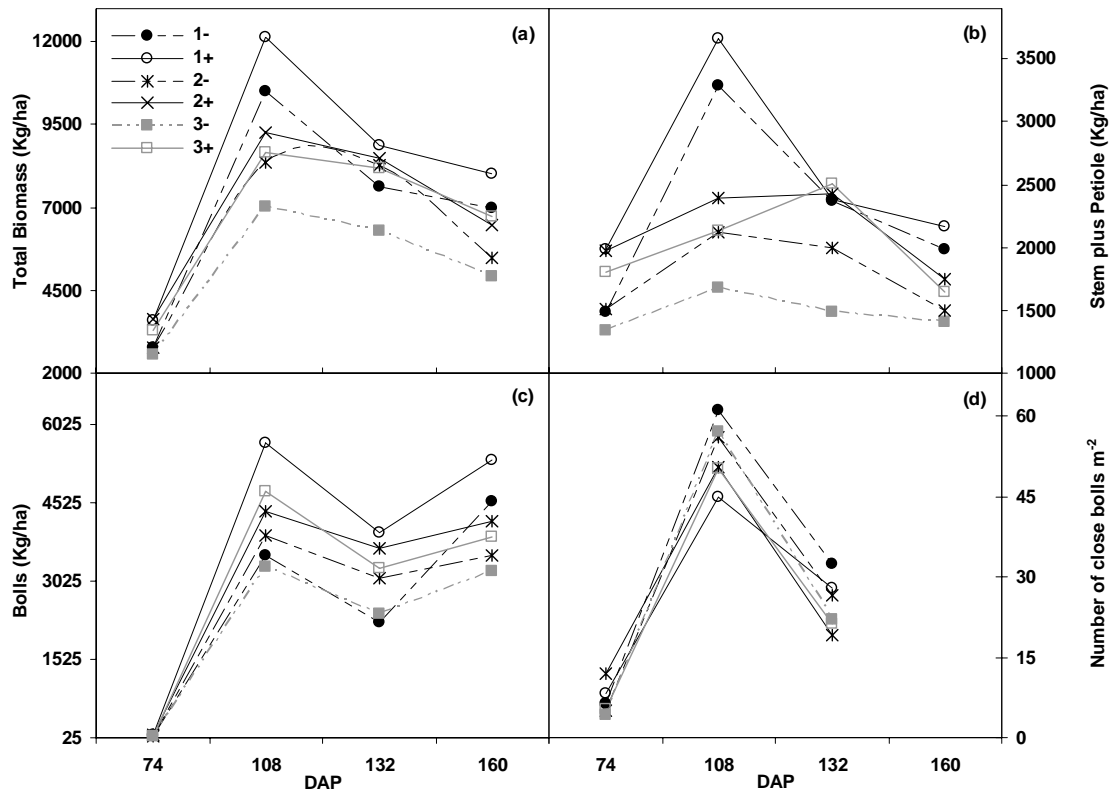


Figure 4.5. Total biomass (a) and stem plus petiole (b), boll biomass (c), and number of closed bolls m<sup>-2</sup> differences between drought stress treatments [low (1), medium (2), severe (3)] and fumigation treatments [nonfumigated (-), and fumigated (+)]. Average of six replications from the Gibbs Farm field.

## CHAPTER 5

### MODELING THE IMPACT OF SOUTHERN ROOT-KNOT NEMATODE ON COTTON BIOMASS AND YIELD<sup>1</sup>

---

<sup>1</sup> Ortiz, B.V., G. Hoogenboom, G. Vellidis, K. Boote, R. F. Davis, C. Perry. To be submitted to *Transactions of ASABE*. October 2008.

## Abstract

Cotton (*Gossypium hirsutum* L.) plants infected with the southern root-knot nematode [*Meloidogyne incognita* (Kofoid & White) Chitwood] (RKN) do not exhibit any symptoms until significant damage has been caused. This makes it, therefore, difficult to estimate the potential yield losses for a particular production area. Because crop models have the potential to take into account the effect of biotic and abiotic factors, the objectives of this study were to: (i) adapt the Cropping System Model (CSM)-CROPGRO-Cotton for simulating growth and yield of cotton plants infected with RKN, (ii) study the potential impact of the interaction RKN population-drought stress through simulations of growth and yield. Additionally, the model was used to predict yield on a producer's field having three management zones with different risk levels for RKN damage. Data from an experiment conducted in 2007 to study the interaction of RKN infection and drought stress were used for model calibration. The experiment consisted of a split plot design with drought stress levels assigned to the main plots and fumigation levels assigned to the subplots all of them replicated six times. The fumigation treatments were used to create various levels of RKN population densities. Data collected from six replications of nonfumigated treatments were used for model adaptation. The control treatment (low drought stress-fumigation) over six replications was used for model calibration. Data collected in 2001 from a similar experiment were used for model evaluation. The model was modified by coupling RKN population for removal of daily assimilate and decreasing root length per unit mass as strategies to mimic RKN damage. The modified model accurately simulated growth and yield of cotton plants infected with RKN. The model simulations indicated that LAI, total biomass, boll weight and seed cotton decreased with elevated RKN population for the nonfumigated plots. The impact of RKN varied among drought stress levels, with the combination of high RKN population-severe drought stress the most harmful. The CSM-CROPGRO-Cotton model underpredicted maximum LAI especially for the fumigated treatments with medium and severe drought stress. Biomass was simulated with a prediction error within a range of 6% to 18.4% and seed cotton with a range of -11.2% to 2.7%. Seed cotton losses associated with RKN infection increased with the level drought stress (9%, 20% and 18% for the low, medium and severe drought stress). Simulation of volumetric soil water content for the 15-60 cm soil depth agreed with the observed values (Index of agreement within a range of 0.51 to 0.92). Model evaluation showed that seed cotton was slightly overpredicted more for the fumigated than for the nonfumigated treatments exhibiting prediction errors of 28.2%, 15.8%, and 2.0% for the low, medium and severe drought stress, respectively. Similar to the calibration of the model, the yield losses increased with the combination of RKN and drought stress (20% and 29% for the low and severe drought stress). The results from this study show the potential for using the CSM-CROPGRO-Cotton model to quantify yield losses related with nematode infection. However, further model evaluation might be needed to evaluate the values of assimilate consumption and root length per unit weight for different environmental conditions and management practices.

Keywords: Crop simulation, cotton, drought stress, DSSAT, southern root-knot nematode.

## 5.1 Introduction

Southern root-knot nematode [*Meloidogine incognita* (Kofoid & White) Chitwood] (RKN) is considered the most harmful plant-parasitic roundworm for cotton (*Gossypium hirsutum* L.) production in the USA. The most important yield losses attributed to nematode pressure across the U.S. cotton belt occurred in the period 1987-2000, when damage increased from 1.0% to 4.39% (NCC, 2008). In Georgia, the third largest upland cotton producer in the U.S. (USDA, 2008), estimated losses attributed to nematodes in 2007 totaled \$50.2 million, with RKN contributing to 75% of losses compared to 19% for reniform (*Rotylenchulus reniformis*) and 6% for Columbia lance (*Hoplolaimus columbus*) nematodes (UGA, 2007). A survey carried out between 2002 and 2003 showed that major cotton-producing counties had RKN populations that were above the threshold [100 second juveniles of RKN per 100 cm<sup>3</sup> of soil, Davis et al. (1996)], which indicated that cotton producers lost approximately 77,000 bales of cotton annually due to RKN damage (Blasingame and Patel, 2001; Kemerait et al., 2004).

The response of cotton to RKN parasitism is manifested in several metabolic and physiologic changes. The second stage juveniles of RKN (RKN-J2) penetrate the roots, feed on the cytoplasm of living root cells, and induce their nuclear division. RKN-J2 grow from eggs expelled from the roots and deposited into the soil after root feeding has begun. The galls or root-knots developed in the root system between the nematode and the syncytia are considered as metabolic sinks of plant resources (McClure, 1977; Williamson and Gleason, 2003). The sink of assimilates (CH<sub>2</sub>O) caused by adult female nematodes feeding on the roots, generates a change in partitioning that impacts the growth of above-ground biomass. Direct and indirect physiological changes in cotton plants as a consequence of root feeding include: reduction in the flow of water and nutrients through intact roots due to the presence of galls (Kirkpatrick et al.,

1991), low stomatal conductance and a reduction in the transpiration rate, a reduction in photosynthesis, and an increase in leaf temperature due to drought stress caused by the earlier listed factors (Wallace, 1987; Wilcox-Lee and Loria, 1987, Kirkpatrick et al., 1995). The combination of assimilate translocation by the roots and the physiological changes explain the production of above-ground symptoms described as chlorosis, stunting, and inhibition of leaf expansion (Kirkpatrick et al., 1995), and increase of root/shoot ratio (Wilcox-Lee and Loria, 1987) which are mainly detected after damage has occurred. The reduction in yield and yield components, e. g. fiber length, seed cotton, lint percentage, and boll weight reported by Colyer et al. (1997) and Davis and May (2005) can be associated with a potential reduction of leaf area, particularly subtending leaves which are coupled to the translocation of assimilate to cotton bolls (Brown, 1968, Ashley, 1972). Root mass and length of cotton plants are also impacted by RKN infection. Zhang et al. (2006) found that the root systems of susceptible genotypes were smaller than resistant genotypes, which had much larger plants and root mass. Khoshkhoo et al. (1994) associated high levels of glucose in leaves of susceptible cotton genotypes with a reduction of root mass due to RKN feeding.

The management of RKN in the southern U.S. has been characterized by the use of chemical nematicides, which are applied at uniform rates to control population density. Crop rotation is another control option in which the host plant, cotton, is replaced by a non-host or poor-host plant. Planting moderately resistant or tolerant cotton cultivars has been implemented to reduce yield losses. The implementation of one of these strategies or their combination is needed to reduce the risk of RKN damage on a particular production area. However, the selection of strategies for site specific management (SSM) by producers can still be improved if

the impact of RKN on cotton plants grown under specific environmental and field conditions can be identified.

During the last decade, crop models have been used broadly in agriculture to simulate the crop response to different biotic and abiotic factors. The Cropping System Model (CSM)-CROPGRO-Cotton model is part of the suite of crop simulation models that encompass the Decision Support System for Agrotechnology Transfer – DSSAT (Jones et al., 2003; Hoogenboom et al., 2004). The model simulates growth and yield of cotton under different weather, soil, and management conditions. Therefore, the weight of leaves, stems, roots, shells, and seed is computed as well as growth stages, leaf area index (LAI), root length density and depth, soil water availability, and soil water extraction on a daily basis during the growing season.

One of the advantages of these type of models is its use to simulate pest damage on a crop. According to Boote et al. (1983), pests can be classified as stand reducers, photosynthetic rate reducers, leaf senescence accelerators, light stealers, tissue consumers, assimilate sappers, and turgor reducers. These types of damage and their effects can be simulated with crop models by coupling population density or specific damage type, expressed in percentage or rate basis, to state variables such as leaf, stem, seed, shell, or root mass, LAI, as well as photosynthetic rate or rate of tissue senescence (Batchelor et al., 1992). Different crop models and simulation strategies have been used to quantify the effects of pest and diseases on crops. Boote et al. (1983) simulated the reduction of water uptake from damaged roots by soybean cyst nematode (SCN) through an increment of carbon allocation to roots using the CROPGRO-Soybean model. Batchelor et al. (1992) simulated the effect of soybean defoliation caused by velvetbean caterpillar (*Anticarsia gemmatalis*) using SOYGRO model. They coupled weekly data of the

cumulative defoliation levels to leaf area through the cumulative leaf damage variable (LAID). Pinnschmidt et al. (1995) coupled the damage effects of defoliators, weed competition, leaf blast, and sheath blight disease to CERES-Rice model. Simulations using different pest scenarios of onset times and pest intensity indicated nonlinear increases in yield losses when the pest intensities were increased and onset times decreased. The CROPGRO-Soybean model was used to quantify the effects of SCN on soybean yield (Paz et al., 2001; Fallick et al., 2002; Irmak et al., 2002). Fallick et al.(2002) developed and evaluated a monomolecular function for coupling damage of various levels of SCN population to daily photosynthesis and root water uptake of soybean. Nabb et al. (2004) simulated yield losses in peanut caused by leaf defoliation associated with the late leafspot disease (*Cercosporidium personatum*). To simulate the impact of late leafspot in leaf weight, total biomass and pod weight, they provided a scouting report to the CROPGRO-Peanut model, in which the observed leaf damage was presented.

Even though the CSM provide options to simulate cotton growth and development and yield as influenced by the environment and agronomic practices, few attempts have been made to simulate the effects of RKN population levels on cotton plants growing under the environmental conditions of the southeastern U.S. The impact of RKN population densities on different cotton plant components and the interaction with different soil types and weather are still not well understood. Therefore, the CSM-CROPGRO-Cotton model offers the opportunity to simulate different scenarios of RKN damage which may guide the definition of the most effective RKN management strategies for different production areas.

The objective of this study were to: (i) adapt the Cropping System Model (CSM)-CROPGRO-Cotton for simulating growth and yield of cotton plants infected with RKN, (ii) study the potential impact of the interaction RKN population-drought stress, and (iii ) simulate

soil water dynamics on three levels of drought stress. Additionally, the model was used to predict yield losses on a producer's field having three management zones with different risk levels for RKN damage. Two specific objectives were related with the evaluation of two different hypotheses to simulate RKN damage: (i) a first hypothesis was that RKN acts as sink of soluble assimilate, and (ii) a second hypothesis was that RKN induced a reduction of root length per root mass and root density.

## **5.2 Materials and Methods**

### **5.2.1 Experimental field**

Data from two years of a long-term field experiment were used to calibrate and evaluate the model. The experiment was conducted at the Gibbs Farm of the University of Georgia in Tifton, GA (-83° 34' 47.9" N, 31° 26' 24" , 90 m elevation above mean sea level). The first year of data were collected in 2001 and used for model evaluation and data collected in 2007 was used for model evaluation. The long-term experiment was conducted to study the differences in cotton (*Gossypium hirsutum* L.) biomass and yield caused by high population of RKN and the interaction RKN population-drought stress. The soil type at the experimental site was a Tifton loamy sand (fine, loamy, siliceous, thermic Plinthic Paleudults) with an approximate depth of 2.0 m depth. The experiment consisted of six treatments as factorial combination of three drought stress levels, including low (1), medium (2), and high drought stress (3), and two fumigation levels, including nonfumigated (-), and fumigated (+) with 1,3-dichloropropene at 65 L ha<sup>-1</sup> [Telone II, Dow AgroSciences, Indianapolis, Indiana] to create different levels of RKN population densities. Irrigation volumes and frequency were selected to create the three levels of drought stress. A split-plot design with six replications was used. The three drought stress

treatments were assigned as the main plots and the two fumigation levels were assigned to the sub plots. Each plot or experimental unit consisted of four 15.2 m rows spaced at a distance of 91 cm. The cotton cultivar Delta & Pineland (DPL) 458 Boll-Guard<sup>®</sup>, Round-Up-Ready<sup>®</sup> cotton; was planted on May 11, 2007. The same variety has also been grown during the previous seven years in this field. Seeds were sown at a depth of 1.2 cm depth and plants were thinned to a density of 14 plants per m<sup>2</sup>.

Before planting the field was disc-plowed, harrowed and the winter cover crop, hairy vetch, incorporated into the soil. The experiment was fertilized two days prior to sowing with NPK (0-20-20, 392 Kg ha<sup>-1</sup>). Liquid nitrogen (114 Kg ha<sup>-1</sup>) was applied approximately one month after planting.

### **5.2.2 Producer field**

Previous research has shown that a differential control of RKN population by management zones could result in more efficient nematode suppression, yield improvements, and an increase in profits (Ortiz et al., 2008; Wolcott, 2007). A parallel study (Ortiz et al., 2007) developed techniques for delineating management zones with different risk levels for RKN damage in producers' fields. The CSM-CROPGRO-Cotton model was run to one of these fields to determine if it could effectively predict the relative differences in management zone yield observed in the field study. The field was 20 ha in size and located near Norman Park, Georgia, USA. The predominant soil in this field is the excessive-drained Kershaw sand characterized by having 91% sand, 6% silt, 3% clay in the first 85- cm. Ortiz et al. (2007) had previously identified three management zones (MZ) for RKN population in this field, which were delineated through fuzzy clustering of various surrogate data for soil texture. The surrogate data for soil

texture included in the MZ delineation were: terrain elevation and slope, apparent soil electrical conductivity ( $EC_a$ ), and bare soil spectral reflectance combined into a single layer through the use of the normalized difference vegetation index (NDVI) formula. Each zone has a different risk level for RKN damage, which was defined according to the occurrence of high RKN population and soil texture properties promoting RKN occurrence and reproduction for each zone (Figure 5.1).

The field was planted on May 18, 2006 at a 91 cm row spacing with cultivar Delta & Pineland (DPL) 555 Boll-Guard<sup>®</sup>, Round-Up-Ready<sup>®</sup>. The preceding winter crop was rye which was planted in the fall of 2005 and harvested prior to planting of cotton.

### **5.2.3 Weather and soil data**

Weather measurements [daily rainfall (mm), maximum and minimum temperature ( $^{\circ}C$ ), and solar radiation ( $MJ\ m^{-2}$ )] were recorded by a weather station (Campbell Scientific, Logan, UT), located at the Gibbs Farm where the experiment was conducted.

Although the soil type of the experimental site was classified as Tifton loamy sand (Table 5.1) by Perkins et al. (1986), soil cores of 90 cm depth were collected at the center of the 36 experimental plots for soil type and texture verification. Each core was divided into four sections: 0-15, 15-30, 30-60, and 60-90 cm and the soil texture of each soil sample was determined by the Bouyoucos hydrometer method (Bouyoucos, 1936; Day, 1965) and compared with the values reported by Perkins et al. (1986).

A smart sensor array for measuring soil water tension and soil temperature was installed at the experimental site. The array consisted of a receiver antenna that was connected to a laptop computer and 12 sensor nodes. Each node comprised of three Watermark<sup>®</sup> sensors, circuit board,

and a radio frequency identification (RFID) tag to send the data to the receiver (Vellidis et al., 2008). The Watermark<sup>®</sup> sensors were installed on each node at three depths (20, 40, and 60 cm) in two plots of each treatment and recorded soil water tension every two hours on a daily basis. Soil water retention curves (SWRC), derived by Perkins et al. (1986) at four different depths for the Tifton loamy sand were used to convert soil water tension readings into volumetric soil water content. When the soil texture at a particular depth or plot did not match the description of the Tifton soil (Perkins et al., 1986), several SWRC, derived from the Perkins's study, with soil texture similar to those measured at the experimental plots were chosen and the average volumetric soil water content was calculated.

#### **5.2.4 Biomass, leaf area index and nematode population measurements**

Biomass samples at the experimental field were collected four times during the growing season including harvest (74, 108, 132, and 160 days after planting – DAP). For the first three samples, one-meter of row, covering an area of 0.914 m<sup>2</sup>, was harvested from the central rows of each plot. At final harvest, two 1-m rows were harvested, covering a total area of 1.828 m<sup>2</sup>. From each biomass sample, a three-plant subsample was removed from the sample and separated into leaves, stems plus petioles, closed and open bolls, lint plus seed (seed cotton), and shells. All the plant material, including the subsample, was oven dried at 70 °C to constant weight to determine the total biomass dry weight. The dry weight per area of each plant component (leaves, stem-petiole, bolls, lint, seed) was calculated as the product of the total biomass dry weight and the fraction of each plant component in the subsample (Fallick et al., 2002). Leaf area index (LAI) was measured with the LAI-2000 Plant Canopy Analyzer (LI-COR, Lincoln, NE) every two weeks at four different locations within each plot.

Soil samples for RKN population density determination [second stage juveniles (RKN-J2)] were collected from each experimental plot four times during the growing season at 18, 65, 127, and 172 DAP. The soil samples consisted of a composite sample of 8 to 10 cores per plot (3 cm diameter opening and approximately 20 cm deep) collected from the root zone. RKN-J2 were extracted from 150 cm<sup>3</sup> of each soil sample by centrifugal flotation (Jenkins, 1964).

At the producer field, a 50 x 50 m grid (0.25 ha cell size) was superimposed over the field and sampling nodes were established at the center of each grid. Soil samples for RKN-J2 determination were collected three times during the growing season: 75, 110, and 167 days after planting (DAP). At each sampling event, eight individual subsamples were collected around the center of each grid and composited into a single sample representing RKN population density within each grid cell. Nematodes were extracted from 100 cm<sup>3</sup> of each soil sample by centrifugal flotation (Jenkins, 1964). Nematode counts were then converted into population on soil volume basis using the equation 1:

$$TRKN = MRKN * MV/SV \quad (1)$$

where TRKN is the total RKN-J2 population, MRKN is the mean population of RKN-J2 in the soil sample, MV is the volume of soil in the area of 1 m<sup>2</sup> to the sampling depth of 15 cm (150,000 cm<sup>3</sup>) and SV is the volume of one subsample (150 cm<sup>3</sup> or 100 cm<sup>3</sup>).

### **5.2.5 Model calibration**

Model calibration is an essential step for simulating the real world conditions as close as possible. This step is required to guarantee that the constants and response functions being used

are correct and to ensure the model performs very well in simulating the growth and yield for a specific cultivar grown under specific environmental conditions (Hunt and Boote, 1998).

Data collected from the control treatment (low drought stress-fumigation) over six replications on the experimental field was used for calibration, which consisted of adjusting the values of some cultivar and ecotype coefficients as well as soil properties for simulating the local conditions.

#### Soil water holding characteristics

Because soil water content was estimated at the depths of 20- cm, 40- cm, and 60- cm, the volumetric soil water was simulated for the conditions of soil depths: 15- to 30-, 30- to 45-, and 45- to 60- cm. The soil properties required by the model [permanent wilting point or lower limit (LL,  $\text{cm}^3 \text{cm}^{-3}$ ), field capacity or drained upper limit (DUL,  $\text{cm}^3 \text{cm}^{-3}$ ), saturated water content (SAT,  $\text{cm}^3 \text{cm}^{-3}$ ), saturated hydraulic conductivity (KSAT,  $\text{cm h}^{-1}$ ) and soil hospitality factor (SRGF)] for each layer were initially estimated with the SBuild program of DSSAT Version 4.0 (Hoogenboom et al., 2004). This program generates a soil file based on data of soil texture (percentage clay and silt) and other soil properties such as bulk density and soil organic carbon. The soil water characteristics were calibrated using a preliminary set of cultivar coefficients. The volumetric soil water measured between 0- cm to 60- cm soil depth from the control treatment [low drought stress-fumigated (1+)] was used to adjust some of the soil water characteristics (LL, DUL, SAT, SRGF) in order to match the simulated values and made them more specific for the conditions of the experimental field. The LL soil moisture for the first four layers was initially replaced by a value of 2/3 of the moisture at 100 kPa soil water tension calculated from the SWRC. This value was later adjusted if the simulated water content did not match the lowest observed water content during drying cycles. The values of DUL were adjusted

for the first three layers by analyzing changes in water content with time after events of rain or irrigation. Constant soil water content for three days after wetting was selected as the DUL value. Because the DUL was modified according to measured values, the SAT was set as the volumetric soil water content measured at 0.4 kPa soil water tension from SWRC derived from the Perkins study (1986). The values of soil albedo (0.13), soil drainage (0.6), and runoff curve number (76) were calculated with the SBuild program from data of soil color and drainage, slope and potential runoff for the Tifton soil.

The soil parameters selected were those that minimized the root mean square error (RMSE) between simulated and observed volumetric soil water content for each soil depth of the control treatment.

#### Cultivar coefficients

The CSM-CROPGRO-Cotton model requires specific cultivar coefficients which characterize phenology, as well as vegetative and reproductive growth traits. These cultivar coefficients allow the model to simulate the response of a particular cultivar to different weather and soils conditions and crop management scenarios. The control treatment was used to calibrate the model for phenology timing and vegetative and reproductive traits unique to the studied cultivar. The cultivar coefficients were obtained following a series of steps starting with prediction of: (i) life cycle expressed as flowering and maturity dates, (ii) dry matter accumulation and LAI, (iii) seed size, (iv) timing of boll and seed, (v) seed size, filling period and shelling percentage, and (vi) final adjustment of dry matter accumulation of biomass and seed (Boote, 1999). A modification of the soil fertility factor (SLPF) was also considered when calibrating biomass accumulation, as this factor affects crop growth rate through a modification of daily canopy photosynthetic rate. Model calibration of cultivar coefficients was conducted

after the calibration of soil water holding characteristics. Sensitivity analyses for phenology dates as well as biomass components (LAI, leaf weight, stem-periole weight), yield (seed cotton weight) and yield components (boll weight, bolls  $\text{m}^{-2}$ , seed  $\text{m}^{-2}$ ) were conducted to estimate the appropriate values of the cultivar coefficients that minimized the root mean square error (RMSE) between the simulated and observed values of the control treatment.

### **5.2.6 Modeling RKN damage**

The quantification of the effect that a particular pest population has at a crop growth stage and final yield is very important to decide the most appropriate management strategy. Teng et al. (1998) suggested that pest damage simulation using crop models can be implemented by subtracting biomass from the pools being consumed or reducing the rates affected by the damage. In this study, the objective was to implement RKN damage in the CSM-CROPGRO-Cotton model by: (i) coupling RKN population levels to daily assimilate [ $\text{g}(\text{CH}_2\text{O}) \text{m}^{-2}\text{d}^{-1}$ ] available for growth and respiration, and (ii) reducing the root length per root weight.

#### *Assimilate consumption by RKN*

In the CSM-CROPGRO-Cotton model, daily assimilates were removed by coupling RKN population density into the model. For each treatment, the daily changes of RKN-J2 population throughout the season were calculated by the model from interpolation of the average RKN-J2 population measured four times during the growing season (Table 5.1).

In this study, it was assumed that each RKN-J2 count reduces the same amount of assimilates. The daily assimilative consumption expressed as C loss [ $\text{ASMDOT}, \text{g}(\text{CH}_2\text{O}) \text{m}^{-2}\text{d}^{-1}$ ] was calculated in the CSM-CROPGRO-Cotton model by eq. 2 as:

$$PGAVL = PGAVL - ASMDOT \quad (2)$$

where

$$PGAVL = \text{total available CH}_2\text{O available for growth and respiration} \\ [\text{g}(\text{CH}_2\text{O}) \text{ m}^{-2}]$$

$$ASMDOT = \text{daily assimilative damage } [\text{g}(\text{CH}_2\text{O}) \text{ m}^{-2}\text{d}^{-1}]$$

Initially, it was assumed that the daily rate of consumption was  $0.0016 \text{ g juveniles}^{-1} \text{ d}^{-1}$  based on the consumption rates from other pests included into DSSAT database. Using sensitivity analyses with the low drought stress-nonfumigated treatment (1-), this daily rate was modified to identify the daily rate of assimilate consumption by the RKN-J2 population that reduced the error between simulated and observed biomass, bolls, and seed cotton weight. Some adjustment of the cultivar coefficients were necessary after the rate of assimilate consumption was set to improve the predicted values of seed and boll weight at harvest.

#### Root length per unit root weigh

In the CSM-CROPGRO-Cotton model, a reduction in the root length per unit root weight (RFAC1) as a consequence of RKN damage will lead to a decrease of plant extractable soil water, root density over the soil profile (RLINIT) and new root growth (eqs. 3 and 4). Therefore, processes such as nutrients uptake, water flow to above ground biomass, transpiration, and growth among others will be impacted resulting in a decrease of yield and total biomass.

The RLINIT can be expressed by:

$$RLINIT = WTNEW * FRRT * PLTPOP * RFAC1 * DEP / (RTDEP * 10000) \quad (3)$$

where

RLINIT	= initial root density [cm([root) cm <sup>-2</sup> (ground)]
WTNEW	= initial weight of the seed or seedling (g plant <sup>-1</sup> )
FRRT	= fraction of vegetative tissue growth that goes to roots on a day [g(root) g(veg) <sup>-1</sup> ]
RFAC1	= root length per unit root weight [cm(root) g <sup>-1</sup> ]
RTDEP	= root depth (cm)
PLTPOP	= plant population (# plants m <sup>-2</sup> )
DEP	= cumulative soil depth (cm)

Changes in the root length per unit mass (RFAC1) also impact the new root growth density (RLNEW) which is calculated as:

$$RLNEW = WRDOTN * RFAC1 / 10000 \quad (4)$$

where

RLNEW	= new root growth added [cm(root) cm <sup>-2</sup> (ground) d <sup>-1</sup> ]
WRDOTN	= dry weight growth rate of new root tissue including N but not C reserves [g(root) m <sup>-2</sup> (ground) d <sup>-1</sup> ]
RFAC1	= root length per unit root weight [cm(root) g <sup>-1</sup> ]

Because the assimilate consumption depends on the population of RKN-J2 extracted from the soil after root damage has been caused, reductions in leaf biomass that occurred early during the

growing season may not be entirely accounted for. Therefore, the reductions in root mass and root density through modifications of the RFAC1 could account for early symptoms of low LAI and vegetative biomass by RKN damage.

### 5.2.7 Model evaluation and statistical methods for performance assessment

The cultivar coefficients for the 458 BG/RR cotton variety as well as the rate of assimilate consumption by RKN and the RFAC1 values obtained from calibration and adjustment of the CSM-CROPGRO-Cotton model were evaluated with data collected from the same experiment conducted in 2001. The two hypotheses for simulation RKN damage were evaluated with commercial data collected from three different management zones delineated for a producer's field.

The deviation of predicted phenology dates, biomass at harvest, maximum LAI, seed cotton, and volumetric soil water content at various depths from the observed values were evaluated using three type of statistical properties: (i) root mean square error (RMSE), (ii) percentage prediction deviation, and (iii) index of agreement- $d$  (Willmott, 1982). The time series of measured data of biomass components, seed weight, LAI, and soil water content were also visually compared with the predicted curves as another way to assess the accuracy of the simulations. RMSE, PD (%), and  $d$  were computed using equations 5, 6, and 7 as follows:

$$\text{RMSE} = \left[ N^{-1} \sum_{i=1}^n (P_i - O_i)^2 \right]^{0.5} \quad (5)$$

$$\text{PD (\%)} = \left( \frac{P_i - O_i}{P_i} \right) \times 100 \quad (6)$$

$$d = 1 - \left[ \frac{\sum_{i=1}^n (P_i - O_i)^2}{\sum_{i=1}^n (|P_i'| + |O_i'|)^2} \right], \quad 0 \leq d \leq 1 \quad (7)$$

where  $N$  is the number of observed values,  $P_i$  and  $O_i$  are the predicted and observed values for the  $i$ th data pair,  $P_i' = P_i - \bar{O}$  and  $O_i' = O_i - \bar{O}$ ; with  $\bar{O}$  as the mean of the observed values. When evaluating the performance of the simulations, the closer the RMSE to 0, the better the agreement between simulated and observed values. Model over predictions were also detected when PD values were positive contrasting with under predictions in which PD had negative values. The index of agreement- $d$  values close to 1 indicates a good simulation of time series data.

## 5.3 Results and Discussion

### 5.3.1 Weather

The 2007 season received less rainfall than the climate average, especially during the months of March, April, and May (Figure 5.2a). In contrast, the month of August received a larger amount of rainfall compared to the normal climate average (182 mm compared to the climate average of 120 mm) as well as the months of October and December.

The 2001 weather conditions under which the model evaluation data were collected contrasted with those observed in 2007. Monthly rainfall in 2001 was less than the climatic average and only the months of March, June and October received larger amount of rainfall compared to the normal climatic average (Figure 5.2b).

### **5.3.2 Model calibration**

#### *Soil water holding characteristics*

The soil texture analyses from soil samples collected at four depths within the range of 0-cm to 90-cm validated the description of the Tifton soil by Perkins et al. (1986), which was based on soil samples extracted from a location nearby our experimental field. Therefore, the soil profile described by Perkins et al. (1986) was used as input data prior to generation of the initial soil properties calculated with the SBuild program of DSSAT Version 4.0 (Table 5.1). For most of the soil layers, the final values for the soil properties of LL, DUL, and SAT were higher than the initial values which were used in the simulations reported in this study.

Volumetric water content values for the first three soil layers were adjusted according to the soil water dynamics measured in the field at 20-cm, 40-cm and 60-cm soil depths; and values derived from SWRC were used to modify the soil parameters for the deeper layers. Large differences were found between the final and initial values of LL, DUL and SAT for the soil layers at 51- to 76-, 76- to 104-, and 104- to 135- cm depth. To match the soil water holding characteristics observed in the top layers, these larger values resulted from adjustments based on the SWRC derived from Perkins et al. (1986). The final soil properties at the bottom layers did not exhibit much difference with respect to the initial values.

The soil hospitality factor (SRGF), which determines the ability of roots to grow and proliferate in a soil layer, was increased for the top layers and decreased for the bottom layers with respect to the initial values. These changes were intended to improve the simulation of the soil water dynamics observed in the shallow layers.

### Cultivar coefficients

Model calibration required the modification of some cultivar coefficients of the cotton cultivar DP 458 BR included into the CSM-CROPGRO-Cotton model for an accurate simulation of phenology, growth and yield (Table 5.2). First, the cultivar coefficients related to the photothermal days for duration of flowering (EM-FL), and beginning of seeds to maturity (SD-PM) were adjusted to match the flowering and physiological maturity dates. The difference between observed and simulated values for the flowering and physiological maturity dates of the control treatment were two days for each one respectively. The coefficients were higher than other commercial cotton cultivars in the DSSAT database suggesting that the cultivar growing under the conditions of this experiment required more days to start the reproductive phase. These cultivar coefficients also improved the total biomass and boll weight predictions by 14.3% and 6.1%, respectively.

Second, simulated values of maximum LAI and total biomass were improved by decreasing the soil fertility factor (from 1.0 to 0.75) while increasing the specific leaf area (SLAVR). The effect of a decrease on the soil fertility factor was a reduction of the growth rate through modification of daily canopy photosynthetic rate. The *d-index* for LAI and total biomass of the control treatment were 0.94 and 0.63, respectively.

Third, the onset of boll formation, photothermal days for seed filling and final boll load were increased to match boll initiation and weight as well as rate of bolls accumulation. The *d-index* values for boll and seed cotton weight on the control treatment were 0.80 and 0.70, respectively.

### 5.3.3 Modeling RKN damage

#### Hypothesis 1: RKN as sink for soluble assimilates

Following the calibration of the soil properties and cultivar coefficients for the control treatment [low drought stress-fumigated (1+)], the model was modified to account for RKN damage. For the implementation of this hypothesis, the initial value of assimilate consumption rate [ $0.0016 \text{ g}(\text{CH}_2\text{O}) \text{ RKN-J2}^{-1} \text{ d}^{-1}$ ] was based on the consumption rates from other pests included into DSSAT database. This value was adjusted through comparisons between simulated and observed values of biomass and yield components (boll and seed cotton weight) for the low drought stress-nonfumigated (1-) treatment. A final assimilate consumption rate value of  $0.0008 \text{ g}(\text{CH}_2\text{O}) \text{ RKN-J2}^{-1} \text{ d}^{-1}$  was obtained after minimizing the error between simulated and observed biomass and yield components at harvest as well as the time series data.

The differences in RKN population levels between treatments influenced the amount of assimilate removed from the shoot, although a constant rate of assimilate consumption was used (Table 5.3, Figure 5.3). This showed that high populations of RKN-J2 increase the number of feeding sites by increasing the amount of removed assimilate. In this study, the highest amount of assimilate was removed from 90 to 120 DAP corresponding to the stages of flowering and boll filling. Therefore, the implementation of this strategy to mimic RKN damage should account for reductions in yield and yield components.

Total biomass. The model simulations showed that cotton biomass severely decreased as the RKN population and the level of drought stress increased, especially for severe drought stress (Figure 5.4). The model overpredicted biomass at maturity for all treatments; this was more severe for the nonfumigated treatments, with values of percentage prediction deviation (PD) of 16.5%, 11.5%, and 18.4% for the 1-, 2-, and 3- treatments respectively (Table 5.4). The over

prediction of biomass could be associated with high simulated values of stem-petiole biomass throughout the growing season (data not shown). The time series of total biomass for the low drought stress treatment were fairly well simulated, with *d-index* values of 0.63 and 0.74 for the 1+ and 1- treatments, respectively (Table 5.4, Figure 5.4a). Due to the high RKN population levels observed for the nonfumigated treatments, there was a higher amount of assimilate removed compared to fumigated treatment, which suggested a high contribution of RKN population to reductions in biomass (Figure 5.3 – 5.4). The percentage reduction in biomass between the fumigated and nonfumigated treatments increased with the level of stress being 8%, 16% and 15% less for the low, medium and severe drought stress levels, respectively.

The second biomass sample (100 DAP) was very high with respect to the other sample dates, which could explain the high value of the overall RMSE. This high biomass value could be associated with moisture in the sample after it was removed from the oven. Contrasting with the over prediction of biomass at harvest, the predicted biomass values at 75 and 135 DAP for all the treatments were within one standard deviation of the measured mean biomass.

Similarities in the removed assimilate by RKN-J2 population throughout the growing season for the 1+ and 2+ treatments showed that the differences in biomass between these two treatments (9345 kg ha<sup>-1</sup> vs. 7427 kg ha<sup>-1</sup>) could be attributed to drought stress observed in the top 45- cm soil depth for the medium drought stress compared to the low drought level. Similarly, the differences between the amount of assimilates that were removed between the 1+ and 3+ treatments were not significantly different. Therefore, the 20% reduction of biomass for the 3+ treatment could be due to the changes in soil water content associated with the severe drought stress.

Boll weight. The changes in boll weight accumulation throughout the season and the final boll weight at harvest were fairly well predicted by the CSM-CROPGRO-Cotton model (Table 5.5, Figure 5.5a – 5.5c). The dynamics of boll weight accumulation were best predicted for the nonfumigated treatments with RMSE values of 1346, 1730, and 1602 kg ha<sup>-1</sup> for the 1-, 2-, and 3- treatments, respectively (Table 5.5). For the nonfumigated (-) plots, predictions of final boll weight for the treatments under medium and severe drought stress (2- and 3-) were close to the observed values compared with the same drought stress levels for the fumigated treatment (2+ and 3+). The PD values for the 2- and 3- treatments (-0.7 and -1.9%) were lower than PD values for the 2+ and 3+ treatments (4.6 and -0.1%). For the 3+ treatment, the final boll weight was underpredicted by 3 kg ha<sup>-1</sup>, which was the most accurate simulation of all treatments. The highest differences between simulated and observed final boll weight (610 kg ha<sup>-1</sup>) was observed for the 1 – treatment.

The high RKN population of the 2- and 3- treatments compared to the 1- treatment caused an increase in the removal of assimilates, especially during the flowering and boll filling stage, suggesting a high contribution of the RKN population to the reduction in boll weight (Figure 5.3). Boll weight was reduced 32% (1668 kg ha<sup>-1</sup>) for the 2- treatment compared to the 1- treatment, and 38% (1989 kg ha<sup>-1</sup>) for the 3- treatment compared to the 1- treatment. Additionally, the percentage reduction of boll weight between the fumigated and nonfumigated treatments increased as the level of stress increased: 9%, 20% and 18% for the low, medium and severe drought stress, respectively. Because the irrigation for the medium and severe drought stress treatments was reduced in July, which corresponded to the squaring and flowering period, the reductions in boll weight could be associated with squares and flowers loss.

For the fumigated (+) plots, the difference in boll weight between the 1+ and 2+ treatments ( $5696 \text{ kg ha}^{-1}$  vs.  $4371 \text{ kg ha}^{-1}$ ) could be attributed to the level of drought stress because of a similar assimilate consumption by RKN-J2 population in these treatments (Figure 5.5a – 5.5b). The simulations showed a higher impact of severe drought stress for the fumigated treatments compared to the low drought stress (32% reduction in boll weight). However, this reduction in boll biomass is the result of the interaction between severe drought stress and fumigation.

It was common for all treatments that the simulated boll weight at 135 DAP was within one standard deviation (SD) of the measured mean for boll weight. In contrast, the measured boll weight at 100 DAP was very high compared to the simulated values, which could indicate that the samples were not dried sufficiently and remained moist even after they were removed from the oven. The high value for the overall RMSE that was found for all treatments could be affected by the inclusion of the boll biomass sampled at 100 DAP.

Seed cotton weight. The dynamics of seed cotton were well simulated with values within one standard deviation of the measured mean for all the treatments (Figure 5.5d – 5.5f). The RMSE for seed cotton at harvest for the fumigated treatments ranged from  $707 \text{ kg ha}^{-1}$ ,  $965 \text{ kg ha}^{-1}$ ,  $885 \text{ kg ha}^{-1}$  for the low, medium and drought stress treatments, respectively. The same drought stress treatments under nonfumigation had RMSE values of  $896 \text{ kg ha}^{-1}$ ,  $1119 \text{ kg ha}^{-1}$ , and  $1009 \text{ kg ha}^{-1}$ , respectively (Table 5.5).

The most accurate predictions were observed for the 2+ treatment followed by the 1+, and 1- treatments with PD values of -0.1, 1.0 and 2.7, respectively. Seed cotton for the severe drought stress treatment exhibited the highest PD values with -10.3% and -11.2% for the 3+ and 3- treatments, respectively. This could be explained by the high variation of seed cotton between

replications evidenced by standard deviation values of 712 kg ha<sup>-1</sup> for the 3+ treatment and 889 kg ha<sup>-1</sup> for the 3- treatment. The highest RMSE was 1119 kg ha<sup>-1</sup> for the cotton plants grown under medium drought stress-nonfumigated (2-) conditions.

The model simulation indicated that seed cotton was highly impacted by the RKN population as well as drought stress. Final seed cotton weight decreased by an average of 1440 kg ha<sup>-1</sup> when the level of drought and the amount of removed assimilate increased from low to severe for the nonfumigated plots (Table 5.5, Figure 5.3 – 5.5). A similar trend was observed for the measured seed cotton weight at harvest, where the reduction in weight of the severe drought level compared to the low drought for the nonfumigated plots was 1096 kg ha<sup>-1</sup>. An increased assimilate consumption by RKN-J2 for the nonfumigated treatments caused reductions in seed cotton that were higher for the medium and severe drought stress compared to the low drought stress treatments, e.g., 14% 18%, and 11%, respectively.

For the fumigated treatments, although there were no big differences in assimilate consumption, the simulations showed a reduction of 27% for seed cotton for the severe drought stress treatments (3+) compared to the low drought stress treatments (1+). This reduction suggests a combined negative effect of drought stress and high RKN population. Seed cotton weight decreased significantly with an increase in drought stress, with a reduction of 21% for the 2+ treatment (3179 kg ha<sup>-1</sup>) compared to the 1+ treatment (4017 kg ha<sup>-1</sup>), although the assimilate consumption by RKN-J2 population was similar for these treatments (Table 5.5). This shows that seed weight is affected by the available water in the soil profile as determined by the differences in drought stress levels.

Hypothesis 2: RKN induces a reduction in root length per unit root mass and root length density

When the hypothesis of RKN as sink of soluble assimilate was tested for the three nonfumigated (-) treatments, the simulated LAI was still overpredicted, which was more evident under severe drought stress (Table 5.6). This showed the need for using an additional strategy of the RKN-J2 as a sink of soluble assimilates to account for early reduction in LAI, perhaps because RKN-J2 are extracted from the soil after root damage has been caused. The second hypothesis, i.e., a reduction in root length per unit root mass and root length density as a result of RKN damage, was implemented by modifying the root length to weight ratio in the model (RFAC1). It was reduced from 17000 cm root g<sup>-1</sup> for the fumigated treatments to 11000 cm root g<sup>-1</sup> for the 1- and 2- nonfumigated treatments, and 8600 cm root g<sup>-1</sup> for the 3- treatment. These final values were obtained after minimizing the error between simulated and observed LAI and improving the overall prediction of LAI throughout the growing season (Table 5.6).

Leaf area index. The implementation of this hypothesis appeared to predict the time series of LAI fairly well for all the treatments compared to hypothesis one (Table 5.7, Figure 5.6). The most accurate simulations of LAI occurred for the treatments 1+, 2-, and 3- with the lowest RMSE (0.69, 0.71, and 0.65 m<sup>2</sup> m<sup>-2</sup>) and high *d-index* values (0.94, 0.86, 0.86) (Table 5.6). The highest RMSE observed from the 1- treatment (0.95 m<sup>2</sup> m<sup>-2</sup>) showed the lack of the model to accurately simulate leaf senesce at the end of the growing season for this particular condition (Figure 5.6a). For the fumigated (+) treatments, particularly the 2+ and 3+ treatments, maximum LAI (occurred around 90 DAP) was underestimated and the RMSE was 0.78 and 0.77 respectively, while for 2- and 3- treatments (nonfumigated) maximum LAI was very well simulated. The reduction in LAI for the nonfumigated compared to the fumigated treatments at a particular drought stress level showed the impact of high population of RKN on LAI.

Additionally, the effects of drought stress on LAI changes were observed by comparing the 1+ and 2+ treatments (Figure 5.6a – 5.6b). Because a similar amount of assimilates was removed for these two treatments, the reduction in LAI for the 2+ treatment compared to the 1+ treatment could be attributed to the differences in soil water content. The simulations showed that the difference in maximum LAI between fumigated and nonfumigated cotton plants increased as the level of drought stress increased. The percentage reduction in maximum LAI due to an increase in RKN population for the nonfumigated treatments compared to the fumigated treatments was 11%, 11% and 17% for the low, medium, and severe drought stress levels, respectively (Table 5.7).

#### **5.3.4 Soil water dynamics**

Observed and simulated volumetric soil water content at three soil depths ( 15- to 30-, 30- to 45-, and 45- to 60- cm depth) are shown for all the drought stress-fumigation treatment combinations (Figure 5.7 – 5.9). For most of the treatments, the predictions of volumetric soil water content at the three evaluated soil depths were close to the observed values resulting in low RMSE (0.015 to 0.099  $\text{cm}^3 \text{cm}^{-3}$ ) and *d-index* values (0.51 to 0.92) (Table 5.8). An example of a good agreement was found for the top 45- cm, where the simulation of increases and decreases of volumetric soil water content occurred at rainfall events followed by drying (Figure 5.7).

There were no significant differences in volumetric soil water content between the fumigated treatments (+) for the top 30-cm soil depth. However, the low drought stress treatment had a higher level of soil water dynamics than the medium and severe drought stress treatments, especially for the top 45- cm of soil depth for the months of July and August. This can be due to the high frequency of irrigation received by this treatment and/or low impact of RKN population

on the root system resulting in a more active one root system (Figure 5.7a – 5.7c). The effects of irrigation frequency on soil water content were demonstrated in the 30-45 cm soil layer of the 2+ and 3+ treatments which experienced a depletion of soil water from July 15 to August 28 (Figure 5.8b and 5.9b).

For the top 30-cm soil layer, the less accurate simulations in volumetric water content were found for the 1+ and 1- treatments with RMSE values of 0.024 and 0.028  $\text{cm}^3 \text{cm}^{-3}$  and *d-index* values of 0.63 and 0.69, respectively (Table 5.8). The underpredictions observed for these treatments can be also explained by the rapid changes in soil moisture for the shallow layers due to both rainfall and irrigation events (Figure 5.7a).

For the 30- to 45- cm soil depth, the most accurate predictions were found for the 1+, 2+, and 3+ treatments; resulting in the lowest RMSE (0.017, 0.015, and 0.018  $\text{cm}^3 \text{cm}^{-3}$ ) and the highest *d-index* values (0.84, 0.92, and 0.88). The least accurate predictions were found for the 3- treatment. This could be due to the incorrect transformation of soil water tension into soil moisture. Although there is not evidence of this, the error could also be due to an undetected sensor problem. This treatment had RMSE and *d-index* values of 0.099  $\text{cm}^3 \text{cm}^{-3}$  and 0.51 respectively (Table 5.8).

For the 45- to 60- cm soil depth, the simulation of soil water content showed less of a pronounced water depletion compared to the observed soil moisture during the flowering and bolls setting periods for the 1+ treatment compared to the 2+ treatment (Figure 5.7c and 5.8c).

### 5.3.5 Model evaluation

#### Experimental field

Data collected in 2001 from a study using the same experimental design and planted at the same site as the experiment in 2007 were used for model evaluation. The RKN-J2 population was collected three times during the growing season and was used as input for the model to simulate the impact of RKN on cotton growth (Table 5.3). The same hypotheses used for model calibration were assumed for model evaluation. From the model simulations it was evident a reduction in seed cotton weight as RKN population increased on nonfumigated plots which reaffirmed the results from model calibration. The reductions of seed cotton weight on nonfumigated plots compared to fumigated plots were 20.5%, 18.7%, and 29% for the low, medium, and severe drought stress, respectively (Table 5.9, Figure 5.10). For all the treatment combination of drought stress-fumigation (1+, 2+, and 3+), the seed cotton weight was overpredicted with PD values of 28%, 15.8%, 2%, respectively (Table 5.9). In contrast, the predicted seed cotton weight for 3- treatment was the most accurate with a PD value of -1.7%. In conclusion, the simulation was better for the nonfumigated treatments compared to the fumigated. This validated the significance of using the two hypotheses here evaluated to account for RKN damage into the CSM-CROPGRO-Cotton model

#### Producer's field

For the producer's field, the differences between the management zones were mainly related with the soil type and RKN population density. Zone 1, with the lowest risk for RKN damage, had an Albany sandy soil (poorly drained in the subsoil); and zones 2 and 3 with moderate and high risk levels, respectively, had a Kershaw sandy soil (excessively drained) (Table 5.10). A soil fertility factor of 0.86 was used for both soils.

Because the RKN population data were collected at 99 different locations through the field, the RKN data from locations within each zone were averaged and the mean value assigned to each zone. Due to the differences in RKN population between the zones, the simulation of yield differences was implemented through the use of assimilate consumption by the nematodes and reduction of root length per unit mass using the RFAC1 factor of the model as described in the previous section. The same rate of assimilate consumption derived from the model calibration with the experimental plots data [ $0.0008 \text{ g}(\text{CH}_2\text{O}) \text{ RKN-J2}^{-1} \text{ d}^{-1}$ ] was used to simulate the levels of consumption by zone (Figure 5.11). The highest amount of assimilates allocated to the roots was observed for zone 3 compared to zone 1, which had the lowest amount of assimilate consumption. The RFAC1 values selected for the simulation of RKN damage were based on the population levels of RKN observed for the different management zones. The zones with low, medium, and high RKN population had RFAC1 values of 17000, 11000, and 8600 cm root  $\text{g}^{-1}$ , respectively. Because the management zones also had low, medium and high RKN populations, the three RFAC1 values used for the experimental plots were applied to the zones.

The model simulation indicated that seed cotton weight was impacted highly by the RKN population. Seed cotton decreased by an average of  $793 \text{ kg ha}^{-1}$  (22% reduction) in zone 3 compared to zone 1. It could be associated with elevated RKN population observed in zone 3 (Table 5.10, Figure 5.12). Although zones 2 and 3 had the same soil type, there was a difference in seed cotton weight of  $225 \text{ kg ha}^{-1}$  which could be related with high amount of assimilate removed by the high RKN population located in zone 3.

Cotton seed weight was overpredicted for all the management zones with PD values of 7%, 3% and 15.1% for zones 1, 2, and 3, respectively. However, the simulated values followed the same trend as the observed value. The results showed that the rate of assimilate consumption

and the RFAC1 values derived from model calibration can be used to simulate yield losses due to nematodes under the conditions of a commercial field.

#### **5.4 Summary and Conclusions**

The CSM-CROPGRO-Cotton model was modified by coupling RKN population for removal of daily assimilate and decreasing root length per unit mass as strategies to mimic RKN damage. Once the RKN effects were accounted for in the CSM-CROPGRO-Cotton model, the simulated vegetative and reproductive biomass components were close to the observed values for the three drought stress levels and fumigation levels. Changes in LAI and boll weight were very well simulated by the model, especially under the conditions of the nonfumigated treatments. Model simulations indicated that LAI, total biomass, boll weight and seed cotton weight decreased with an increase in RKN population for the nonfumigated plots. The impact of RKN is more pronounced under severe drought stress. For both the fumigated and nonfumigated treatments, LAI, biomass weight and seed cotton weight decreased with an increase in the drought stress level. The model underpredicted maximum LAI for most of the treatments. This was more pronounced for the fumigated treatment under medium and severe drought stress. In addition, there was less reliability in prediction of total biomass by the model for all the fumigated treatments. Total biomass values were overpredicted by an average of 12% for all the treatments. The simulations indicated that seed cotton losses from RKN population increased with the level of water stress. The simulations with the evaluation data set showed seed cotton losses of 20%, 19% and 29% for the low, medium and severe drought stress, respectively. In conclusion, the CROPGRO-Cotton model in DSSAT v4.0 was able to simulate growth and yield due to RKN damage and drought stress within  $\pm 30\%$  error from the measured values. It also

simulated soil water dynamics for the different drought stress levels. The two hypotheses to account for RKN damage were successfully tested and implemented to simulated LAI, biomass and cotton seed weight in plots having high population of RKN. The first hypothesis considered RKN as a sink of soluble assimilates targeted reductions in biomass and yield components (bolls and seed cotton). The second hypothesis accounts for reductions in root length per unit mass due to RKN parasitism allowed the simulations of LAI under different levels of RKN population.

The results presented in this study showed the potential of CSM-CROPGRO-Cotton model for determining the potential impact of RKN and drought stress in cotton and understanding the effect of these stressor factors on growth and final yield when changing management strategies. In addition, the CSM-CROPGRO-Cotton model seemed a promissory tool for forecasting relative differences between management zones with different RKN risk levels delineated for the conditions of a producer's field. It was evidenced by the small percentage of error when simulating the yield between the management zones.

Future research should involve the identification and implementation of other methods to improve prediction of RKN damage, for example the addition of disease progress functions to better simulate within season changes in RKN population and its effect on growth and yield. Additionally, there is a need for additional evaluation of the model under other conditions of cultivar, soil and weather in order to establish the levels of risk for high population of nematode and define the most appropriate management strategies.

### **Acknowledgments**

This research was partially supported by grants from Cotton Incorporated and the Georgia Cotton Commission and the Flint River Water Planning and Policy Center for supporting this work. We express our gratitude to Dr. Kenneth Boote from the University of

Florida for his guidance carrying out this research. We also thank Dr. Cecilia Tojo Soler for assistance with different aspects related with the operation of DSSAT v4.0.

## References

- Ashley, D. A. 1972.  $^{14}\text{C}$ -Labeled photosynthate translocation and utilization in cotton plants. *Crop Sci.* 12: 69-74.
- Batchelor, W. D., J. W. Jones, and K. J. Boote. 1992. Assessing pest and disease damage with DSSAT. *Agrotech. Trans.* 16: 1-8.
- Blasingame, D. and Patel, M. V. 2001. Cotton disease loss estimate committee report . In *Proc. 2001 Beltwide Cotton Conference*. Anaheim, CA.: National Cotton Council.
- Boote, K. J. 1999. Concepts for calibrating crop growth models. In *DSSAT, Version 3. A Decision Support System for Agrotechnology Transfer*. Vol. 4, p. 179-194. Eds G. Hoogenboom, P. W. Wilkens and G. Y. Tsuji. Honolulu, HI.: University of Hawaii.
- Boote, K. J., J. W. Jones, J. W. Mishoe, and R. D. Berger. 1983. Coupling pest to growth simulators to predict yield reductions. *Phytopathology* 73:1581-1587.
- Bouyoucos, G. J. 1936. Directions for making mechanical analysis of soils by the hydrometer method. *Soil Sci.* 42: 3.
- Brown, K. L. 1968. Translocation of carbohydrate in cotton: Movement to fruiting bodies. *Annals Bot.* 32: 703-713.
- Colyer, P. D., T. L. Kirkpatrick, W. D. Caldwell, and P. R. Vernon. 1997. Influence of nematicide application on the severity of the root-knot nematode-fusarium wilt disease complex in cotton. *Plant. Dis.* 81: 66-70.
- Davis, R. F., and O. L. May. 2005. Relationship between yield potential and percentage yield suppression caused by the southern root-knot nematode in cotton. *Crop. Sci.* 45: 2312-2317.
- Davis, R. F., P. Bertrand, J. D. Gay, R. E. Baird, G. B. Padgett, E. A. Brown, F. F. Hendrix, and J. A. Balsdon. 1996. Guide for interpreting nematode assay results. Circular No. 834, 16 p.: University of Georgia Cooperative Extension Service.
- Day, P. R. 1965. Particle fractionation and particle-size analysis. Madison, WI.: Black, C. A.
- Fallick, J. B., W. D. Batchelor, G. L. Tylka, T. L. Niblack, and J. O. Paz. 2002. Coupling soybean cyst nematode damage to CROPGRO Soybean. *Trans. ASAE* 45: 433-441.
- Hoogenboom, G., J. W. Jones, P. W. Wilkens, C. H. Porter, W. D. Batchelor, L. A. Hunt, K. J. Boote, U. Singh, O. Uryasev, W. T. Bowen, A. J. Gijsman, A. S. Du Toit, J. W. White, G. Y. Tsuji. 2004. *Decision Support System for Agrotechnology Transfer*. Ver. 4.0. Honolulu, HI.:University of Hawaii.

- Hunt, L. A. and K. J. Boote. 1998. Data model operation, calibration, and evaluation. In *Understanding options for agricultural production*. Dordrecht, The Netherlands.: Kluwer Academic Publishers.
- Irmak, A., J. W. Jones, W. D. Batchelor, and J. O. Paz. 2002. Linking multiple layers of information for diagnosing causes of spatial yield variability in soybean *Trans. ASAE* 45: 839-849.
- Jenkins, W. R. 1964. A rapid centrifugal flotation technique for separating nematodes from soil. *Plant Dis.* 48: 692.
- Jones, J. W., G. Hoogenboom, C. H. Porter, K. J. Boote, W. D. Batchelor, L. A. Hunt, P. W. Wilkens, U. Singh, A. J. Gijsman, and J. T. Ritchie. 2003. DSSAT Cropping System Model. *Eur. J. Agron.* 18:235-265.
- Kemerait, R. C., R. F. Davis, P. H. Jost, C. L. Brewer, S. N. Brown, B. Mitchell, W. E. Harrizon, R. Joyce, and E. McGriff. 2004. Assessment of nematicides for management of the southern root-knot nematode, *Meloidogyne incognita*, in Georgia. Tifton, GA.: The University of Georgia.
- Khoshkhoo, N., P. A. Hedin, and J. C. J. McCarthy. 1994. Free sugars in root-knot nematode susceptible and resistant cotton plant roots and leaves. *J. Agric. Food Chem.* 42: 366-368.
- Kirkpatrick, T.L., D.M. Oosterhuis, and S.D. Wullschleger. 1991. Interaction of *Meloidogyne incognita* and water stress in two cultivars. *J. Nematol.* 23: 462-467.
- Kirkpatrick, T.L., M.W. van Iersel, and D.M. Oosterhuis. 1995. Influence of *Meloidogyne incognita* on the water relations of Cotton growth in microplots. *J. Nematol.* 27: 465-471.
- McClure, M.A. 1977. *Meloidogyne incognita*: A metabolic sink. *J. Nematol.* 9: 88-90.
- Naab, J. B., P. Singh, K. J. Boote, J. W. Jones, and K. O. Marfo. 2004. Using the CROPGRO-peanut model to quantify yield gaps of peanut in the guinean savanna zone of Ghana. *Agron. J.* 96: 1231-1242.
- NCC. 2008. Beltwide yield losses to nematode damage. Cordova, TN.: National Cotton Council of America. Available at: [www.cotton.org/tech/pest/nematode/losses.cfm](http://www.cotton.org/tech/pest/nematode/losses.cfm). Accessed August 17, 2008.
- Ortiz, B. V., D. G. Sullivan, C. Perry, G. Vellidis, L. Seymour, and K. Rucker. 2007. Delineation of management zones for site specific management of parasitic nematodes using geostatistical analysis of measured field characteristics. In *Proc. Sixth European Conference of Precision Agriculture (6ECPA)*., CD-ROOM. Stafford, J., and A. Werner, eds. Skiathos. Greece.

- Ortiz, B. V., C. Perry, D. G. Sullivan, R. C. Kemerait, A. Ziehl, R. Davis, G. Vellidis, and K. Rucker. 2008. Evaluation of Variable Rate of Nematicides on Cotton According to Nematode Risk Zones. In *Proc. 2008 Beltwide Cotton Conference*. Nashville, TN.: National Cotton Council.
- Paz, J. O., W. D. Batchelor, G. L. Tylka, and R. G. Hartzler. 2001. A modeling approach to quantify the effects of spatial soybean yield limiting factors. *Trans. ASAE* 44: 1329-1334.
- Perkins, H. F., J. E. Hook, and N. W. Barbour. 1986. Soil characteristics of selected areas of the coastal plain experiment station and ABAC research farms. The University of Georgia.
- Pinnschmidt, H. O., W. D. Batchelor, and P. S. Teng. 1995. Simulation of multiple species pest damage in rice using CERES-Rice. *Agric. Syst.* 48: 193-222.
- Teng, P. S., W. D. Batchelor, H. O. Pinnschmidt, G. G. Wilkerson. 1998. Simulation of pest effects on crop using coupled pest-crop models: the potential for decision support. In *Understanding options for agricultural production*. Dordrecht, The Netherlands.: Kluwer Academic Publishers.
- UGA, 2007. Georgia plant disease loss estimate. Cooperative Extension. Athens, GA: University of Georgia. Available at: <http://pubs.caes.uga.edu/caespubs/pubs/PDF/SB41-10.pdf>. Accessed 23 August 2008.
- USDA. 2008. Crop production. National Agricultural Statistics Service. Washington, D.C.: USDA National Agricultural Statistics Service. Available at: [www.usda.gov/nass/PUBS/TODAYRPT/crop0808.txt](http://www.usda.gov/nass/PUBS/TODAYRPT/crop0808.txt). Accessed 17 August 2008.
- Vellidis, G., M. Tucker, C. Perry, C. Kvien, and C. Bednarz. 2008. A real-time wireless smart sensor array for scheduling irrigation. *Comput. Electron. Agric.* 61: 44-50.
- Wallace, H.R. 1987. Effects of nematode parasites on Photosynthesis. In *Vistas on nematology*, 253-259. Hyattsville, MD. Society of Nematologists.
- Wilcox-Lee, D.A., and R. Loria. 1987. Effects of nematode parasitism on plant-water relations. In *Vistas on nematology*, 260-266. Hyattsville, MD. Society of Nematologists.
- Williamson, V.M., and C.A. Gleason. 2003. Plant-nematode interactions. *Current Opinion in Plant Biology* 6(4): 327-333
- Willmott, C.J. 1982. Some comments on the evaluation of the model performance. *Bulletin of the American Meteorological Society* 63: 1309-1313.
- Wolcott, M. 2007. Cotton yield response to residual effects of Telone Fumigant. In *Proc. 2007 Beltwide Cotton Conference*. New Orleans, LS.: National Cotton Council.

Zhang, J., C. Waddell, C. Sengupta-Gopalan, C. Potenza, and R.G. Cantrell. 2006. Relationships between root-knot nematode resistance and plant growth in upland cotton: Galling index as a criterion. *Crop Sci.* 46: 1581-1586.

Table 5.1. Description of the Tifton soil profile for the experiment conducted at the Gibbs Farm, GA, USA.

Depth (cm)	Horizon name	Clay (%)	Silt (%)	Permanent wilting point LL ( $\text{cm}^3 \text{cm}^{-3}$ )		Field capacity DUL ( $\text{cm}^3 \text{cm}^{-3}$ )		Saturated water content SAT ( $\text{cm}^3 \text{cm}^{-3}$ )		Bulk density ( $\text{g cm}^{-3}$ )	Organic carbon (%)
				Initial <sup>[a]</sup>	Final <sup>[b]</sup>	Initial <sup>[a]</sup>	Final <sup>[b]</sup>	Initial <sup>[a]</sup>	Final <sup>[b]</sup>		
0-30	Apc	4.2	10.9	0.051	0.069	0.107	0.125	0.317	0.300	1.76	0.74
30-51	Btc1	18.6	11.9	0.092	0.096	0.150	0.163	0.259	0.320	1.76	1.08
51-76	Btc2	20.9	12.6	0.102	0.212	0.159	0.340	0.280	0.480	1.74	0.34
76-104	Btv1	32.6	13.9	0.183	0.180	0.261	0.300	0.362	0.400	1.77	0.19
104-135	Btv2	28.8	15.6	0.156	0.185	0.231	0.282	0.342	0.345	1.68	0.25
135-183	Bt	32.5	15.6	0.176	0.134	0.254	0.205	0.353	0.344	1.73	0.04
183-216	BC	36.5	15.4	0.200	0.147	0.283	0.225	0.365	0.365	1.55	0.23

<sup>[a]</sup> Adjusted volumetric water content ( $\text{cm}^3 \text{cm}^{-3}$ ) at the permanent wilting point (LL) and field capacity (DUL) using calculated volumetric soil water content from soil water tension values measured in the field.

<sup>[b]</sup> Volumetric water content estimated by the DSSAT V 4.0 software.

Table 5.2. Cultivar coefficients of cultivar DP 458 B/RR used for model simulations in 2001 and 2007.

Cultivar coefficient	Abbreviation	Calibrated	Original value
Photothermal days from emergence to flower appearance	EM-FL	44	38
Photothermal days from beginning flower to beginning boll	FL-SH	10	12
Photothermal days from beginning flower to beginning seed	FL-SD	22	15
Photothermal days from beginning seed to maturity	SD-PM	51	42
Maximum leaf photosynthesis rate, CO <sub>2</sub> m <sup>-2</sup> s <sup>-1</sup>	LFMAX	1.1	1.1
Specific leaf area, cm <sup>2</sup> g <sup>-1</sup>	SLAVR	252	170
Maximum size of full leaf, cm <sup>2</sup>	SIZLF	300	300
Maximum fraction of daily growth partitioned to seed + shell	XFRT	0.79	0.85
Maximum weight per seed, g	WTPSD	0.308	0.18
Photothermal days for seed filling per individual seed	SFDUR	38	30
Average seed numbers per boll, no. boll <sup>-1</sup>	SDPDV	28	27
Photothermal days to reach final boll load	PODUR	10	8

Table 5.3. Average RKN population (second stage juveniles-J2 per 150,000 cm<sup>3</sup> soil) measured at different days after planting for the six treatments of the calibration and evaluation experiments.

Treatment <sup>[a]</sup>	RKN population density (second stage juveniles 150000 cm <sup>-3</sup> of soil)						
	2007 <sup>[b]</sup>				2001 <sup>[c]</sup>		
	DAP <sup>[d]</sup>						
	18	66	118	175	51	71	197
1+	5000	10000	100000	265000	30000	7000	101667
1-	23333	36667	210000	211667	76667	304000	160000
2+	0	16667	111667	221667	20000	16667	70000
2-	28333	38333	345000	288333	61667	200333	181667
3+	5000	6667	191667	213333	15000	15000	176667
3-	28333	0	361667	205000	60000	250333	435000

<sup>[a]</sup> Treatments: Low drought stress-fumigated (1+), low drought stress-nonfumigated (1-), medium drought stress-fumigated (2+), medium drought stress-nonfumigated (2-), severe drought stress-fumigated (3+), severe drought stress-nonfumigated (3-)

<sup>[b]</sup> RKN population density data for model calibration

<sup>[c]</sup> RKN population density data for model evaluation

<sup>[d]</sup> Days after planting

Table 5.4. Simulated and observed total biomass at harvest for the six treatments in 2007 at the Gibbs Farm, GA, USA.

Treatment <sup>[a]</sup>	Total biomass (kg ha <sup>-1</sup> )				
	Simulated	Observed	RMSE <sup>[b]</sup>	PD (%) <sup>[c]</sup>	d <sup>[d]</sup>
1+	9345	8013	3707	14.3	0.63
1 -	8570	7159	2254	16.5	0.74
2+	7427	6805	3069	8.4	0.61
2 -	6208	5493	2872	11.5	0.55
3+	7123	6709	3194	5.8	0.57
3 -	6033	4925	2433	18.4	0.54

<sup>[a]</sup> Treatments: Low drought stress-fumigated (1+), low drought stress-nonfumigated (1-), medium drought stress-fumigated (2+), medium drought stress-nonfumigated (2-), severe drought stress-fumigated (3+), severe drought stress-nonfumigated (3-)

<sup>[b]</sup> Root mean square error, average over dates

<sup>[c]</sup> Percentage prediction deviation

<sup>[d]</sup> Index of agreement

Table 5.5. Simulated and observed bolls weight and seed cotton weight at maturity for the six treatments in 2007 at the Gibbs Farm, GA, USA.

Treatment <sup>[a]</sup>	Boll weight (kg ha <sup>-1</sup> )					Seed cotton weight (kg ha <sup>-1</sup> )				
	Simulated <sup>[b]</sup>	Observed <sup>[c]</sup>	RMSE <sup>[d]</sup>	PD (%) <sup>[e]</sup>	d <sup>[f]</sup>	Simulated <sup>[g]</sup>	Observed <sup>[h]</sup>	RMSE <sup>[d]</sup>	PD (%) <sup>[e]</sup>	d <sup>[f]</sup>
1+	5696	5347	2025	6.1	0.80	4017	3972	707	1.1	0.70
1 -	5151	4541	1346	11.8	0.87	3635	3536	896	2.7	0.69
2+	4371	4170	1788	4.6	0.78	3179	3181	965	-0.1	0.49
2 -	3483	3508	1730	-0.7	0.71	2547	2738	1119	-7.5	0.48
3+	3853	3856	2326	-0.1	0.64	2687	2964	885	-10.3	0.65
3 -	3162	3223	1602	-1.9	0.67	2195	2440	1009	-11.2	0.53

<sup>[a]</sup> Treatments: Low drought stress-fumigated (1+), low drought stress-nonfumigated (1-), medium drought stress-fumigated (2+), medium drought stress-nonfumigated (2-), severe drought stress-fumigated (3+), severe drought stress-nonfumigated (3-)

<sup>[b]</sup> Simulated weight at maturity

<sup>[c]</sup> Observed weight at maturity

<sup>[d]</sup> Root mean square error, average over dates

<sup>[e]</sup> Percentage prediction deviation

<sup>[f]</sup> Index of agreement

<sup>[g]</sup> Simulated seed cotton weight at maturity

<sup>[h]</sup> Observed seed cotton weight at maturity

Table 5.6. Prediction accuracy of simulated maximum leaf area index before and after modeling RKN damage. Values correspond to the nonfumigated treatment (-) with low (1), medium (2), and severe (3) drought stress.

Treatment <sup>[a]</sup>	LAI (m <sup>2</sup> m <sup>-2</sup> ) <sup>[b]</sup>			Prediction assessment			
	Observed	Initial	Final	RMSE <sup>[c]</sup>		d <sup>[d]</sup>	
				Initial	Final	Initial	Final
1 -	4.57	4.80	4.38	1.07	0.95	0.84	0.85
2 -	3.67	4.02	3.65	0.74	0.70	0.86	0.86
3 -	3.39	4.13	3.43	0.75	0.65	0.86	0.86

<sup>[a]</sup> Treatments: Low drought stress-nonfumigated (1-), medium drought stress-nonfumigated (2-), severe drought stress-nonfumigated (3-)

<sup>[b]</sup> Values of maximum LAI: measured in the field, initially simulated using the 1<sup>st</sup> hypothesis, and finally simulated using the 2<sup>nd</sup> hypothesis.

<sup>[c]</sup> Root mean square error, average over dates

<sup>[d]</sup> Index of agreement

Table 5.7. Simulated and observed maximum leaf area index for the six treatments in 2007 at the Gibbs Farm, GA, USA.

Treatment <sup>[a]</sup>	LAI (m <sup>2</sup> m <sup>-2</sup> )				
	Simulated <sup>[b]</sup>	Observed <sup>[c]</sup>	RMSE <sup>[d]</sup>	PD (%) <sup>[e]</sup>	d <sup>[f]</sup>
1+	4.93	5.08	0.69	-3	0.94
1 -	4.38	4.57	0.95	-4.3	0.85
2+	4.11	4.62	0.78	-12.4	0.87
2 -	3.65	3.67	0.71	-0.5	0.86
3+	4.13	4.97	0.77	-20	0.88
3 -	3.43	3.39	0.65	1.16	0.86

<sup>[a]</sup> Treatments: Low drought stress-fumigated (1+), low drought stress-nonfumigated (1-), medium drought stress-fumigated (2+), medium drought stress-nonfumigated (2-), severe drought stress-fumigated (3+), severe drought stress-nonfumigated (3-)

<sup>[b]</sup> Simulated maximum LAI

<sup>[c]</sup> Observed maximum LAI

<sup>[d]</sup> Root mean square error, average over dates

<sup>[e]</sup> Percentage prediction deviation

<sup>[f]</sup> Index of agreement

Table 5.8. Prediction accuracy of simulated volumetric soil water content for the six treatment combinations of drought stress and fumigation evaluated at the 15- to 30- cm, 30- to 45- cm, and 45- to 60- cm soil depth.

Treatment <sup>[a]</sup>	RMSE <sup>[b]</sup>	d <sup>[c]</sup>	N <sup>[d]</sup>
<u>Depth (15-30 cm)</u>			
1+	0.024	0.63	109
1-	0.028	0.69	118
2+	0.022	0.83	118
2-	0.018	0.85	120
3+	0.022	0.82	115
3-	0.036	0.71	115
<u>Depth (30-45 cm)</u>			
1+	0.017	0.84	120
1-	0.032	0.63	110
2+	0.015	0.92	120
2-	0.021	0.83	124
3+	0.018	0.88	122
3-	0.099	0.51	124
<u>Depth (45-60 cm)</u>			
1+	0.028	0.82	121
1-	0.041	0.67	122
2+	0.94	0.78	124
2-	0.03	0.85	124
3+	0.029	0.83	122
3-	0.032	0.84	124

<sup>[a]</sup> Treatments: Low drought stress-fumigated (1+), low drought stress-nonfumigated (1-), medium drought stress-fumigated (2+), medium drought stress-nonfumigated (2-), severe drought stress-fumigated (3+), severe drought stress-nonfumigated (3-)

<sup>[b]</sup> Root mean square error, average over dates

<sup>[c]</sup> Index of agreement

<sup>[d]</sup> Number of observations

Table 5.9. Simulated and observed seed cotton weight at harvest for the six treatments in 2001 at the Gibbs Farm, GA, USA.

Treatment <sup>[a]</sup>	Seed cotton weight (kg ha <sup>-1</sup> ) <sup>[b]</sup>			
	Simulated <sup>[c]</sup>	Observed <sup>[d]</sup>	RMSE <sup>[e]</sup>	PD (%) <sup>[f]</sup>
1+	4275	3069	1290	28.2
1 -	3397	2895	621	14.8
2+	3638	3064	643	15.8
2 -	2958	2785	445	5.8
3+	2999	2939	219	2.0
3 -	2124	2160	906	-1.7

<sup>[a]</sup> Treatments: Low drought stress-fumigated (1+), low drought stress-nonfumigated (1-), medium drought stress-fumigated (2+), medium drought stress-nonfumigated (2-), severe drought stress-fumigated (3+), severe drought stress-nonfumigated (3-)

<sup>[b]</sup> Seed cotton weight is equivalent to seed plus lint weight

<sup>[c]</sup> Simulated weight at harvest maturity. Simulations were run using cultivar and damage coefficients from the calibration data set collected in 2007

<sup>[d]</sup> Observed weight at harvest maturity. Data correspond to the validation data set collected in 2001.

<sup>[e]</sup> Root mean square error

<sup>[f]</sup> Percentage prediction deviation

Table 5.10. Description of the Albany and Kershaw soil profiles predominant one each of the management zones at the producer field in Norman Park, GA, USA.

Zone <sup>[a]</sup>	Depth (cm)	Horizon name	Sand (%)	Clay (%)	Silt (%)	Permanent wilting point	Field capacity	Saturated water content	Bulk density (g cm <sup>-3</sup> )
						LL	DUL	SAT	
						(cm <sup>3</sup> cm <sup>-3</sup> )			
<i>1 (Low risk - 6.0 ha)</i>									
Albany soil	0-13	A	89	2	9	0.041	0.116	0.416	1.48
	13-53	E1	91	3	6	0.046	0.118	0.413	1.49
	53-81	E2	87	6	7	0.064	0.143	0.398	1.53
	81-114	BE	83	11	6	0.091	0.171	0.38	1.58
	114-132	Bt	76	17	7	0.119	0.202	0.373	1.6
<i>2 (Moderate risk - 6.6 ha) and 3 (High risk - 7.6 ha)</i>									
Kershaw soil	0-18	Ap	93.4	3	3.6	0.052	0.102	0.413	1.49
	18-43	E	87.7	5.7	6.6	0.059	0.111	0.389	1.56
	43-66	A	87.6	5.5	6.9	0.056	0.108	0.386	1.57
	66-89	B1	82.9	9.9	7.2	0.078	0.132	0.369	1.62
	89-102	B2	84.9	8.6	6.5	0.071	0.123	0.369	1.62
	102-132	Btg	78.6	16.3	5.1	0.108	0.16	0.344	1.69

<sup>[a]</sup> Zone 1 = Low risk, Zone 2 = Moderate risk, Zone 3 = High risk for RKN damage

Table 5.11. Simulated and observed average seed cotton weight at harvest for the three management zones in 2006 at the producer field in Norman Park, GA, USA.

Zone <sup>[a]</sup>	Seed cotton weight (kg ha <sup>-1</sup> ) <sup>[b]</sup>		
	Simulated	Observed <sup>[c]</sup>	PD (%) <sup>[d]</sup>
1	3566	3316	7.0
2	2998	2909	3.0
3	2773	2354	15.1

<sup>[a]</sup> Zone 1 = Low risk, Zone 2 = Moderate risk, Zone 3 = High risk for RKN damage

<sup>[b]</sup> Seed cotton weight is equivalent to seed plus lint weight

<sup>[c]</sup> Observed average value of the yield data within each zone

<sup>[d]</sup> Percentage prediction deviation

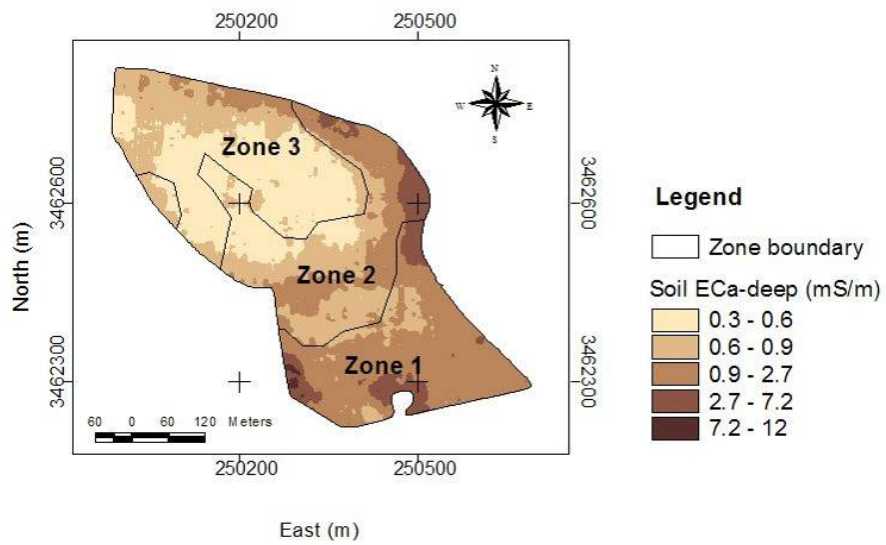


Figure 5.1. RKN management zones for a producer's field (Zone 1 = Low risk, Zone 2 = Moderate risk, Zone 3 = High risk for RKN damage).

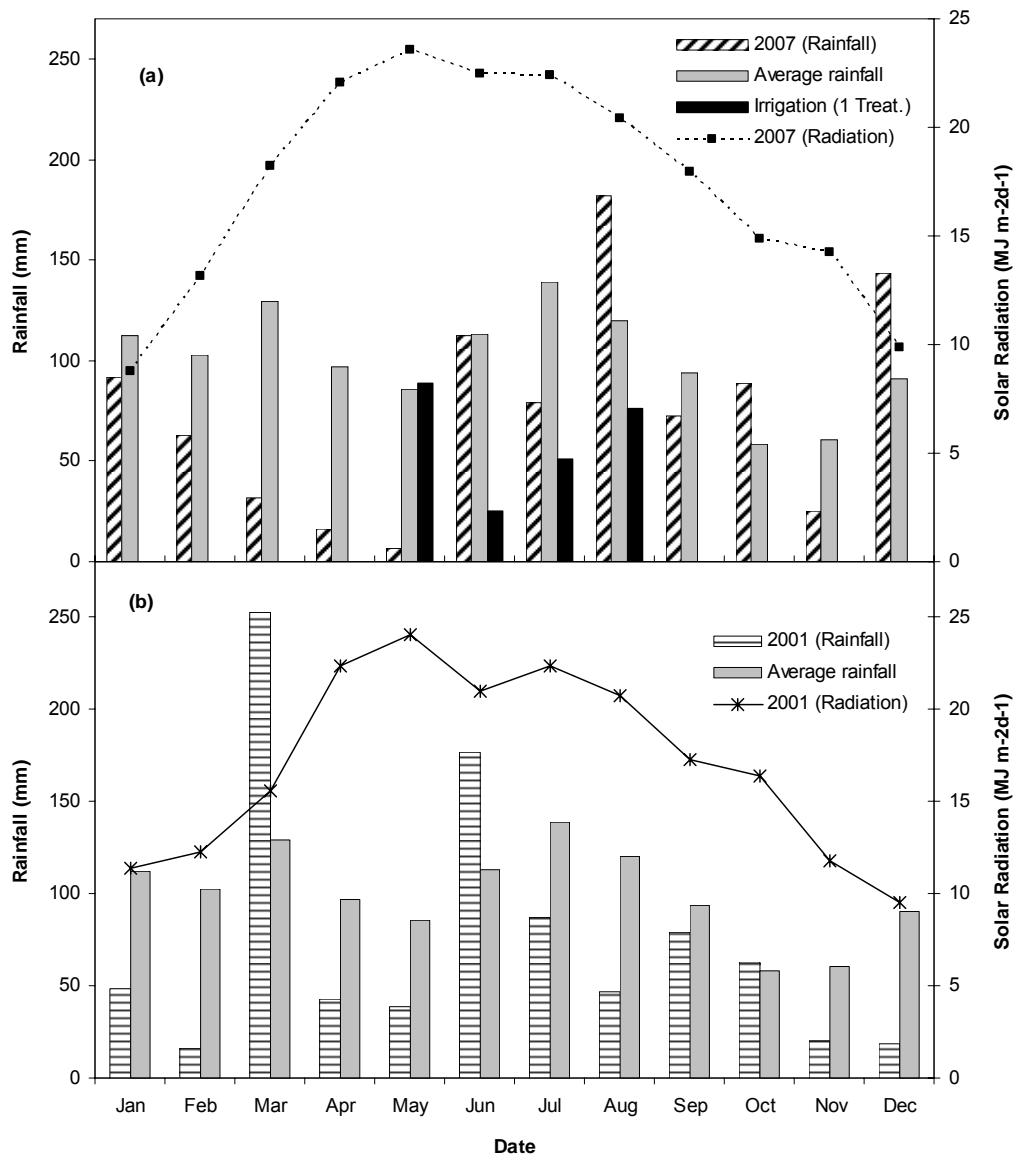


Figure 5.2. Average monthly solar radiation, average monthly total rainfall, and monthly total irrigation applied on the low drought stress treatment [1] in 2007 (a) and 2001 (b), and the climatic average rainfall (1912-2003) at the Gibbs Farm, Tifton, USA.

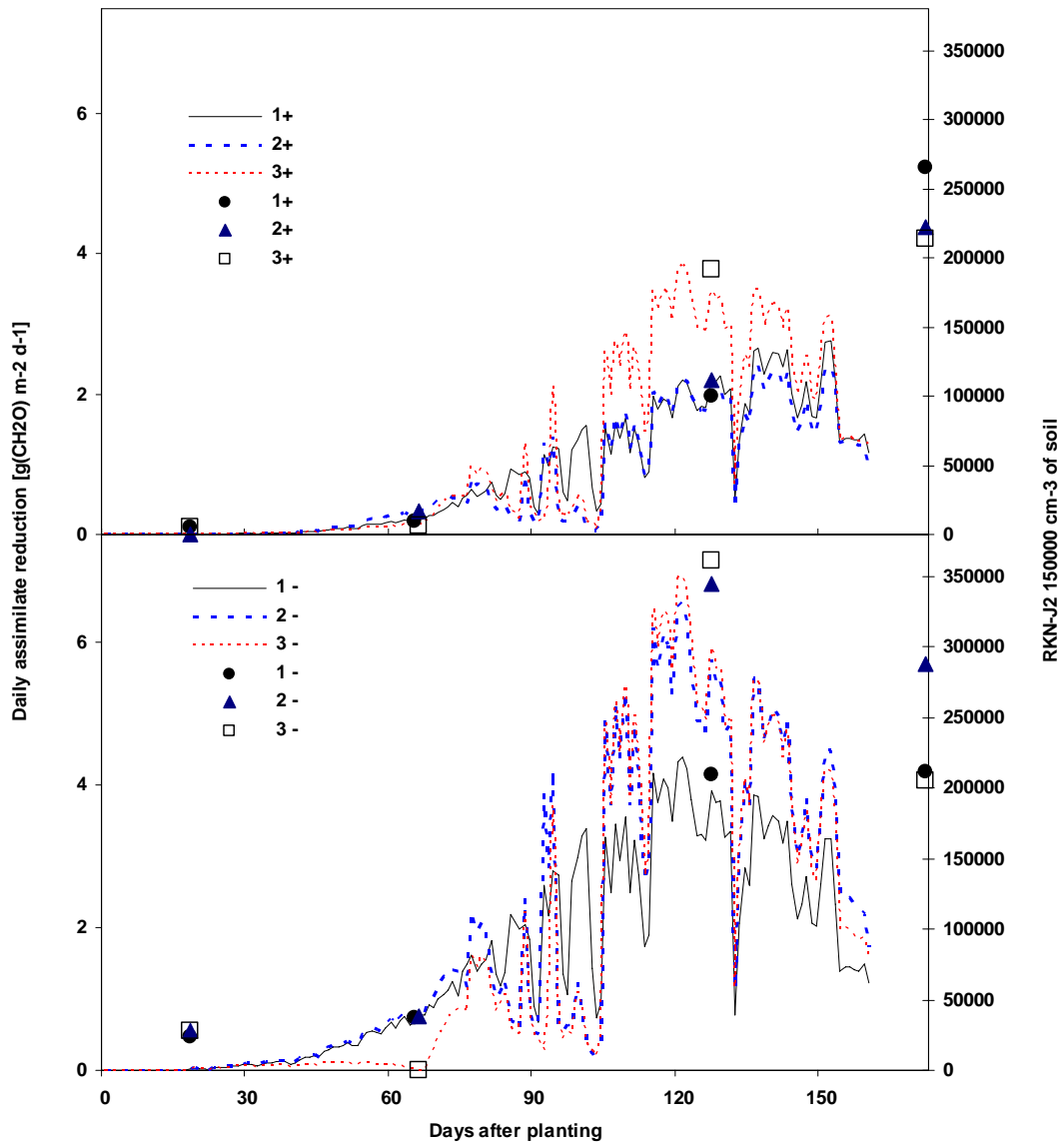


Figure 5.3. Differences in RKN-J2 population density (dots) and daily assimilate removal (lines) by calculated by the CMS-CROPGRO-Cotton model for the treatment combinations of drought stress [low (1), medium (2), and high (3)] with fumigation levels [ (a) fumigated (+), and (b) nonfumigated (-)].

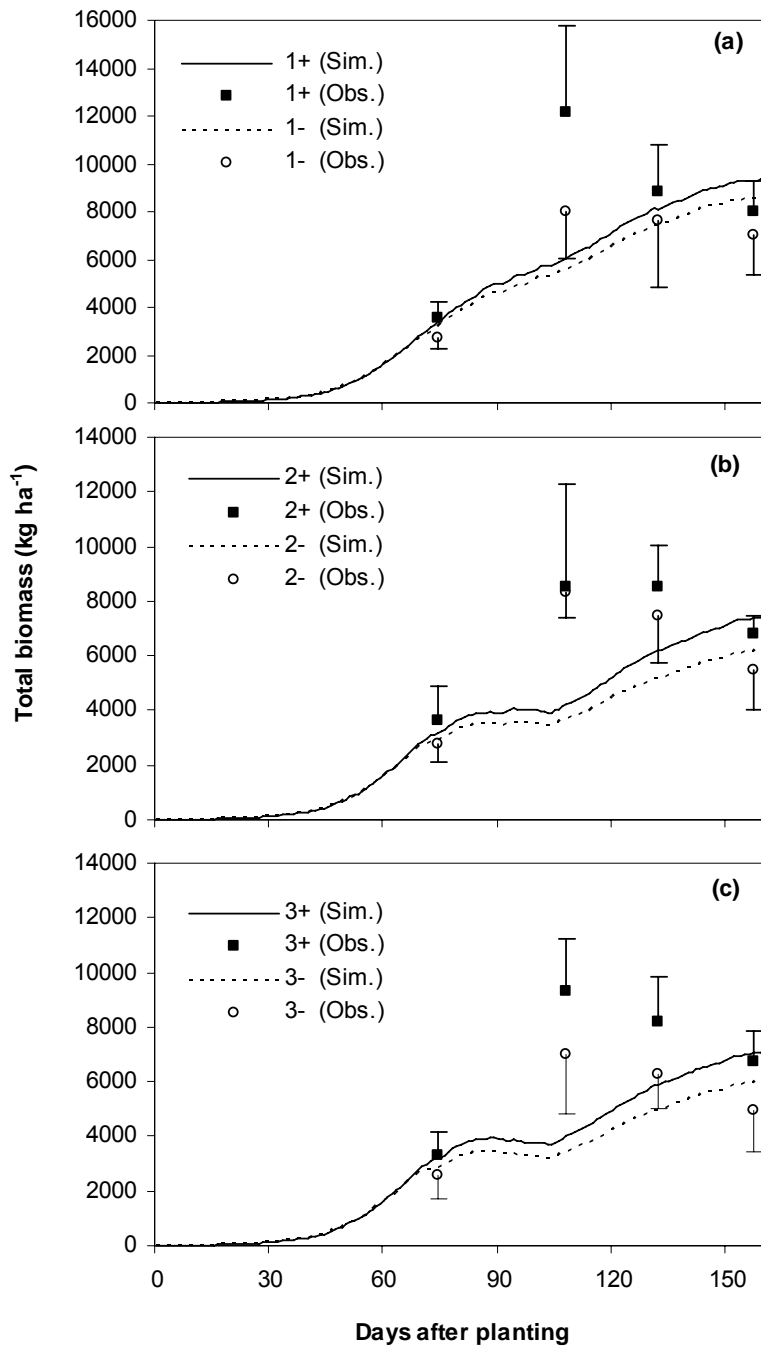


Figure 5.4. Simulated and observed total biomass for the 2007 experiment corresponding to treatment combinations: low (1), medium (2), and severe (3) drought stress with the fumigated (+) and nonfumigated (-). Error bars represent one standard deviation, and points represent the mean of measured data.

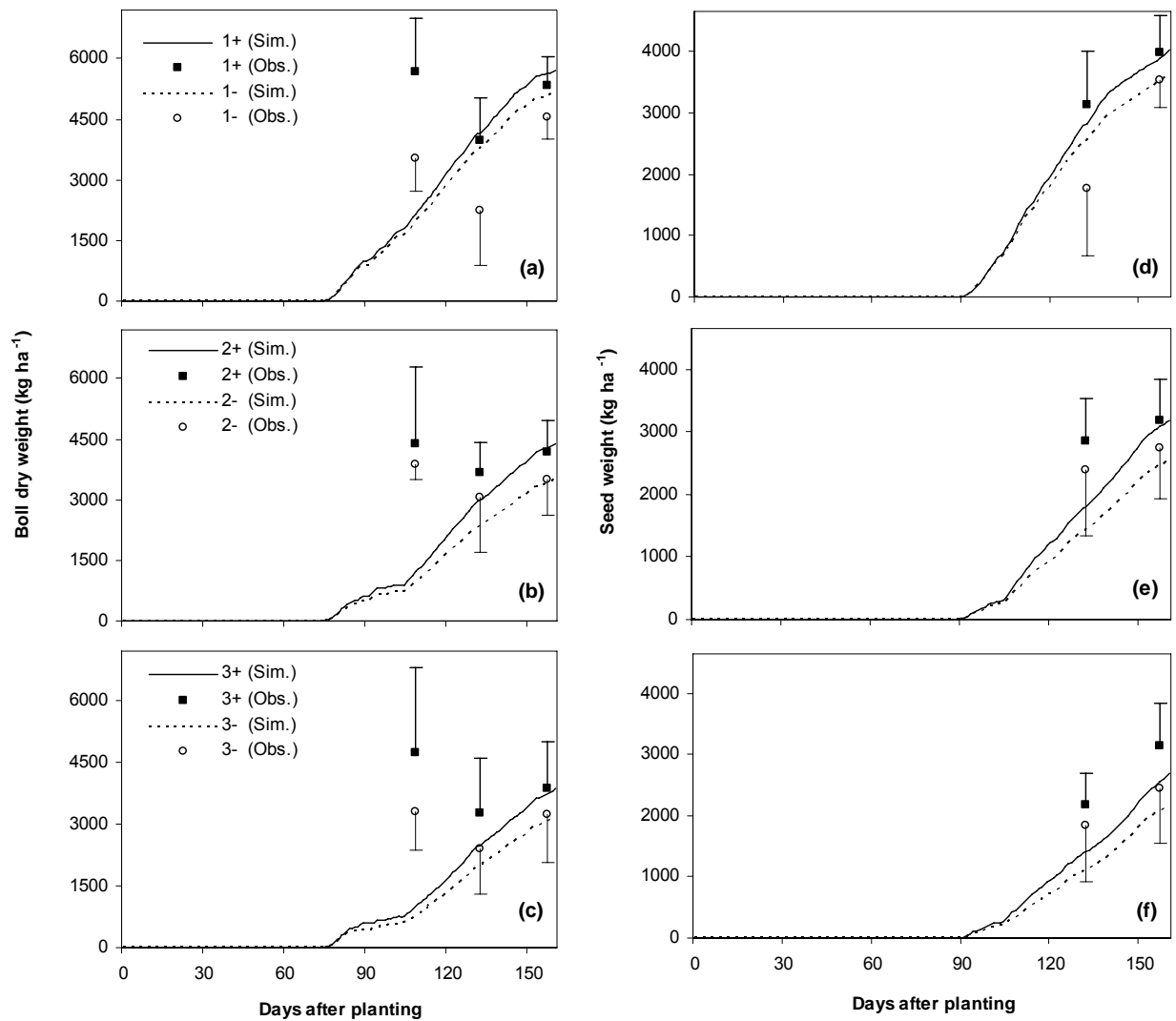


Figure 5.5. Simulated and observed boll dry weight and seed cotton weight for the 2007 experiment corresponding to treatment combinations: low (1), medium (2), and severe (3) drought stress with the fumigated (+) and nonfumigated (-). Error bars represent one standard deviation, and points represent the mean of measured data.

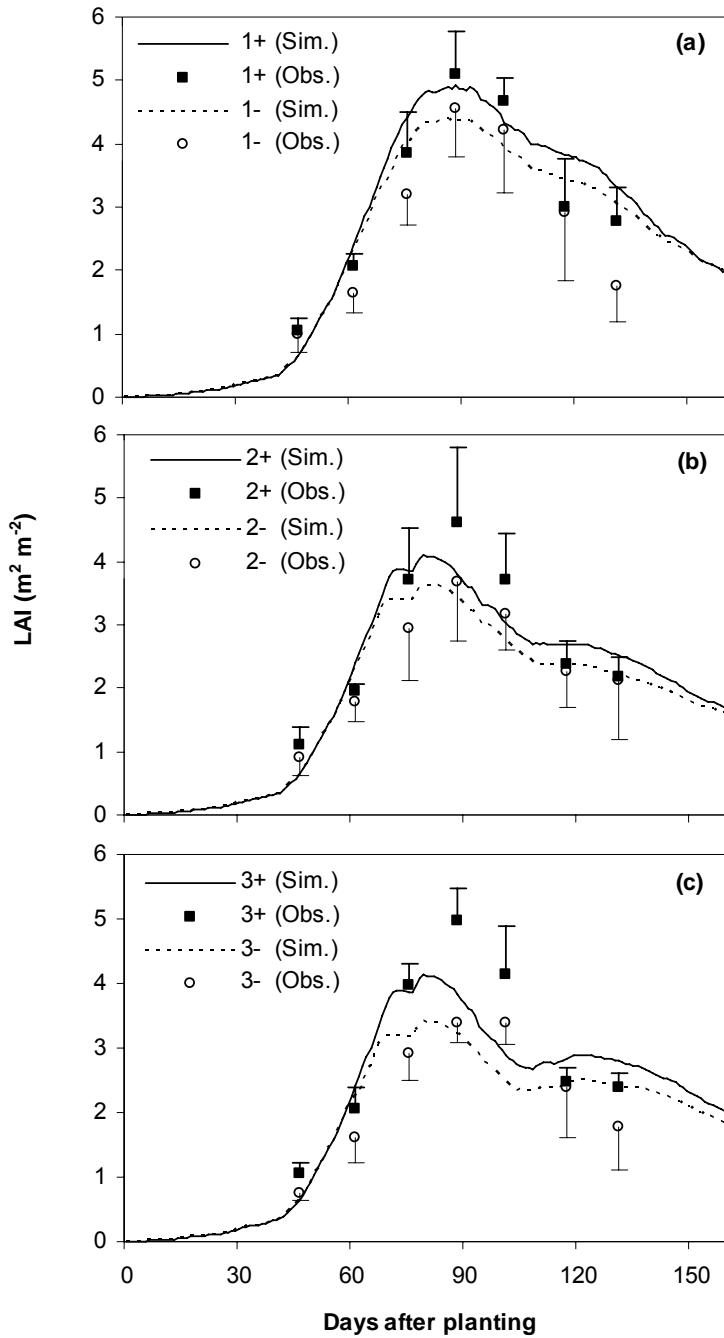


Figure 5.6. Simulated and observed leaf area index for the 2007 experiment corresponding to treatment combinations: low (1), medium (2), and severe (3) drought stress with the fumigated (+) and nonfumigated (-). Error bars represent one standard deviation, and points represent the mean of measured data.

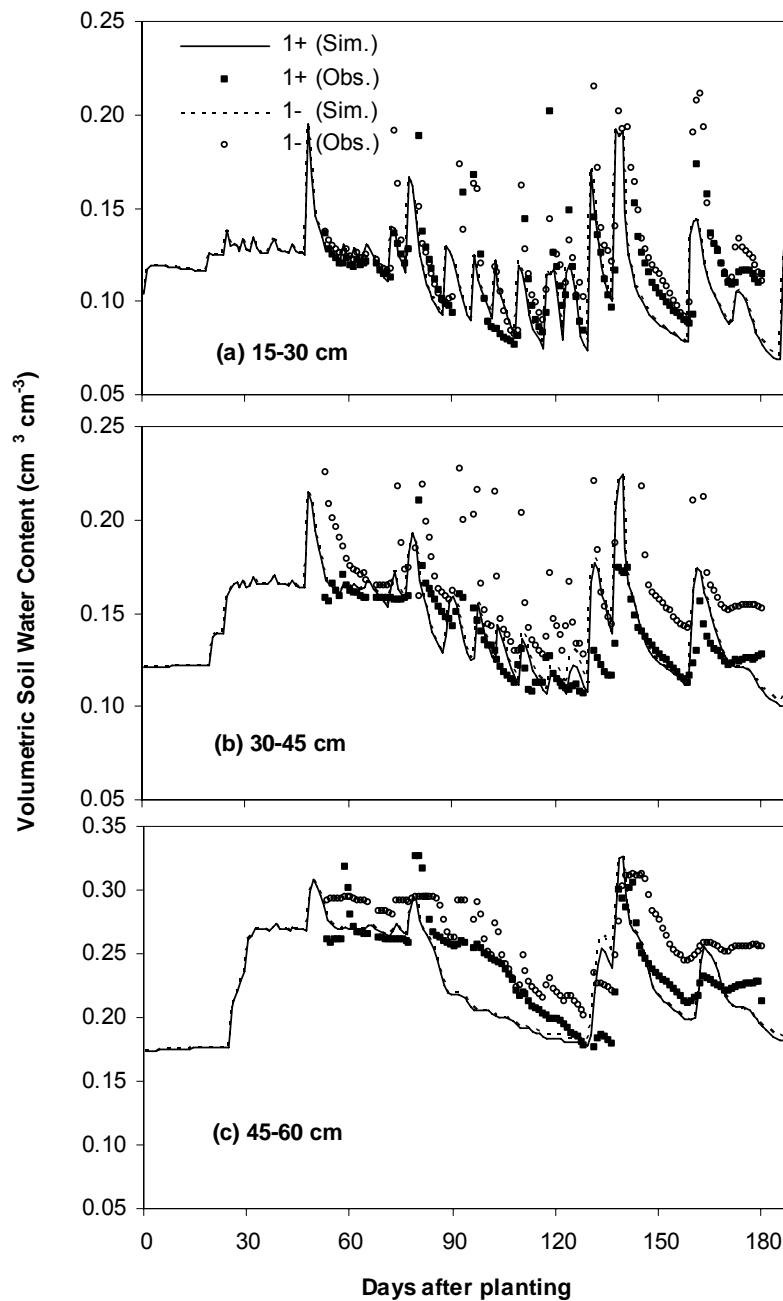


Figure 5.7. Simulated and observed volumetric soil water content at the 0- to 60- cm soil depth during the 2007 experiment for the treatment combinations: low (1) drought stress with the fumigated (+) and nonfumigated (-) levels.

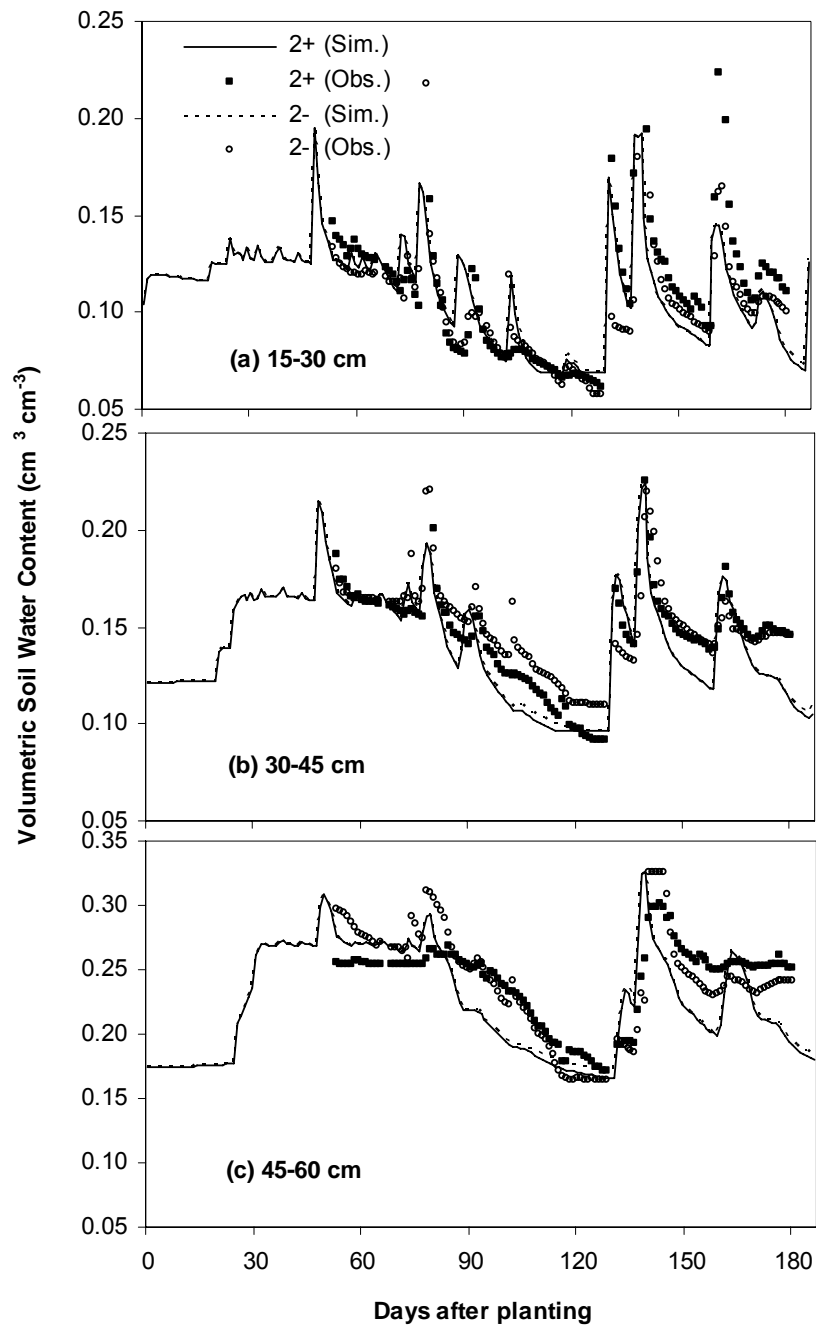


Figure 5.8. Simulated and observed volumetric soil water content at the 0- to 60- cm soil depth during the 2007 experiment for the treatment combinations: medium (2) drought stress with the fumigated (+) and nonfumigated (-) levels.

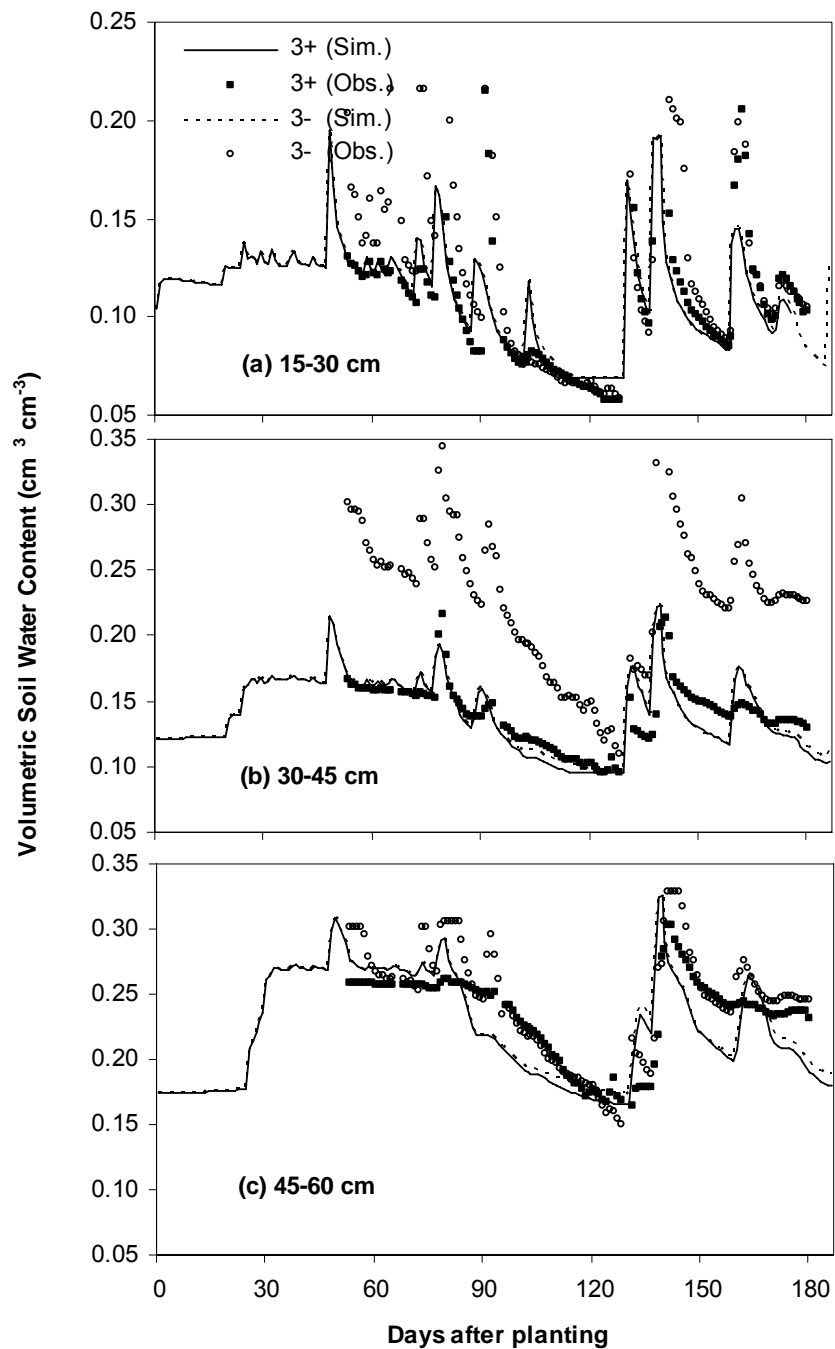


Figure 5.9. Simulated and observed volumetric soil water content at the 0- to 60- cm soil depth during the 2007 experiment for the treatment combination severe drought stress (3) with fumigated (+) and nonfumigated (-) levels.

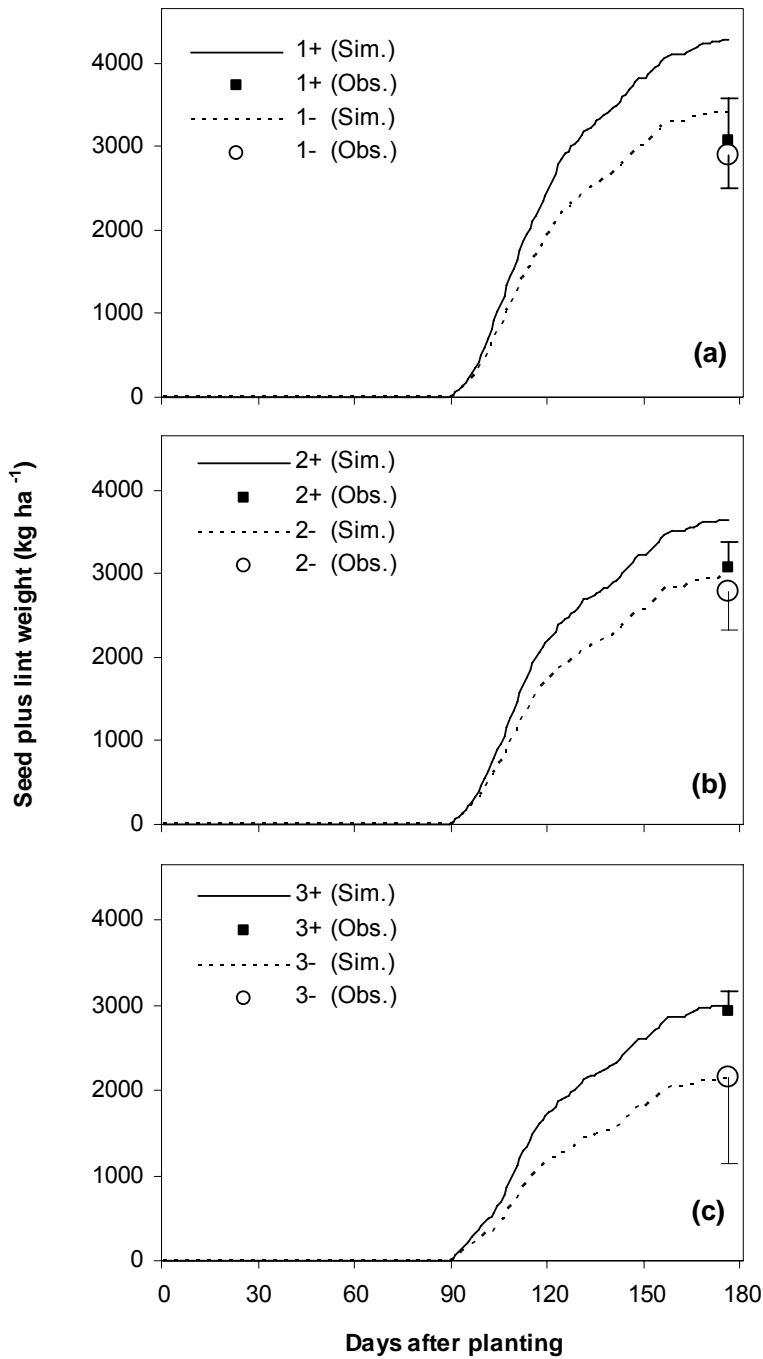


Figure 5.10. Simulated and observed seed cotton weight for the 2001 experiment corresponding to treatment combinations: low (1), medium (2), and severe (3) drought stress with the fumigated (+) and nonfumigated (-). Error bars represent one standard deviation, and points represent the mean of measured data.

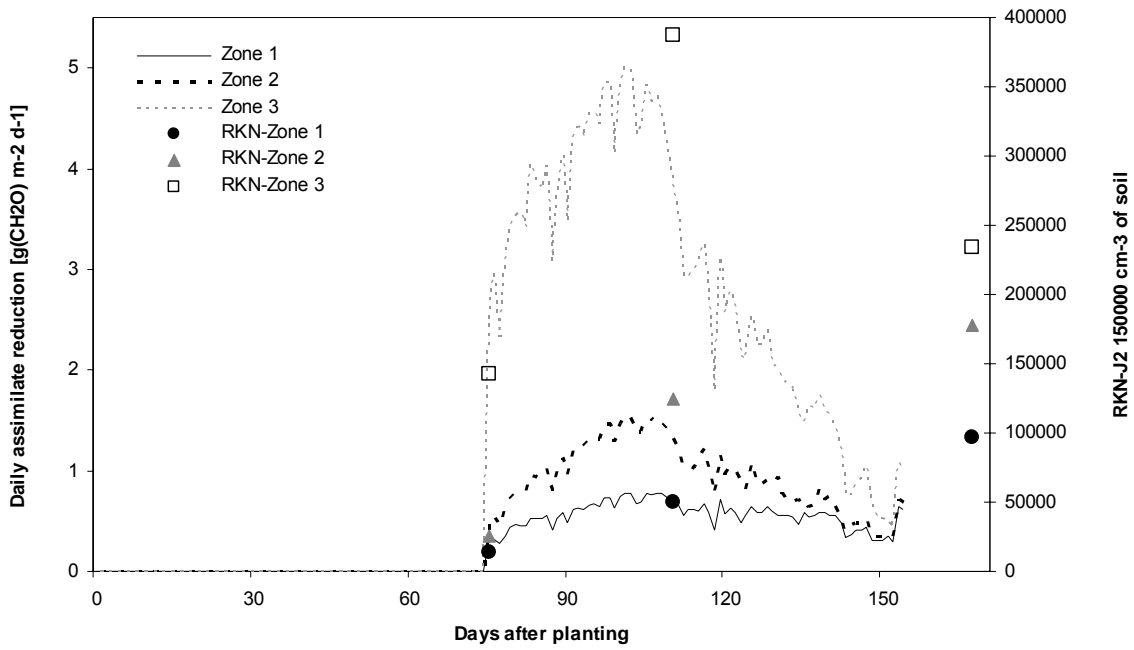


Figure 5.11. Differences in RKN-J2 population density (dots) and daily assimilate removal (lines) calculated by the CROPGRO-Cotton model for the three management zones [low risk (Zone 1), moderate risk (Zone 2), and high risk for RKN damage (Zone 3)] at the producer field.

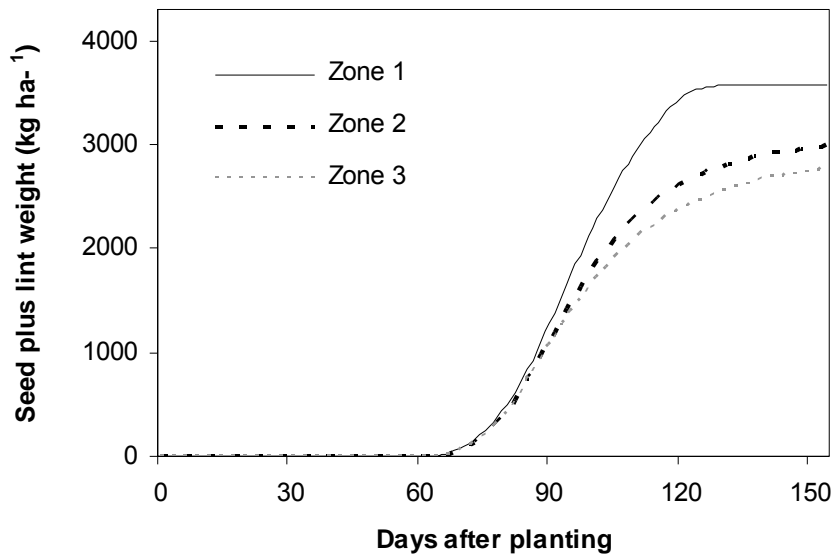


Figure 5.12. Simulated seed plus lint weight in 2006 for the three management zones [low risk (Zone 1), moderate risk (Zone 2), and high risk for RKN damage (Zone 3)] at the producer field.

## CHAPTER 6

### SUMMARY AND CONCLUSIONS

In order to implement a site specific management of the southern root-knot nematode (RKN), understanding of its spatial variability of RKN and the field features promoting their presence or absence is necessary. Additionally, the study and simulation of cotton growth and development under different levels of RKN population and drought stress will contribute to an understanding of the effect of these stressor factors when ecological and environmental conditions might change. Also, the identification and evaluation of strategies for modeling RKN damage on cotton plants will bring new options of accounting for RKN damage when running simulations for site specific management (SSM).

Southern root-knot nematode ecology is strongly related with soil properties and the root system of the host plant. In contrast, the plant response to the RKN infection changes with the growth stage and the combination of other stressor factors, especially drought stress. Therefore, it is necessary to study how RKN aggregates in producer fields and their impact on cotton growth and yield under different conditions. The purpose of this study was to identify through geostatistical and statistical methods field features in producer's fields that can be used as surrogate data for RKN when delineating management zones for a site specific management of RKN. In addition, cotton growth data and analyses were provided for testing different strategies and estimation of parameters required to couple the effects of RKN into the CSM-CROPGRO Cotton model. Each one of the four studies included in this dissertation is part of the study to

understand and manage the RKN-plant-environment system. In the first study a geostatistical approach is used to study the spatial variability of RKN population, establish the relationship between RKN occurrence and the spatial variability of soil properties; and delineate areas at risk for RKN over a threshold value. In the second, canonical correlation analyses with data collected from 11 fields were included as part of the identification of edaphic and terrain properties as surrogate data for RKN. In addition, a framework of procedures for delineation of management zones with purposes of SSM for RKN is presented. The third study, include an analysis of the impact of RKN parasitism-drought stress on different cotton biomass components and yield. The fourth study included an adaptation to the CSM-CROPGRO-Cotton model for simulating the growth and development of cotton plants infected by RKN and under the combined effects of high RKN population and drought stress.

Spatial variability of RKN and soil properties were monitored in 11 cotton producer fields located in the TVU ecoregion of the southeastern Coastal Plain. A 50 x 50 m grid (0.25 ha cell size) was superimposed over each study field and sampling locations for RKN population density determination were established at the center of each grid. Soil samples were collected four times during the growing season: June (planting, RKN-S0), July (first square, RKN1), late August (flowering, RKN2), and October-November (harvest, RKN3).

Dry matter accumulation was monitored under the conditions of a controlled experiment and a producer's field. For the controlled experiment, plots were subject to six different combinations of fumigation and drought stress levels. Fumigation with 1,3-dichloropropene at 65 L ha<sup>-1</sup> [Telone II, Dow AgroSciences, Indianapolis, Indiana] was used to create different levels of RKN population densities. The drought stress treatments differed with respect to the frequency and amount of the irrigation water applied.

Crop dry matter was sampled monthly while leaf area and plant height were sampled weekly throughout the season and used to estimate leaf area index (LAI) and growth of some cotton biomass components such as leaves, stem and petiole, bolls, and lint plus seed. Differences in development throughout the season were assessed by monitoring progress of vegetative and reproductive stages. Biomass samples at the producer field were collected at 14 locations exemplifying areas with differences for natural occurrence of RKN population and drought stress.

The findings presented here showed that at two fields where the spatial variability of RKN was studied, the RKN population was aggregated and stable through time, which indicated potential for implementation of RKN site specific management. The aggregated pattern of RKN distribution and its strong spatial correlation with apparent soil electrical conductivity deep ( $EC_{a-d}$ ) facilitated the segregation of RKN risk areas through the development of indicator kriging maps. The combination of hard (RKN samples) and soft data ( $EC_{a-d}$ ) data for mapping took advantage of the dense set of  $EC_{a-d}$  data which is less expensive and easier for a producer to collect than the RKN samples. The biggest advantage of this data combination is the reduced number of RKN samples required to assess the areas at risk for high population of RKN. This study also showed that if RKN populations exhibit short and large variability, then the short range of spatial dependence can be used as a guideline for sampling RKN population density in fields with low topographic relief.

In chapter three, data from 11 producer's fields were analyzed to identify potential RKN surrogate data and posterior development of management zones delineation method, the results indicated that areas likely to have high levels of RKN population may be identified based on edaphic variables, apparent soil electrical conductivity (shallow-  $EC_{a-s}$  or deep- $EC_{a-d}$ ) and bare

soil spectral reflectance patterns. However, if the field exhibits significant variability in terrain properties, flat lying areas will be more likely to have high RKN levels. This study showed that the zone with the highest RKN population (high risk zone) was characterized by having the lowest mean values of  $EC_{a-s}$ ,  $EC_{a-d}$ , NDVI and SL. In contrast, the zone with the lowest RKN population density (low risk zone) exhibited the highest values of  $EC_{a-s}$ ,  $EC_{a-d}$ , NDVI and SL with respect to the average values of the field. This type of characterization is fundamental for guided sampling.

The results from the management zones delineation study confirmed that the presence of RKN population is related to soil texture. However, it is important to understand that in south Georgia there is not a high variability in soil textural classes within the fields; in contrast there is a high predominance of coarse sandy textures. Therefore, this study indicated that differentiation of the zones at risk for nematode occurrence must be based on the segregation of sandy areas with different particle size that are possible to identify through sensing changes in apparent soil electrical conductivity ( $EC_a$ ) or bare soil spectral reflectance.

The fact that management zones can be delineated using field edaphic and terrain properties and that RKN population density increased in areas of coarse textured soils where leaching of nematicides is most likely to occur, indicates the importance of differentiating RKN levels not only for RKN management but also for soil fertility management. However, if there is neither structured within-field spatial variability for RKN population nor edaphic or terrain properties, a uniform management would be preferred to one by management zones.

When the impact of RKN parasitism on cotton plants was studied, chapter four, a reduction of growth and development of cotton biomass components (plant height, LAI, stem-petiole biomass, number of bolls, number of closed bolls, lint plus seed yield) was found. The

effects of high RKN population density were exacerbated by drought stress. Plant height and boll dry weight from plots with RKN population above the threshold (100 second juveniles per 100 cm<sup>3</sup> of soil) were highly reduced when the level of drought increased from low to severe, which showed that high RKN population density and drought limit vegetative and reproductive growth. Another effect of RKN parasitism was the high number of closed bolls observed on nonfumigated plots (RKN population above the threshold), caused by a delay in the onset of fruiting and resulting in a delay in harvest maturity. This delay in maturity, along with a reduction of boll biomass, might be considered directly related to the decline of lint plus seed yield. Differences in partitioning were more evident when the reductions in biomass components were compared by sampling date. In general, when the growth of biomass components in nonfumigated plots under low drought was compared with conditions of severe drought stress the reductions were 20%, 14%, 29%, 22.5%, 25%, and 14% for leaf area index, plant height, stem and petiole dry weight, total biomass dry weight, bolls dry weight, and lint plus seed weight, respectively.

In chapter five, the CSM-CROPGRO-Cotton model was adapted to couple RKN effects on cotton growth. The two hypotheses to account for RKN damage were successfully tested and implemented to simulate LAI, biomass and cotton yield in plots having different levels of RKN population. The first hypothesis considering RKN as sink of soluble assimilate targeted reductions in biomass and yield components. The second hypothesis accounting for reductions in root length per unit mass due to RKN parasitism allowed the simulations of LAI under different levels of RKN population. Once the RKN effects were accounted for, the CROPGRO-Cotton model in DSSAT v4.0 was able to simulate growth and yield of the DP 458 BR cotton variety impacted by RKN population and drought stress, and also simulated soil water dynamics with

respect to different drought stress levels from an experimental site in Tifton, GA, USA. The simulated weight of vegetative and reproductive biomass components were close to the observed values for three drought stress and two fumigation levels. Model simulations reinforced the observations from the experimental plots where leaf area index, total biomass, boll weight and seed cotton weight decreased with elevated RKN population on nonfumigated plots. Simulations showed that the impact of RKN changed among drought stress levels being the combination RKN-severe drought stress the most harmful.

The results presented in this study showed the potential of CSM-CROPGRO-Cotton model for forecasting the impact of RKN and drought stress in cotton and understanding the effect of these stressor factors on growth and final yield when changing management strategies. Additionally, CSM-CROPGRO-Cotton model seemed a promising tool for forecasting yield losses by RKN population under the conditions of a producer's field. It was evidenced by the small percentage of error when simulating the yield differences between management zones having different levels of risk for high RKN population.

This dissertation provides insights into what and how surrogate data for RKN should be collected for site specific management of nematodes by zones. This approach might bring the opportunity to decide various threshold values for nematicide application within a single field as well as different rates for fertilization and irrigation management. In addition, the identification of strategies for coupling RKN damage into the CSM-CROPGRO-Cotton model opened new opportunities for evaluating the damage on different varieties and environments as well as test the same and new modeling strategies with other nematodes impacting cotton production.

Future research should involve the evaluation of the cotton yield and RKN population response to differential application of nematicides based on the management zones. Also, to test

if at a producer's field it is possible to grow tolerant and resistant varieties according to the levels of risk for RKN existing in each management zone. In the case of modeling cotton growth impacted by RKN damage, it is important to identify and implement additional methods for coupling RKN damage in order to improve prediction of RKN damage. For example the addition of disease progress functions to better simulate within season changes in RKN population and its effect on growth and yield could be utilized. Additionally, it is necessary to evaluate the model under other conditions of cultivar, soil and weather in order to establish the levels of risk for high populations of nematodes and define the most appropriate management strategy.

## REFERENCES

- Aaron, R.S., J.F. Shanahan, M.A. Liebig, J.S. Schepers, S.H. Johnson, and A.J. Luchiari. 2004. Appropriateness of management zones for characterizing spatial variability of soil properties and irrigated corn yields across years. *Agron. J.* 96: 195-203.
- Ashley, D.A. 1972. <sup>14</sup>C-Labeled photosynthate translocation and utilization in cotton plants. *Crop Sci.* 12: 69-74.
- Avendaño, F., O. Schabenberger, F. J. Pierce, and H. Melakeberhan. 2003. Geostatistical analysis of field spatial distribution patterns of soybean cyst nematode. *Agron. J.* 95: 936-948.
- Avendaño, F., F. J. Pierce, O. Schabenberger, and H. Melakeberhan. 2004. The spatial distribution of soybean cyst nematode in relation to soil texture and soil map unit. *Agron. J.* 96: 181-194.
- Avruskin G., G. Jacquez, J. Meliker, M. Slotnick, A. Kaufmann, and J. Nriagu. 2004. Visualization and exploratory analysis of epidemiologic data using a novel space time information system. *Intl. J. Health Geogr.* 3: 26.
- Barnes, E.M., and M.G. Baker. 2000. Multispectral data for mapping soil texture: possibilities and limitations. *Trans. ASAE* 16(6): 731-741.
- Basnet, B., R. Kelly, T. Jensen, W. Strong, A. Apan, and D. Butler. 2003. Delineation of management zones using multiple crop yield data. In *Proc. International Soil Tillage Research Organization Conference, 16th Triennial Conference*. Brisbane, AU.: The University of Queensland.
- Batchelor, W. D., J. W. Jones, and K. J. Boote. 1992. Assessing pest and disease damage with DSSAT. *Agrotech. Trans.* 16: 1-8.
- Bird, A.F. 1974. Plant response to root- knot nematode. *Ann. Rev. Phytophat.* 12: 69-85.
- Bird, A.F., and R.R. Loveys. 1975. The incorporation of photosynthates by *Meloidogyne javanica*. *J. Nematol.* 7:111-113.
- Blasingame, D., and M. V. Patel. 2001. Cotton disease loss data base . In *Proc. 2002 Beltwide Cotton Conference*. Anaheim, CA.: National Cotton Council.
- Bond, C.R., and J. D. Mueller. 2007. Delayed maturity and associated yield loss in cotton infected by the Columbia Lance (*Hoplolaimus Columbus* Sher) nematode. *J. Cotton Sci.* 11: 275-287.

- Boote, K. J. 1999. Concepts for calibrating crop growth models. In *DSSAT, Version 3. A Decision Support System for Agrotechnology Transfer*. Vol. 4, p. 179-194. Eds G. Hoogenboom, P. W. Wilkens and G. Y. Tsuji. Honolulu, HI.: University of Hawaii.
- Boote, K. J., J. W. Jones, J. W. Mishoe, and R. D. Berger. 1983. Coupling pest to growth simulators to predict yield reductions. *Phytopathology* 73:1581-1587.
- Bouyoucos, G.J. 1936. Directions for making mechanical analysis of soils by the hydrometer method. *Soil Sci.* 42: 3.
- Boydell, B., and B. McBratney. 2002. Identifying potential within-field management zones from cotton-yield estimates. *Prec. Agric.* 3:9-23.
- Bronson, K.F., J.D. Booker, S.J. Officer, R.J. Lascano, S.J. Maas, S.W. Searcy, and J. Booker. 2005. Apparent electrical conductivity, soil properties and spatial covariance in the U.S. Southern High Plains. *Prec. Agric.* 6: 297-311.
- Brown, K.L. 1968. Translocation of carbohydrate in cotton: Movement to fruiting bodies. *Ann. Bot.* 32: 703-713.
- Cadet, P., S. Berry, and V. Spaul. 2004. Mapping of interactions between soil factors and nematodes. *Eur. J. Soil Biol.* 40(2): 77-86.
- Castrignanò, A., G. Buttafuoco, R. Puddu, and C. Fiorentino. 2007. A multivariate geostatistical approach to delineate areas at soil salinization risk. In Proc. *Sixth European Conference of Precision Agriculture (6ECPA)*, 199-205. Stafford, J., and A. Werner, eds. Skiathos. Greece.
- Castro, C. E., N. O. Belser, H. E. McKinney, and I. J. Thomasson. 1990. Strong repellency of the root knot nematode, *Meloidogine incognita* by specific inorganic ions. *J. Chem. Ecol.* 16(4): 1199-1205.
- Chang, J., D.E. Clay, C.G. Carlson, S.A. Clay, D.D. Malo, R. Berg, J. Kleinjan, and W.J. Wiebold. 2003. Different techniques to identify management zones impact nitrogen and phosphorus sampling variability. *Agron. J.* 95: 1550-1559.
- Chen, F., D.E. Kissel, L.T. West, and W. Adkins. 2000. Field-scale mapping of surface soil organic carbon using remotely sensed imagery. *Soil Sci. Soc. Am. J.* 64: 746-753.
- Colyer, P. D., T. L. Kirkpatrick, W. D. Caldwell, and P. R. Vernon. 1997. Influence of nematicide application on the severity of the root-knot nematode-fusarium wilt disease complex in cotton. *Plant. Dis.* 81: 66-70.
- Corwin, D.L., and S.M. Lesch. 2005. Apparent soil electrical conductivity measurements in agriculture. *Comput. Electron. Agric.* 46: 11-43.

- Creech, R.G., J.N. Jenkins, B. Tang, G.W. Lawrance, and J.C. McCarthy. 1995. Cotton Resistance to Root-Knot Nematode: I. Penetration and Reproduction. *Crop Sci.* 35: 365-368.
- Davis, R. F., P. Bertrand, J. D. Gay, R. E. Baird, G. B. Padgett, E. A. Brown, F. F. Hendrix, and J. A. Balsdon. 1996. Guide for interpreting nematode assay results. Circular No. 834, 16 p.: University of Georgia Cooperative Extension Service.
- Davis, R.F., and O.L. May. 2003. Relationships between tolerance and resistance to *Meloidogyne incognita* in Cotton. *J. Nematol.* 35: 411-416.
- Davis, R.F., and O.L. May. 2005. Relationship between yield potential and percentage yield suppression caused by the southern root-knot nematode in cotton. *Crop Sci.* 45: 2312-2317.
- Day, P.R. 1965. Particle fractionation and particle-size analysis. Black, C. A., Madison, Wisconsin.
- Dieleman J. A., D. A. Mortensen, D. D. Buhler, C. A. Cambardella, and T. B. Moorman. 2000. Identifying associations among site properties and weed species abundance: I Multivariate analysis. *Weed Sci.* 48: 567-575.
- Doberman, A., J.L. Ping, V.I. Adamchuk, G.C. Simbahan, and R.B. Ferguson. 2003. Classification of crop yield variability in irrigated production fields. *Agron. J.* 95: 1105-1120.
- Doerge, T.A. 1999. Management zone concepts. In *Site-Specific Management Guidelines*. P. P. Institute. Series Norcross.
- Dorhout, R., F.J. Gommers, and C. Kollöffel. 1991. Water transport through tomato roots infected with *Meloidogyne incognita*. *Phytopathology* 81: 379-385.
- Ehwaeti, M.E., M.J. Elliott, J.M. McNicol, M.S. Phillips, and D.L. Trudgill. 2000. Modelling nematode population growth and damage. *Crop Prot.* 19: 739-745.
- ESRI. 2004a. ArcGIS Spatial Analyst 9.0. ESRI, Redlands, CA.
- ESRI. 2004b. ArcGIS Geostatistical Analyst. ESRI, Redlands, CA.
- Evans, K., R.M. Webster, P.D. Halford, A.D. Barker, and M.D. Russell. 2002. Site-specific management of nematode - Pitfalls and practicalities. *J. Nematol.* 34: 194-199.
- Fallick, J.B., W.D. Batchelor, G.L. Tylka, T.L. Niblack, and J.O. Paz. 2002. Coupling soybean cyst nematode damage to CROPGRO Soybean. *Trans. ASAE* 45: 433-441.

- Fraisse, C.W., K.A. Sudduth, and N.R. Kitchen. 2001a. Delineation of site-specific management zones by unsupervised classification of topographic attributes and soil electrical conductivity. *Trans. ASAE* 44(1): 155-166.
- Fraisse, C.W., K.A. Sudduth, and N.R. Kitchen. 2001b. Calibration of the ceres-maize model for simulating site-specific crop development and yield on claypan soils. *Appl. Eng. Agric.* 17: 547-556.
- Fridgen, J.J., C.W. Fraisse, N.R. Kitchen, and K.A. Sudduth. 2000. Delineation and analysis of site-specific management zones. In *Proc. 2<sup>nd</sup> International Conference on Geospatial Information in Agriculture and Forestry*, CD-ROM. Lake Buena Vista, FL.
- Fridgen, J.J., N.R. Kitchen, K.A. Sudduth, S.T. Drummond, W.J. Wiebold, and C.W. Fraisse. 2004. Management zone analyst (MZA): software for subfield management zone delineation. *Agron. J.* 96: 100-108.
- Garson, D.G. 2007. Canonical Correlation. North Carolina State University. Available at: <http://www2.chass.ncsu.edu/garson/pa765/canonic.htm>. Accessed 24 August 2008.
- Geovariances, 2007. ISATIS technical references, version 7.0.6.
- Goodell, P. B., and H. Ferris. 1980. Plant-parasitic nematode distributions in an alfalfa field. *J. Nematol.* 12: 136-141.
- Goovaerts, P. 1994. Study of spatial relations between two set of variables using multivariate geostatistics. *Geoderma* 62: 93-107
- Goovaerts, P. 1997. *Geostatistics for Natural Resources*. Oxford University Press, New York, USA.
- Goovaerts, P., R. Webster, and J. P. Dubois. 1997. Assessing the risk of soil contamination in the Swiss Jura using indicator geostatistics. *Environ. Ecol. Stat.* 4: 31-48.
- Goovaerts, P. 1998. Geostatistical tools for characterizing the spatial variability of microbiological and physico-chemical soil properties. *Biol. Fert. Soils* 27: 315-334.
- Goovaerts, P., G. AvRusking, J. Meliker, M. Slotnick, G. Jacquez, and J. Nriagu. 2005. Geostatistical modeling of the spatial variability of arsenic in ground water of southeast Michigan. *Water Resour. Res.* 41: 1-19.
- Grunwald, S., P. Goovaerts, C. M. Bliss, N. B. Comerford, and S. Lamsal. 2006. Incorporation of auxiliary information in the geostatistical simulation of soil nitrate nitrogen. *Vadose Zone J.* 5: 391-404

- Hoogenboom, G., J. W. Jones, P. W. Wilkens, C. H. Porter, W. D. Batchelor, L. A. Hunt, K. J. Boote, U. Singh, O. Uryasev, W. T. Bowen, A. J. Gijssman, A. S. Du Toit, J. W. White, G. Y. Tsuji. 2004. *Decision Support System for Agrotechnology Transfer*. Ver. 4.0. Honolulu, HI.:University of Hawaii.
- Hunt, L. A. and K. J. Boote. 1998. Data model operation, calibration, and evaluation. In *Understanding options for agricultural production*. Dordrecht, The Netherlands.: Kluwer Academic Publishers.
- Irmak, A., J. W. Jones, W. D. Batchelor, and J. O. Paz. 2002. Linking multiple layers of information for diagnosing causes of spatial yield variability in soybean *Trans. ASAE* 45: 839-849.
- Jaynes, D.B., T.C. Kaspar, T.S. Colvin, and D.E. James. 2003. Cluster analysis of spatiotemporal corn yield patterns in an Iowa field. *Agron. J.* 95: 574-586.
- Jaynes, D.B., T.S. Colvin, and T.C. Kaspar. 2005. Identifying potential soybean management zones from multi-year yield data. *Comput. Electron. Agric.* 46: 309-327.
- Jenkins, W.R. 1964. A rapid centrifugal flotation technique for separating nematodes from soil. *Plant Dis.* 48: 692.
- Johnson, R. A., and D. W. Wichern. 2002. *Applied multivariate analysis*. 5th ed. Upper Saddle River, NJ.: Prentice Hall.
- Jones, J. W., G. Hoogenboom, C. H. Porter, K. J. Boote, W. D. Batchelor, L. A. Hunt, P. W. Wilkens, U. Singh, A. J. Gijssman, and J. T. Ritchie. 2003. DSSAT Cropping System Model. *Eur. J. Agron.* 18:235-265.
- Kemerait, R. C., R. F. Davis, P. H. Jost, C. L. Brewer, S. N. Brown, B. Mitchell, W. E. Harrison, R. Joyce, and E. McGriff. 2004. Assessment of nematicides for management of the southern root-knot nematode, *Meloidogyne incognita*, in Georgia. Tifton, GA. In 2004 Georgia cotton research and extension reports.: The University of Georgia. Available at: <http://commodities.caes.uga.edu/fieldcrops/cotton/rerpubs/2004/p202.pdf>. Accessed 10 October 2008
- Khalilian A., J. D. Mueller, S. C. Blackville, Y. J. Han, and F. J. Wolak. 2001. Predicting cotton nematodes distribution utilizing soil electrical conductivity. In *Proc. 2001 Beltwide Cotton Conference*, 146-149. Memphis, TN.:National Cotton Council.
- Khoshkhoo, N., P.A. Hedin, and J.C.J. McCarthy. 1994. Free sugars in root-knot nematode susceptible and resistant cotton plant roots and leaves. *J. Agric. Food Chem.* 42: 366-368.
- Kerry, R., M. A. Oliver. 2003. Co-kriging when soil and ancillary data are not co-located. In *Proc. 4<sup>th</sup> European Confence of Precision Agriculture*. 303-308. Wageningen Academic Publishers.

- Kirkpatrick, T.L., D.M. Oosterhuis, and S.D. Wulschleger. 1991. Interaction of *Meloidogyne incognita* and water stress in two cultivars. *J. Nematol.* 23: 462-467.
- Kirkpatrick, T.L., M.W. van Iersel, and D.M. Oosterhuis. 1995. Influence of *Meloidogyne incognita* on the water relations of Cotton growth in microplots. *J. Nematol.* 27: 465-471.
- Kitchen, N. R., K.A. Sudduth, and S. T. Drummond. 1999. Soil electrical conductivity as a crop productivity measure for claypan soils. *J. Prod. Agric.* 12: 607-617.
- Kitchen, N. R., S. T. Drummond, E. D. Lund, K.A. Sudduth, and G. W. Buchleiter. 2003. Soil electrical conductivity and topography related to yield for three contrasting soil-crop systems. *Agron. J.* 95: 483-495.
- Kleinschmidt, I., M. Bagayoko, G.P.Y. Clarke, M. Craig, and D. Le Sueur. 2000. A spatial statistical approach to malaria mapping. *Intl. J. Epidemiol.* 29: 355-361.
- Koenning, S.R., and K.R. Barker. 1995. Soybean photosynthesis and yield as influenced by *Heterodera glycines*, soil type and irrigation. *J. Nematol.* 27: 51-62.
- Koenning, S. R., S. A. Walters, and K. R. Barker. 1996. Impact of soil texture on the reproductive and damage potential of *Rotylenchulus reniformis* and *Meloidogyne incognita* on Cotton. *J. Nematol.* 28: 527-536.
- Koenning, S.R., T.L. Kirkpatrick, J.L. Starr, J.A. Wrather, N.R. Walker, and J.D. Mueller. 2004. Plant-parasitic nematodes attacking cotton in the United States: old and emerging production challenges. *Plant Dis.* 88: 100-113.
- Li, H., R.J. Lascano, E.M. Barnes, J. Booker, L.T. Wilson, K.F. Bronson, and E. Segarra. 2001. Multispectral reflectance of cotton related to plant growth, soil water and texture, and site elevation. *Agron. J.* 93: 1327-1337.
- Li, Y., Z. Shi, F. Li, and H.Y. Li. 2007. Delineation of site-specific management zones using fuzzy clustering analysis in a coastal saline land. *Comput. Electron. Agric.* 56: 174-186.
- Lin, Y., T. Chang, C. Shih, and C. Tseng. 2002. Factorial and indicator kriging methods using a geographic information system to delineate spatial variation and pollution sources of soil heavy metals. *Environ. Geol.* 42: 900-909.
- Littel, R.C., G.A. Milliken, W.W. Stroup, and R.D. Wolfinger. 1996. *SAS Systems for Mixed Models*, Cary, NC.
- Loveys, R.R., and A.F. Bird. 1973. The influence of nematodes on photosynthesis in tomato plants. *Physiol. Plant Pathol.* 3: 525-529.

- Lyon, S. W., A. J. Lembo Jr, M. T. Walter, and T. S. Steenhuis. 2006. Defining probability of saturation with indicator kriging on hard and soft data. *Adv. Water Resour.* 29: 181-193.
- Martin, N. F., G. Borrero, and D. G. Bullock. 2005. Association between field characteristics and soybean plant performance using canonical correlation analysis. *Plant and Soil* 237: 39-55.
- Matheron, G. 1963. Principles of geostatistics. *Econ. Geol.* 58: 1246-1266.
- Matheron, G. 1982. Pour une analyse krigéante de données regionalices. Centre de Géostatistique, Report N-732, Fontainebleau.
- Melakeberhan, H., J. Dey, V. C. Baligar, and T. E. Carter Jr. 2004. Effect of soil pH on the pathogenesis of *Heterodera glycines* and *Meloidogyne incognita* on *Glycine max* genotypes. *Nematology* 6: 585-592.
- McBratney, A.B., and J.J. DeGrujter. 1992. A continuum approach to soil classification by modified fuzzy means with extragrades. *J. Soil Sci.* 43: 159-175.
- McClure, M.A. 1977. *Meloidogyne incognita*: A metabolic sink. *J. Nematol.* 9: 88-90.
- McWilliams, D. 2003. Drought strategies for cotton. New Mexico State University, Las Cruces. 6 p.
- Monfort, W. S., T. L. Kirkpatrick, C. S. Rothrock, and A. Mauromoustakos. 2007. Potential for site-specific management of *Meloidogyne incognita* in cotton using soil textural zones. *J. Nematol.* 39 (1): 1-8.
- Naab, J. B., P. Singh, K. J. Boote, J. W. Jones, and K. O. Marfo. 2004. Using the CROPGRO-peanut model to quantify yield gaps of peanut in the guinean savanna zone of Ghana. *Agron. J.* 96: 1231-1242.
- NCC. 2008. Beltwide yield losses to nematode damage. Cordova, TN.: National Cotton Council of America. Available at: [www.cotton.org/tech/pest/nematode/losses.cfm](http://www.cotton.org/tech/pest/nematode/losses.cfm). Accessed August 17, 2008.
- Noe, J. P., and K. R. Barker. 1985. Relation of within-field spatial variation of plant-parasitic nematode population densities and edaphic factors. *Phytopatology* 75: 247-252.
- O'Bannon, J.H., and H.W. Reynolds. 1965. Water consumption and growth of root-knot nematode-infected and uninfected cotton plants. *Soil Sci.* 99: 251-255.
- Oka, Y., N. Tkachi, S. Shuker, R. Rosenberg, S. Suriano, L. Roded, and P. Fine. 2006. Field studies on the enhancement of nematicidal activity of ammonia-releasing fertilizers by alkaline amendments. *Nematology* 8(6): 881-893.

- Oka, Y., N. Shapira, and P. Fine. 2007. Control of root-knot nematodes in organic farming systems by organic amendments and soil solarization. *Crop Prot.* 26(10): 1556-1565.
- Ortiz, B. V., D. G. Sullivan, C. Perry, and G. Vellidis. 2006. Geospatial solutions for precision management of cotton root knot nematodes. ASAE paper No. 061147. Portland, OR.: ASAE.
- Ortiz, B. V., D. G. Sullivan, C. Perry, G. Vellidis, L. Seymour, and K. Rucker. 2007. Delineation of management zones for site specific management of parasitic nematodes using geostatistical analysis of measured field characteristics. In *Proc. Sixth European Conference of Precision Agriculture (6ECPA)*., CD-ROOM. Stafford, J., and A. Werner, eds. Skiathos. Greece.
- Ortiz, B. V., C. Perry, D. G. Sullivan, R. C. Kemerait, A. Ziehl, R. Davis, G. Vellidis, and K. Rucker. 2008. Evaluation of Variable Rate of Nematicides on Cotton According to Nematode Risk Zones. In *Proc. 2008 Beltwide Cotton Conference*. Nashville, TN.: National Cotton Council.
- Paz, J. O., W. D. Batchelor, G. L. Tylka, and R. G. Hartzler. 2001. A modeling approach to quantify the effects of spatial soybean yield limiting factors. *Trans. ASAE* 44: 1329-1334.
- Perkins, H.F., J.E. Hook, and N.W. Barbour. 1986. Soil characteristics of selected areas of the coastal plain experiment station and ABAC research farms. The University of Georgia.
- Perry, C., G. Vellidis, D. G. Sullivan, K. Rucker, and R. Kemerait. 2006. Predicting nematode hotspots using soil EC<sub>a</sub> data. In *Proc. 2006 Beltwide Cotton Conference*. San Antonio, TX.: National Cotton Council.
- Pettigrew, W.T., W.R. Meredith, Jr., and L.D. Young. 2005. Potassium fertilization effects on cotton lint yield, yield components, and reniform nematode populations. *Agron. J.* 97: 1245-1251.
- Pinnschmidt, H. O., W. D. Batchelor, and P. S. Teng. 1995. Simulation of multiple species pest damage in rice using CERES-Rice. *Agric. Syst.* 48: 193-222.
- Robinson, A.F. 2007. Reniform in U. S Cotton: When, where, why, and some remedies. *Ann. Rev. Phytophatol.* 45: 263-288.
- Rodgers, S. E., and M. A. Oliver. 2007. A geostatistical analysis of soil, vegetation, and image data characterizing land surface variation. *Geogra. Anal.* 39: 195-216.
- SAS Institute Inc. 2007. SAS OnlineDoc (R) 9. 1. 3. Cary, NC.: SAS Institute Inc.
- Shepherd, R.L., and M.G. Huck. 1989. Progression of root-knot nematode symptoms and infection on resistant and susceptible cotton. *J. Nematol.* 21: 235-241.

- Smit, A.L., and T. Vamerali. 1998. The influence of potato cyst nematodes (*Globodera pallida*) and drought on rooting dynamics of potato (*Solanum tuberosum* L.). *Eur. J. Agron.* 9: 137-146.
- Shurley, W.D., R.C. Kemerait, S. Brown, E. McGriff, B. Mitchell, and R. Reed. 2004. Economic analysis of southern root knot nematode controls. University of Georgia.
- Stanton, M. A. 1986. Effects of root-knot nematode (*Meloidogyne* spp.) on growth and yield of 'Cobb' soybean (*Glycine max* (L.) merrill). MS thesis. Gainesville, Fl.: University of Florida, Agronomy Department.
- Starr, J.L., C.M. Heald, A.F. Robinson, R.G. Smith, and J.P. Krausz. 1993. *Meloidogyne incognita* and *Rotylenchulus reniformis* and associated soil textures from some cotton production areas of Texas. *J. Nematol.* 25: S895-899.
- Steel, R.G.D., and J.H. Torrie. 1980. Principles and procedures of statistics. 2<sup>nd</sup> ed. New York, N.Y.: McGraw-Hill.
- Sudduth, K. A., N. R. Kitchen, W.J. Wiebold, W. D. Batchelor, G. A. Bollero, D. G. Bullock, D. E. Clay, H. L. Palm, F. J. Pierce, R. T. Schuler, and K. D. Thelen. 2005. Relating apparent electrical conductivity to soil properties across the north-central USA. *Comp. Electron. Agric.* 46: 263-283.
- Sullivan, D.G., J.N. Shaw, and D. Rickman. 2005. IKONOS imagery to estimate surface property variability in two Alabama physiographies. *Soil Sci. Soc. Am. J.* 69: 1789-1798.
- Tarr, A.B., K.J. Moore, P.M. Dixon, C.L. Burras, and M.H. Wiedenhoef. 2003. Use of soil electroconductivity in a multistage soil-sampling scheme. *Crop Mgmt.* 10:1094/CM-2003-1029.
- Teng, P. S., W. D. Batchelor, H. O. Pinnschmidt, G. G. Wilkerson. 1998. Simulation of pest effects on crop using coupled pest-crop models: the potential for decision support. In *Understanding options for agricultural production*. Dordrecht, The Netherlands.: Kluwer Academic Publishers.
- UGA, 2005. 2005 Georgia cotton research and extension reports. Cooperative Extension Service.: The University of Georgia. Available at : <http://commodities.caes.uga.edu/fieldcrops/cotton/rerpubs/2005/p242.pdf>. Accessed 25 August 2008.
- UGA, 2007a. Georgia plant disease loss estimate. Cooperative Extension. Athens, GA: University of Georgia. Available at: <http://pubs.caes.uga.edu/caespubs/pubs/PDF/SB41-10.pdf>. Accessed 23 August 2008.

- UGA. 2007b. 2007 Georgia cotton production guide. Cooperative Extension Service.: The University of Georgia. Available at:  
<http://commodities.caes.uga.edu/fieldcrops/cotton/2007cottonguide/appendixIII.pdf>.  
Accessed 06 October 2008.
- USDA. 2002. Soil survey geographic (SSURGO) database. U.S. Department of Agriculture, Natural Resources Conservation Service.
- USDA. 2008. Crop production. National Agricultural Statistics Service. Washington, D.C.: USDA National Agricultural Statistics Service. Available at:  
[www.usda.gov/nass/PUBS/TODAYRPT/crop0808.txt](http://www.usda.gov/nass/PUBS/TODAYRPT/crop0808.txt). Accessed 17 August 2008.
- Vellidis, G., M. Tucker, C. Perry, C. Kvien, and C. Bednarz. 2008. A real-time wireless smart sensor array for scheduling irrigation. *Comput. Electron. Agric.* 61: 44-50.
- Walker, N.R., T.L. Kirkpatrick, and C.S. Rothrock. 1998. Interaction between *Meloidogyne incognita* and *Thielaviopsis basicola* on cotton (*Gossypium hirsutum*). *J. Nematol.* 30: 415-422.
- Walker, N.R., T.L. Kirkpatrick, and C.S. Rothrock. 1999. The interaction between the root-knot nematode (*Meloidogyne incognita*) and black root rot (*Thielaviopsis basicola*) on cotton (*Gossypium hirsutum*). *J. Nematol.* 30: 415-422.
- Wallace, H.R. 1987. Effects of nematode parasites on Photosynthesis. In *Vistas on nematology*, 253-259. Hyattsville, MD. Society of Nematologists.
- Webster, R., and B. Boag. 1992. Geostatistical analysis of cyst nematodes in soil. *J. Soil Sci.* 43: 583-595.
- Wheeler, T. A., K.R. Barker, and S. M. Schneider. 1991. Yield-loss models for tobacco infected with *Meloidogyne incognita* as affected by soil-moisture. *J. Nematol.* 23: 365-371.
- Wilcox-Lee, D.A., and R. Loria. 1987. Effects of nematode parasitism on plant-water relations. In *Vistas on nematology*, 260-266. Hyattsville, MD. Society of Nematologists.
- Williamson, V.M., and C.A. Gleason. 2003. Plant-nematode interactions. *Curr. Opin. Plant Biol.* 6(4): 327-333
- Willmott, C.J. 1982. Some comments on the evaluation of the model performance. *Bulletin of the American Meteorological Society* 63: 1309-1313.
- Windham, G. L. and K. R. Barker. 1993. Spatial and temporal interactions of *Meloidogyne incognita* and soybean. *J. Nematol.* 25: 738-745 Suppl. S.

- Wolcott, M. 2007. Cotton yield response to residual effects of Telone Fumigant. In *Proc. 2007 Beltwide Cotton Conference*. New Orleans, LS.: National Cotton Council.
- Wyse-Pester, D. Y., L.J. Wiles, and P. Westra. 2002. The potential for mapping nematode distribution for site-specific management. *J. Nematol.* 34: 80-87.
- Wyss, U., F.M.W. Grundler, and A. Munch. 1992. The parasitic behaviour of second stage juveniles of *Meloidogyne incognita* in root of *Arabidopsis thaliana*. *Nematologica* 38: 98-111.
- Zhang, J., C. Waddell, C. Sengupta-Gopalan, C. Potenza, and R.G. Cantrell. 2006. Relationships between root-knot nematode resistance and plant growth in upland cotton: galling index as a criterion. *Crop Sci.* 46: 1581-1586.
- Zimet, D.J., J.L. Smith, R.A. Kinloch, and J.R. Rich. 2002. Improving cotton returns using nematicides in Northwestern Florida infested with Root-Knot Nematode. *J. Cotton Sci.* 6: 28-33.